MOUNTAIN-PLAINS CONSORTIUM

MPC 22-459 | F. Ting and B. Kidd

FLOOD HYDROGRAPH
GENERATION FOR
PREDICTING BRIDGE
SCOUR IN COHESIVE SOILS

Flood Hydrograph Generation for Predicting Bridge Scour in Cohesive Soils

Francis C.K. Ting
Brian Kidd

Department of Civil and Environmental Engineering
South Dakota State University
Brookings, SD 57007

May 2022

Acknowledgements

Disclaimer

The contents of this report reflect the views of the authors, who are responsible for the facts and the accuracy of the data presented. This document is disseminated under the sponsorship of the Department of Transportation, University Transportation Centers Program, in the interest of information exchange. The U.S. Government assumes no liability for the contents or use thereof.

ABSTRACT

Three bridge sites in South Dakota with streamflow records ranging from 50 to 67 years were selected to compute the histories of pier or contraction scour using the Scour Rates In COhesive Soils (SRICOS) method. Scour depths were computed using a range of soil erosion functions representative of cohesive and non-cohesive soils. The results show that a continuous hydrograph spanning several decades may be replaced by a series of maximum annual floods. A tiered approach for using the SRICOS method was developed. In the Level I analysis, the results of soil classification or soil erosion rate testing are used with simple calculations to eliminate bridge sites where use of the SRICOS method is not recommended. In the Level II analysis, recorded hydrographs are used to predict the final scour depths produced by floods of different return periods to assess scouring potential. In the Level III analysis, annual maximum series are generated and used with the SRICOS method to compute the exceedance probabilities associated with different scour depths and project lives. Each flood in the annual maximum series has a constant discharge sampled randomly from the Log Pearson Type III (LP-III) distribution and an equivalent duration computed using a regression equation.

TABLE OF CONTENTS

LIST OF FIGURES

ix

LIST OF TABLES

1. EXECUTIVE SUMMARY

1.1 Introduction

The method currently used by the South Dakota Department of Transportation (SDDOT) for designing bridge foundation assumes that the bed material is sand and designs for a single (worst-case) flood event, such as the 100-year or 500-year flood using the peak flow magnitude. This approach is generally regarded as conservative because the duration of flooding events in many watersheds in South Dakota is not long enough to generate equilibrium scour and the bed material is more likely to be cohesive. The Scour Rate In COhesive Soils (SRICOS) method is included in Hydraulic Engineering Circular No. 18 (HEC-18; Arneson et al., 2012) as an alternative approach for evaluating bridge scour in cohesive soils. The method considers the time rate of scour but will require the input of a hydrograph. There is no guidance in HEC-18 on how to generate hydrographs for use with the SRICOS method. It is unclear what level of detail in the temporal record of flows (e.g., a continuous hydrograph for multiple years with an annual flooding cycle, a series of design floods with short-term correlation up to a few days) is required to correctly predict the final scour depth in cohesive soils. Some hydrograph generation methods require a great deal of effort to use and are difficult to apply routinely by engineers. SDDOT also needs guidelines to define the site conditions where the SRICOS method is more appropriate, and more cost effective than the traditional method.

This research has three main objectives. First, select three bridge sites in South Dakota with long streamflow records (> 50 years) to compute scour histories using the SRICOS method. The results will be analyzed to understand the relationship between time sequence of flows, rate of scour, and final scour depth to answer the fundamental question of how the characteristics of a hydrograph, such as flood magnitude and duration, and the order of flood occurrence would influence scour development in cohesive soils. Second, develop a decision tool to identify the types of field situations where the SRICOS method is appropriate and beneficial. Third, provide guidelines for hydrologic analysis and hydrograph generation for using the SRICOS method based on the site conditions and project requirements.

1.2 Importance/Potential Applications of Research

The immediate benefits of this project will be an alternative approach to evaluating bridge scour in cohesive soils. SDDOT currently uses methods developed for non-cohesive soils to evaluate bridge scour. The SRICOS method could reduce foundation costs in cohesive soils and increase the confidence level of foundation designs for some bridge sites and projects. The SRICOS method may also be useful for evaluating scour critical bridges and scheduling substructure repair and scour remediation projects.

The SRICOS method is most useful when the design life of the bridge is short compared with the expected duration of the scouring floods, and for sites with slow rates of scour. Potential situations may include:
- Bridges scheduled to be replaced in few years
- Bridges over ephemeral streams
- Scour critical bridges, which may be safe if the slower rates of scour in cohesive soils are considered, and
- Bridges on low volume roads that can be temporarily closed during a flood

The results of this research are directly applicable to practice, first by giving the design engineer a screening tool to identify bridge sites where the SRICOS method may be more appropriate than the traditional HEC-18 method, and second by providing a step-by-step procedure to generate flood hydrographs for scour prediction using the SRICOS method and assessing the scour risk. When use of the SRICOS method is advisable, substantial savings in foundation costs and scour countermeasures may result, and this can be measured by the dollars saved in highway projects.

The bridge scour evaluation procedure developed in this project is an extension of the HEC-18 method, first by including the time effect of scour, and second by using a stochastic approach to predict the probability of exceedance of the predicted scour depth. The new procedure can be used to assess the susceptibility of bridges to scour damages during extreme flooding events where the structures would probably be classified as unsafe based on the traditional HEC-18 method. A broader impact of this project will be a new engineering tool that can be incorporated into a future statewide hazard assessment program to identify flood vulnerable bridges in South Dakota, which would have considerable benefits to the resiliency of the state's transportation system.

1.3   Research Approach

The central hypothesis of this project is that even for highly erosion-resistant cohesive soils, it is not necessary to predict scour using a continuous hydrograph to cover the service life of a bridge. Due to pre-existing scour, most of the floods in a continuous hydrograph will not achieve their maximum scour potential. Therefore, a sequence of design floods should be all that is needed to predict scour over the project life. This hypothesis was tested by analyzing the computed scour histories at three bridge sites with long streamflow records to determine how the characteristics of a hydrograph, such as the magnitude and duration of floods, and their order of occurrence may influence the time development of scour. SRICOS simulations were conducted for pier scour at the SD13 bridge over the Big Sioux River near Flandreau and the Interstate 90 bridges over the Split Rock Creek at Brandon, and for contraction scour at the SD37 bridges over the James River north of Mitchell. These three sites were chosen for the case studies because the SD13 bridge and SD37 bridges have long streamflow records (around 70 years) and large potential for pier scour (SD13 bridge) and contraction scour (SD37 bridges). The Interstate 90 bridges were chosen to evaluate the QPPQ method (Archfield et al., 2013) for estimating streamflow in a stream with incomplete flow records. To expand the dataset to include soil types other than those found at the three bridge sites, a sensitivity analysis was conducted by varying the soil critical shear stress and erosion rates over a range of values representative of cohesive and non-cohesive soils. The findings from the case studies were synthesized to develop a hydrograph generation method for using the SRICOS method and a screening tool for the engineer to determine whether use of the SRICOS method is beneficial for a given project.

The basic framework for hydrograph generation is a series of maximum annual floods. A flood frequency analysis is performed on historical flow data to determine the peak discharges and their return periods. The equivalent duration that will produce the same final scour depth as the one created by the recorded hydrograph is also determined for each flood. The probability distribution of peak discharge is sampled randomly to create a series of maximum annual floods (annual maximum series) that satisfies the parameters of the Log Pearson Type III (LP-III) distribution. A set of equally probable future hydrographs are generated and used with the SRICOS method to compute the distribution of final scour depths, which is then used to determine the risk values associated with different project lives and scour depths.

1.4 Research Findings

SRICOS simulations conducted using recorded hydrographs at the three bridge sites show that significant reduction in the predicted final scour depth occurred only in regions III (medium erodibility) and IV (low erodibility) of the soil erodibility charts by Briaud et al. (2011). Cohesive soils that fall into this category include high plasticity silt and clay. Scour history analyses further show that a continuous hydrograph may be replaced by a sequence of maximum annual floods for the purpose of scour prediction. Based on these research findings, three levels of assessment in increasing order of complexity are proposed for evaluating pier and contraction scour in cohesive soils.

The Level I assessment will be a basic hydrologic, hydraulic, geotechnical, and scour analysis like the procedure for scour evaluation in HEC-18. A flood frequency analysis is conducted to determine the moments of the log Pearson Type III (LP-III) distribution and peak discharges for floods of different return periods. A bridge hydraulic analysis is then performed using a one-dimensional (1D) or two-dimensional (2D) flow model. Borehole data are obtained to delineate the soil stratigraphy and for geotechnical testing, and thin-walled tube samples may be collected and tested in an erosion function apparatus (EFA) to measure the erosion-rate-versus-shear-stress curve. Alternatively, USCS soil classification may be used with the soil erodibility chart by Briaud et al. (2011) to estimate the critical shear stress and soil erosion rates. The SRICOS method is run with the estimated 100-year peak discharge for five days. If the soil type falls into category I or II and/or the computed final scour depth is close to the equilibrium scour depth, the maximum scour depth can be reached during a single flooding event and no reduction in the predicted scour depth from the HEC-18 method is recommended. The engineer may also adopt the equilibrium scour depth for design if the scour depth predicted by the HEC-18 method is judged to be reasonable or other considerations (e.g., high traffic volume, long design life) dictate a more conservative approach.

In the Level II assessment, scour histories of past floods are computed using a measured soil erosion function to determine the final scour depth z_f and equivalent time t_e of the individual floods. The results are plotted on a $\frac{t_e}{t_{90}}$ versus $\frac{z_f}{z_{max}}$ curve, where z_{max} is equilibrium scour depth and t_{90} is time to reach 90% of z_{max} to assess the potential of floods of different return periods to produce scour. A decision is made to adopt the scour depth predicted using the HEC-18 method or proceed to a full SRICOS analysis.

In the Level III assessment, the LP-III distribution is used to generate a sequence of peak flows, and their equivalent times are computed using a regression equation. Many annual maximum series are generated and used with the SRICOS method to predict the exceedance probability of final scour depth. A design scour depth is selected based on the risk values associated with different project lives.

The general procedure for a full SRICOS analysis with hydrograph generation at a bridge site consists of the following five steps:

(1) SRICOS simulations are conducted using recorded hydrographs to predict the scour histories produced by the maximum annual floods. For ungauged streams, recorded hydrographs may be transferred from a gauged stream using the QPPQ method if the two streams have similar hydrologic characteristics.

(2) The computed scour histories are used to determine the equivalent times of the maximum annual floods that will produce the same predicted scour depths as the recorded hydrographs. Regression analysis is conducted to relate the computed equivalent time to peak discharge.

(3) The LP-III distribution is sampled randomly to create a sequence of equivalent rectangular floods. Each flood is assigned a duration using the regression equation developed in step (2).

(4) A set of equally probable future hydrographs is generated using Monte Carlo simulation and employed with the SRICOS method to compute final scour depths. Each hydrograph consists of a series of maximum annual floods. The total number of floods in the annual maximum series is equal to the expected project life of the bridge in years.

(5) The distribution of computed final scour depth is used to determine the exceedance probability associated with different predicted scour depths and project lives.

1.5 Research Recommendations

It is recommended that:

(1) When scour depth is the controlling factor in bridge design, an additional check be included in the current SDDOT bridge design procedure to determine whether time effect of scour may be an important factor in predicting the final scour depth.

(2) The HEC-18 pier scour equation for the equilibrium scour depth in non-cohesive soils be used to compute the equilibrium scour depth in cohesive soils when using the SRICOS method. Thus, any reduction in the predicted scour depth in cohesive soils is due to the time effect of scour only.

(3) For bridge sites with large contraction scour depth, the critical shear stress be measured instead of estimated based on grain sizes.

(4) A workshop be conducted for SDDOT engineers and consultants on the use of the SRICOS method in evaluating bridges for scour.

It is suggested that SDDOT:

(1) Acquires the capability to measure soil erodibility

(2) Develops a research project to investigate the occurrence of long duration floods and their effects on bridge scour

(3) Conducts additional cases studies on using the QPPQ method for estimating streamflow in ungauged streams in South Dakota

(4) Conducts a study on flooding trends in South Dakota streams.

2.   PROBLEM DESCRIPTION

The method currently used by the South Dakota Department of Transportation (SDDOT) for designing bridge foundation assumes that the bed material is sand and designs for a single (worst-case) flood event such as the 100-year or 500-year flood using the peak flow magnitude. Many bridges in South Dakota are founded on cohesive soils consisting of silts and clays (Niehus, 1996). Since silts and clays scour more slowly than sands, using the traditional methods for evaluating scour at bridges may over-predict the extent of scour. This could result in over-design of new bridge foundations or installation of unnecessary scour countermeasures at existing bridges. Furthermore, bridges that are classified as scour critical may in fact be safe. With more reliable methods for predicting scour in cohesive soils, SDDOT could save significant time and money on bridges built over waterways.

Using the results of flume tests and numerical modeling, the Scour Rate In COhesive Soils (SRICOS) method was developed by researchers at Texas A&M University (TAMU) to predict the time rate of scour as well as the final scour depth at bridges (Briaud et al., 1999). While traditional methods only predict the equilibrium scour depth, SRICOS uses site-specific measurements of critical shear stress and soil erosion rates to predict scour depth as a function of time. For soils that erode slowly, scouring may take a long time to achieve equilibrium condition and the final scour depth produced by a single flood or a series of floods could be considerably less than the equilibrium scour depth.

The SRICOS method has been evaluated for pier and contraction scour by comparing the predicted and measured scour depths at eight bridge sites in Texas (Briaud et al., 2001b), two sites in Alabama (Curry et al., 2003), five sites in Maryland (Ghelardi, 2004), 15 sites in Illinois (Straub and Over, 2010), and four sites in South Dakota (Ting et al., 2010, 2017). These studies showed that the amount of scour predicted by the SRICOS method is consistent with the observed scour and is always less than the predicted equilibrium scour depth in sand.

The SRICOS method is included in the current edition of Hydraulic Engineering Circular No. 18 (HEC-18; Arneson et al., 2012) as an alternative approach for predicting bridge scour in cohesive soils. In order to apply the SRICOS method, a hydrograph is required. For new bridges, this means generating a synthetic hydrograph with daily or sub-daily flow values or assumes that a recorded hydrograph will repeat itself. HEC-18 provides no guidance on how to generate a hydrograph for using the SRICOS method. It is unclear what level of detail (e.g., a continuous hydrograph for multiple years with an annual flooding cycle, a series of design floods) is required in the temporal record of flows to predict the final scour depth in cohesive soils with confidence. It is also unclear how to apply the SRICOS method to small watersheds and ungauged streams where flow records may be lacking. SDDOT needs guidelines to define the site conditions where the SRICOS method is more appropriate and cost effective than the traditional methods, and to select a hydrograph generation method for using the SRICOS method.

3.   RESEARCH OBJECTIVES AND APPROACHES

3.1   Determine the Relationship Between Flood Hydrograph, Soil Erodibility, and Scour History in Cohesive Soils

The central hypothesis in this study is that even for highly erosion-resistant cohesive soils, a small number of design floods can produce the same amount of scour as a long sequence of large and small floods. This is because most of the floods in a continuous hydrograph would not achieve their equilibrium scour depths due to pre-existing scour. Three bridge sites in South Dakota with streamflow records ranging from 50 to 67 years were selected to compute the histories of pier or contraction scour using the SRICOS method. To cover a wide range of critical shear stress and soil erosion rate values representative of cohesive and non-cohesive soils, scour histories were computed using the erosion-rate-versus-shear-stress curves of different geo-materials in the soil erosion chart proposed by Briaud et al. (2011), in addition to measured soil erosion functions where they are available. The final scour depth computed using the complete hydrograph was compared with the cumulative scour depth produced by the maximum annual floods to show that a continuous hydrograph spanning several decades may be replaced by an annual maximum series for the purpose of scour prediction. The computed scour histories of the maximum annual floods were used to determine the equivalent time required for the peak discharge of each flood to produce the same scour depth as the one created by the recorded hydrograph. A multiple regression was performed on the results to obtain an empirical relationship for the equivalent time as a function of the duration of the hydrograph and the peak discharge for floods of different return periods.

3.2   Develop a Screening Tool for Adopting the SRICOS Method at a Bridge Site

Based on the results of scour history analysis described in Section 3.1, a step-by-step procedure was developed to identify bridge sites where use of the SRICOS method would be beneficial. The screening process is divided into three different levels of increasing complexity. In the Level I analysis, the results of soil classification and/or EFA testing are used with simple calculations to eliminate bridge sites where use of the SRICOS method is not recommended. In the Level II analysis, recorded hydrographs are used with the SRICOS method to predict the final scour depths produced by floods of different return periods. The results are normalized and plotted on a $\frac{z_f}{z_{max}}$ versus $\frac{t_e}{t_{90}}$ graph where z_f is computed final scour depth, z_{max} is equilibrium scour depth, t_e is equivalent time, and t_{90} is the time to reach 90% of equilibrium scour depth to assess the scour potential of the recorded floods in different soil types. In the Level III analysis, many future hydrographs are generated using the hydrograph method described in Section 3.3 and used with the SRICOS method to determine the risk values associated with different predicted scour depths and project lives.

3.3 Develop Hydrograph Generation Method for Using the SRICOS Method

The basic framework for hydrograph generation used in this study is a series of maximum annual floods (an annual maximum series). The advantage in working with maximum annual floods is that the peak discharge in one year can be assumed to be independent from the peak discharge in another year. Therefore, a sequence of annual peak flows can be generated by sampling from a suitable distribution such as the Log Pearson Type III (LP-III) distribution, which is commonly used for flood frequency analysis in the United States. The parameters of the LP-III distributions were computed from the mean, standard deviation, and skew coefficient of the recorded peak discharges. Based on the method for accumulating scour depths resulting from multiple floods in the SRICOS method, an annual maximum series can be represented by a sequence of equivalent rectangular floods. Each flood has a constant discharge given by the annual peak flow and an equivalent duration obtained using the regression equations described in Section 3.1. The rectangular hydrograph would produce the same final scour depth as the recorded hydrograph of a flood with the same return period. A stochastic approach is used to generate many annual maximum series to compute the distribution of final scour depth using the SRICOS method.

4.   TASK DESCRIPTION

4.1   Review Project Scope and Work Plan

The principal investigator met with the technical panel on April 20, 2017, at the SDDOT office in Pierre for an organizational meeting. The SD13 bridge over the Big Sioux River near Flandreau and SD37 bridges over the James River near Mitchell were selected to study pier and contraction scour, respectively, by using the SRICOS method. The mechanism for conducting the national survey was discussed, and arrangements were made with Ryan Thompson of the United States Geological Survey (USGS) to obtain streamflow records and results of flood frequency analysis for the project sites.

4.2   Literature Review

The equations and methods used to predict the time history of pier and contraction scour in cohesive soils are reviewed. Also reviewed are the different soil erosion rate relationships published in the literature. The soil erosion rate chart proposed by Briaud et al. (2011) is compared with the results of erosion function apparatus (EFA) testing conducted on field and laboratory soil samples found in the literature. It is concluded that the soil erosion rate chart proposed by Briaud et al. (2011) may be used for preliminary analysis to determine if time rate of scour is an important factor. However, EFA testing should be conducted on soil samples collected from the bridge site to determine the critical shear stress and erosion-rate-versus-shear-stress curve for detailed scour analysis.

The concept of equivalent time is introduced, and the method used to analyze computed scour histories is described. The functional relationship between equivalent time and peak discharge and flood duration is derived by dimensional analysis to provide the theoretical basis for performing regression analysis on the computed equivalent times. A stochastic method for generating future hydrographs is presented. The method assumes that a continuous hydrograph may be replaced by a series of maximum annual floods (an annual maximum series) for the purpose of scour prediction. Individual floods in the annual maximum series are represented by a rectangular hydrograph with a constant discharge that follows the Log Pearson Type III distribution and an equivalent time that is a function of the peak discharge and flood duration. The equivalent flood will produce the same final scour depth as the actual hydrograph. Monte Carlo simulations are preformed to generate many equally probable annual maximum series to predict the distribution of final scour depth and compute the exceedance probability of a given scour depth using the SRICOS method. The literature review and theoretical background of the study are presented in Chapter 5.

4.3   Conduct National Survey

A questionnaire on bridge scour in cohesive soils and hydrograph generation was prepared by the researchers and submitted to the technical panel for review and approval. After revision, the survey was conducted through the AASHTO Research Advisory Council (RAC). The online survey was conducted in summer 2018. The questionnaire for the survey is presented together with a discussion of the survey results in Chapter 9. A summary of the survey results is included in Appendix I.

4.4   Select Bridge Sites

The SD13 bridge over the Big Sioux River near Flandreau and the Interstate 90 Bridges over Split Rock Creek near Brandon were selected to study pier scour using the SRICOS method. Contraction scour was studied using the SD37 bridges over the James River near Mitchell. Recorded hydrographs from streamflow gauging stations near the bridge sites were used with measured erosion functions

(where available) and the soil erosion chart proposed by Briaud et al. (2011) to compute scour histories. The results of analysis for the SD13 bridge, SD37 bridges, and Interstate 90 bridges are presented in Chapters 6, 7, and 8, respectively.

4.5   Conduct Scour History Analysis

Computed scour histories at the three bridge sites were analyzed to determine if a continuous hydrograph can be replaced by a sequence of maximum annual floods for the purpose of scour prediction. Scour histories were computed using the soil erosion chart proposed by Briaud et al. (2011) in addition to measured soil erosion functions where they are available. The cumulative scour depth predicted using the entire flow record was compared with the cumulative scour depth predicted using the maximum annual floods. The results show that omitting the smaller floods has negligible effects on the predicted final scour depth. Therefore, an annual maximum series may be used to predict the accumulated scour depth over the lifetime of a bridge. It is found that the predicted final scour depths are significantly less than the equilibrium scour depths only for region IV (low erodibility) of the soil erosion rate chart.

To compute the scour-depth-versus-time curve for an annual maximum series, both the magnitude and duration of the maximum annual floods need to be specified. The distribution of peak discharge is assumed to follow the Log Pearson Type III distribution, but methods for computing flood durations for peak flows of different return periods have not been developed. Using the computed scour histories of the recorded maximum annual floods, the equivalent time for the peak discharge to produce the same final scour depth as the one created by the actual hydrograph was determined for each flood. The computed equivalent times were correlated to the recorded peak discharges and flood durations to develop regression equations for predicting the equivalent time. The results of scour history analysis are presented in Sections 6.2, 7.2, and 8.3, respectively, for the three bridge sites. Regression equations for the equivalent time are presented in Sections 6.3, 7.4, and 8.4.

4.6   Prepare Technical Memorandum I

The first technical memorandum was submitted in December 2017 and an oral presentation was given to the technical panel by the principal investigator at a project meeting in Pierre on January 25, 2018. In the meeting, the Interstate 90 bridges over Split Rock Creek near Brandon were approved to be the third study site.

4.7   Develop Decision Tool for Using the SRICOS Method

Based on the results of scour history analysis performed in Section 4.5, a step-by-step procedure was developed to identify bridge sites where use of the SRICOS method may be beneficial. The screening process is divided into three different levels of increasing complexity. In the Level I analysis, the results of soil classification and/or EFA testing are used with simple calculations to eliminate bridge sites where use of the SRICOS method is not recommended. In the Level II analysis, recorded hydrographs are used with the SRICOS method to predict the final scour depths produced by floods of different return periods. The results are normalized and plotted on a $\frac{z_f}{z_{max}}$ versus $\frac{t_e}{t_{90}}$ graph to assess the rates of scour produced by the recorded floods in different soil types. In the Level III analysis, future hydrographs are generated based on the Log Pearson Type III distribution and scour histories are computed using the SRICOS method to determine the risk values associated with different predicted scour depths and project lives. The screening process and different levels of scour assessment are described in Chapter 10.

4.8 Develop Hydrograph Generation Method for Using the SRICOS Method

The Log Pearson Type III distribution was employed with Monte Carlo simulation to construct future hydrographs at the three bridge sites. The constructed annual maximum series were used with the SRICOS method and the soil erosion chart proposed by Briaud (2011) to predict the distribution of final scour depth for different project lives and their risk values (exceedance probabilities). The results were used to evaluate several simplified methods for predicting pier and contraction scour in cohesive soils. Generation of future hydrographs and scour risk analysis are presented in Sections 6.4, 7.5, and 8.5, respectively, for the three bridge sites. Comparison with other scour prediction methods in cohesive soils is presented in Sections 6.5, 7.6, and 8.6.

The QPPQ method was employed to extend the streamflow record at the Split Rock Creek site by using the Skunk Creek at Sioux Falls gauging station as an index station. Daily-to-hourly streamflow disaggregation was performed for the maximum annual floods using the method described in Straub and Over (2010) for comparison with the recorded peak flows. The Split Rock Creek at Corson station operated as a crest-stage partial-record gauging station from 1990 to 2001. This site provides an excellent example of how the SRICOS method may be applied to streams that do not have complete flow records. The QPPQ method and daily-to-hourly streamflow disaggregation are described with the results of the streamflow analysis in Section 8.2. A method for computing the scour histories for ungauged streams using the NRCS unit triangular hydrograph and the SRICOS method is presented in Section 13.5.

4.9 Prepare Technical Memorandum II

A second technical memorandum was submitted to SDDOT on October 1, 2018, and an oral presentation was given to the technical panel by the principal investigator at a project meeting in Pierre on December 6, 2018.

4.10 Develop Worked Examples

Three worked examples are presented in Chapters 11, 12, and 13 on pier scour, contraction scour, and ungauged streams, respectively, using the three bridge sites studied in this project. The worked examples use hand calculations to demonstrate step-by-step the procedures for screening a bridge site for using the SRICOS method, conducting scour history analysis for pier and contraction scour, and generating future hydrographs for scour risk analysis. MATLAB scripts developed in this project are described in the worked examples and included as supplementary files to the final report.

4.11 Prepare Technical Memorandum III

A third technical memorandum was submitted to SDDOT on May 15, 2019. An oral presentation was given to the technical panel by the principal investigator at a project meeting in Pierre on July 16, 2019.

4.12 Prepare Final Report

A final report was submitted to SDDOT on October 23, 2019. In addition to the results and findings presented in the three technical memoranda, the final report contains the executive summary, conclusions, recommendations, and implementation plan for the project.

4.13 Make Executive Presentation

An executive presentation of the project findings, conclusions, and recommendations was made by principal investigator to the SDDOT Research Review Board in Pierre on February 13, 2020.

5. BACKGROUND

This chapter provides a summary of the concepts behind the SRICOS method and the equations for scour history analysis and hydrograph generation used in this study. The chapter is organized as follows. The erosion rate relationships for different geo-materials are reviewed in Section 5.1. The SRICOS method for pier scour is summarized in Section 5.2. The SRICOS method for accumulating scour depth for a sequence of flow discharges is described in Section 5.3. The SRICOS method for contraction scour is summarized in Section 5.4, and an alternative method based on the energy equation is presented in Section 5.5. The concept of equivalent time is introduced in Section 5.6. The approach for replacing a continuous hydrograph by a sequence of equivalent floods for scour calculation is described in Section 5.7. The functional relationship between equivalent time and the flow and soil parameters is derived using dimensional analysis in Section 5.8. A stochastic approach for generating future hydrographs and computing scour risk is presented in Section 5.9. Bridge scour assessment procedures employing the SRICOS method are reviewed in Section 5.10.

5.1 Soil Erodibility

Soil erodibility refers to the sensitivity of the soil to erosion by water velocity and hydraulic shear stress and is an important index in assessing the time development of scour. Briaud et al. (2001a) developed the erosion function apparatus (EFA) to measure soil erosion rate as a function of the applied fluid shear stress using thin-walled tube (Shelby tube) samples. The apparatus consists of a rectangular water tunnel, 101.6 mm wide, 50.8 mm high, and 1.25 m long mounted on top of a hydraulic bench (Figure 5.1a). A pump draws water from a tank underneath the bench. The flow rate is regulated using a hand valve and measured by a flow meter. The range of flow velocity that can be achieved is between 0.1 and 6.0 m/s. A thin-walled tube is mounted perpendicular to the flow such that the open end of the tube is flush with the floor of the water tunnel. An electric motor and piston assembly (Figure 5.1b) is used to push the soil out of the thin-walled tube 1 mm into the flow. The amount of time it takes to erode the 1 mm protrusion is measured to determine the soil erosion rate. The fluid shear stress τ is calculated as $\frac{1}{8}\rho f V^2$ where f is friction factor, ρ is fluid density, and V is flow velocity (discharge/cross-sectional area). The friction factor is a function of the pipe Reynolds number Re_p and relative roughness $\frac{\epsilon}{D}$ and is determined using the Moody chart or Colebrook equation (Munson et al., 2013). For a rectangular cross section, the equivalent pipe diameter D is $\frac{4A}{P}$, where A is cross-sectional area and P is wetted perimeter. The Reynolds number is calculated as $\frac{VD}{\nu}$ where ν is kinematic viscosity of water. The roughness height ϵ is assumed to be $\frac{D_{50}}{2}$, where D_{50} is median grain diameter of the soil. Alternatively, the operator may assess the surface texture of the soil sample and estimate the bed roughness. When 1 mm of soil is eroded or after one hour of flow, whichever comes first, the flow velocity is increased, and the soil sample is again pushed 1 mm into the flow. This process is repeated several times with different flow velocities to establish a curve of erosion rate versus shear stress.

Figure 5.2 shows the measured erosion-rate-versus-shear-stress curve for very silty fine sand collected from the SD13 bridge over the Big Sioux River. The weakness of the test procedure is immediately evident from this figure. Two different roughness heights ($\varepsilon = 0$ and 1 mm) were used to calculate the fluid shear stress. The corresponding critical shear stresses are 7.2 and 18.6 N/m². The EFA curve for $\epsilon = 1$ mm produces a predicted pier scour depth comparable to the observed value; whereas, that for

$\epsilon = 0$ yields a predicted scour depth equal to about twice the observed value (Larsen et al., 2011). Therefore, it is extremely important that the bed shear stress is determined accurately in the EFA test.
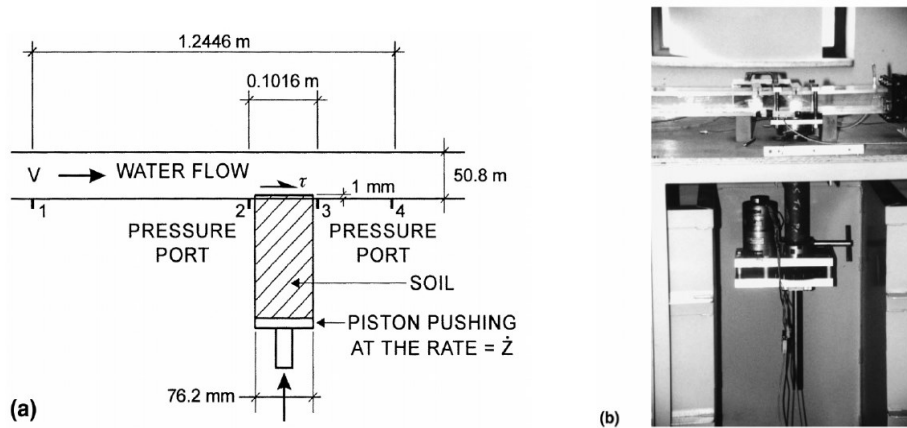
Figure 5.1 Conceptual diagram and photograph of erosion function apparatus *(from Briaud et al., 2001a)*
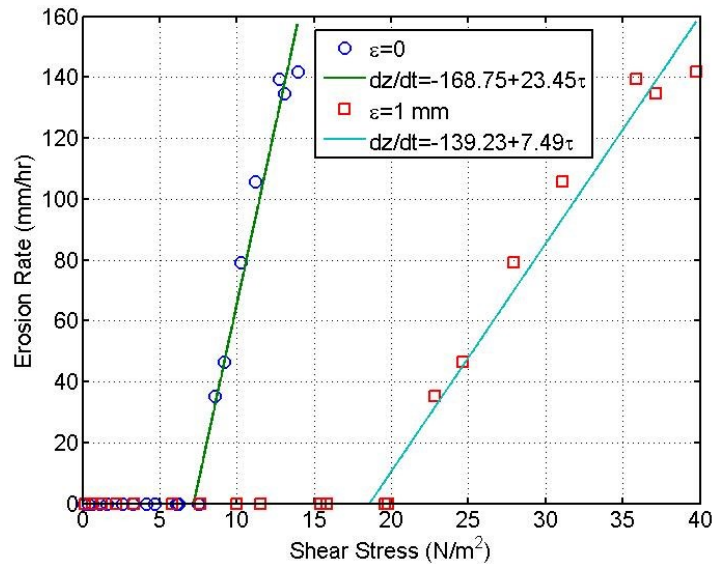
Figure 5.2 Measured curves of erosion rate versus shear stress for very silty fine sand from SD13 bridge over the Big Sioux River *(from Larsen et al., 2011)*

The relationship between soil erodibility and soil properties is very complicated, and direct measurements using soil samples collected from the bridge site are still the most reliable methods for determining the soil critical shear stress and erosion rates. Based on the results of EFA testing conducted on a wide range of geo-materials, Briaud et al. (2011) proposed erosion rate relationships for different categories of soils and rocks (Figure 5.3). These relationships can be expressed by the following equation:

$$\text{Log}\,\dot{z} = a' \log \tau + b' \tag{5.1}$$

13

where $\dot{z}$ is soil erosion rate, τ is bed shear stress, and a' and b' are constants. Defining the critical shear stress τ_c as the bed shear stress corresponding to an erosion rate of 0.1 mm/h, Eq. (5.1) can be re-written as:

$$\dot{z}(\text{mm/h}) = 0.1 \left(\frac{\tau}{\tau_c}\right)^{a'} \tag{5.2}$$

Table 5.1 gives values of τ_c and a' for the erosion-rate-versus-shear stress curves represented by the solid lines separating the different geo-materials in Figure 5.3.
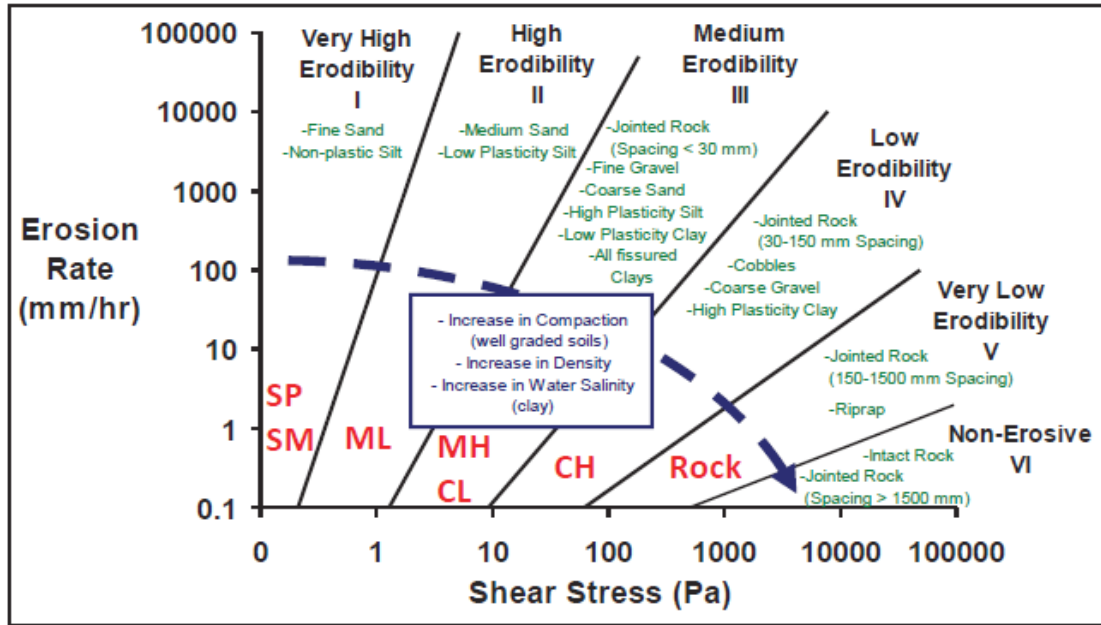
Figure 5.3 Generalized relationships for erosion rate in different geo-materials
(from Briaud et al., 2011)

Table 5.1 Values of τ_c and a' representing different geo-material boundaries in Fig. 5.3

Regions	I and II	II and III	III and IV
τ_c (Pa)	0.21	1.33	9.5
a'	4.02	2.53	1.62

The erosion categories proposed by Briaud et al. (2011) were compared with the test results obtained by others. The published datasets include 13 soil samples from five bridge sites in Maryland (Brubaker et al., 2004), 22 samples from 15 sites in Illinois (Straub and Over, 2010), 70 samples from 15 sites in Kansas (Tucker-Kulesza and Karim, 2017), and 17 samples prepared by the Hydraulics Research Laboratory at the Turner Fairbank Highway Research Center (Shan et al., 2015). Measured soil erosion rates and applied fluid shear stresses are grouped by the United Soil Classification System (USCS) soil types and plotted in Figures 5.4 to 5.7 for each dataset. Referring to Figure 5.3, gravelly sands (SP) and silty sands (SM) are found in region I (very high erodibility); low plasticity silts (ML) in region II (high erodibility); high plasticity silts (MH) and low plasticity clays (CL) in region III (medium erodibility); and high plasticity clays (CH) in region IV (low erodibility).

The samples from Maryland were classified as sands, low plasticity silts, and low plasticity clays. The EFA test results (Figure 5.4) fall in region I (very high erodibility) for sands, and on the borderline between region II (high erodibility) and region III (medium erodibility) for low plasticity silts and clays. The samples from Illinois were classified as high plasticity silts and low plasticity clays. The EFA test results (Figure 5.5) generally fall in region III, consistent with soils of medium erodibility. The samples from Kansas include a wide range of soil types (Figure 5.6). Clayey sands (SC) and gravelly sands (SW) were found to have high erodibility (region II). Low plasticity clays (CL) were found to be in region III and on the borderline between region III and region IV. Discrepancies were found in the EFA test results for high plasticity clays (CH), which should be in region IV (low erodibility) but instead are in region III (medium erodibility). The prepared soils (Figure 5.7) were classified as low plasticity silts and clays (ML and CL). These soil specimens were found to have medium to high erodibility. Overall, the EFA results from the different studies are consistent with the erosion rate chart proposed by Briaud et al. (2011).
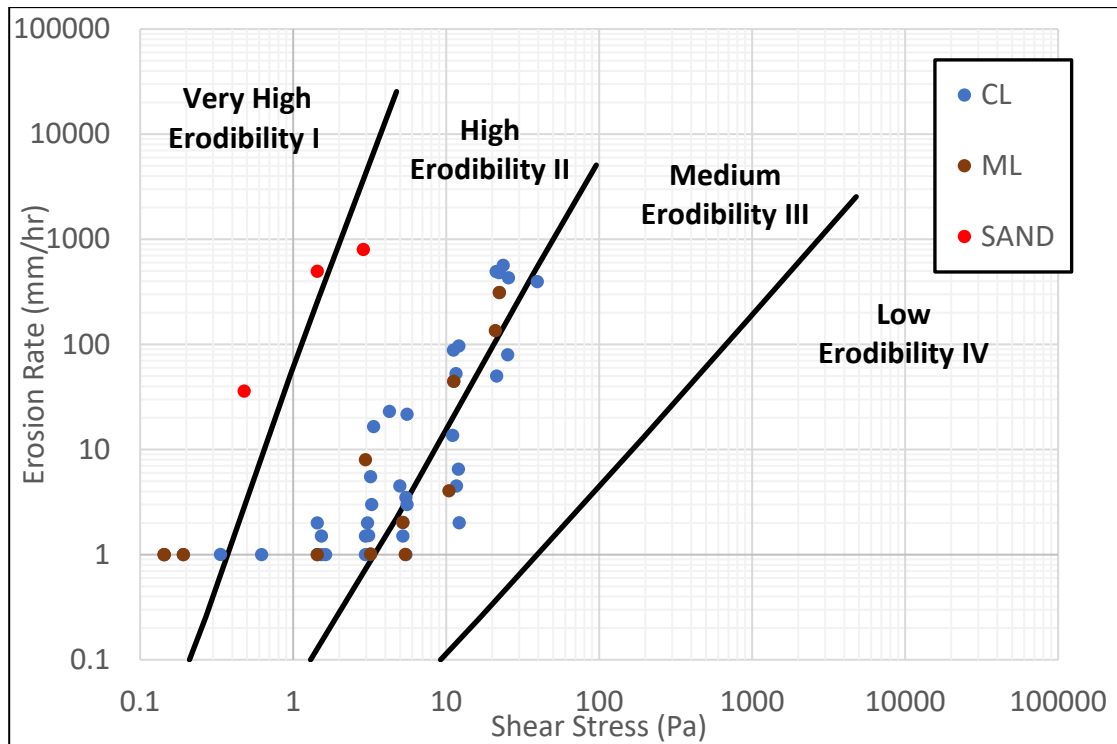
Figure 5.4 Measured data of erosion rate versus shear stress for soil samples from Maryland
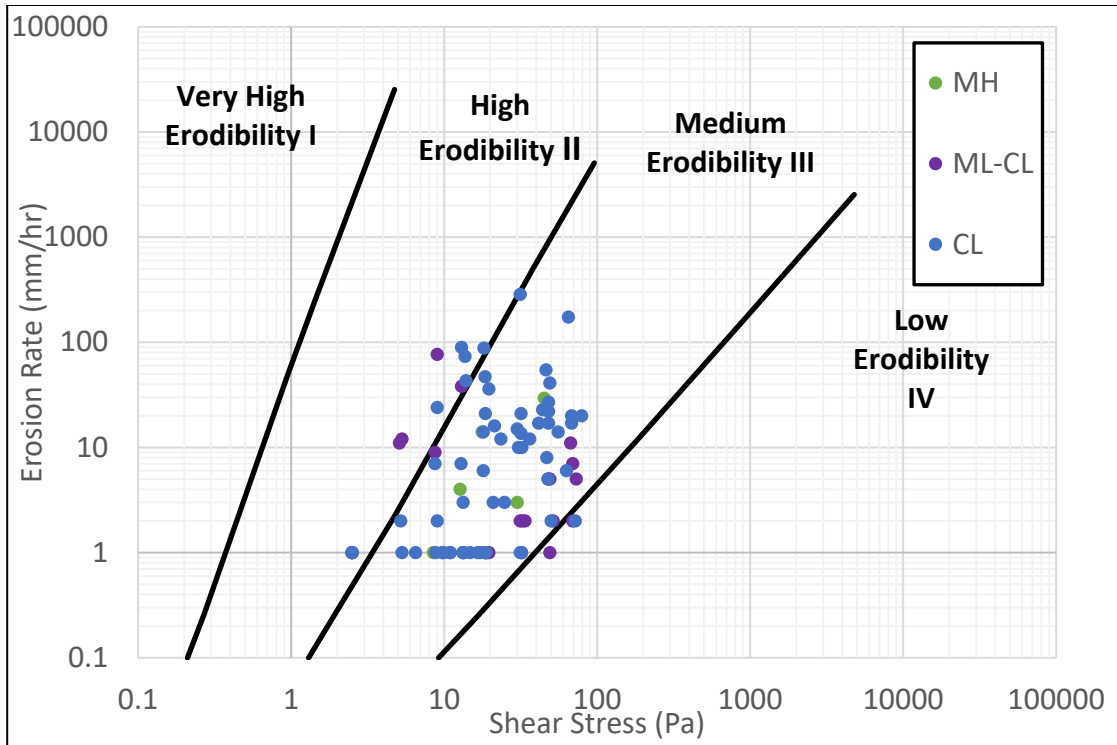
Figure 5.5 Measured data of erosion rate versus shear stress for soil samples from Illinois
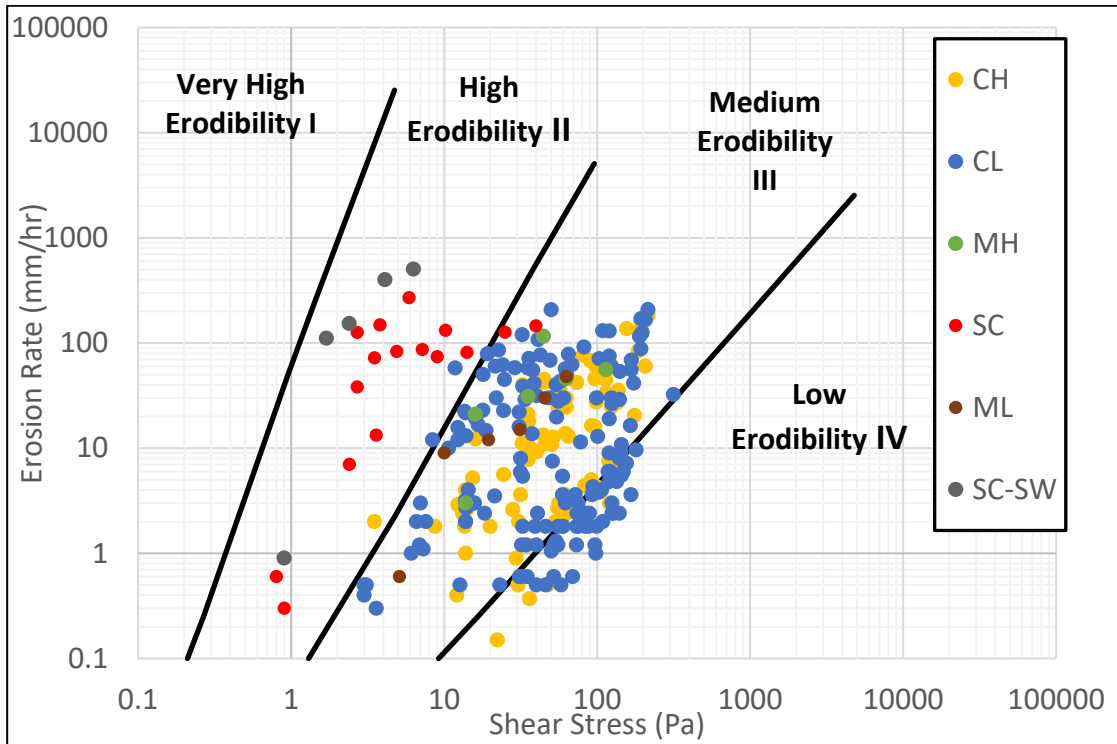
Figure 5.6 Measured data of erosion rate versus shear stress for soil samples from Kansas
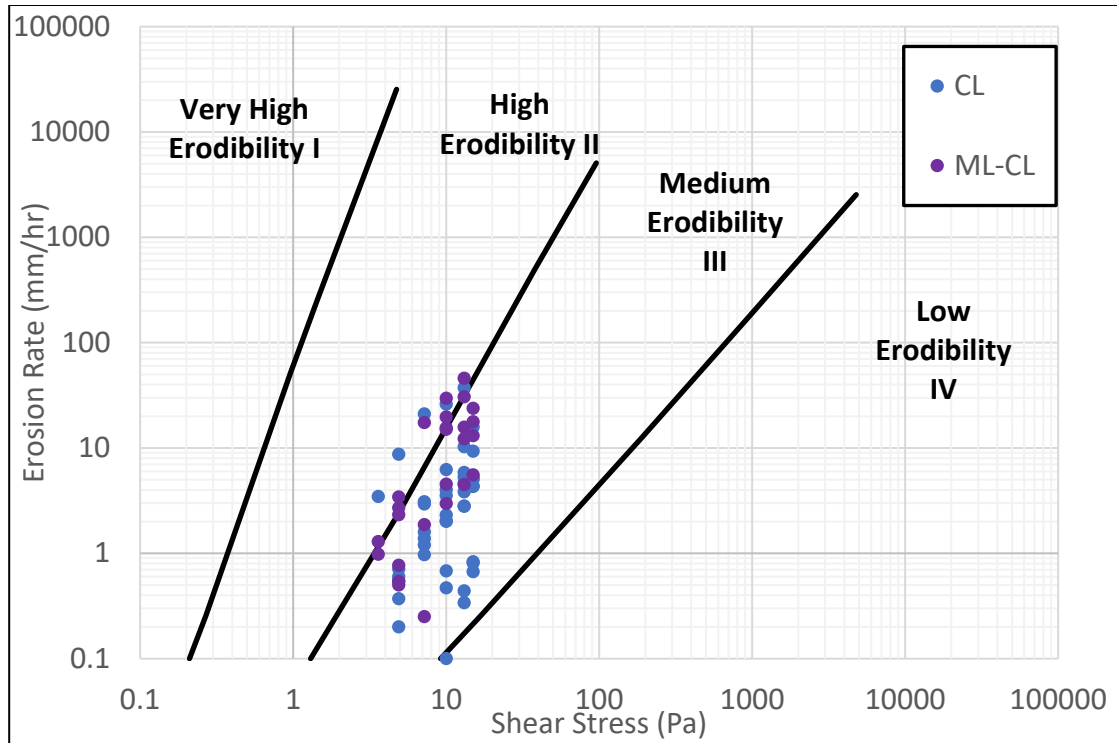
Figure 5.7 Measured data of erosion rate versus shear stress for prepared soil specimens

The erodibility of cohesive soils is dependent on many factors. Briaud et al. (2001a) found poor correlations between the critical shear stress or initial slope of the measured erosion-rate-versus-shear-stress curve and the common soil properties. They concluded that a simple regression equation for τ_c or the initial slope is unlikely to exist because many parameters are involved. In a more recent study, Straub and Over (2010) investigated the relationship between soil erosion rate and excess shear stress (bed shear stress minus critical shear stress) given by the following equation:

$$\dot{z} = a'(\tau - \tau_c)^{b'} \tag{5.3}$$

which gives a straight line on a plot of $\log \dot{z}$ versus $\log(\tau - \tau_c)$. Eq. (5.3) is fitted to the EFA test results of 22 soil samples collected from 15 sites in Illinois to determine the values of the coefficient a' and exponent b'. They found a linear relationship between τ_c and the natural logarithm of the unconfined compressive strength Q_u. The best-fit line is given by:

$$\tau_c = 5.098 \ln Q_u + 10.01 \tag{5.4}$$

where τ_c is in Pascals and Q_u in tons/ft². Eq. (5.4) has a coefficient of determination (R^2) of 0.95. The best-fit equation ($R^2 = 0.61$) for the exponent b' is given by:

$$b' = 1.089 Q_u^{-0.353} \tag{5.5}$$

For the coefficient a', no equation using any of the soil parameters was found to give a R^2 value greater than 0.3. The median value of a' is 0.276.

Shan et al. (2015) developed an ex-situ erosion testing device (ESTD) to measure soil erodibility. As in the EFA, the ESTD measures soil erosion rates by pushing a soil sample out of a thin-walled tube into a water tunnel as fast as the soil can be eroded. Unlike the close conduit flow in the EFA, the ESTD employs a moving belt and a pump to generate a log-law velocity profile to simulate an open-

channel flow (Figure 5.8). The bed shear stress is directly measured using a direct force gage, thus eliminating the need to estimate the roughness height ϵ using the Moody chart, which is one of the biggest sources of uncertainty in the EFA test. In addition, the soil sample is automatically elevated to maintain a constant bed shear stress throughout the test period to determine the erosion rate. Shan et al. (2015) found that the difference between the bed shear stress measured by the direct force gage and estimated using the Moody chart is around 20%.
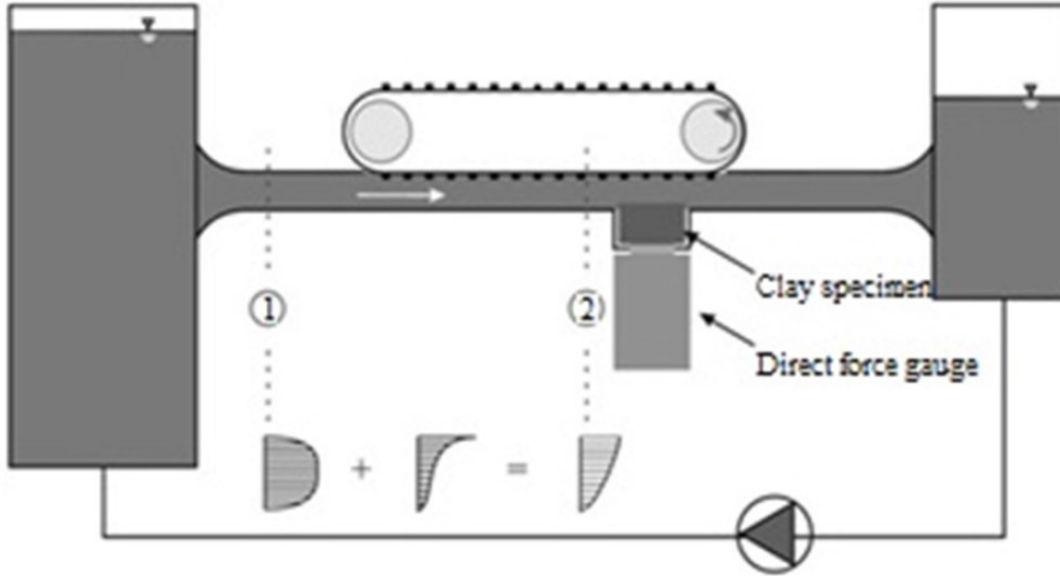
Figure 5.8 Conceptual diagram of the ESTD *(from Shan et al., 2015)*

Shan et al. (2015) prepared cohesive soil specimens with different percentages of Red Art clay, silt, and non-uniform sand with a range of water contents to create 17 unique soil specimens for testing using the ESTD. They found a weaker correlation between the measured critical shear stress and unconfined compressive strength. They developed the following empirical relationships for τ_c and a':

$$\tau_c = 0.07 \left(\frac{W}{F}\right)^{-2.0} PI^{1.3} Q_u^{0.4} \tag{5.6}$$

$$a' = (Q_u)^{-1.0} PI^{-1.1} \tag{5.7}$$

where W is water content, F is percent of particles finer than 0.075 mm, PI is plasticity index, and Q_u is unconfined compressive strength of the soil. The units of τ_c and Q_u are Pascal and lbf/ft^2. The R^2 values for Eqs. (5.6) and (5.7) are 0.73 and 0.35, respectively. Shan et al. (2015) found that when compared with the EFA test results from Texas (Briaud et al., 2011) and Illinois (Straub and Over, 2010), Eq. (5.6) under-predicts the Illinois data but significantly over-predicts the Texas data. They also found that a constant value of 1.8 for b' provides the best fit to their erosion rate data. The resulting best-fit model ($R^2 = 0.61$) for the erosion function is given by:

$$\dot{z} = a'(\tau - \tau_c)^{1.8} \tag{5.8}$$

with τ_c and a' given by Eqs. (5.6) and (5.7), respectively. Equation (5.8) was found to over-predict the erosion rate of the Illinois data.

In summary, direct measurement of critical shear stress and soil erosion rates is recommended for detailed design; the relationship between soil erodibility and soil properties is extremely complicated and still poorly understood. Figure 5.3 is the most detailed information currently available for different geo-materials. However, this chart should only be used for preliminary analysis. If the results show that the time rate of scour is an important factor, the erosion-rate-versus-shear-stress curve should be determined by conducting EFA testing on soil samples collected from the bridge site.

5.2 Pier Scour

The HEC-18 pier scour equation is recommended in the Federal Highway Administration (FHWA) document entitled "Evaluating Scour at Bridges," Hydraulic Engineering Circular No. 18, or HEC-18 (Arneson et al., 2012) for predicting the maximum scour depth in cohesionless soils:

$$\frac{z_{max}}{a} = 2.0K_1K_2K_3\left(\frac{y_1}{a}\right)^{0.35}\left(\frac{V_1}{\sqrt{gy_1}}\right)^{0.43} \tag{5.9}$$

where z_{max} is equilibrium scour depth, a is pier width, y_1 is approach flow depth, V_1 is approach flow velocity, g is acceleration of gravity; and K_1, K_2, and K_3 are correction factors for pier nose shape, flow angle of attack, and bed condition. The dimensionless parameter $\frac{V_1}{\sqrt{gy_1}}$ is called the Froude number (Fr_1). Eq. (5.9) was developed from flume tests in sands. This equation shows that equilibrium scour depth is proportional to flow velocity to the power of 0.43 and flow depth to the power of 0.135. Therefore, the equilibrium scour depth is sensitive to flow velocity but relatively insensitive to flow depth.

Several empirical equations for predicting the equilibrium scour depth in clay and clay-sand mixtures have been proposed by researchers (e.g., Molinas and Honsy, 1999; Briaud et al., 1999; Debnath and Chaudhuri, 2010; Kothayri et al., 2014). Each of these equations may be valid only for the conditions under which it was derived. The scour equation in Briaud et al. (1999) is given by:

$$z_{max} \text{ (mm)} = 0.18Re^{0.635} \tag{5.10}$$

where $Re = \frac{V_1a}{\nu}$ is pier Reynolds number, a is pier diameter, and ν is kinematic viscosity of water. Equation (5.10) was developed from 43 flume tests on circular piers, of which 30 were conducted in Porcelain clay, four in Armstone clay, two in Bentonite clay, and seven in sand. The pier Reynolds number ranges from 5,100 to 84,840; the Froude number ranges from 0.12 to 0.42; and the flow-depth-to-pier-diameter ratio ranges from 1.43 to 16 (Ting et al., 2001).

Briaud et al. (2004) introduced correction factors for Eq. (5.10) to account for shallow water, pier spacing, pier shape, and flow angle of attack effects. The flume tests used to develop the correction factors were conducted in Porcelain clay. The revised equation is given by:

$$z_{max}(\text{mm}) = 0.18k_wk_{sp}k_{sh}k_\alpha Re^{0.635} \tag{5.11}$$

The correction factor for shallow water effect, k_w, is given by

$$k_w = 0.85\left(\frac{y_1}{a}\right)^{0.34} \qquad \frac{y_1}{a} < 1.62$$

$$= 1 \qquad \frac{y_1}{a} > 1.62 \tag{5.12}$$

A correction factor, k_{sp}, was introduced to account for pier spacing effect. However, most bridge sites have pier-spacing-to-pier-width ratio much greater than unity. Therefore, pier spacing effects would be small in most cases.

The same correction factor for pier shape in the HEC-18 equation was recommended for cohesive soils (i.e., $k_{sh} = K_1$). Similarly, the K_2 factor in the HEC-18 equation was adopted for the flow angle of attack effect in cohesive soils, i.e.,

$$k_\alpha = \left(\cos \alpha + \frac{L}{a} \sin \alpha\right)^{0.65}$$ (5.13)

where α is the angle between the approach flow direction and long axis of the pier (= 0 for circular pier) and L is length of pier.

The value of z_{max} in Eq. (5.11) is greater than zero except when $V_1 = 0$. In addition, the Reynolds number is not considered to be an important parameter at field scale. Oh (2009) re-analyzed the flume test results conducted at Texas A& M University (TAMU) and proposed the following revised equation for the maximum pier scour depth:

$$\frac{z_{max}}{a} = 2.2 K_1 K_2 \left(2.6 \frac{V_1}{\sqrt{ga}} - \frac{V_c}{\sqrt{ga}}\right)^{0.7}$$ (5.14)

In Eq. (5.14), V_c is the critical velocity for initiation of sediment erosion, which is related to the critical shear stress τ_c through the Manning's equation (Akan, 2006):

$$V_c(\text{m/s}) = \sqrt{\frac{\tau_c y_1^{\frac{1}{3}}}{\rho g n^2}}$$ (5.15)

where n is Manning's coefficient. Using the Shields relationship, the critical velocity for non-cohesive soils may be found as $K_u y_1^{\frac{1}{6}} D_{50}^{\frac{1}{3}}$, where $K_u = 6.19$ (SI units) or 11.17 (English units) and D_{50} is median sediment diameter (Arneson et al., 2012). Equation (5.14) is included in HEC-18 for calculating the equilibrium scour depth in cohesive soils.

The parameter $\frac{V_1}{\sqrt{ga}}$ is known as the pier Froude number and represents the square root of the stagnation pressure head at the leading edge of the pier normalized by the pier width. This parameter is useful for describing the flow gradients around the pier (Ettema et al., 1998). Dividing Eq. (5.14) by Eq. (5.9) and take $K_3 = 1.1$ for clear-water scour, the ratio of equilibrium scour depths from the two equations is given by:

$$\text{Scour Depth Ratio} = \left(2.6 - \frac{V_c}{V_1}\right)^{0.7} \left(\frac{V_1}{\sqrt{gy_1}}\right)^{0.27}$$ (5.16)

Since the condition $\frac{V_1}{V_c} \geq 1$ will almost certainly be met during large floods, the scour depth ratio in Eq. (5.16) would be greater than 1.0 for Froude number as low as 0.3. Therefore, Eq. (5.14) would generally predict a larger maximum or equilibrium scour depth than Eq. (5.9) for the large floods. Ting et al. (2001) found that the measured equilibrium scour depths in clay and sand are similar, while pier scour studies with clay-sand mixtures have found that the equilibrium scour depth generally decreases with increase in clay content. Harris and Whitehouse (2017) further showed that the measured equilibrium scour depths given in Ting et al. (2001) encompass other published datasets. Hence, there is no evidence that the equilibrium scour depth can be greater in cohesive soils than in non-cohesive soils. However, a reduction factor is not recommended when calculating the equilibrium

scour depth in cohesive soils until more data are available. The HEC-18 equation has been used to predict the value of z_{max} in this report. Therefore, any reductions in the predicted scour depths are attributed to the time effect of scour only.

Numerical simulations were used to develop empirical equations for calculating the maximum initial bed shear stress around a complex pier (Briaud et al., 2004):

$$\tau_{max} = k_w k_{sp} k_{sh} k_\alpha \times 0.094 \rho V_1^2 \left[\frac{1}{\log\left(\frac{aV_1}{\nu}\right)} - \frac{1}{10} \right] \tag{5.17}$$

$$k_w = 1 + 16e^{\frac{-4y_1}{a}} \tag{5.18}$$

$$k_{sp} = 1 + 5e^{\frac{-1.1S}{a}} \tag{5.19}$$

$$k_{sh} = 1.15 + 7e^{\frac{-4L}{a}} \tag{5.19}$$

$$= 1 \text{ for circular shape} \tag{5.20}$$

$$k_\alpha = 1 + 1.5 \left(\frac{\alpha}{90°}\right)^{0.57} \tag{5.21}$$

Eq. (5.17) is used with a soil erosion function such as Eq. (5.2) or Eq. (5.3) to calculate the initial rate of scour $\dot{z}$. The initial rate of scour and equilibrium scour depth are the two parameters that need to be determined to compute the scour-depth-versus-time curve for a given discharge.

5.3   Scour-Depth-Versus-Time Curve

In the SRICOS method, the scour-depth-versus-time (z-versus-t) curve is modeled by a hyperbolic equation:

$$z = \frac{t}{\frac{1}{\dot{z}} + \frac{t}{z_{max}}} \tag{5.22}$$

Eq. (5.22) shows that the scour history is defined by two parameters: the initial rate of scour $\dot{z}$ and the equilibrium scour depth z_{max}. The equilibrium scour depth can be calculated using the HEC-18 (Eq. 5.9) or TAMU (Eq. 5.14) equation, and the maximum bed shear stress around the pier before scour starts is calculated using Eq. (5.17) – Eq. (5.21). The initial rate of scour is then obtained from a measured erosion-rate-versus-shear-stress curve (Eq. 5.2 or Eq. 5.3) with the computed maximum bed shear stress around the pier.

To predict the cumulative scour produced by a hydrograph, the latter is represented by a sequence of constant discharges such as the hourly or daily mean flow (Figure 5.9). A hyperbolic function is generated for each time step in the hydrograph. The series of hyperbolic functions are fitted together to create a continuous scour-depth-versus-time curve (Briaud et al., 2001b). The scour depth at the end of the hydrograph is the predicted final scour depth. The basic equations involved in an unsteady flow analysis are illustrated using an example below.

In Figure 5.9, flood 1 has velocity V_1 and duration t_1, flood 2 has velocity V_2 and duration t_2, and flood 3 has velocity V_3 and duration t_3. Assume an initial scour depth of zero at $t = 0$, the scour depth at $t = t_1$ due to flood 1 is given by:

$$z_1 = \frac{t_1}{\frac{1}{\dot{z}_1} + \frac{t_1}{z_{max,1}}} \tag{5.23}$$

where subscript 1 denotes flood 1. The scour depth z_1 becomes the pre-existing scour depth for flood 2. Scour depth would increase from z_1 to z_2 during flood 2 because z_1 is smaller than the equilibrium scour depth for flood 2 (small flood followed by big flood). The scour depth at the end of flood 2 is given by:

$$z_2 = \frac{t^*+t_2}{\frac{1}{\dot{z}_2}+\frac{t^*+t_2}{z_{max,2}}} \tag{5.24}$$

where t^* is the equivalent time for flood 2 to produce a scour depth equal to z_1 from zero. The equivalent time t^* is determined by replacing t_1 with t_*, $\dot{z}_1$ with $\dot{z}_2$ and $z_{max,1}$ with $z_{max,2}$ in Eq. (5.23). Thus, we have

$$t^* = \frac{z_1}{\dot{z}_2\left(1-\frac{z_1}{z_{max,2}}\right)} \tag{5.25}$$

The scour depth z_2 then becomes the pre-existing scour depth for flood 3. Scour depth would increase from z_2 to z_3 during flood 3 if z_2 is less than $z_{max,3}$. This situation can occur even if V_3 is smaller than V_2 (large flood followed by small flood). If $z_2 > z_{max,3}$ the scour-depth-versus time curve would remain flat during flood 3 and z_3 would be equal to z_2. The equivalent time t^{**} and scour depth z_3 can be found using Eq. (5.24) and Eq. (5.25) by replacing $t^*, t_2, z_1, z_2, \dot{z}_2$, and $z_{max,2}$ with $t^{**}, t_3, z_2, z_3, \dot{z}_3$, and $z_{max,3}$, respectively. This procedure is repeated to compute the scour depths at all the time steps.
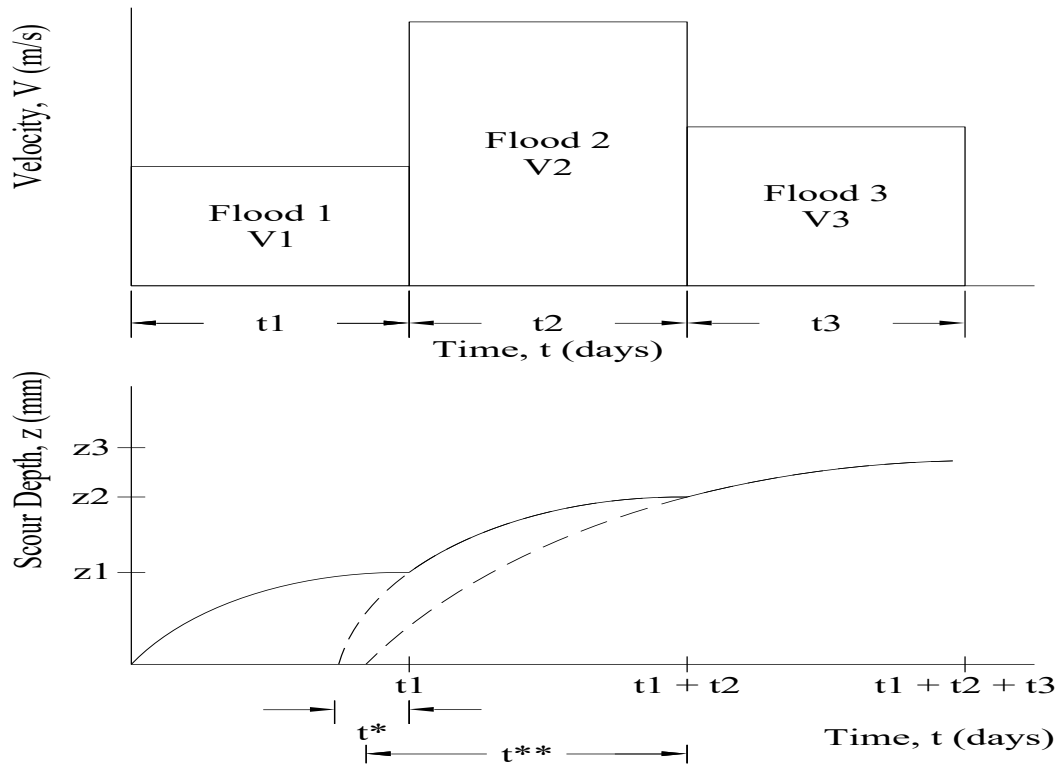
Figure 5.9 Method for accumulating scour depth from multiple floods (discharges) in the SRICOS method

5.4   Contraction Scour (TAMU Model)

Prediction of contraction scour depth is based on the same approach as pier scour. The equilibrium scour depth z_{max} is obtained using regression equations developed from flume tests in Porcelain clay, and the maximum initial bed shear stress τ_{max} in the contracted channel is obtained using regression equations developed from numerical simulations. Empirical equations were developed for both the maximum local contraction scour depth and maximum uniform contraction scour depth. The equation for the maximum uniform contraction scour depth z_{max} is written in SI units (Briaud et al., 2011):

$$\frac{z_{max}}{y_1} = 0.94 \left(\frac{1.83 V_2}{\sqrt{g y_1}} - \frac{\sqrt{\frac{\tau_c}{\rho}}}{g n y_1^{\frac{1}{3}}} \right) \tag{5.26}$$

where y_1 is main channel depth in the approach section, V_2 is average velocity in the contracted section, τ_c is critical shear stress of the bed material, ρ is density of water, g is acceleration of gravity, and n is Manning's coefficient.

The equation for calculating the initial (maximum) shear stress within the contracted length of a channel τ_{max} before scour starts is given by:

$$\tau_{max}(\text{N/m}^2) = k_R k_\theta k_L \rho g n^2 V_1^2 R_h^{-\frac{1}{3}} \tag{5.27}$$

where V_1 is upstream flow velocity, R_h is hydraulic radius of the uncontracted channel, and k_R, k_θ, k_L are correction factors for contraction ratio, contraction transition angle, and contraction length, respectively. These correction factors are given by:

$$k_R = 0.62 + 0.38 \left(\frac{B_1}{B_2} \right)^{1.75} \tag{5.28}$$

$$k_\theta = 1 + 0.9 \left(\frac{\theta}{90} \right)^{1.5} \tag{5.29}$$

$$k_L = \begin{cases} 1, & \text{for } \frac{L}{(B_1 - B_2)} \geq 0.35 \\ 0.77 + 1.36 \left(\frac{L}{B_1 - B_2} \right) - 2 \left(\frac{L}{B_1 - B_2} \right)^2, & \text{for } \frac{L}{(B_1 - B_2)} \leq 0.35 \end{cases} \tag{5.30}$$

where B_1 is upstream channel width, B_2 is contracted channel width, θ is contraction transition angle in degrees, and L is length of contracted channel. Note that Eqs. (5.26) to (5.30) are developed for a rectangular channel with vertical sidewalls (straight riverbanks). Depending on the channel alignment and floodplain configuration, the flow conditions at the bridge crossing in a compound channel can be very complicated (see Rossell and Ting, 2013). Therefore, these equations may be difficult to apply in practice. It is also noted that the flume experiment was conducted using Porcelain clay so there was no deposition in the contracted channel. Because of this, these equations are only valid for clear-water scour conditions. The latter can be determined by calculating the ratio of the friction velocity $V^* = \left(\frac{\tau}{\rho} \right)^{\frac{1}{2}}$ in the contracted section and the sediment fall velocity ω. If the ratio is much larger than 2, then the bed material from the upstream reach will be mostly suspended discharge and may be washed through the contracted section (Arneson et al., 2012).

5.5 Contraction Scour (Energy Method)

The clear-water contraction scour equations in HEC-18 are derived assuming that scour depth in the contracted channel will increase until the bed shear stress is reduced to the critical shear stress of the bed material. The maximum flow depth in the contracted section after scour is given by:

$$y_{max}(m) = \left(\frac{\rho g n^2 q^2}{\tau_c}\right)^{\frac{3}{7}} \tag{5.31}$$

where q is discharge per unit width. For non-cohesive soils, the critical shear stress can be determined using the Shields relation, and the maximum flow depth can be written as (Arneson et al., 2012):

$$y_{max} = \left(\frac{q^2}{C_u D_m^{\frac{2}{3}}}\right)^{\frac{3}{7}} \tag{5.32}$$

where $C_u = 40$ m/s^2 or $130 \frac{ft}{s^2}$, and $D_m = 1.25 D_{50}$ is the effective bed material size. For cohesive soils, both the critical shear stress and soil erosion rates would have to be measured. The measured soil erosion function (Eq. 5.2 or 5.3) can then be used to compute scour depth as a function of time by increasing the flow depth in the contracted channel in a stepwise fashion. An approach based on the energy equation was developed by Güven (2002) for steady flows and extended to unsteady flows by Rossell and Ting (2013). The model can compute clear-water contraction scour in a long contraction created by abutments projecting into or ending at the edge of the mail channel (cases 1a and 1b in HEC-18). The model has the advantage that it does not rely on any empirical equations or assume that the scour history follows a hyperbolic function. A hydraulic analysis is first performed using a 1D or 2D flow model to establish the variations of the flow depth y and unit discharge q in the contracted section with the flow discharge Q. The procedure for contraction scour calculations is summarized below (see also Rossell, 2012):

The model is based on energy balance between the contracted/bridge section (BR) and a section downstream of the bridge (BD). The model assumes that the flow remains subcritical through the bridge section. The total head at section BD, H_{BD}, is then known from gradually varied flow calculations further downstream and is not affected by the flow condition at the bridge section (i.e., H_{BD} would be the same before and after scour). Writing the energy equation between sections BR and BD for a given discharge, we get:

$$H_{BD} = \underbrace{y_i + z_0 + \frac{V_i^2}{2g} - h_{L,i}}_{\text{(before scour)}} = \underbrace{y_{BR} + (z_0 - z) + \frac{V_{BR}^2}{2g} - h_{L,BR}}_{\text{(after scour)}} \tag{5.33}$$

where y and V are flow depth and flow velocity in the contracted section, z_0 is vertical distance from the datum to the channel bed before scour, z is contraction scour depth, and h_L is head loss between sections BR and BD. The subscript i is used to denote the initial flow condition before scour; the subscript BR is used to denote the flow condition at any time after scour starts.

The head loss between the contracted section and downstream section is modeled as expansion loss:

$$h_{L,i} = C_e \left(\frac{V_i^2}{2g} - \frac{V_{BD}^2}{2g}\right) \tag{5.34a}$$

$$h_{L,BR} = C_e \left(\frac{V_{BR}^2}{2g} - \frac{V_{BD}^2}{2g}\right) \tag{5.34b}$$

where C_e is the expansion loss coefficient (typically taken to be 0.5). Note that in sub-critical flows, the flow velocity at the downstream section BD, V_{BD}, remains constant during the scouring process. Substituting Eq. (5.34a, b) in Eq. (5.33) and writing $V = \frac{q}{y}$, we get

$$z = y_{BR} + (1 - C_e)\frac{q^2}{2gy_{BR}^2} - \left[y_i + (1 - C_e)\frac{q^2}{2gy_i^2}\right] \tag{5.35}$$

Taking the derivative of z with respect to time and rearranging, the time rate of change of flow depth in the contracted channel can be expressed as:

$$\frac{dy_{BR}}{dt} = \frac{\frac{dz}{dt}}{\left[1 - \frac{(1-C_e)q^2}{gy_{BR}^3}\right]} \tag{5.36}$$

since the initial flow depth y_i is constant for a given discharge. In Eq. (5.36), the rate of scour $\frac{dz}{dt}$ is equal to the soil erosion rate $\dot{z}$, which is assumed to be a function of the bed shear stress τ. The latter may be computed as (Akan, 2006):

$$\tau \ (\text{N/m}^2) = \frac{\rho g n^2 q^2}{y_{BR}^{\frac{7}{3}}} \tag{5.37}$$

Starting with $y_{BR} = y_i$ and $z = 0$, the bed shear stress is computed using Eq. (5.37) and the corresponding erosion rate $\dot{z}$ using Eq. (5.2) or (5.3). The time rate of change of flow depth in the contracted channel $\frac{dy_{BR}}{dt}$ is computed using Eq. (5.36). The new flow depth is then given by $y_{BR} + \frac{dy_{BR}}{dt} \cdot \Delta t$, and the new scour depth by $z + \frac{dz}{dt} \cdot \Delta t$, where Δt is length of time step. This procedure is repeated to give the variations of bed shear stress, flow depth, and scour depth with time in the contracted section.

A similar procedure can be applied to a sequence of constant discharges represented by a hydrograph to compute the contraction scour depth for unsteady flows. However, the relationship between the flow depth and flow discharge in the contracted section was developed for an un-scoured channel. The unit discharge q may be assumed to remain constant, but the flow depth must be modified to account for pre-existing scour. The total head at section BD at the beginning of a time step can be written as (see Eq. 5.33):

$$H_{BD} = y_{BR} + (z_0 - z) + \frac{q^2}{2gy_{BR}^2} - C_e\left(\frac{q_{BR}^2}{2gy_{BR}^2} - \frac{q_{BD}^2}{2gy_{BD}^2}\right) \tag{5.38}$$

where z is the pre-existing scour depth and y_{BR} is the flow depth in the contracted section with pre-existing scour. For sub-critical flow through the bridge opening, H_{BD} is computed from gradually varied flow calculations in the upstream direction. Therefore, the value of H_{BD} is the same at a given discharge with or without pre-existing scour. Thus, we have:

$$H_{BD} = y_{BR,WI} + z_0 + \frac{q^2}{2gy_{BR,WI}^2} - C_e\left(\frac{q_{BR}^2}{2gy_{BR,WI}^2} - \frac{q_{BD}^2}{2gy_{BD}^2}\right) \tag{5.39}$$

where $y_{BR,WI}$ is the flow depth in the contracted section at a given discharge without pre-existing scour. Equating Eq. (5.38) and (5.39), we get:

$$y_{BR} = y_{BR,WI} + z + (1 - C_e)\frac{q^2}{2g}\left(\frac{1}{y_{BR,WI}^2} - \frac{1}{y_{BR}^2}\right) \tag{5.40}$$

If the change in velocity head in the contracted section due to scour is small, Eq. (5.40) can be approximated by:

$$y_{BR} \approx y_{BR,WI} + z \qquad (5.41)$$

Hence, for a given discharge, the flow depth in the contracted section is increased approximately by the pre-existing scour depth from the flow depth without scour. Eq. (5.41) may be used as a first approximation in an iteration scheme with Eq. (5.40) to compute the flow depth y_{BR} with pre-existing scour.

The procedure for computing the scour-depth-versus-time curve for unsteady flows is like that for steady flows. For each discharge value in the hydrograph, Eq. (5.40) and the computed scour depth from the previous time step are used to calculate the flow depth y_{BR} at the beginning of the new time step. The bed shear stress is computed using Eq. (5.37) and the erosion rate $\dot{z}$ using Eq. (5.2) or (5.3). The time rate of change of flow depth $\frac{dy_{BR}}{dt}$ is computed using Eq. (5.36). Then, the new flow depth and scour depth at the end of the time step is given by $y_{BR} + \frac{dy_{BR}}{dt} \cdot \Delta t$ and $z + \frac{dz}{dt} \cdot \Delta t$, respectively.

5.6 Equivalent Time

In order to apply the SRICOS method, a hydrograph is required. For new bridges, this means generating a synthetic hydrograph with daily or sub-daily flow values or assume that a recorded hydrograph will repeat itself. To avoid the problem of constructing a future hydrograph for each bridge site, Briaud et al. (2001b) developed the Simple-SRICOS or S-SRICOS method. They introduced the concept of an equivalent time, which is the time required for the maximum discharge or velocity in a hydrograph to create the same predicted final scour depth as the one created by the complete hydrograph (Figure 5.10). The equivalent time for pier scour was computed for 55 cases generated from eight bridge sites in Texas. In each case, the recorded hydrograph from the nearest gauging station was used with the SRICOS method to predict the final scour depth. The maximum flow velocity in the recorded hydrograph was determined from the measured discharge using a hydraulic model, and the equivalent time needed to produce the same predicted final scour depth as the one produced by the recorded hydrograph was calculated. A multiple regression was performed on the results to obtain an empirical relationship for the equivalent time as a function of the duration of the hydrograph t_{hydro}, the maximum velocity in the hydrograph $V_{\max}$, and the initial erosion rate at the maximum velocity $\dot{z}_i$ as follows:

$$t_{e,\text{pier}}(h) = 73[t_{\text{hydro}}(\text{years})]^{0.126}[V_{\max}(\text{m/s})]^{1.706}[\dot{z}_i(\text{mm/h})]^{-0.20} \qquad (5.42)$$

Using the same approach, Wang (2004) developed the following empirical equation for the equivalent time for contraction scour based on 28 cases generated from six bridge sites in Texas:

$$t_{e,\text{contraction}}(h) = 644.32[t_{\text{hydro}}(\text{years})]^{0.4242}[V_{\max}(\text{m/s})]^{1.648}[\dot{z}_i(\text{mm/h})]^{-0.605} \qquad (5.43)$$

To predict pier or contraction scour at a new bridge, t_{hydro} is taken to be the design life of the bridge and $V_{\max}$ the flow velocity produced by a design flood (e.g., the 100-year peak flow). The initial erosion rate $\dot{z}_i$ is determined using a soil erosion function and the computed bed shear stress before scour starts, and the equilibrium scour depth $z_{\max}$ is calculated using Eq. (5.14) or (5.26). The equivalent time is then determined using Eq. (5.42) or (5.43) and substituted in Eq. (5.22) with the values of $\dot{z}_i$ and $z_{\max}$ to compute the final scour depth. Briaud et al. (2009) adopted the S-SRICOS method to develop simplified procedures for scour assessment in Texas without the need to generate a future hydrograph (see Section 5.10)
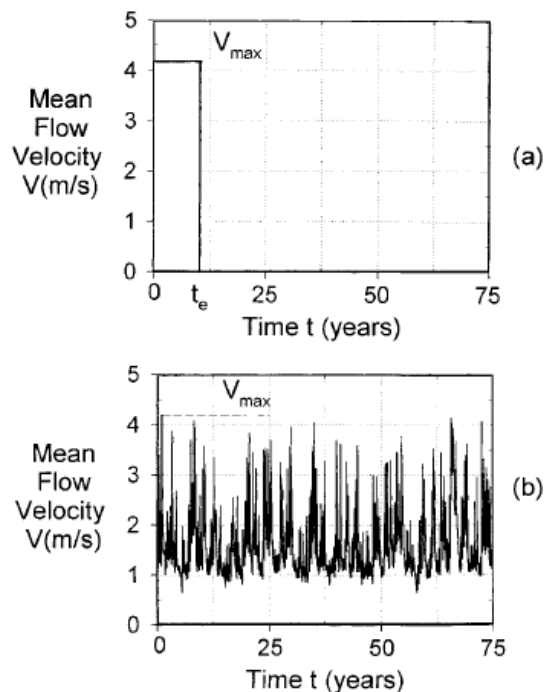
Figure 5.10 (a) Hydrograph with a constant velocity V_{max} and equivalent time t_e and (b) the actual hydrograph
Both hydrographs would produce the same predicted final scour depth.(from Briaud et al., 2001b)

Equations (5.42) and (5.43) are limited by the database from which they were derived. For pier scour, this database includes recorded hydrographs with duration ranging from 10 to 50 years at eight bridge sites in Texas. For contraction scour, six bridge sites with recorded hydrographs ranging from two to 35 years were used to develop the regression equation. Therefore, the scour predictions from these equations must be treated with caution when they are applied to other bridge sites. For example, the maximum velocity V_{max} is influenced by the bridge hydraulics as well as the hydrologic characteristics of the drainage basin. If the hydraulic and hydrologic conditions are significantly different at another site, the temporal structure of flow and flow distribution around the bridge would be different from those used to develop the regression equations.

In addition to the variation in distribution of flow velocity from site to site, a recorded hydrograph represents only one possible outcome in the temporal distribution of floods. Therefore, using Eq. (5.42) or (5.43) to predict future scour implicitly assumes that the sequences of flows used to develop the regression equations will be repeated, which ignores the stochastic nature of the hydrologic process. The latter is influenced by many factors, including the shape of the drainage basin, soil type, and vegetation cover. A recorded hydrograph consisting of a multitude of large and small floods may not be adequately replaced by a single equivalent flood. In general, more temporal information on the sequence of flows would be required. A more robust approach is to determine an equivalent time for each of the floods in the recorded hydrograph so that only the time sequence of flows in the individual flood is repeated when computing the scour history.

5.7 Scour History Analysis

Pier scour at the SD13 bridge over the Big Sioux River near Flandreau and Interstate 90 bridges over Split Rock Creek near Brandon were studied using the SRICOS method. Contraction scour at the SD37 bridges over the James River near Mitchell was studied using the energy method. Recorded hydrographs from the streamflow gauging stations at Big Sioux River near Brookings (#06480000), Split Rock Creek at Corson (#06482610), and James River near Forestburg (#06477000) were used to compute pier or contraction scour history at each site. The computed scour histories were analyzed to determine the equivalent times of the individual floods, which were then correlated to the flood magnitudes and durations. Scour histories were computed using a measured soil erosion function (if available) and Eq. (5.2) with the values of τ_c and a' given in Table 5.1.

The central hypothesis in this study is that a few large floods can produce the same amount of scour as a long sequence of large and small floods, since most of the floods in a continuous hydrograph would not achieve their maximum scour depths due to pre-existing scour. The Big Sioux River near Brookings and James River near Forestburg streamflow gauging stations have been operated since 1953 and 1950, respectively. For the Split Rock Creek at Corson streamflow gauging station, daily mean flow data from 1966 to 1989 and 15-minute flow data from 2002 to the present are available. Only peak flow data were recorded between 1990 and 2001 when the station was operated as a crest-stage partial-record gauging station. The recorded hydrographs were used to compute scour histories at the three sites. To study the potential of each flood to produce scour, we replace the continuous hydrograph by a series of floods to create a flood sequence. For each scouring flood in the recorded hydrograph, the SRICOS method is used to compute the final scour depth. This computed scour depth represents the maximum scour depth that would be produced by the flood if there were no pre-existing scour. We also compute the equivalent time (t_e) required for the peak discharge (Q_{max}) in each flood to create the same scour depth as that created using the recorded hydrograph. Then, we replace the continuous time series of daily or sub-daily flow values by a series of N rectangular hydrographs with discharge $Q_{max,i}$ and equivalent duration $t_{e,i}$ ($i = 1,..,N$). The return period of each flood is also determined by a flood frequency analysis. Note that Briaud et al. (2001b) replaced a multi-year hydrograph with a single equivalent flood. Consequently, information on the potential of the individual floods to produce scour is lost. In the current approach, this information is retained for each scouring flood in the recorded hydrograph using the flood's peak discharge and equivalent duration. The sequence of equivalent floods would produce the same final scour depth as the recorded hydrograph. Hence, we can use these equivalent floods to construct other flood sequences to predict future scour.

Three different types of hydrologic data series may be used for flood frequency analysis (Bedient and Huber, 1992). An annual maximum series is a series of maximum annual floods consisting of the largest flood in each year. A series of annual exceedances is given by the n-largest independent floods from an n-year period, regardless of the year the floods occur. A partial duration series is a series of floods that are selected so their magnitude is greater than a base value (e.g., the 10-year flood). It is preferred to use annual peak flows for flood frequency analysis because the largest flood in one year can be assumed to be independent of the largest flood in any other year. Thus, annual maximum series may be constructed to predict the occurrence of large floods. We will show in Chapters 6, 7, and 8 that, for both pier scour and contraction scour, the final scour depth predicted using the maximum annual floods is essentially the same as that obtained using the complete, recorded hydrograph except for soils with very slow erosion rates.

5.8 Dimensional Analysis

By replacing the recorded hydrograph of a flood with the maximum discharge and equivalent time, the problem of hydrograph construction for scour prediction is reduced to determining the equivalent times for floods of different return periods, since the maximum discharges can be obtained by randomly sampling from a suitable probability distribution such as the Log Pearson Type III distribution. To determine the equivalent times for different floods, a multiple regression is performed to relate the equivalent durations of the scouring floods to the important hydrologic, hydraulic, and soil parameters at the bridge site. The relevant dimensionless groups are constructed by dimensional analysis. The procedure is similar for pier scour and contraction scour and is presented for pier scour in the following.
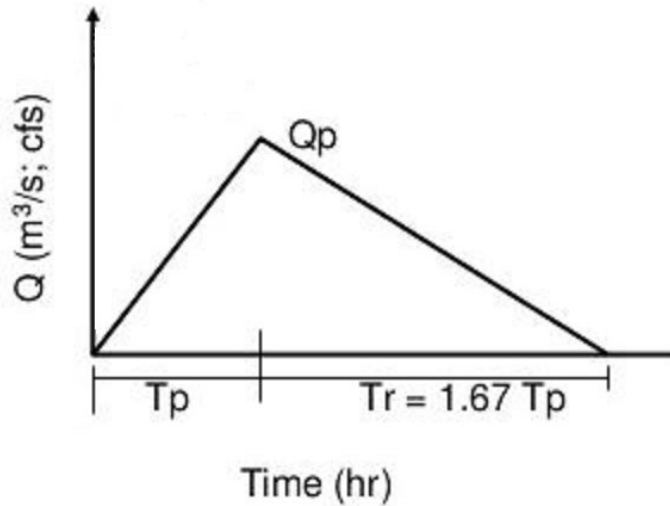
Figure 5.11 NRCS synthetic unit triangular hydrograph

For each discharge in the hydrograph, the equilibrium scour depth can be found using Eq. (5.9) or (5.14) and the maximum initial bed shear stress around the pier using Eq. (5.17). With the measured critical shear stress τ_c and erosion rate constant a', the initial rate of scour can be found using Eq. (5.2). The scour-depth-versus-time-curve can then be computed using the SRICOS method by following the procedure for accumulating scour depths produced by multiple discharges described in Section 5.3. Hence, the predicted final scour depth z_f for a given flood can be described by the following functional relationship:

$$z_f = f\left(Q_{\max}, a, t_{\text{hydro}}, \rho, \tau_c, a'\right) \tag{5.44}$$

where $Q_{\max}$is peak discharge, a is pier width, t_{hydro} is duration of the hydrograph, ρ is density of water, τ_c is critical shear stress, and a' is soil erosion constant. Note that Eq. (5.44) is written for a specific site. It is not necessary to include the flow depth and approach flow velocity as independent variables because they are related to $Q_{\max}$. In Eq. (5.44), the pier width a is chosen as the representative length scale for the bridge site.

Using the equilibrium scour depth at peak discharge $z_{\max}$ instead of a as the representative length scale and combining ρ and τ_c into a velocity scale represented by Q_c, the discharge at critical shear stress, Eq. (5.44) can be re-written as:

$$z_f = f\left(Q_{\max}, Q_c, z_{\max}, t_{\text{hydro}}, a'\right) \tag{5.45}$$

By the Buckingham π-theorm, Eq. (5.45) yields $n - k = 6 - 2 = 4$ dimensionless groups. A dimensionless form of Eq. (5.45) is given by:

$$\frac{z_f}{z_{max}} = f\left(\frac{Q_{max}}{Q_c}, \frac{Q_{max}t_{hydro}}{z_{max}^3}, a'\right)$$

(5.46)

which is applicable to different floods at the same site.

The equivalent time is the time required for the maximum discharge in a hydrograph to create the same predicted final scour depth as the one created by the complete hydrograph. Thus, we have:

$$z_f = \frac{t_e}{\frac{1}{\dot{z}_i} + \frac{t_e}{z_{max}}}$$

(5.47)

where $\dot{z}_i$ is initial erosion rate at peak discharge Q_{max}. Define t_{90} as the time required for the maximum discharge to develop 90% of the equilibrium scour depth, we have:

$$0.9z_{max} = \frac{t_{90}}{\frac{1}{\dot{z}_i} + \frac{t_{90}}{z_{max}}}$$

(5.48)

or $t_{90} = \frac{9z_{max}}{\dot{z}_i}$. Combining Eq. (5.47) and Eq. (5.48) yields:

$$\frac{t_e}{t_{90}} = \frac{\frac{z_f}{z_{max}}}{9\left(1 - \frac{z_f}{z_{max}}\right)}$$

(5.49)

Hence, $\frac{t_e}{t_{90}}$ is a function of $\frac{z_f}{z_{max}}$ and we can write:

$$\frac{t_e}{t_{90}} = \phi\left(\frac{Q_{max}}{Q_c}, \frac{Q_{max}t_{hydro}}{z_{max}^3}, a'\right)$$

(5.50)

Eq. (5.49) assumes that the scour history follows a hyperbolic function. We will show in Chapter 7 that the history of contraction scour does not generally follow the hyperbolic model. Nevertheless, $\frac{z_f}{z_{max}}$ and $\frac{t_e}{t_{90}}$ are still related. Therefore, the equivalent time for contraction scour can also be represented functionally by Eq. (5.50). The relationship between the dimensionless groups is determined by multiple regression. The results are presented for pier scour in Chapters 6 and 8, and for contraction scour in Chapter 7 for the three bridge sites.

5.9 Future Hydrograph Generation and Risk Approach to Scour Prediction

A stochastic approach to scour prediction is presented in this section. The method was employed to predict pier or contraction scour at three bridge sites in South Dakota. A flood frequency analysis is first performed on the historical flow records to determine the recurrence intervals of the annual peak flows and the parameter values of the Log Pearson Type III (LP-III) distribution. The equivalent times of the maximum annual floods are then determined. The LP-III distribution is sampled randomly to create a sequence of maximum annual floods that satisfies the LP-III distribution. An equivalent duration is assigned to each flood based on the peak discharge. A set of equally probable annual maximum series is generated and used with the SRICOS method to compute the final scour depth. The set of computed final scour depths is then used to determine the risk values associated with different predicted scour depths and project lives.

The Log Pearson Type III distribution is recommended for flood flow frequency analysis in Bulletin 17B (U.S. Interagency Advisory Committee on Water Data, 1982), and the procedure was recently revised in Bulletin 17C (England Jr. et al., 2018). The probability distribution $p(y)$ for LP-III is represented by the following equation:

$$p(y) = \frac{\lambda^\beta (y-\varepsilon)^{\beta-1} \exp[-\lambda(y-\varepsilon)]}{\Gamma(\beta)} \tag{5.51}$$

In Eq. (5.51), the distribution parameters λ, β and ε are related to the moments of the data by the following equations:

$$\lambda = \frac{\sqrt{\beta}}{\sigma_y}, \qquad \beta = \left(\frac{2}{C_y}\right)^2 \quad \text{and} \quad \varepsilon = \mu_y - \frac{\beta}{\lambda} \tag{5.52}$$

where $\mu_y = \text{mean}(y)$, $\sigma_y = \text{Stdev}(y)$, $C_y = \text{skew}(y)$, and y is the base-10 logarithm of the measured annual peak flow. The mean, standard deviation and skew coefficient of y may be calculated using the following equation (Roberson et. al., 1998):

$$\mu_y = \frac{\sum_{i=1}^n y_i}{n} \tag{5.53a}$$

$$\sigma_y = \sqrt{\frac{\sum_{i=1}^n (y_i - \mu_y)^2}{n-1}} \tag{5.53b}$$

$$C_y = \frac{n^2 \sum_{i=1}^n (y_i^3) - 3n \sum_{i=1}^n (y_i) \sum_{i=1}^n (y_i^2) + 2(\sum_{i=1}^n y_i)^3}{n(n-1)(n-2)\sigma_y^3} \tag{5.53c}$$

where n is the number of maximum annual floods. The probability distribution $p(y)$ can be sampled randomly to create a flood series that satisfies the parameters of the LP-III distribution. However, it is more convenient to evaluate the exceedance probability $P(y)$ of the distribution using the frequency factor. The frequency factor K is a function of the skew coefficient C_y and return period T ($P = \frac{1}{T}$). The equation used to represent any probability distribution is (Chow et al., 1988):

$$y = \mu_y + K \cdot \sigma_y \tag{5.54}$$

For the LP-III distribution, the frequency factor can be computed using the Wilson-Hilferty's approximation (Wilson and Hilferty, 1931) or the equation by Kite (1977).

Wilson-Hilferty:

$$K \approx \frac{2}{C_y}\left\{\left[1 - \left(\frac{C_y}{6}\right)^2 + \left(\frac{C_y}{6}\right)(z)\right]^3 - 1\right\} \tag{5.55}$$

Kite:

$$K \approx z + (z^2 - 1)\left(\frac{C_y}{6}\right) + \frac{1}{3}(z^3 - 6z)\left(\frac{C_y}{6}\right)^2 - (z^2 - 1)\left(\frac{C_y}{6}\right)^3 + z\left(\frac{C_y}{6}\right)^4 + \frac{1}{3}\left(\frac{C_y}{6}\right)^5 \tag{5.56}$$

where z is the standard normal variate. The standard normal variate is related to the exceedance probability P and can be calculated using the following equation (Chow et al., 1988):

(for $0 < P \le 0.5$),

$$z = w - \frac{2.515517 + 0.802853w + 0.010328w^2}{1 + 1.432788w + 0.189269w^2 + 0.001308w^3}, \quad w = \sqrt{\ln\left(\frac{1}{P^2}\right)} \tag{5.57}$$

When $P > 0.5$, $1 - P$ is substituted for P in Eq. (5.57) and the value of z computed is given a negative sign.

Monte Carlo simulation is employed to generate a set of equally probable future hydrographs. To create a hydrograph consisting of a series of maximum annual floods, the MATLAB function *rand* is used to generate a sequence of uniformly distributed random numbers between 0 and 1. The series of uniform random numbers represents the exceedance probability P_i ($i = 1, \ldots, n$) of the individual maximum annual floods. The flood magnitudes are then computed using Eqs. (5.54) – (5.57), and the equivalent durations of the floods are computed using regression equations developed from historical flow data as described in Section 5.8. Because a constructed hydrograph represents only one probable outcome of flooding events in the design life of a bridge, the procedure is repeated to create 20,000 annual maximum series. The set of equally probable future hydrographs is used with the SRICOS method to compute the final scour depth. The set of computed final scour depths is then used to determine the risk values associated with different scour depths and project lives.

Briaud et al. (2004) conducted a scour risk analysis for the Woodrow Wilson Bridge. Their procedure differs from ours in two important ways. First, they constructed future hydrographs by sampling from the lognormal distribution. The frequency factor is equal to the standard normal variate when the skew coefficient is equal to zero, and the Log Pearson Type III distribution then reduces to the lognormal distribution. Therefore, the lognormal distribution is a special case of the Log Pearson Type III distribution. Second, the mean and standard deviation of the lognormal distribution were computed from daily mean flow record at the Little Falls station on the Potomac River in Washington, D. C. Each flow value is treated as an individual flood with a duration of one day. This approach eliminates the need to estimate the flood duration. However, daily mean flows are not independent and therefore may not be related to the return period.

In the updated *Guidelines for Determining Flood Flow Frequency – Bulletin 17C*, the expected moments algorithm (EMA) is adopted as an improved method of moments approach to fitting the LP-III distribution to flood peaks. EMA employs a wide range of data that include historical flood information and paleo flood information to produce improvements to the moment estimates in the Bulletin 17B method. EMA's estimates of mean, standard deviation and skew coefficient can be obtained by running the USGS program PeakFQ (https://water.usgs.gov/software/PeakFQ/). The values of μ_y σ_y, and C_y can then be used with Eqs. (5.54) – (5.57) to generate annual maximum series for SRICOS simulations. Hence, the proposed hydrograph generation method based on the LP-III distribution is consistent with the USGS's method for flood frequency analysis and takes advantage of the recent advances in statistical methods described in Bulletin 17C.

5.10 Bridge Scour Assessment Methods

One of the key objectives of this study is to develop a screening tool to determine whether accounting for the time rate of scour would be worthwhile for a given project. The final decision will need to consider the site conditions, design requirements, and other project factors such as data availability and time scheduling. Instead of a full SRICOS-EFA analysis, researchers have developed several simplified methods to predict bridge scour in cohesive soils. These methods include (see Briaud et al., 2009; Straub and Over, 2010):

1. Apply a reduction factor to the scour depth computed using the scour equations for non-cohesive soils in HEC-18 based on the measured soil properties;

2. Adopt the equilibrium scour depth for the 100- or 500-year flood computed using the scour equations for cohesive soils such as Eqs. (5.14) and (5.26) (the SRICOS z_{max} method);

3. Use a recorded hydrograph with the SRICOS method to predict future scour;

4. Run the SRICOS method with the 500-year peak flow for five days;

5. Use the S-SRICOS method with an equivalent time calculated using Eq. (5.42) or (5.43).

Based on the results of geotechnical laboratory testing, EFA testing and SRICOS simulations for 15 bridge sites in Illinois, Straub, and Over (2010) found that on average the HEC-18 method predicts the highest amount of scour, followed by the SRICOS z_{max} method, and then other simplified SRICOS methods. They determined the reduction factors that would match the results from the HEC-18 method to those from the SRICOS method. They developed a tiered approach to predicting pier and contraction scour in cohesive soils. Their approach is built upon four levels (1-4) in increasing order of complexity. In Level 1, the reduction factors shown in Table 5.2 are used to adjust the scour depths predicted using the equations in HEC-18. In Level 2, the SRICOS z_{max} value for the 100-year flood is used for sites where the reduction factor method predicts higher scour depths. In Level 3, SRICOS simulations are performed using critical shear stress and soil erosion rates estimated by soil property regressions. Level 4 is like Level 3 but uses measured critical shear stress and erosion rates from EFA tests conducted on soil samples collected from the bridge site. Note that a hydrograph is not required in the Levels 1 and 2 analysis. In the Levels 3 and 4 analysis, the SRICOS-EFA program developed by Texas A&M University is used to conduct the SRICOS simulations.

Table 5.2 Reduction factor for HEC-18 based on unconfined compressive strength Q_u
(from Straub and Over, 2010)

Q_u (tons/ ft^2)	Reduction Factor (%)
0 to 0.4	0
> 0.4 to 1.0	25
>1.0 to 8.0	50

Briaud et al. (2009) developed a three-level Bridge Scour Assessment (BSA 1 to 3) procedure that does not require site-specific erosion testing and a full SRICOS-EFA analysis. The first level, BSA 1, uses the observed scour depth Z_{mo}, the maximum flow velocity experienced at the bridge V_{m0}, and the age of the bridge t_{hyd} to predict the scour depth Z_{fut} corresponding to a future flood with maximum velocity V_{fut}. Simulations of pier and contraction scour depths were carried out using the S-SRICOS method to develop extrapolation charts (Z-Future charts) that relate the ratios $\frac{Z_{fut}}{Z_{mo}}$ and $\frac{V_{fut}}{V_{mo}}$. Their simulations assume that the duration of the future flood is 72 hours, and the soil type belongs to one of the erosion categories (I through V) shown in Figure 5.3. Category VI is excluded because the materials are considered non-erodible and thus would produce no future scour. Z-Future charts were developed for different bridge parameters and soil categories so the user can use the appropriate chart to obtain the value of Z_{fut}.

The second level, BSA 2, assumes that the bridge will experience the maximum possible scour depth (equilibrium scour depth) under V_{fut} within its lifetime. The equilibrium scour depth is calculated using Eq. (5.14) for pier scour and Eq. (5.26) for contraction scour. These equations require the critical velocity as one of the inputs. The critical shear stress τ_c is estimated using the generalized erosion function chart (Figure 5.3) based on the soil type, and the critical velocity V_c is then calculated using Eq. (5.15).

The third level, BSA 3, uses Eq. (5.42) or (5.43) to calculate the equivalent time of the design flood, which is then substituted into Eq. (5.22) to compute the final scour depth. In Eqs. (5.42) and (5.43), t_{hydro} is taken to be the design life of the bridge and V_{max} the flow velocity produced by the design flood (e.g., the 100-year peak flow). The initial erosion rate $\dot{z}_i$ in Eq. (5.22) is estimated using the generalized erosion function chart (Figure 5.3) and the equilibrium scour depth Z_{max} is calculated using Eq. (5.14) (for pier scour) or Eq. (5.26) (for contraction scour).

Although several methods have been proposed by researchers for predicting bridge scour in cohesive soils, no guidelines exist to define the site conditions where use of these methods is appropriate and determine the associated risk. In Chapters 6, 7, and 8, probability distributions of predicted scour depth at three bridge sites are obtained using Monte Carlo simulations. These results are used to assess the risk levels of other simplified methods for predicting scour in cohesive soils. Once the risk level of a method has been determined, the engineer can either use the method with confidence, or reject it for another method. A decision tool is presented in Chapter 9 to help the engineer decide whether to conduct a full SRICOS-EFA analysis when evaluating a bridge site for scour. The step-by-step procedures are demonstrated using worked examples in Chapter 11 for pier scour and Chapter 12 for contraction scour. Preliminary results on hydrograph generation at an ungauged site are presented in Chapter 13.

6. PIER SCOUR ANALYSIS, SD13 BRIDGE OVER BIG SIOUX RIVER AT FLANDREAU, SOUTH DAKOTA

6.1 Site Description

The SD13 bridge (51-150-099) over the Big Sioux River is located on South Dakota Highway No. 13, 0.3 miles north of the City of Flandreau in east-central South Dakota (Figures 6.1 and 6.2). The bridge was built in 1964 and has four spans, with an overall length of 436 ft. It has three octagonal pier sets with webs located on piling. Each pier set is 3-ft wide and 30-ft long. The bridge opening is classified as a spill-through abutment with three horizontal to one vertical slope embankments protected by riprap. The United States Geological Survey (USGS) has measured river bottom profiles at the bridge site on December 5, 1991 (low flow), June 20, 1992 (discharge 1,624 ft^3/s), June 22, 1992 (4,346 ft^3/s), March 30, 1993 (9,090 ft^3/s), and July 7, 1993 (7,774 ft^3/s), as part of a detailed scour assessment for selected bridge sites in South Dakota (Niehus, 1996). These measurements show 7 to 8 ft of local scour around the northern-most pier (bent 2) and up to 1 ft of contraction scour. Between December 5, 1991, and July 7, 1993, the peak flow occurred on July 4, 1993, with a recorded hourly mean flow of 13,300 ft^3/s at the streamflow gauging station near Brookings (06480000) located 22 miles upstream. The USGS collected flow velocity data at the bridge site on March 30 and July 7, 1993. These measurements show a flow concentration around bent 2. The estimated drainage areas at the Brookings gauging station and bridge site are 3,898 mi^2 and 4,096 mi^2, respectively. The estimated two-year, 100-year, and 500-year peak discharges at the gauging station are 2,572, 29,293, and 49,063 ft^3/s, respectively. These estimates were obtained by fitting the Log Pearson Type III distribution to the measured annual peak flows from water years 1954 to 2016.

A bathymetric and topographical survey of the bridge site was conducted most recently by the USGS on August 3 to 6, 2009, using a GPS (global positioning system) topographic survey system. Figure 6.1 shows the locations of the survey points overlaid on a geo-referenced image of the study area. The Flandreau site has complex channel and floodplain geometry, and the water level is also affected by a low-head dam located ¼ mile downstream. During low flows, the stream flow approaches at an angle of about 45 degrees to the upstream face of the bridge at bent 2 (Figure 6.7). At about 4,000 ft^3/s, the river overflows its banks, and the overbank flow takes a more direct path to the bridge opening over the left floodplain. Computer models predict that, during high flows, the overbank flow significantly affects the velocity distribution at the bridge crossing (Larsen et al., 2011).

Figure 6.3 shows the generalized subsurface conditions at the bridge site. The general site soil materials include about 15 ft of loose to medium dense fill soils overlying alluvial soils consisting of inter-bedded layers of silts, clays, and sands. At a depth of about 20 ft, black organic silt was encountered at the south abutment. Coarser grained materials were observed at the north abutment. Figure 6.4 shows the measured curves of erosion rate versus shear stress for the very silty fine sand collected from the north abutment. Two different roughness heights ($\varepsilon = 0$ and 1 mm) were used to calculate the applied fluid shear stress. The EFA curve for $\epsilon = 1$ mm produces predicted pier scour depth comparable to the observed value in 1993; whereas, that for $\epsilon = 0$ yields predicted scour depth equal to about twice the observed value (Larsen et al., 2011).

Figure 6.1 Aerial photograph of SD13 bridge site near Flandreau, South Dakota, showing the bridge crossing over the Big Sioux River and field survey points for the 2D flow model
(background image courtesy of United States Geological Survey)

A two-dimensional (2D) flow model of the bridge site was created in the Surface Water Modeling System (SMS) using the depth-averaged model FESWMS. Figures 6.5 to 6.7 show the variations of computed water surface elevation, approach flow velocity, and flow angle of attack with flow discharge at bent 2. The best-fit curves were used to compute the equilibrium scour depth z_{max} and initial rate of scour $\dot{z}_i$ at different discharge values as described in Section 6.2. Table 6.1 summarizes the input parameters used in the SRICOS simulations. A drainage area ratio adjustment of 1.025 was used to transfer the recorded hydrograph at the Brookings station to the bridge site. Note that all the discharges given in this chapter already have the drainage area ratio adjustment applied. SRICOS simulations were conducted using daily mean flow from August 1, 1953, to September 30, 1990; hourly mean flow from October 1, 1990, to November 10, 1998; and 15-minute mean flow from November 24, 1998, to April 21, 2017.

Figure 6.2 SD13 bridge from left bank facing along upstream face toward right bank
The pier sets in the photograph are, from left to right, bents 4, 3, and 2.
The photograph was taken by Francis Ting on April 6, 2007.
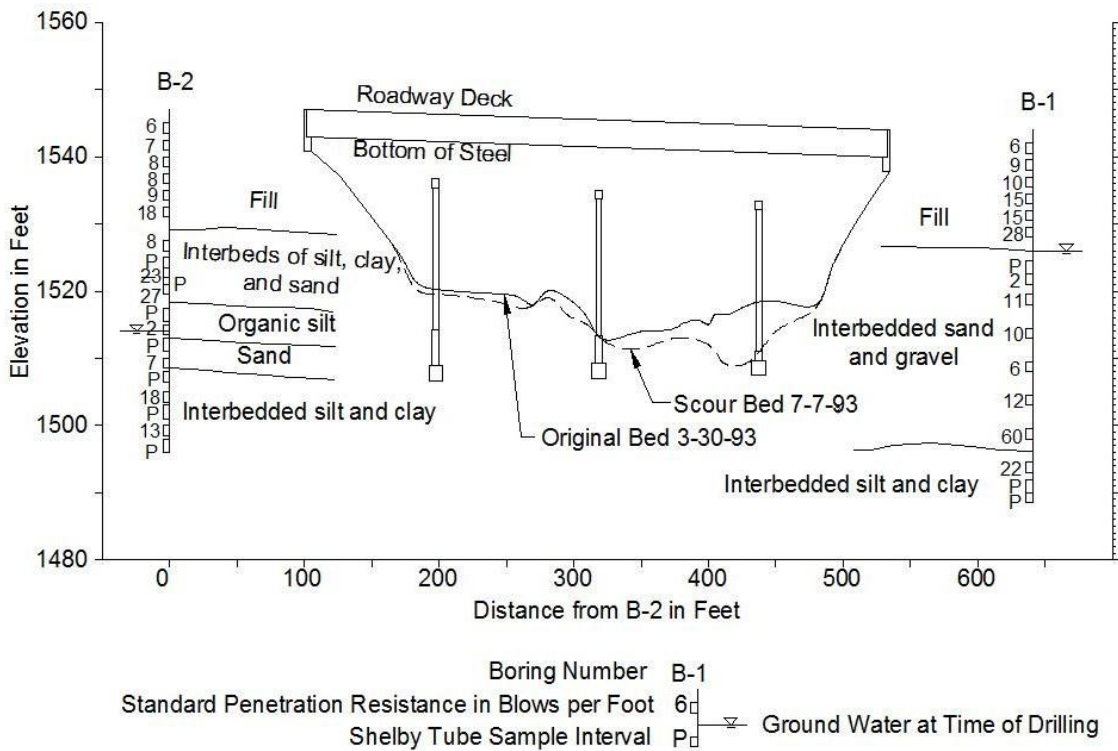
Figure 6.3 Subsurface profile at the SD13 bridge site
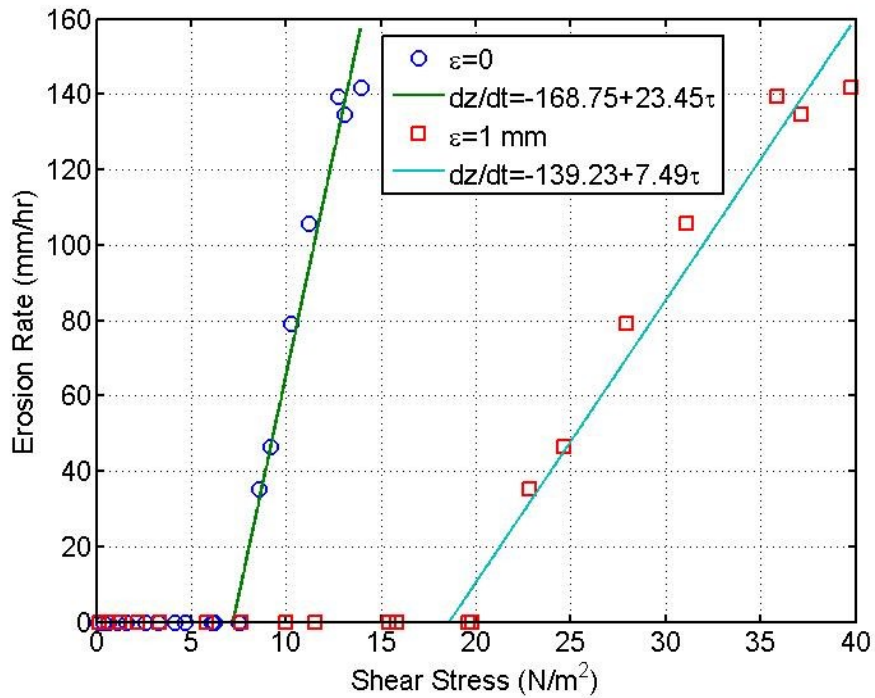
Figure 6.4 Curve of measured erosion rate versus shear stress for very silty fine sand from depth 19.5 to 21.5 ft on the north abutment
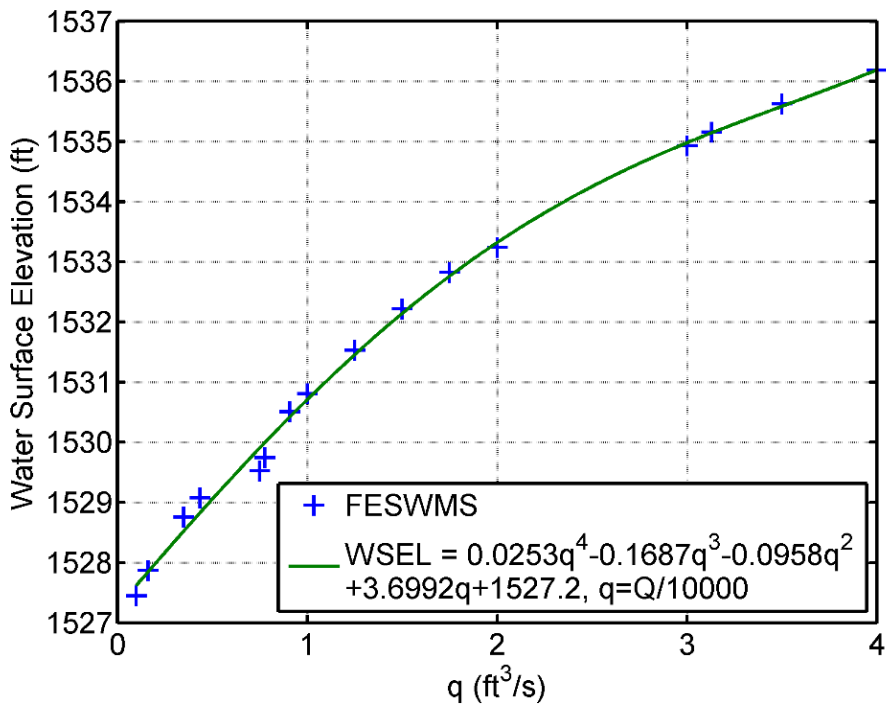
Figure 6.5 Computed curve of water surface elevation versus flow discharge at bent 2
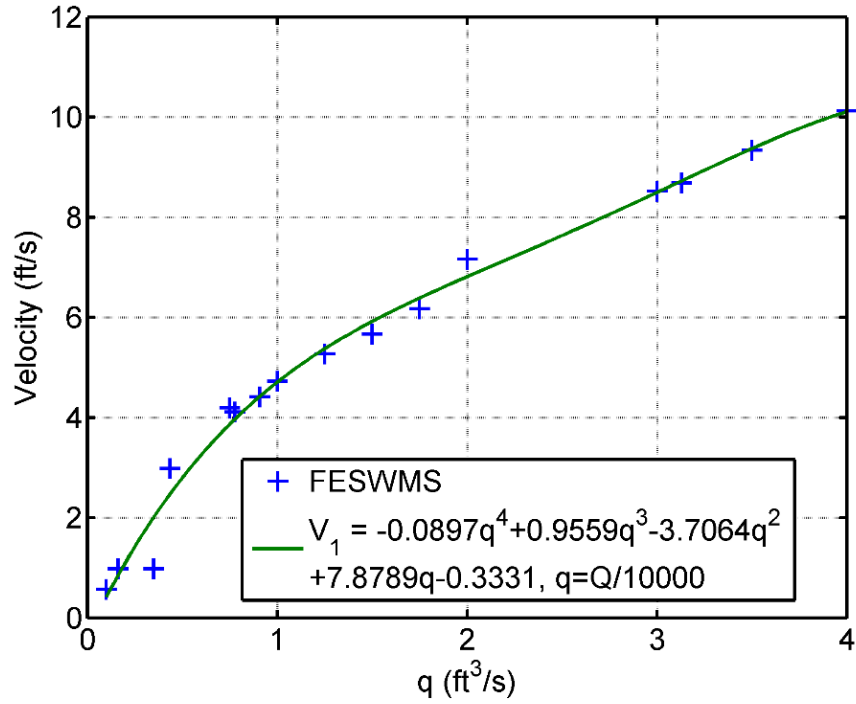
Figure 6.6 Computed curve of approach flow velocity versus flow discharge at bent 2
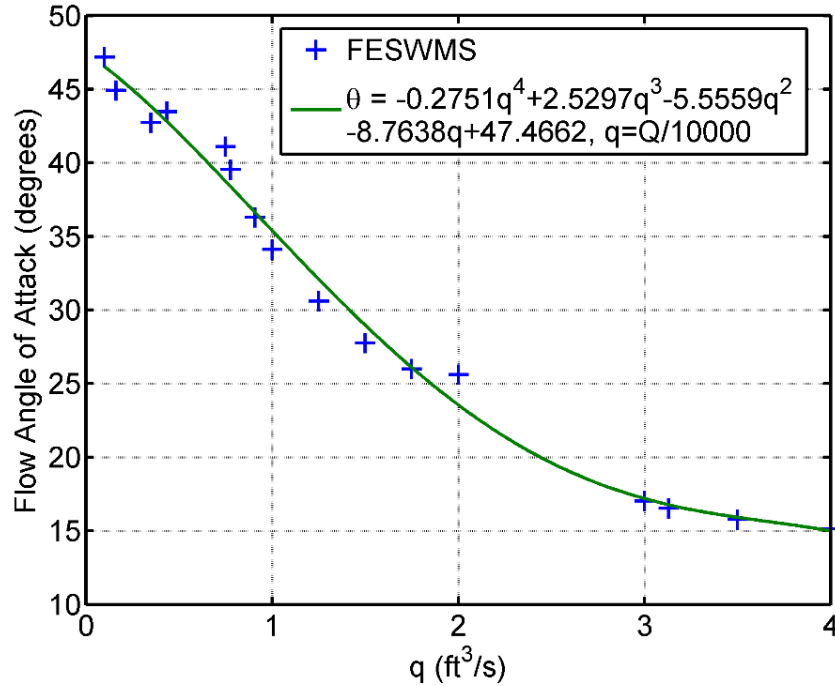
Figure 6.7 Computed curve of flow angle of attack versus flow discharge at bent 2

Table 6.1 Summary of input parameters for SRICOS simulation at bent 2

Pier geometry	Pier width B = 3 ft, pier length L = 30 ft, pier shape = octagonal pier sets with webs
Channel geometry	Channel width W_1 = 436 ft, number of piers N = 3, pier spacing S = 120 ft, initial bed elevation Y_0 = 1523.61 ft (August 4, 2009)
Flow parameters	Figs. 6.5, 6.6 and 6.7
Fluid parameters (20˚ C)	Density ρ = 998.2 kg/m^3, kinematic viscosity v = 1.004 × 10^{-6} m^2/s
Soil parameters	Fig. 6.4 (with ε = 1 mm)
Hydrograph	USGS streamflow data at Brookings, SD

6.2   Scour History Analysis

The purpose of the scour history analysis was to investigate the potential of the historical floods to produce scour. Therefore, scour histories were computed using all the available flow records, including those collected before the bridge was built. SRICOS simulations were conducted for bent 2 using the measured soil erosion function (Figure 6.4). To assess the effect of soil erodibility on the predicted scour depth, scour histories were also computed using the soil erosion function given by Eq. (5.2) and the soil parameters in Table 5.1.

Table 6.2 and Figure 6.8 show the computed results obtained using the measured soil erosion function. The return periods shown in Table 6.2 were obtained by fitting the Log Pearson Type III distribution to the measured annual peak flows from water years 1954 to 2016 using the Bulletin 17B method. The results are like those obtained by running the expected moment algorithm (EMA) without historical and regional information in the Bulletin 17C method, but they are more conservative than the results obtained by the EMA runs with historical and regional information. The peak flow estimates and return periods computed using the different methods are compared in a worked example in Chapter 11.

The SRICOS method predicts that the maximum annual floods produce scour in only nine (1960, 1962, 1969, 1984, 1985, 1993, 1997, 2010, and 2011) out of 63 years. The largest flood occurred on April 9, 1969, and has a peak discharge of 34,748 ft^3/s, which is about a 150-year flood. This flood alone produces a predicted final scour depth of 14.7 ft or 80% of the equilibrium scour depth at peak discharge. The smallest scouring maximum annual flood occurred on March 19, 1985. On its own, this flood would produce a predicted final scour of about 1 ft.

Table 6.2 shows that as the discharge decreases, the equilibrium scour depth remains about the same. This is due to the increase in flow angle of attack at the long pier (Figure 6.7). The SD13 bridge is located on a sharp bend. Concentrated flow develops upstream of the bridge crossing where the thalweg (a line connecting the lowest points of successive cross sections along the course of a river) runs adjacent to the right bank and the approach flow to bent 2 has a large flow angle of attack at low to medium flows. The flow concentration diminishes at high flows when the river overflows its banks, and the direction of the approach flow becomes more aligned with the long axis of the pier. Although the equilibrium scour depth varies little with discharge, the predicted final scour depth generally decreases with discharge because the maximum bed shear stress around the pier decreases, which reduces the rate of scour as well as the period when the bed shear stress exceeds the critical shear stress.

Table 6.2 Summary of results from SRICOS simulations for bent 2

The results were obtained for all scouring maximum annual floods between 1953 and 2016 using the measured soil erosion function with $\varepsilon = 1$ mm in Fig. 6.4. The critical discharge Q_c is 7,345 ft³/s.

Year	Peak Discharge Date	Peak Discharge Q_{max} (ft³/s)	Return Period (yr)	Final Scour Depth z_f (ft)	Initial Erosion Rate (ft/hr)	Equilibrium Scour Depth z_{max} (ft)	$\dfrac{z_f}{z_{max}} \times 100\%$
1969	4/9/1969	34,748	152	14.7	1.4102	18.2	80
2010	9/25/2010	20,295	37	10.5	0.7075	18.5	56
2011	3/25/2011	15,785	21	8.9	0.5181	18.9	47
1984	6/22/1984	14,043	17	8.9	0.4344	19.0	47
1993	7/4/1993	13,633	16	8.1	0.4133	19.0	43
1997	4/2/1997	11,275	11	10.2	0.2787	18.7	54
1962	3/29/1962	10,865	10	4.3	0.2529	18.6	23
1960	3/31/1960	9,861	9	0.44	0.1862	18.4	2
1985	3/19/1985	8,651	7	1.03	0.0999	17.9	6

Year	Flow Duration Exceeding Critical Discharge t_s (hr)	Equivalent Time t_e (hr)	t_{90} (hr)	$\dfrac{t_e}{t_{90}}$	$\dfrac{Q_{max}}{Q_c}$	$\dfrac{Q_{max}t_s}{z_{maz}^3}$
1969	120	53.19	116.29	0.4574	4.73	691.67
2010	69	33.96	236.23	0.1438	2.76	221.17
2011	75	32.06	328.94	0.0975	2.15	175.36
1984	72	38.68	392.94	0.0984	1.91	147.41
1993	61	34.30	412.8	0.0831	1.86	121.24
1997	171	80.28	604.18	0.1329	1.54	294.84
1962	48	22.04	663.12	0.0332	1.48	81.05
1960	24	2.42	888	0.0027	1.34	37.99
1985	24	10.94	1,615.28	0.0068	1.18	36.2

The equivalent time t_e is the time required for the peak discharge in a flood to create the same predicted final scour depth as the one created by the recorded hydrograph. The value of t_e is included in Table 6.2 and varies from 2.4 to 80 hours. Also shown in Table 6.2 is the flow duration t_s when the computed bed shear stress exceeds the critical shear stress. The equivalent time of the maximum annual flood in 1997 is considerably longer than those of the other floods. This is due to the long period of time ($t_s = 171$ hr) when the bed shear stress is above the critical shear stress. The flood in April 1997 is about a 10-year flood. This flood produces a predicted final scour depth of 10.2 ft, which is about the same as the scour depth (10.5 ft) produced by a much larger flood in September 2010.

The predicted cumulative scour depth from August 1953 to April 2017 is 16.9 ft, which is close to the equilibrium scour depths of the maximum annual floods shown in Table 6.2. No flood with peak discharge less than 7,345 ft³/s was found to produce any scour. Figure 6.8 shows the results of SRICOS simulation for the period from August 1953 to April 2017. From top to bottom, the plots represent the time history of flow discharge Q, approach flow velocity V_1, approach flow depth Y_1, initial bed shear stress τ, initial rate of scour $\dfrac{dz}{dt}$, maximum (equilibrium) scour depth z_{max}, and computed scour depth z. The critical shear stress τ_c is shown as a dashed line in the initial bed shear stress plot. Note that the length of the hydrograph in the SRICOS simulation is less than 63 years because no flow was recorded during the winter months (December to February) when the river iced up. About a 10-year flood (peak discharge 10,865 ft³/s) in March 1962 was followed by about a 150-year-flood (peak discharge 34,748 ft³/s) in April 1969 to produce a cumulative scour depth close to 15

ft. In comparison, all the following floods from 1969 to 2007 together produce less than of 2 ft of additional scour, although five of these floods (1984, 1993, 1997, 2010, and 2011) have return periods greater than 10 years. This is due to pre-existing scour. The time rate of scour decreases with time, and scouring would stop if the existing scour depth is greater than the equilibrium scour depths of the following floods.

Although the measured critical shear stress is very high at this bridge site (τ_c = 18.6 N/m^2), the high initial soil erosion rate (1.4 ft/hr at a discharge of 34,748 ft^3/s) enables scouring to proceed rapidly once the bed shear stress exceeds the critical shear stress. For the flood of April 1969, the predicted final scour depth is equal to about 80% of the equilibrium scour depth at peak discharge. For those floods with return periods between 10 and 100 years, the ratio of the predicted final scour depth to equilibrium scour depth is around 50%. The predicted cumulative scour depth from August 1953 to April 2017 is close to the equilibrium scour depths of the large floods. This means that the equilibrium scour depth of a major flood such as the 100-year flood can be reached during the lifetime of the bridge. Hence, accounting for the time rate of scour would not substantially reduce the design scour depth at this site.

Table 6.3 and Figure 6.9 show the results obtained using the erosion-rate-versus-shear-stress curve that separates region III (medium erodibility) and region IV (low erodibility) in Figure 5.3. This curve has a soil critical shear stress of 9.5 N/m^2 compared with 18.6 N/m^2 measured at the bridge site. However, the initial soil erosion rate above the critical shear stress is extremely low (0.0096 ft/hr or about 3 mm/hr at a discharge of 34,748 ft^3/s). Consequently, all the predicted final scour depths are very small (< 1 ft). This is the situation where using the SRICOS method instead of the traditional HEC-18 method could result in substantial reduction in the predicted scour depth. Figure 6.9 shows the computed scour-depth-versus-time curve from August 1953 to April 2017. The predicted final scour depth is 2.7 ft, which is considerably less than the equilibrium scour depths of the floods shown in Table 6.3.

Table 6.3 shows that the maximum annual floods in 1997, 2001, and 2011 have very long equivalent times. SRICOS simulations were typically run for a period of two months for each flood, with the start date chosen to be the point in time when the discharge begins to increase from the base flow. For most floods, scouring ceases shortly after the stream flow has peaked when the flood is receding; this is due to pre-existing scour. The scour depth is already so large that a reduced discharge would not produce additional scour. For the floods of 1997, 2001, and 2011, however, the base flow is so high that scouring continues slowly for many days after the peak flow has passed.
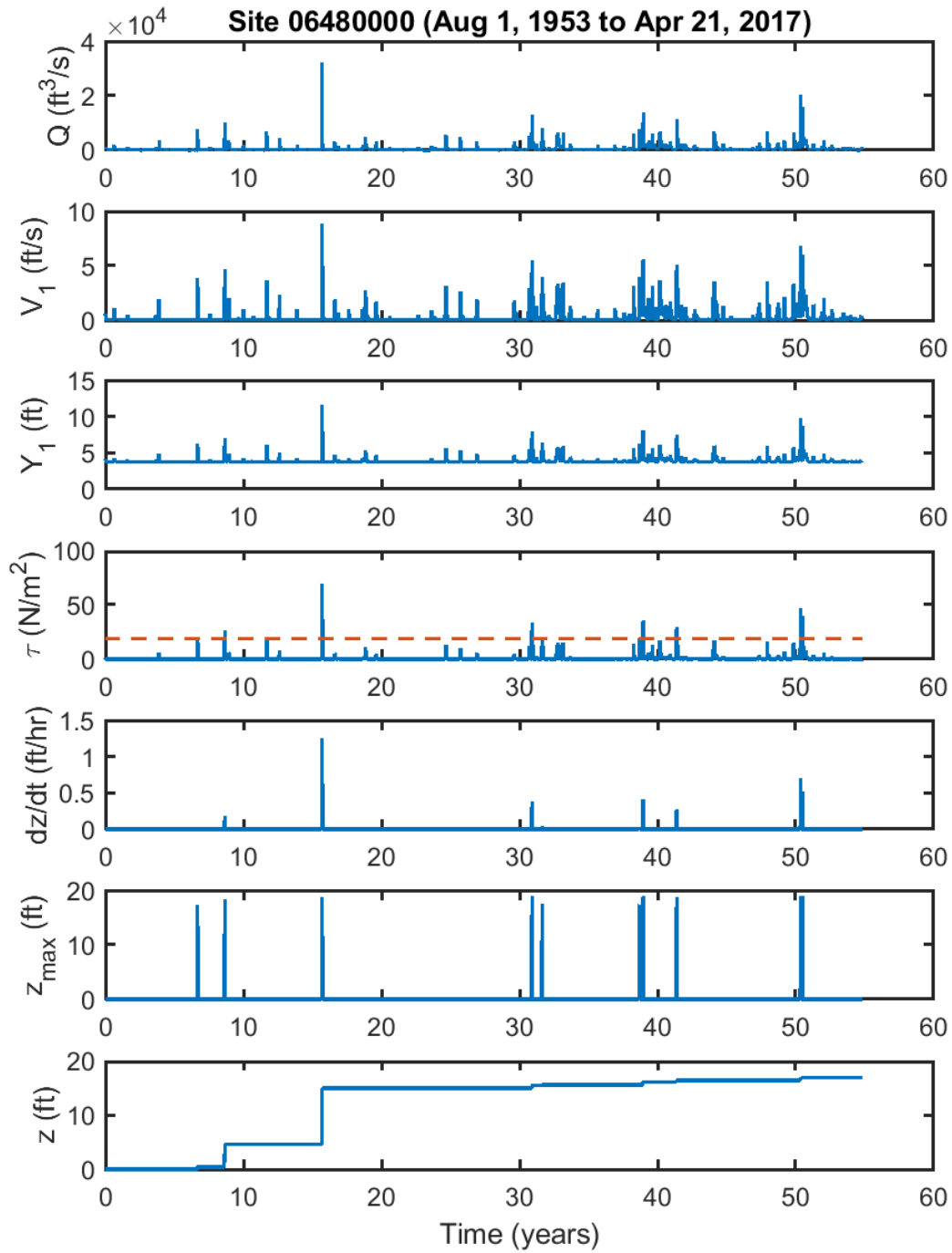
Figure 6.8 Computed scour history from August 1, 1953, to April 21, 2017, using the measured EFA curve
The red dashed line represents the critical shear stress.

Figure 6.9 shows that the final scour depth continues to increase with time, and a multitude of large and small floods contribute to the cumulative scour depth. If the maximum annual floods are used to compute the scour history, the predicted final scour depth will be 2.04 ft. This is somewhat less than the 2.7 ft computed using the complete recorded hydrograph. Hence, using only the maximum annual floods to predict scour may underestimate the final scour depth for soils with very slow rates of scour. However, the predicted final scour depths are also small in such cases. Instead of constructing a long sequence of large and small floods to predict a final scour depth that is small anyway, it may be more economical to apply a safety factor to account for the contributions of the smaller floods.

Table 6.3 Summary of results from SRICOS simulations for bent 2 for the maximum annual floods between 1953 and 2017 with return periods of 5 years and higher

The results were obtained using the erosion-rate-versus-shear-stress curve that separates soil regions III and IV in Fig. 5.3. The critical discharge Q_c is 4,581 ft³/s.

Year	Peak Discharge Date	Peak Discharge Q_{max} (ft³/s)	Return Period (yr)	Final Scour Depth z_f (ft)	Initial Erosion Rate (ft/hr)	Equilibrium Scour Depth z_{max} (ft)	$\dfrac{z_f}{z_{max}} \times 100\%$
1969	4/9/1969	34,748	152	0.51	0.0096	18.2	2.8
2010	9/25/2010	20,295	36.7	0.21	0.0044	18.5	1.1
2011	3/25/2011	15,785	21.1	0.48	0.0033	18.9	2.5
1984	6/22/1984	14,043	16.7	0.19	0.0029	19.0	1.0
1993	7/4/1993	13,633	15.7	0.16	0.0028	19.0	0.8
1997	4/2/1997	11,275	11.1	0.36	0.0021	18.7	1.9
1962	3/29/1962	10,865	10.4	0.09	0.002	18.6	0.5
1960	3/31/1960	9,861	8.9	0.03	0.0017	18.4	0.2
1985	3/19/1985	8,651	7.2	0.08	0.0013	17.9	0.4
1965	4/7/1965	7,893	6.3	0.05	0.0011	17.6	0.3
1995	4/20/1995	7,083	5.4	0.07	0.0009	17.1	0.4
1986	9/20/1986	6,857	5.2	0.04	0.0008	16.9	0.2
2001	4/25/2001	6,847	5.2	0.25	0.0008	16.9	1.5
2007	3/15/2007	6,683	5	0.04	0.0008	16.8	0.2

Year	Flow Duration Above Critical Discharge t_s (hr)	Equivalent Time t_e (hr)	t_{90} (hr)	$\dfrac{t_e}{t_{90}}$	$\dfrac{Q_{max}}{Q_c}$	$\dfrac{Q_{max} t_s}{z_{maz}^3}$
1969	168	54.88	17,153	0.00320	7.59	968.33
2010	126.5	47.84	37,594	0.00127	4.43	405.48
2011	779.5	147.72	51,124	0.00289	3.45	1822.53
1984	168	66.59	59,228	0.00112	3.07	343.96
1993	136	58.21	61,543	0.00095	2.98	270.31
1997	456	173.88	79,772	0.00218	2.46	786.24
1962	96	45.4	84,176	0.00054	2.37	162.09
1960	48	17.7	97,405	0.00018	2.15	75.98
1985	96	59.8	120,085	0.00050	1.89	144.80
1965	72	44.49	140,270	0.00032	1.72	104.24
1995	114	77.7	170,013	0.00046	1.55	161.49
1986	72	47.46	180,409	0.00026	1.50	102.28
2001	465	301.29	180,908	0.00167	1.49	659.62
2007	87.25	50.14	189,245	0.00027	1.46	122.97
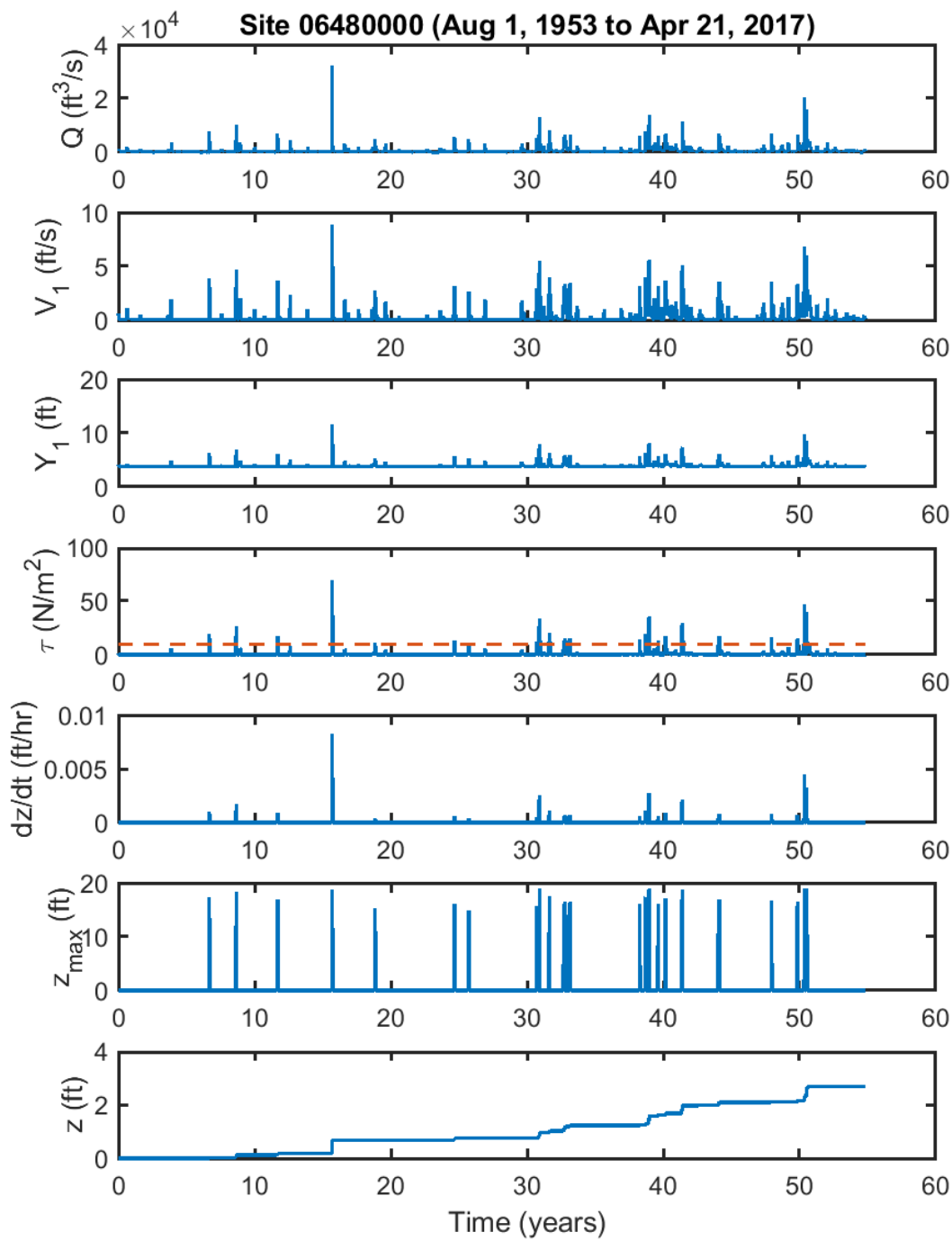
Figure 6.9 Computed scour history from August 1, 1953, to April 21, 2017, using the erosion-rate-versus-shear-stress curve that separates soil regions III and IV

45

Table 6.4 and Figure 6.10 show the results obtained using the erosion-rate-versus-shear-stress curve that separates region II (high erodibility) from region III (medium erodibility) in Figure 5.3. This curve has a soil critical shear stress of 1.3 N/m^2 and an extremely high initial soil erosion rate of 9.2 ft/hr at a discharge of 34,748 ft^3/s. Figure 6.10 shows the predicted scour history from August 1953 to April 2017. The predicted final scour depth is 18.1 ft, which is nearly the same as the equilibrium scour depths of the larger floods shown in Table 6.4. Furthermore, the predicted scour depth is already 17.1 ft by April 1969. All the subsequent floods from 1969 to 2017 together produce only 1 ft of additional scour. This is like the trend shown in Figure 6.8. However, more floods in Figure 6.10 can contribute to scour due to the lower soil critical shear stress and higher initial erosion rates. Therefore, the cumulative scour depth in Figure 6.10 approaches equilibrium condition sooner.

Table 6.4 summarizes the key results from the SRICOS simulations. Only the maximum annual floods with return periods of two years and higher are included in the table. For those floods that are greater than the 10-year flood, the predicted final scour depth is close to the equilibrium scour depth. The computed equivalent time ranges from one to two days, with the flood of April 1997 being an exception.

The duration of time when the measured discharge exceeds the critical discharge cannot be determined for some floods in Table 6.4 because the critical shear stress is so low, and the base flow exceeds the critical discharge for a long period of time. In such cases, flow duration is probably not an important parameter anyway due to the high rates of scour. Scouring would stop long before the base flow falls below the critical discharge.

Figure 6.11 is a plot of the $\frac{z_f}{z_{max}}$ ratio versus $\frac{t_e}{t_{90}}$ ratio for all the computed results in Tables 6.2, 6.3 and 6.4. For the hyperbolic model, the two parameters are related through Eq. (5.49). Thus, all the computed results fall on the solid line represented by Eq. (5.49). By normalizing the computed final scour depth and equivalent time by z_{max} and t_{90}, this plot provides a concise summary of the stage of scour that can be produced by floods of different return periods in different soil categories. For example, when SRICOS simulations are conducted using the erosion-rate-versus-shear-stress curve that separates soil regions III and IV in Figure 5.3, the computed $\frac{z_f}{z_{max}}$ and $\frac{t_e}{t_{90}}$ ratios are all close to zero, which means that the scour depths produced by the maximum annual floods are far from the equilibrium condition. On the other hand, when SRICOS simulations are conducted using the measured EFA curve, the computed $\frac{z_f}{z_{max}}$ and $\frac{t_e}{t_{90}}$ ratios are much larger, suggesting that a sequence of such floods would produce a cumulative scour depth close to the equilibrium scour depth of a major flood such as the 100-year flood. Hence, Figure 6.11 may be used as a screening tool to determine whether time rate of scour is an important factor at a given site and to assess the effect of soil erodibility on the computed scour depth.

Table 6.4 Summary of results from SRICOS simulations for bent 2 for the maximum annual
floods from 1953 to 2017 with return period of 2 years and higher
*The results were obtained using the erosion-rate-versus-shear-stress curve that
separates soil regions II and III in Fig. 5.3. The critical discharge Q_c is 1,609 ft³/s.*

Year	Peak Discharge Date	Peak Discharge Q_{max} (ft³/s)	Return Period (yr)	Final Scour Depth (ft)	Initial Erosion Rate (ft/hr)	Equilibrium Scour Depth z_{max} (ft)	$\dfrac{z_f}{z_{max}} \times 100\%$
1969	4/9/1969	34,748	152	17.41	9.1734	18.22	96
2010	9/25/2010	20,295	36.7	15.4	2.7692	18.54	83
2011	3/25/2011	15,785	21.1	14.72	1.7705	18.94	78
1984	6/22/1984	14,043	16.7	14.55	1.4104	18.97	77
1993	7/4/1993	13,633	15.7	13.71	1.3273	18.96	72
1997	4/2/1997	11,275	11.1	15.25	0.8674	18.71	82
1962	3/29/1962	10,865	10.4	10.79	0.7922	18.63	58
1960	3/31/1960	9,861	8.9	6.2	0.6172	18.37	34
1985	3/19/1985	8,651	7.2	9.35	0.4285	17.93	52
1965	4/7/1965	7,893	6.3	7.06	0.3256	17.56	40
1995	4/20/1995	7,083	5.4	8.72	0.231	17.09	51
1986	9/20/1986	6,857	5.2	6.54	0.2076	16.94	39
2001	4/25/2001	6,847	5.2	8.75	0.2066	16.93	52
2007	3/15/2007	6,683	5	5.78	0.1905	16.81	34
1978	3/29/1978	6,109	4.6	7.78	0.1399	16.37	48
1992	6/20/1992	5,904	4.3	4.31	0.124	16.2	27
1994	6/26/1994	5,802	4.3	6.28	0.1165	16.11	39
1957	6/18/1957	5,453	3.9	0.38	0.093	15.78	2
1972	6/1/1972	5,187	3.8	3.09	0.0771	15.52	20
1979	4/14/1979	4,838	3.4	3.18	0.0591	15.14	21
1966	3/14/1966	4,674	3.3	1.38	0.0517	14.96	9
1980	6/26/1980	3,916	2.8	0.39	0.0252	13.98	3
2009	3/29/2009	3,834	2.7	0.98	0.0231	13.86	7
2013	6/29/2013	3,567	2.5	1.45	0.017	13.46	11
1970	3/6/1970	3,434	2.5	0.36	0.0144	13.25	3
1983	3/7/1983	3,383	2.4	0.44	0.0135	13.17	3
1973	3/8/1973	3,085	2.3	0.41	0.0089	12.66	3
1996	5/30/1996	3,065	2.2	2.15	0.0087	12.62	17
2006	3/20/2006	2,860	2.1	0.57	0.0063	12.24	5
2008	6/10/2008	2,850	2.1	0.48	0.0062	12.22	4
2012	5/9/2012	2,583	2	0.21	0.0039	11.68	2

Table 6.4 Summary of results from SRICOS simulations for bent 2 for the maximum annual floods from 1953 to 2017 with return period of 2 years and higher

Year	Flow Duration Exceeding Critical Discharge t_s (hr)	Equivalent Time t_e (hr)	t_{90} (hr)	$\dfrac{t_e}{t_{90}}$	$\dfrac{Q_{max}}{Q_c}$	$\dfrac{Q_{max}t_s}{z_{maz}^3}$
1969	360	17.88	17.88	1.0000	21.60	2068.2
2010	447.5	32.79	60.27	0.5441	12.61	1425.1
2011	NA	37.33	96.26	0.3878	9.81	NA
1984	480	44.3	121.02	0.3661	8.73	987.41
1993	NA	37.33	128.53	0.2904	8.47	NA
1997	NA	95.04	194.14	0.4895	7.01	NA
1962	168	32.36	211.64	0.1529	6.75	282.29
1960	288	15.16	267.91	0.0566	6.13	458.13
1985	360	45.6	376.61	0.1211	5.38	540.29
1965	216	36.26	485.58	0.0747	4.91	314.86
1995	NA	77.1	665.88	0.1158	4.40	NA
1986	264	51.32	734.18	0.0699	4.26	372.39
2001	NA	87.67	737.53	0.1189	4.26	NA
2007	NA	46.23	794.33	0.0582	4.15	NA
1978	456	105.96	1053.1	0.1006	3.80	635.02
1992	235	47.36	5904	0.0080	3.67	326.34
1994	323	88.38	1244.73	0.0710	3.61	448.22
1957	48	4.19	1528.37	0.0027	3.39	66.613
1972	312	50.03	5186.5	0.0096	3.22	432.91
1979	312	68.07	4838	0.0141	3.01	434.95
1966	144	29.41	4674	0.0063	2.90	201.03
1980	96	15.9	4987.52	0.0032	2.43	137.59
2009	NA	45.68	3833.5	0.0119	2.38	NA
2013	226	95.73	7137.85	0.0134	2.22	330.58
1970	72	25.72	8290.4	0.0031	2.13	106.29
1983	168	33.8	8800	0.0038	2.10	248.80
1973	119	47.45	12759.52	0.0037	1.92	180.93
1996	734	299.14	13113.66	0.0228	1.90	1119.31
2006	180.25	94.91	17490.23	0.0054	1.78	281.12
2008	220.75	80.66	17756.73	0.0045	1.77	344.77
2012	112	55	27048.42	0.0020	1.61	181.56
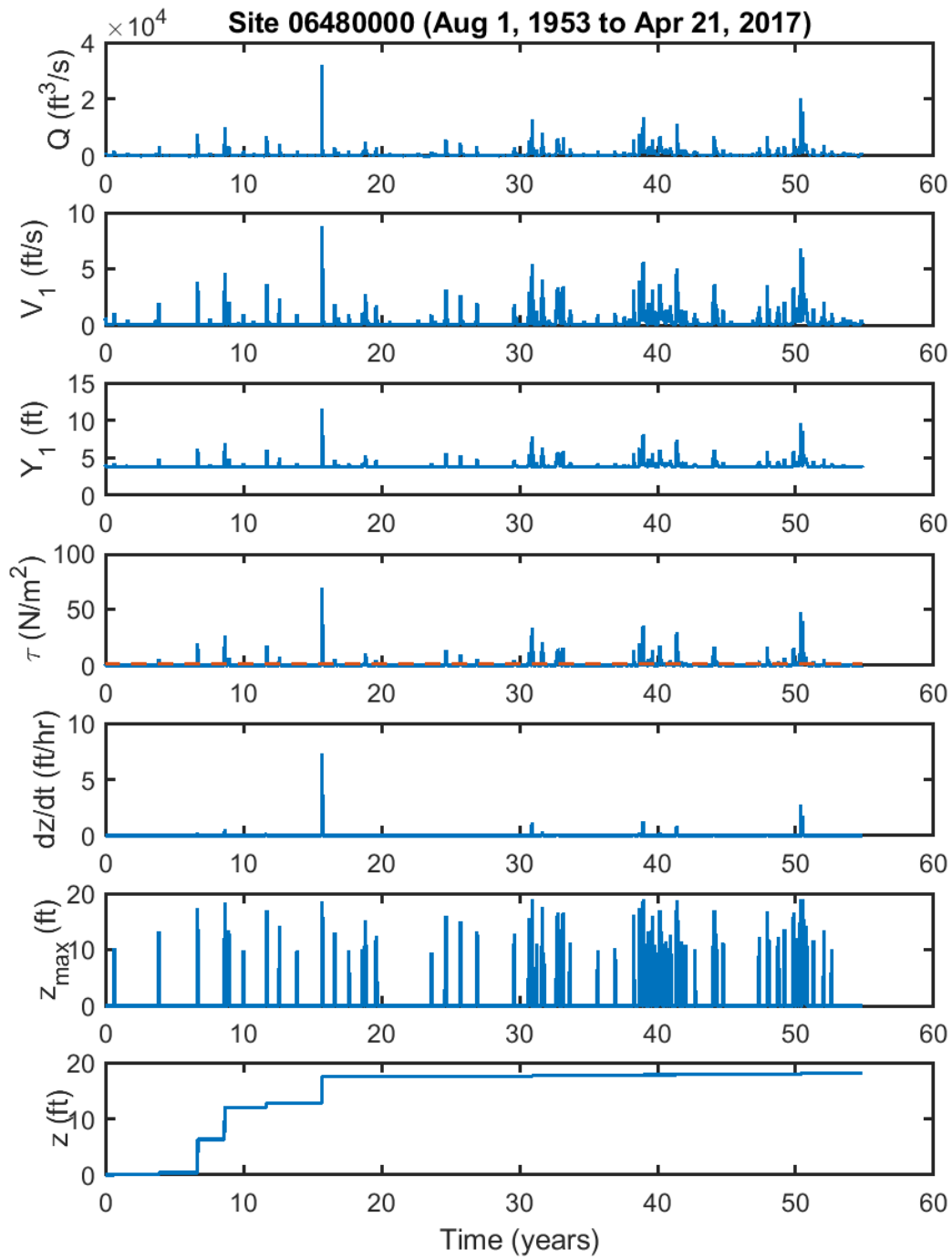
Figure 6.10 Computed scour history from August 1, 1953, to April 21, 2017, using the erosion-rate-versus-shear-stress curve that separates soil regions II and III
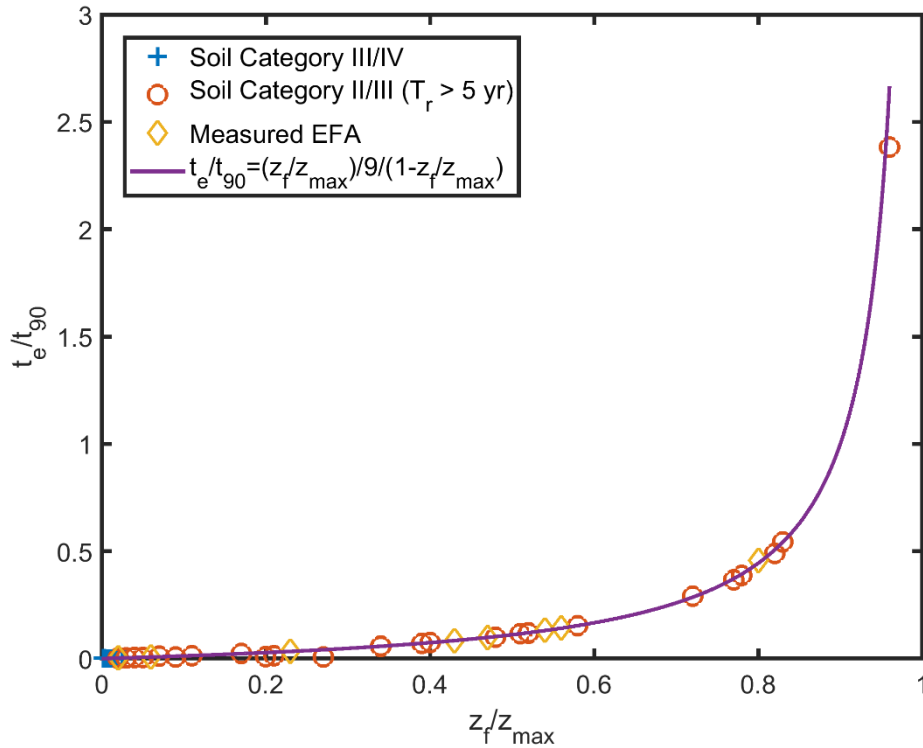
Figure 6.11 Variations of t_e/t_{90} ratio with z_f/z_{max} ratio for the maximum annual floods in Tables 6.2, 6.3, and 6.4

Figure 6.12 show the results of SRICOS simulation obtained using the erosion-rate-versus-shear-stress curve that separates soil region I (very high erodibility) and region II (high erodibility). This EFA curve has a very low soil critical shear stress (0.21 N/m^2) and extremely high initial soil erosion rates. Consequently, equilibrium scour depth is reached by all the maximum annual floods. The predicted final scour depth from August 1953 to April 2017 is 19 ft. Because the equilibrium scour depth is reached practically by every flood in the hydrograph, only a larger following flood can produce additional scour. When a small flood follows a large flood, the existing scour depth is already greater than the equilibrium scour depth of the small flood, and thus no additional can occur. Figure 6.12 shows that the final scour depth is achieved in the first 10 years of the numerical simulation. These results are consistent with the scour development in non-cohesive soils, and the bridge should be evaluated for scour based on the peak discharge of a single flooding event such as the 100-year flood.
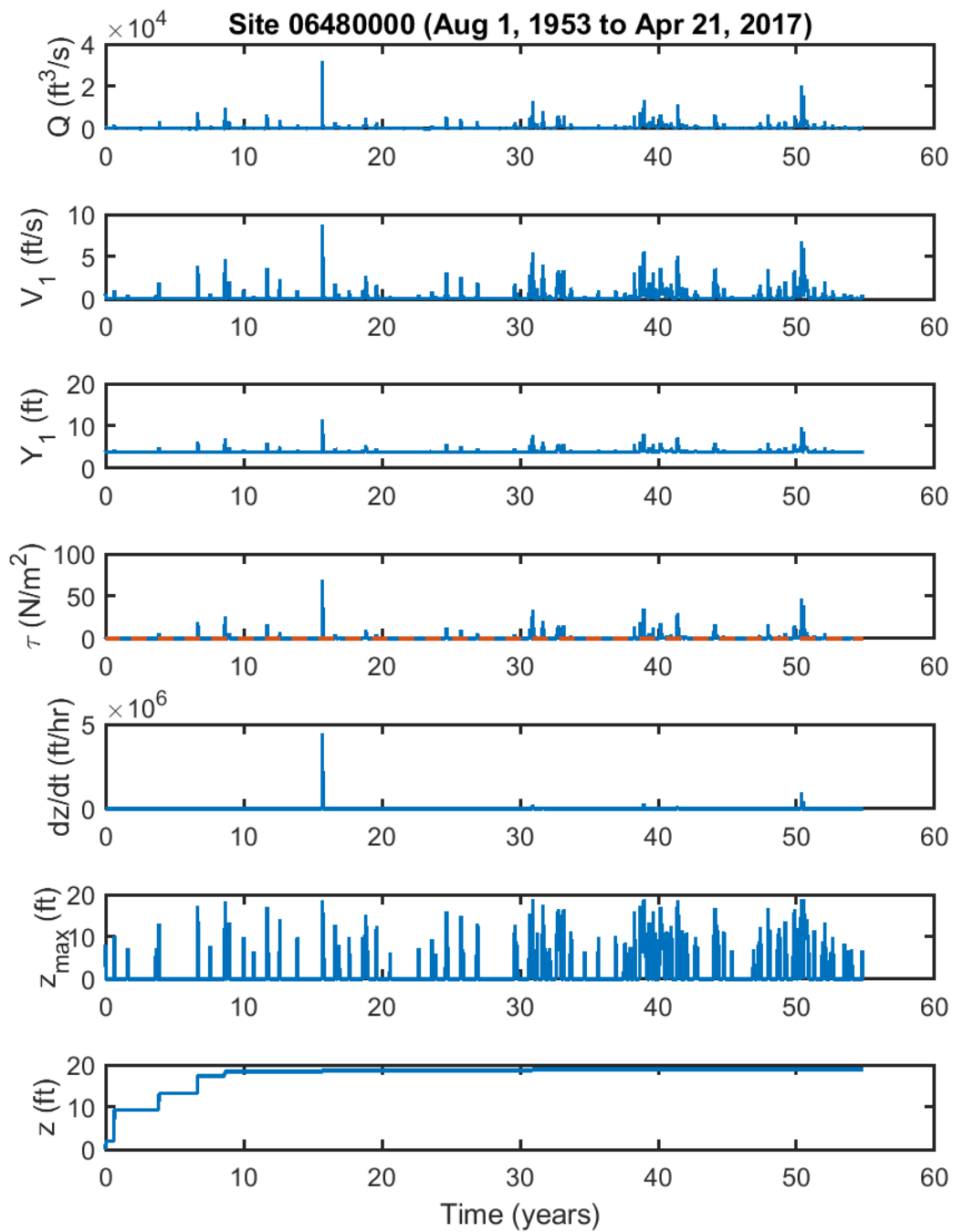
Figure 6.12 Computed scour history from August 1, 1953, to April 21, 2017, using the erosion-rate-versus-shear-stress curve that separates soil regions I and II

6.3   Equivalent Time

The equivalent time t_e of a flood can be functionally related to the flow and soil parameters as follows (see Section 5.8):

$$\frac{t_e}{t_{90}} = \phi\left(\frac{Q_{max}}{Q_c}, \frac{Q_{max}t_{hydro}}{z_{max}^3}, a'\right) \tag{6.1}$$

where t_{90} is the time required to reach 90% of the equilibrium scour depth at peak discharge, Q_{max} is peak discharge, Q_c is discharge at critical shear stress, t_{hydro} is duration of hydrograph, z_{max} is equilibrium scour depth at peak discharge, and a' is a soil erosion rate constant [see, Eq. (5.2)].

Eq. (6.1) shows that the normalized equivalent time $\frac{t_e}{t_{90}}$ is a function of the normalized peak discharge $\frac{Q_{max}}{Q_c}$, dimensionless hydrograph duration $\frac{Q_{max}t_{hydro}}{z_{max}^3}$, and soil erosion rate constant a' [or both a' and b' if $\dot{z}$ is computed using Eq. (5.3)]. Figure 6.13 shows the results of SRICOS simulation for the maximum annual flood in 2010. The scour history is computed for the time period from September 14 to November 19 using the measured soil erosion function (Figure 6.4). The critical discharge and critical shear stress are shown as a dashed line in the Q-versus-t and τ-versus-t plots. The measured discharge exceeds the critical discharge for 69 hours, and the final scour depth is reached long before the flood has subsided. These results suggest that the actual flood duration is not important if the rates of scour are high. When the flood duration is much longer than the time period of scour, the correlation between t_e and t_{hydro} will be poor and the dimensionless group $\frac{Q_{max}t_{hydro}}{z_{max}^3}$ may be neglected. Since the soil erosion rate constant a' does not change for a given site, the equivalent time would vary primarily with discharge. The relationship is shown in Figure 6.14. As seen, there is an almost linear relationship between the $\frac{t_e}{t_{90}}$ and $\frac{Q_{max}}{Q_c}$ ratios. The R^2-value of the regression equation is 0.9233 and the root-mean-square error is 0.04067.
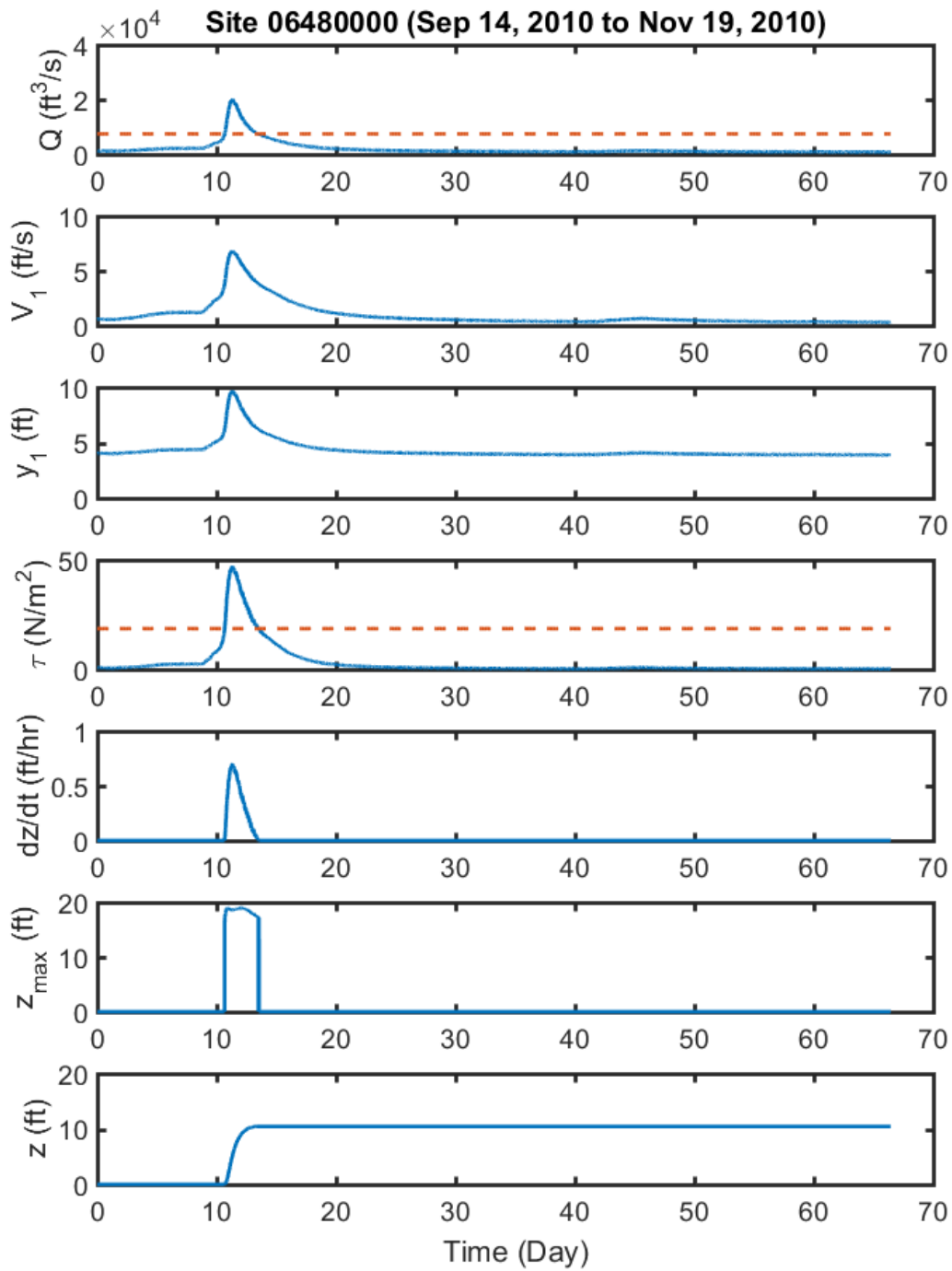
Figure 6.13 SRICOS simulation for bent 2, September 4 to November 19, 2010
The critical discharge and critical shear stress are shown as a dashed line in the discharge and initial bed shear stress plots.
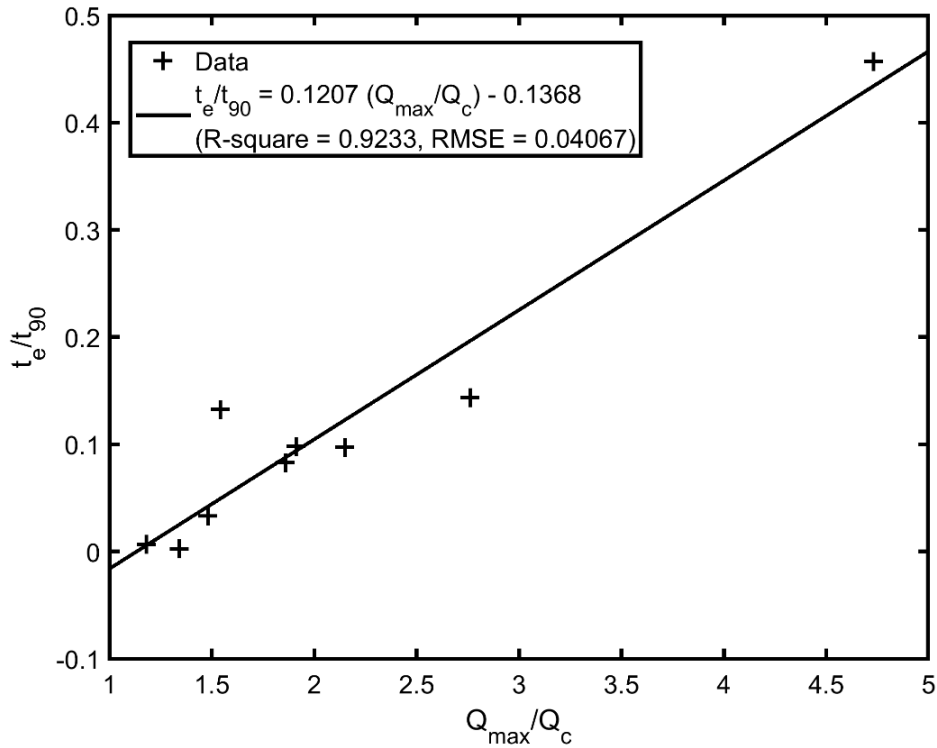
Figure 6.14 Normalized equivalent time versus normalized peak discharge
The equivalent time is computed using the measured soil erosion function.

The regression equation shown in Figure 6.14 significantly under-predicts the equivalent time of the flood of April 1997 ($\frac{Q_{max}}{Q_c} = 1.54$). The value of $\frac{t_e}{t_{90}}$ computed using the regression equation is 0.0491, whereas the $\frac{t_e}{t_{90}}$ value determined using the recorded hydrograph is 0.1329 (Table 6.2). Figure 6.15 shows the SRICOS simulation for this flood. The measured discharge exceeds the critical discharge for more than one week, and the long duration of high flows results in a large equivalent time for a relatively small flood. Such a condition is common for spring floods in South Dakota and is not captured by the regression curve shown in Figure 6.14. Figure 6.16 presents the results of multiple regression with both $\frac{Q_{max}}{Q_c}$ and $\frac{Q_{max}t_s}{z_{max}^3}$ as the independent variables. The time duration when the measured discharge exceeds the critical discharge, t_s, is used to define the length of the hydrograph t_{hydro}. Including $\frac{Q_{max}t_s}{z_{max}^3}$ as an additional parameter improves the prediction of the $\frac{t_e}{t_{90}}$ ratio. The R^2-value is increased from 0.9233 to 0.9956, and the root-mean-squared error is reduced from 0.04067 to 0.01058. More important, the predicted $\frac{t_e}{t_{90}}$ value (0.1374) for the maximum annual flood in 1997 is close to the value of 0.1329 computed using the recorded hydrograph. Table 6.5 compares the $\frac{t_e}{t_{90}}$ ratios computed using the one- and two-parameter regression equations with the values obtained from the SRICOS simulations.
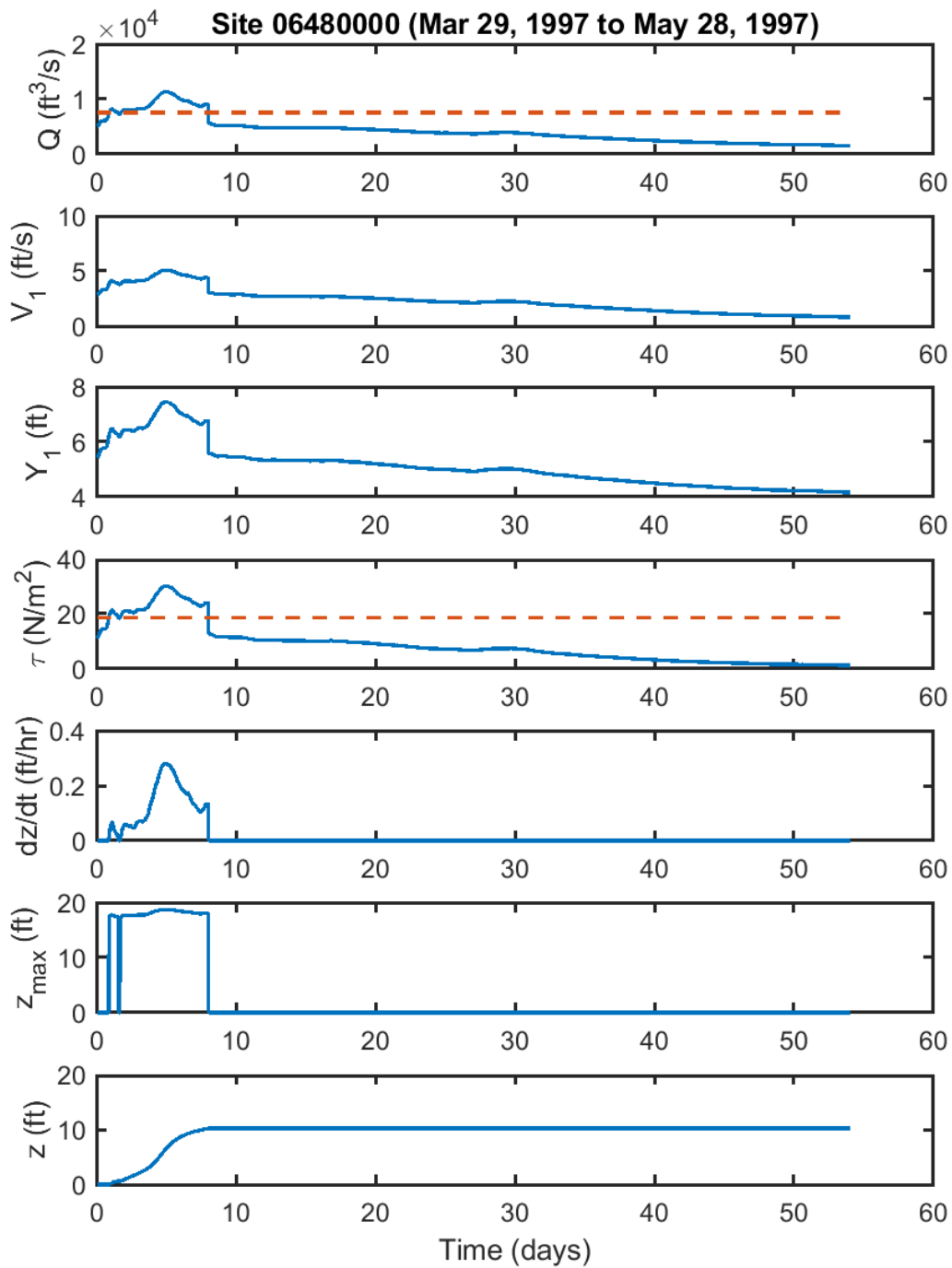
Figure 6.15 SRICOS simulation for bent 2, March 29 to May 28, 1997
The critical discharge and critical shear stress are shown as a dashed line in the discharge and initial bed shear stress plots. The flow record from April 6 to April 12 is missing.

55
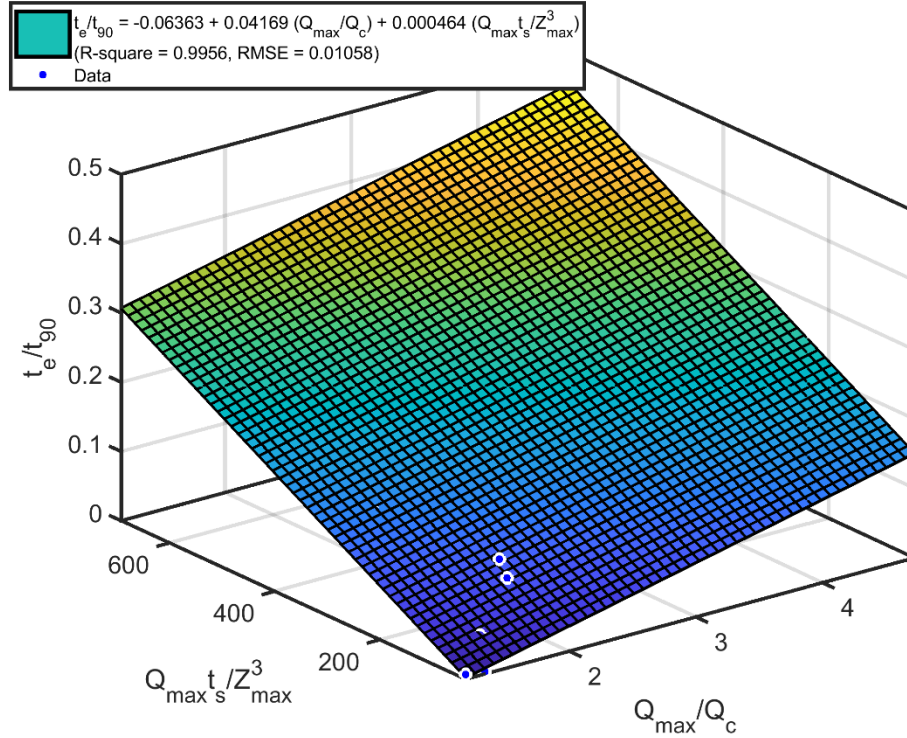
Figure 6.16 Normalized equivalent time versus normalized peak discharge and flood duration
The equivalent time is computed using the measured soil erosion function.

Table 6.5 Comparison of t_e/t_{90} values from the one- and two-parameter equations with the results of SRICOS simulations conducted using the measured soil erosion function

$\dfrac{Q_{max}}{Q_c}$	1.18	1.34	1.48	1.54	1.86	1.91	2.15	2.76	4.73
$\dfrac{t_e}{t_{90}}$ (Table 6.2)	0.0068	0.0027	0.0332	0.1329	0.0831	0.0984	0.0975	0.1438	0.4574
$\dfrac{t_e}{t_{90}}$ (Fig. 6.14)	0.0056	0.0249	0.0418	0.0491	0.0877	0.0937	0.1227	0.1963	0.4340
$\dfrac{t_e}{t_{90}}$ (Fig. 6.16)	0.0024	0.0099	0.0357	0.1374	0.0702	0.0844	0.1074	0.1541	0.4545

Figure 6.17 shows the results of regression analysis for the $\dfrac{t_e}{t_{90}}$ ratio obtained using the erosion-rate-versus-shear-stress curve that separates soil regions III and IV (see Table 6.3). In addition to the maximum annual flood in 1997, the maximum annual floods in 2001 and 2011 also produce long equivalent time. Good correlation between the $\dfrac{t_e}{t_{90}}$ and $\dfrac{Q_{max}}{Q_c}$ ratios is obtained when the three outliners are removed; the R^2-value is 0.9554 and the root-mean-square error is 0.0001936. Figure 6.18 shows the results of SRICOS simulation for the flood of March 2011. The long equivalent time for this flood is produced by a high base flow; the measured discharge was above the critical discharge for four weeks. This has a significant effect on the predicted final scour depth and will need to be addressed in hydrograph generation. One approach is to shift the solid line in Figure 6.17 upward to the dashed line

to create an envelope curve. However, this will increase the equivalent time of all the floods, which will in turn increase the predicted scour depth. Another approach is to include $\frac{Q_{max}t_s}{z_{max}^3}$ as an additional parameter in the regression equation. The relationship is shown in Figure 6.19. The R^2 value of the multiple regression equation is 0.9444 and the root-mean-square error is 0.0002571. The second approach is more satisfactory on theoretical grounds, but the problem is then shifted to determining the values of t_s for the individual floods. Table 6.6 shows a comparison of the $\frac{t_e}{t_{90}}$ values computed using the one- and two-parameter regression equations with the values shown in Table 6.3. As seen, including $\frac{Q_{max}t_s}{z_{max}^3}$ as an additional parameter significantly improves the predicted $\frac{t_e}{t_{90}}$ ratio for the maximum annual floods in 1997 and 2011 ($\frac{Q_{max}}{Q_c}$= 2.46 and 3.45).
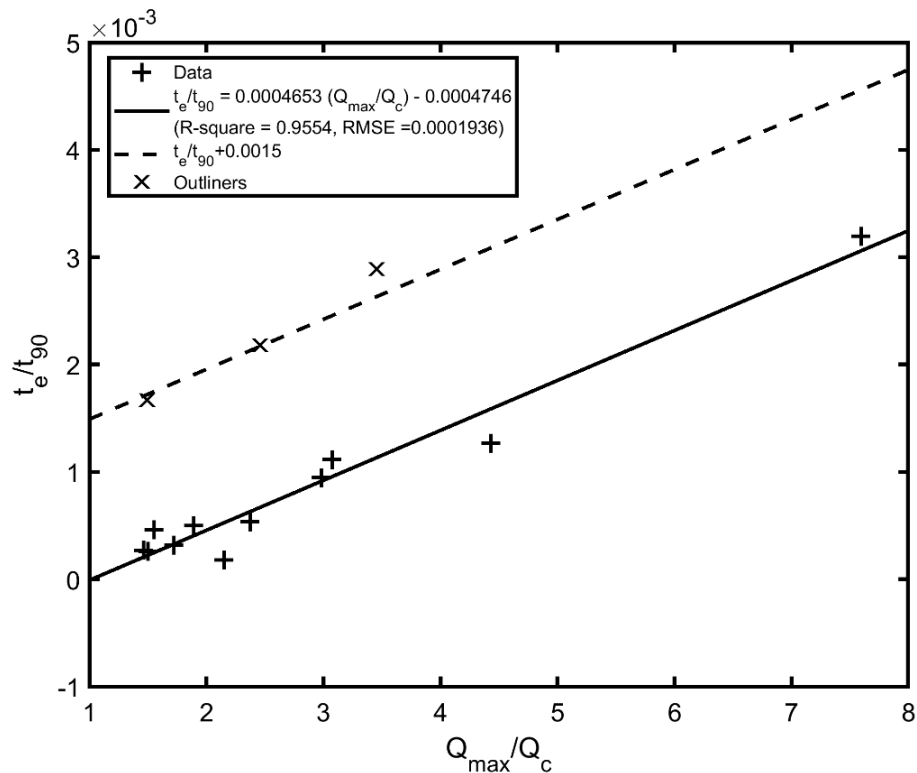
Figure 6.17 Normalized equivalent time versus normalized peak discharge
The equivalent time is computed using the erosion-rate-versus-shear-stress curve that separates soil regions III and IV in Fig. 5.3.
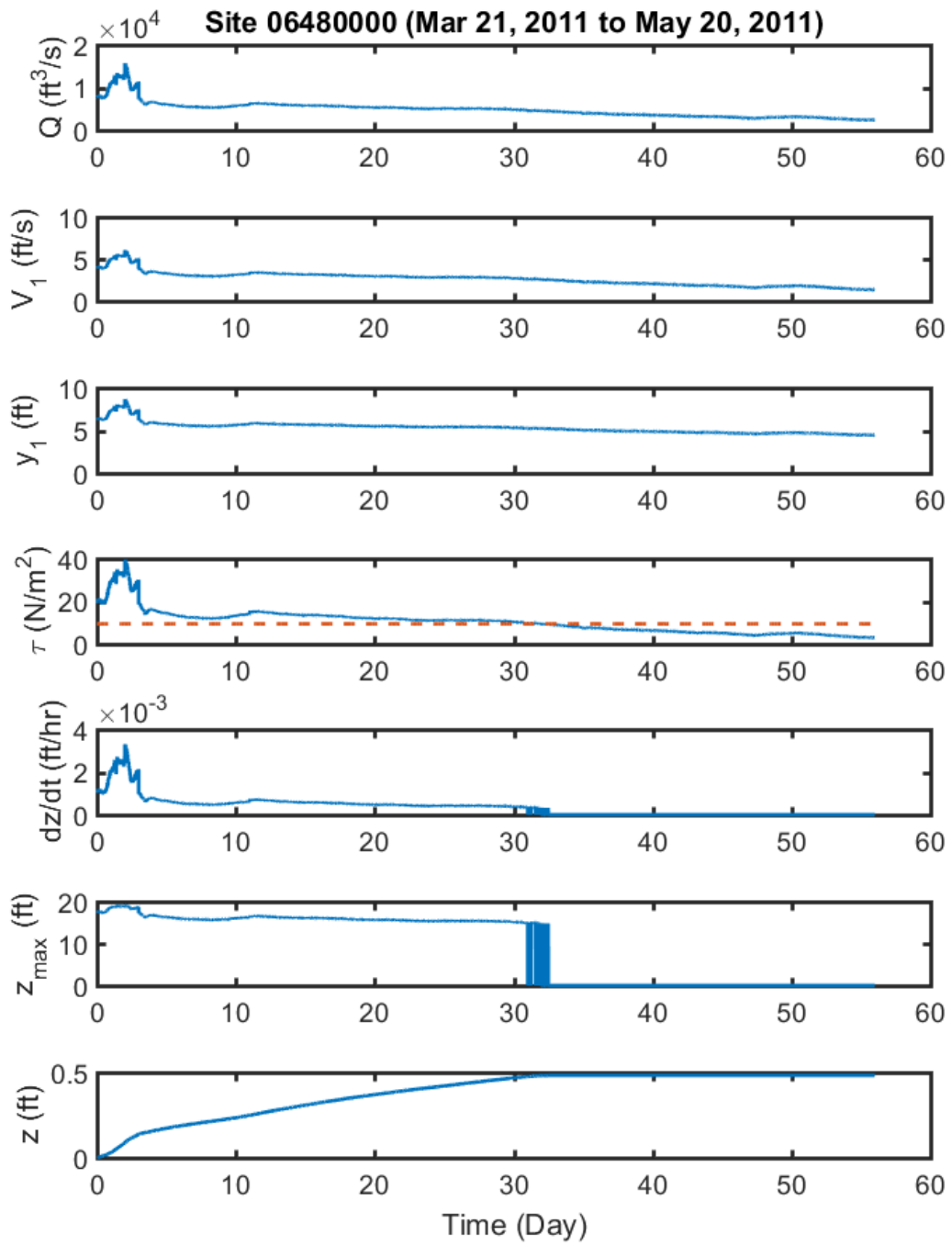
Figure 6.18 SRICOS simulation for bent 2, March 2011 to May 20, 2011
The critical shear stress is shown as a dashed line in the initial bed shear stress plot.
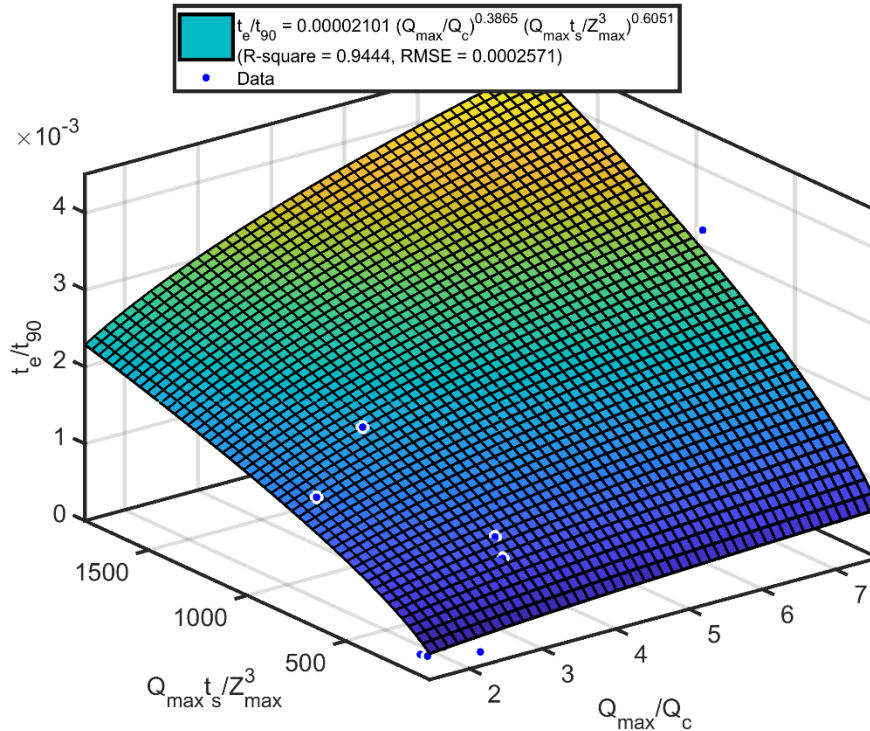
Figure 6.19 Normalized equivalent time versus normalized peak discharge and flood duration
The equivalent time is computed using the erosion-rate-versus-shear-stress curve that separates soil regions III and IV in Fig. 5.3.

Table 6.6 Comparison of t_e/t_{90} values from the one- and two-parameter equations with the results of SRICOS simulations conducted using the erosion-rate-versus-shear-stress curve that separates soil regions III and IV in Fig. 5.3

$\dfrac{Q_{max}}{Q_c}$	2.37	2.46	2.98	3.07	3.45	4.43	7.59
$\dfrac{t_e}{t_{90}}$ (Table 6.3)	0.00054	0.00218	0.00095	0.00112	0.00289	0.00127	0.0032
$\dfrac{t_e}{t_{90}}$ (Fig. 6.17)	0.00063	0.00067	0.00091	0.00095	0.0011	0.0016	0.0031
$\dfrac{t_e}{t_{90}}$ (Fig. 6.19)	0.00064	0.00170	0.00095	0.0011	0.0032	0.0014	0.0029

Figure 6.20 shows the results of regression analysis for the $\dfrac{t_e}{t_{90}}$ ratio computed using the erosion-rate-versus-shear-stress curve that separates soil regions II and III in Figure 5.3. Several floods also produce long equivalent time, but good correlation between the $\dfrac{t_e}{t_{90}}$ ratio and $\dfrac{Q_{max}}{Q_c}$ ratio is obtained when the results are normalized. The R^2-value is 0.9223 and the root-mean-square error is 0.06238. Figure 6.21 shows that the R^2-value is increased to 0.9744 and the root-mean-square error is reduced to 0.0383 when $\dfrac{Q_{max}t_s}{z_{max}^3}$ is included as an additional parameter. Table 6.7 shows a comparison of the $\dfrac{t_e}{t_{90}}$

values computed using the one- and two-parameter regression equations with the values in Table 6.4. In general, adding the parameter $\frac{Q_{max}t_s}{z_{max}^3}$ improves the prediction of the $\frac{t_e}{t_{90}}$ values. However, the differences are not as great when compared with Tables 6.5 and 6.6, especially for the large floods. This is due to the high rates of scour in regions II and III. Consequently, flood duration becomes less important in determining the predicted final scour depth.
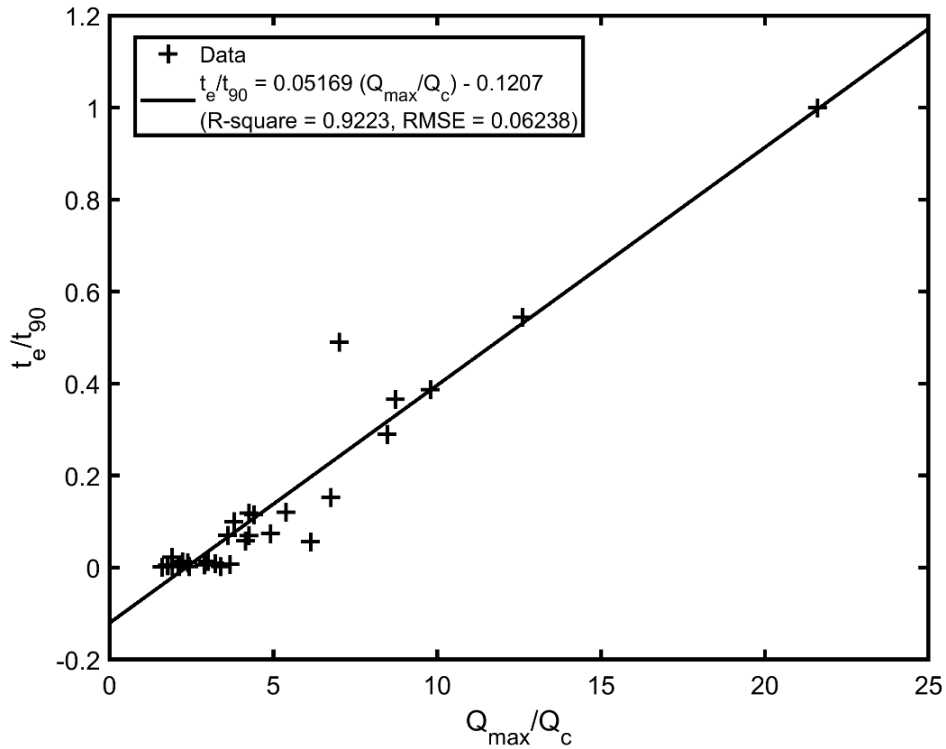
Figure 6.20 Normalized equivalent time versus normalized peak discharge
The equivalent time is computed using the erosion-rate-versus-shear-stress curve that separates soil regions II and III.
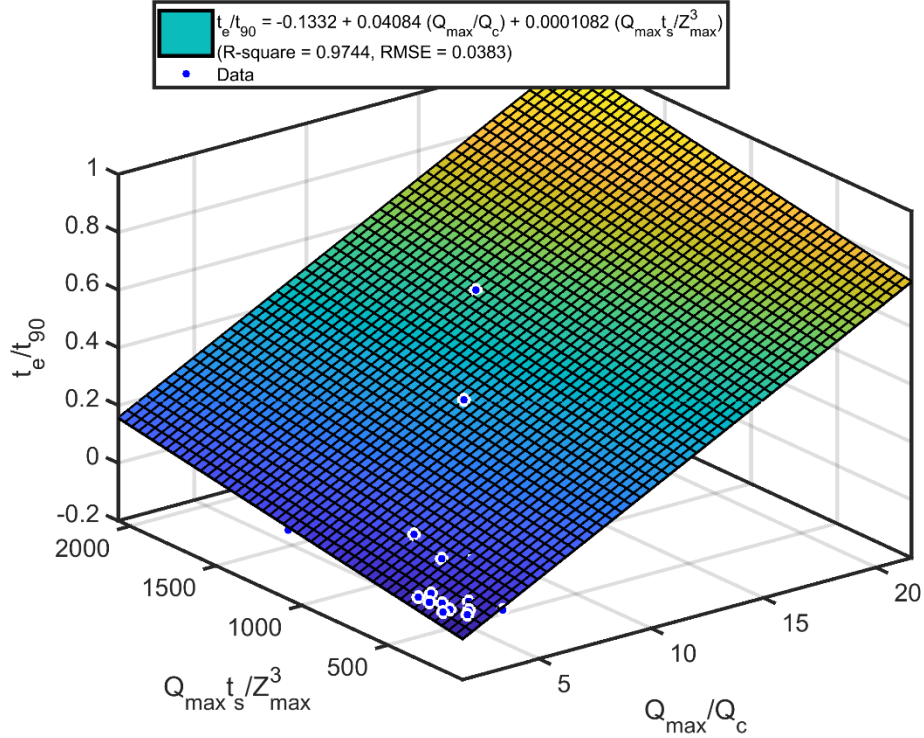
Figure 6.21 Normalized equivalent time versus normalized peak discharge and flood duration
*The equivalent time is computed using the erosion-rate-versus-shear-stress curve that
separates soil regions II and III in Fig. 5.3.*

**Table 6.7 Comparison of t_e/t_{90} values from the one- and two-parameter equations with the
results of SRICOS simulations conducted using the erosion-rate-versus-shear-stress
curve that separates soil regions II and III in Fig. 5.3**

$\dfrac{Q_{max}}{Q_c}$	4.26	4.91	5.38	6.13	6.75	8.73	12.61	21.6
$\dfrac{t_e}{t_{90}}$ (Table 6.4)	0.0699	0.0747	0.1211	0.0566	0.1529	0.3661	0.5441	1
$\dfrac{t_e}{t_{90}}$ (Fig. 6.20)	0.0995	0.1331	0.1574	0.1962	0.2282	0.3306	0.5311	0.9958
$\dfrac{t_e}{t_{90}}$ (Fig. 6.21)	0.0811	0.1014	0.1450	0.1667	0.1730	0.3302	0.5360	0.9727

6.4   Generation of Future Hydrographs and Scour Risk Analysis

In this section, we present the results of hydrograph generation and risk analysis of scour depth for
bent 2 computed using the SRICOS method. The SRICOS simulations were conducted using the
measured EFA curve and the soil erosion chart in Figure 5.3.

The probability of exceedance R that a flood having a return period T_r will be exceeded at least once in
a project life of L_p years is given by:

61

$$R = 1 - \left(1 - \frac{1}{T_r}\right)^{L_p} \tag{6.2}$$

Table 6.8 shows the exceedance probability for the 100-year flood for different project lives. For example, if the design life of a bridge is 75 years and the design flood has a return period of 100 years, there is a 53% chance that the design flood will be exceeded at least once during the design life of the bridge. For non-cohesive soils, it is assumed that the equilibrium scour depth can be reached in the course of a single design flood. Therefore, bridges over waterways are currently operated at a relatively high-risk level. In reality, the risk level could be much lower due to the slow rates of scour in some cohesive soils.

Table 6.8 Exceedance probability for 100-year flood as a function of project life

Project Life (yr)	Exceedance Probability (%)
50	39
75	53
100	63

Figure 6.22 shows the results of SRICOS simulation for one constructed series of 75 maximum annual floods conducted using the measured EFA curve (Fig. 6.4, $\varepsilon = 1$ mm). The measured soil critical shear stress τ_c is 18.6 N/m². The initial erosion rate is 1.4 ft/hr at a discharge of 34,748 ft³/s. The critical discharge to produce scour is 7,345 ft³/s. From top to bottom, the plots represent the magnitude of annual peak flow Q, equivalent time t_e, approach flow velocity V_1, approach flow depth Y_1, initial bed shear stress τ, initial rate of scour $\frac{dz}{dt}$, equilibrium scour depth z_{max}, and cumulative scour depth z. The equivalent time is computed using the regression equation shown in Figure 6.14. Although only a few large floods contribute to scour, the soil erosion rates are so high that the predicted final scour depth (16.3 ft) at the end of the 75-year period is close to the equilibrium scour depth of the 100-year flood (≈ 18 ft). The largest flood in Figure 6.22 has a peak discharge of 24,427 ft³/s and an equivalent time of 49 hours. The return period of this flood is 58 years. Table 6.9 shows the exceedance probabilities associated with different predicted scour depths for the project lives of 50, 75, and 100 years. These statistics are computed based on 20,000 SRICOS simulations (see Section 5.9). Compared with the HEC-18 method, there is a small reduction in the predicted scour depth in using the SRICOS method. For example, if the design life of the bridge is 75 years and the design flood has a return period of 100 years, the probability that this flood will be exceeded at least once during the design life of the bridge is 53% (Table 6.8). This is also the exceedance probability of the equilibrium scour depth for the 100-year flood in non-cohesive soils. However, Table 6.9 shows that the exceedance probability for a scour depth of 18 ft is only 3% if the time rate of scour is considered. However, Table 6.9 also shows that reducing the scour depth from 18 ft to 17 ft would increase the exceedance probability to 52%. This means that using the SRICOS method instead of the traditional HEC-18 method would reduce the predicted scour depth at this site by only 1 to 2 ft if the same risk level is adopted for design. The small benefit hardly justifies the extra effort for conducting a full SRICOS-EFA analysis.

The large, predicted scour depths at the SD13 bridge are due to the unique hydraulic condition at this site. Table 6.2 shows that the equilibrium scour depth at bent 2 is around 18 ft for all the maximum annual floods with return period greater than 10 years. Hence, even small floods can produce large scour depths. It is not safe to evaluate this bridge site for scour based on the 100-year flood alone since the equilibrium scour depth does not decrease with flood magnitude. The SRICOS method in conjunction with Monte Carlo simulations can provide a more complete picture of the risk involved in adopting different design scour depths because the results include the contributions from both large and small floods.
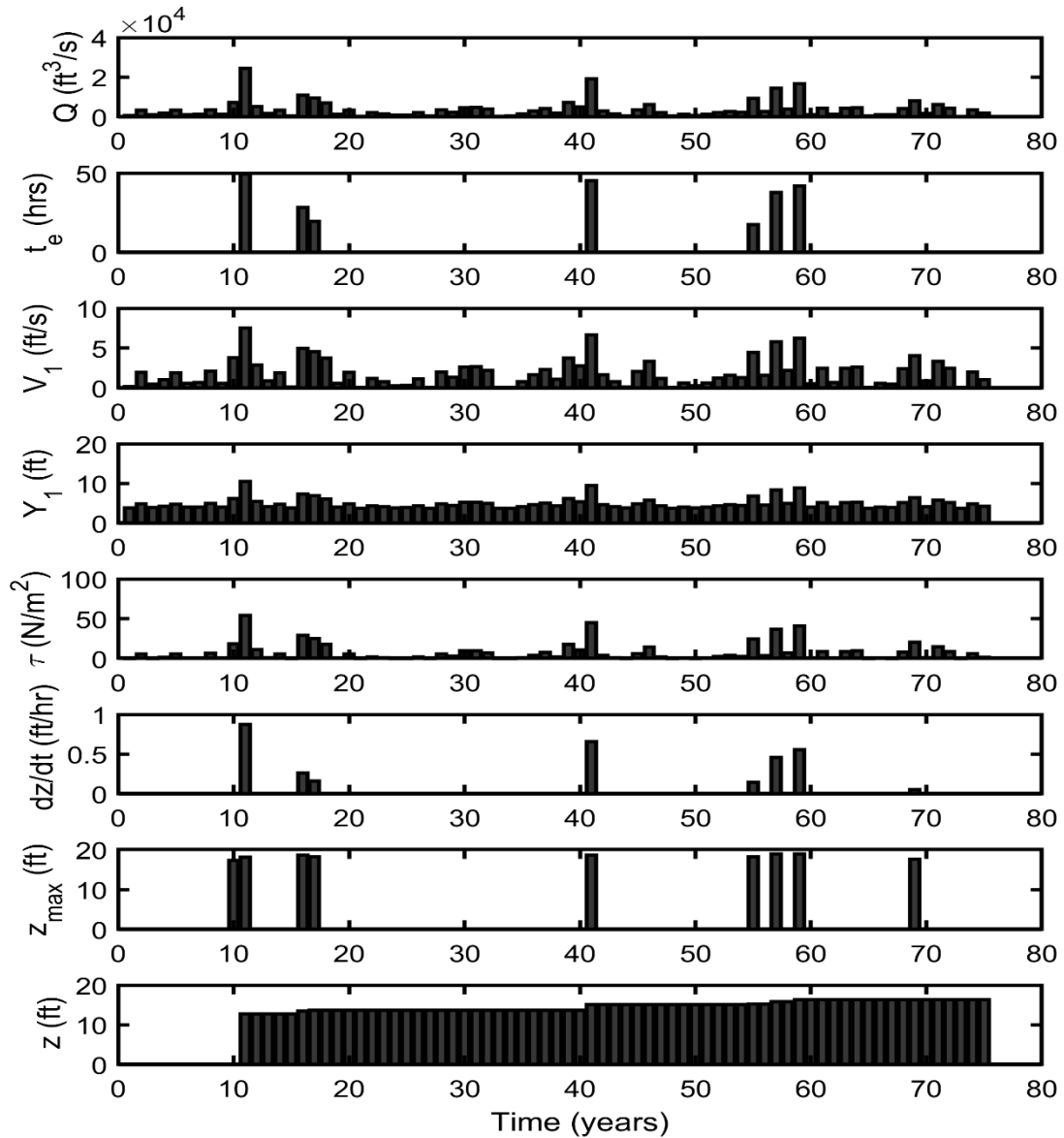
Figure 6.22 SRICOS simulation for a constructed series of 75 maximum annual floods for bent 2
The simulation was conducted using the measured EFA curve (ε=1 mm) shown in Fig. 6.4. The equivalent time is computed using the regression equation in Fig. 6.14.

Table 6.9 Exceedance probabilities associated with predicted final scour depths and project lives for bent 2
The SRICOS simulations were conducted using the measured EFA curve. The equivalent time is computed using the regression equation in Fig. 6.14.

Scour Depth (ft)	14	15	16	17	18
Exceedance Probability (Project life 50 yrs)	89%	80%	59%	22%	<1%
Exceedance Probability (Project life 75 yrs)	98%	96%	87%	52%	3%
Exceedance Probability (Project life 100 yrs)	99.8%	99.4%	97%	78%	8%

63

Figure 6.23 shows the results of SRICOS simulation for one constructed series of 75 maximum annual floods conducted using the erosion-rate-versus-shear-stress curve that separates soil regions III (medium erodibility) and IV (low erodibility) in Figure 5.3. The soil critical shear stress τ_c is 9.5 N/m^2 and the constant a' is 1.62 (see Eq. 5.2 and Table 5.1). The critical discharge to produce scour is 4,581 ft^3/s. The equivalent time is computed using the regression equation given by the solid line in Figure 6.17. The largest flood in Figure 6.23 has a magnitude of 40,215 ft^3/s and an equivalent time of 50 hours. The return period of this flood is approximately 239 years. The predicted final scour depth for the entire series of 75 floods is 2.4 ft, which is much smaller than the equilibrium scour depths of the large floods. Table 6.10 shows the exceedance probabilities associated with different predicted final scour depths for the project lives of 50, 75, and 100 years. These results show that the exceedance probability for a scour depth of 5 ft is less than 1% for a project life of 75 years, compared with an equilibrium scour depth of 18 ft for the 100-year flood.

The exceedance probabilities of the predicted final scour depths increase considerably if the equivalent time is computed using the dashed line in Figure 6.17. This is due to the slow rates of scour for this soil category. Those results show that the design scour depth will have to be increased from 5 ft to 8 ft (not shown) in order to maintain an exceedance probability of less than 1% for a project life of 75 years. However, the dashed line was constructed to match the equivalent time of three maximum annual floods (1997, 2001, and 2011) that have exceptionally long equivalent time. Therefore, using the dashed line would significantly over-estimate the equivalent times of other maximum annual floods and the predicted final scour depth.

Table 6.10 Exceedance probabilities associated with predicted scour depths and project lives for bent 2

The soil critical shear stress τ_c and erosion rate constant a' are 9.5 N/m^2 and 1.62, respectively. The equivalent time is computed using the regression equation given by the solid line in Fig. 6.17.

Scour Depth (ft)	2	3	4	5	6	7
Exceedance Probability (Project life 50 yrs)	14%	1%	<1%	<1%	<1%	<1%
Exceedance Probability (Project life 75 yrs)	51%	7%	<1%	<1%	<1%	<1%
Exceedance Probability (Project life 100 yrs)	85%	28%	3%	<1%	<1%	<1%
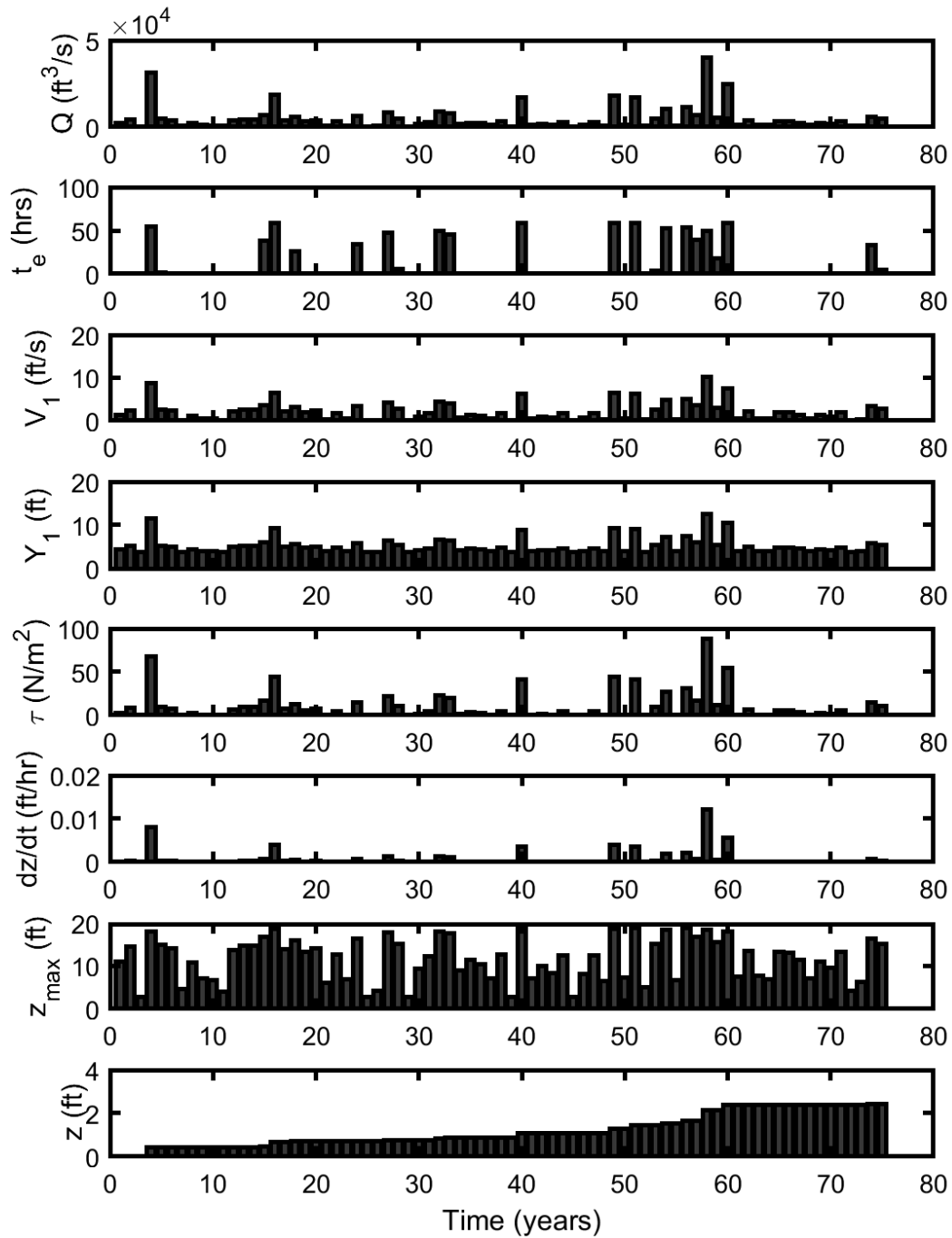
Figure 6.23 SRICOS simulation for a constructed series of 75 maximum annual floods for bent 2
The soil critical shear stress τ_c and erosion rate constant a' are 9.5 N/m² and 1.62, respectively. The equivalent time is computed using the regression equation given by the solid line in Figure 6.17.

Figure 6.24 presents the results of SRICOS simulations for a constructed series of 75 maximum annual floods conducted using the erosion-rate-versus-shear-stress curve that separates soil regions II (high erodibility) and III (medium erodibility) in Figure 5.3. The critical shear stress τ_c is 1.33 N/m^2 and the erosion rate constant a' is 2.53 (see Eq. 5.2 and Table 5.1). The critical discharge to produce scour is 1,609 ft^3/s. The critical shear stress is so low and the soil erosion rates are so high that the equilibrium scour depth of the 100-year flood ($\approx$ 18 ft) is reached long before the end of the hydrograph. The predicted final scour depth is 18.1 ft. The largest flood in Figure 6.24 has a magnitude of 29,894 ft^3/s and an equivalent time of 22 hours. The return period is approximately 100 years. Table 6.11 shows the exceedance probabilities associated with different predicted final scour depths for the project lives of 50, 75, and 100 years. These results confirm that there is a very high probability that the final scour depth would reach the equilibrium scour depth of the 100-year flood during the design life of the bridge.

Table 6.11 Exceedance probabilities associated with predicted scour depths and project lives for bent 2

The soil critical shear stress τ_c and erosion rate constant a' are 1.33 N/m^2 and 2.53, respectively. The equivalent time is computed using the regression equation shown in Fig. 6.20.

Scour Depth (ft)	15	16	17	18	19
Exceedance Probability (Project life 50 yrs)	99.9%	99.4%	95%	32%	<1%
Exceedance Probability (Project life 75 yrs)	>99.99%	99.99%	99.7%	71%	<1%
Exceedance Probability (Project life 100 yrs)	>99.99%	>99.99%	99.98%	91%	<1%

6.5 Comparison with Other Simplified SRICOS Methods

The results obtained in the scour risk analysis may be compared with the scour depths predicted using other bridge scour assessment methods discussed in section 5.10. The SRICOS method as implemented in this study has the following assumptions:

1. The equilibrium scour depth in cohesive soils is the same as in non-cohesive soils. The equilibrium scour depth was calculated using the traditional HEC-18 equation (Eq. 5.9). Two other equations (Eqs. 5.10 and 5.14) have been proposed for predicting the equilibrium scour depth in the SRICOS method. Eq. (5.10) is based on flume tests conducted primarily on Porcelain clay (Ting et al., 2001). Ting et al. (2010) show that Eq. (5.10) will give similar results as Eq. (5.9) for the range of Froude number used in the flume tests. Eq. (5.14) incorporates a critical velocity for initiation of scour, but the equation would predict a larger equilibrium scour depth than Eq. (5.9) when the Froude number exceeds about 0.3 (see Section 5.2). Because of the relatively small dataset used to develop Eqs. (5.10) and (5.14), the HEC-18 equation has been used to calculate the equilibrium scour depth in this study.

2. The initial rate of scour is predicted using a measured erosion function from EFA testing on soil samples collected from the bridge site or the soil erosion rate chart in Figure 5.3.
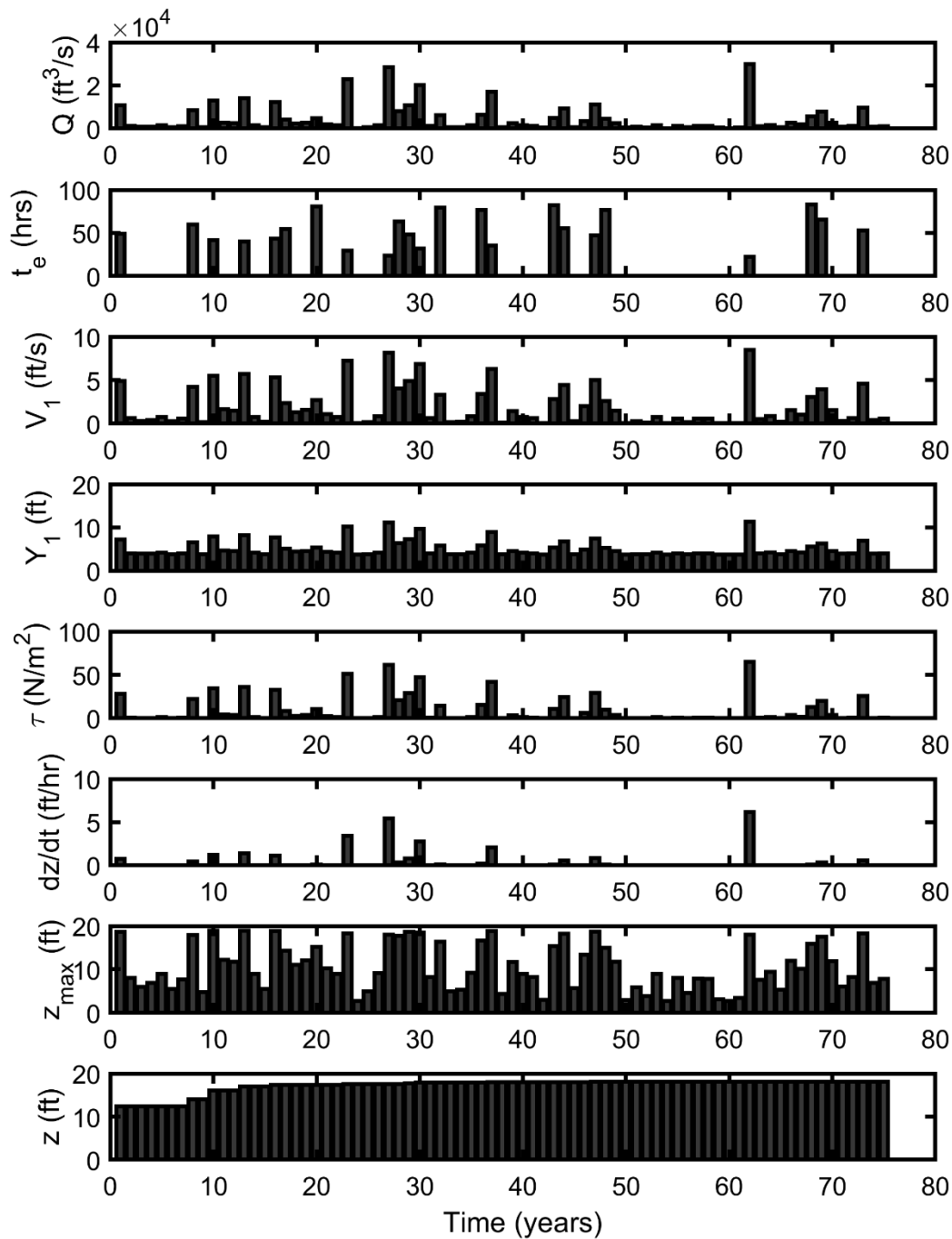
Figure 6.24 SRICOS simulation for a constructed series of 75 maximum annual floods for bent 2
The soil critical shear stress τ_c and erosion rate constant a' are 1.3 N/m² and 2.53, respectively. The equivalent time is computed using the regression equation shown in Figure 6.20.

3. It is assumed that a sequence of large floods would produce the same amount of scour as a continuous series of large and small floods because most of the floods in the time series would not achieve their maximum scour potential due to pre-existing scour. The method of

hydrograph generation utilizes a series of maximum annual floods (an annual maximum series). The flood magnitude is assumed to follow the Log Pearson Type III distribution. The duration of the individual flood is represented by an equivalent time that will produce the same predicted final scour depth as the recorded hydrograph. Short-term autocorrelation as determined by the time sequence of flows in the hydrograph is captured by specifying the flood's peak flow magnitude and equivalent duration. However, long-term changes in flood frequency are not considered.

Table 6.12 presents the results of SRICOS simulations for bent 2 with the 100- and 500-year peak flow run for five days. The soil critical shear stress τ_c and erosion rate constant a' correspond to the erosion-rate-versus-shear-stress curve that separates soil regions III and IV in Figure 5.3. The equilibrium scour depth is computed using the HEC-18 equation for pier scour (Eq. 5.9) in Table 6.12(a) and the equation developed for cohesive soils (Eq. 5.14) in Table 6.12(b). Several conclusions can be drawn from these results. First, the equilibrium scour depths are similar for the 100- and 500-year floods. As discussed before, this is due to the unique hydraulic condition at this site. As the discharge increases, the approach flow velocity increases but the flow angle of attack decreases so that the equilibrium scour depth remains about the same for a wide range of flow discharges. Second, the equilibrium scour depths computed using Eq. (5.14) are greater than those computed using the HEC-18 equation by 40% to 50%. Third, the probability that the equilibrium scour depth for the 100- or 500-year peak flow can be reached during the lifetime of the bridge is extremely low (< 1%) based on the results of the scour risk analysis shown in Table 6.10. Hence, the equilibrium scour depth significantly over-estimates the predicted final scour depth in this soil category.

Table 6.12 shows that the predicted final scour depth obtained by running the 500-year peak flow for five days is about 2 ft. The exceedance probabilities are 14%, 51%, and 85% for the project lives of 50, 75, and 100 years, respectively (Table 6.10). These risk values are quite high; therefore, the 500-year flood alone is not adequate for predicting a safe design scour depth for the lifetime of the bridge. This conclusion is supported by the scour prediction obtained using the recorded hydrograph. If the recorded hydrograph from August 1953 to April 2017 is used with the SRICOS method to predict scour, the predicted final scour depth will be 2.7 ft (Figure 6.9). Due to large equilibrium scour depths over a wide range of discharges, the smaller floods can also contribute to the final scour depth. Therefore, a series of floods are needed to correctly predict the final scour depth over the project life of the bridge.

Table 6.12 Results of SRICOS simulations for bent 2 with the 100- and 500-year peak flow run for 5 days and z_{max}

Computed using: (a) HEC-18 equation for pier scour (Eq. 5.9) and (b) equilibrium scour depth for cohesive soils (Eq. 5.14). The soil critical shear stress τ_c and erosion rate constant a' are 9.5 N/m^2 and 1.62, respectively.

(a)									
T_r (yr)	Q (ft^3/s)	V_1 (ft/s)	Y_1 (ft)	α (°)	τ (N/ m^2)	V_c (ft/s)	z_{max} (ft/s)	$\dot{z}_i$ (ft/hr)	z_f (ft)
100	30,025	8.49	11.32	17.18	65.2	3.6	18.0	0.0075	0.85
500	50,290	11.66	13.56	13.50	110.2	3.7	19.0	0.0175	1.89
(b)									
T_r (yr)	Q (ft^3/s)	V_1 (ft/s)	Y_1 (ft)	α (°)	τ (N/ m^2)	V_c (ft/s)	z_{max} (ft/s)	$\dot{z}_i$ (ft/hr)	z_f (ft)
100	30,025	8.49	11.32	17.18	65.2	3.6	25.0	0.0075	0.86
500	50,290	11.66	13.56	13.50	110.2	3.7	28.8	0.0175	1.95

If the S-SRICOS method is used to predict the final scour depth, the equivalent time will be calculated using Eq. (5.42) with t_{hydro} taken to be the design life of the bridge, V_{max} the flow velocity produced by the design flood (e.g., the 100-year peak flow), and $\dot{z}_i$ the initial erosion rate for the maximum velocity. With $t_{hydro} = 75$ years, $V_{max} = 8.5$ ft/s and $\dot{z}_i = 0.0075 \frac{ft}{hr}$ (Table 6.12), the computed equivalent time is 541 hr. The computed final scour depth is 3.5 ft. From Table 6.10, the corresponding exceedance probability is about 5%. However, this result must be viewed with caution because Eq. (5.42) was developed using field data collected in Texas. Hence, the regression equation may not be applicable in South Dakota.

6.6   Summary

SRICOS simulations show that except for soil region IV (low erodibility), there is no significant reduction in the predicted final scour depth for this site when the time rate of scour is considered. Soils that fall into this category include high plasticity clay and coarse gravel. Using the measured EFA curve for the silty fine sand collected on the north abutment with the SRICOS method to predict scour further confirms that the predicted final scour depth will be like the equilibrium scour depth of the 100-year flood.

Good correlation is found between the equivalent times and peak discharges of historical floods when the results are normalized. A long flood recession time can significantly increase the equivalent time and consequently increase the predicted final scour depth. The equivalent time can be very long for some spring floods. Including the flood duration above the critical discharge as an additional parameter improves the prediction of the equivalent time, but the procedure is difficult to implement since flood duration can vary considerably from year to year even for floods with the same return periods.

 A risk approach was employed with the SRICOS method to compute the exceedance probability of the predicted final scour depth. The stochastic method uses Monte Carlo simulations to generate 20,000 annual maximum series. The magnitudes of the maximum annual floods in the series are sampled from the Log Pearson Type III distribution, and their equivalent times are calculated using regression equations developed by analyzing the computed scour histories of recorded floods. The results provide a benchmark with which the predicted scour depths obtained using other simplified methods may be compared. It was found that a substantial reduction factor (50% to 70%) can be applied to the HEC-18 results only for soil region IV. It was also found that the scour depth predicted by running the 500-year peak flow for five days does not provide an acceptable risk value for this site. The unique hydraulic condition produces similar equilibrium scour depths over a wide range of discharges. Consequently, the lesser floods may also contribute significantly to the predicted final scour depth.

7. CONTRACTION SCOUR ANALYSIS, SD37 BRIDGES OVER JAMES RIVER NEAR MITCHELL, SOUTH DAKOTA

7.1 Site Description

The SD37 bridges (structure number 56-150-176 and 56-149-176) over the James River are located on South Dakota (SD) Highway No. 37 northbound and southbound, respectively, about 20 miles north of the city of Mitchell in southeast South Dakota. The parallel bridges are both three-span, pre-stressed girder bridges, 353 ft in length. The northbound bridge was built in 1992 and the southbound bridge in 2002. Both bridges have two pier sets with three 3.75-ft diameter cylindrical piers per set located on pilings. The bridge opening is classified as a spill-through abutment with two horizontal to one vertical slope embankment protected by riprap. The pier sets and abutments are skewed at an angle of 35° parallel to the general direction of the flow. The low-flow channel is confined between the pier sets.

The James River near Forestburg streamflow gauging station (station number 06477000) is located about 4.5 miles upstream of the bridge site and has a contributing drainage area of 15,549 mi^2. The station has been operated since 1950. The largest recorded peak discharge is 28,400 ft^3/s on March 25, 2011. The predicted 2-, 100-, and 500-year peak discharges are 1,948, 40,025, and 80,351 ft^3/s, respectively. These statistics were obtained by fitting the Log Pearson Type III distribution to the recorded annual peak flows from water years 1950 to 2017. If the flood frequency analysis is conducted using the flood data from 1950 to 2000, the predicted 2-, 100-, and 500-year peak discharges are 1,805, 27,475, and 47,598 ft^3/s, respectively. It is apparent that large floods have occurred more frequently in the last two decades. This trend can be seen in the recorded hydrograph shown in the top plot of Figure 7.10.

Figure 7.1 shows an aerial photograph of the bridge site. The James River flows from west to east. The bridge crossing is located on a straight reach of stream between two meander bends. The river valley is approximately 1 mile wide and bounded by high bluffs. The floodplain is comprised primarily of farmland and pasture, but the left overbank in the meander upstream and downstream of the bridge crossings is heavily vegetated by trees. The channel slope in this reach averages about 0.5 feet per mile. As the channel meanders across the floodplain, exchange of flow takes place constantly between the left and right floodplains. Because all the floodplain flow passes through the bridge opening, the site has a large potential for contraction scour. Figure 7.2 shows the layout and main dimensions of the bridge waterway. The pier sets and abutments are skewed parallel to the flow to minimize scour, and the abutments are protected by riprap extending to the edge of the low-flow channel. Figures 7.3 through 7.6 show pictures of the bridge site taken by Francis Ting on March 24, 2011, around peak flow during the record flood in March 2011 (see Table 7.2).

Figure 7.1 Aerial photograph of SD37 Bridges over the James River north of Mitchell, South Dakota
(image courtesy of United States Geological Survey)
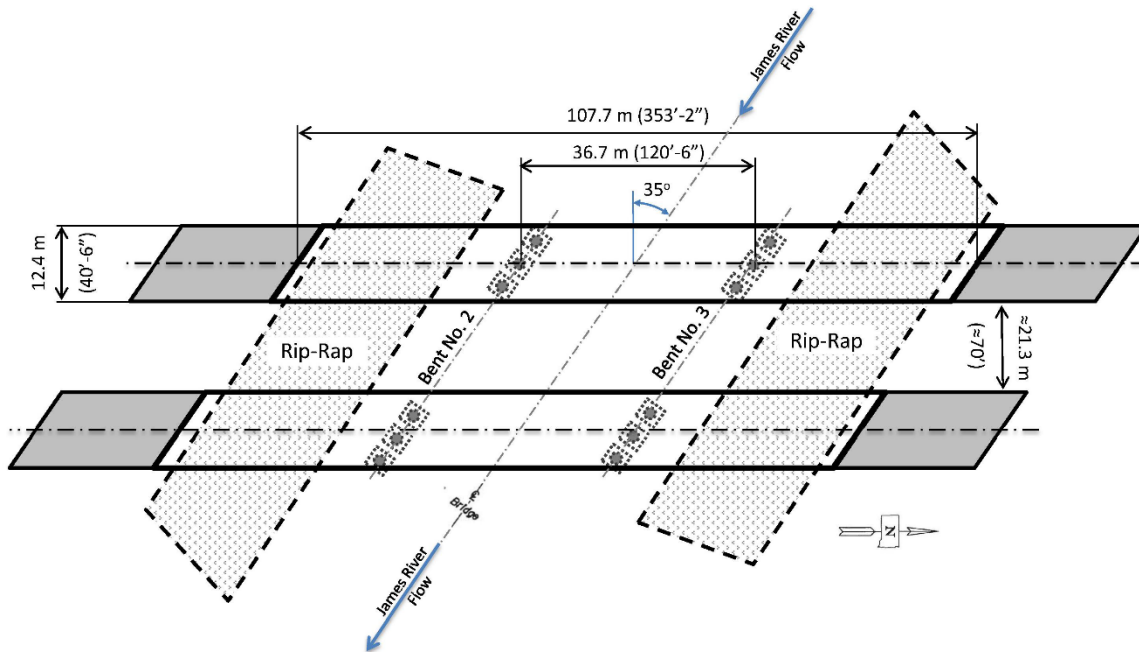
Figure 7.2 Main dimensions and layout of the bridge waterway
(from Rossell and Ting, 2013)

Figure 7.3 Bridge crossing from right bank facing along upstream face of southbound bridge toward left bank during the flood of March 2011

Figure 7.4 Bridge crossing from right bank facing bent 2 of southbound bridge

Figure 7.5 Bridge crossing from right bank facing along downstream face of northbound bridge toward left bank

Figure 7.6 From right bank facing the downstream 90º bend and the floodplain beyond
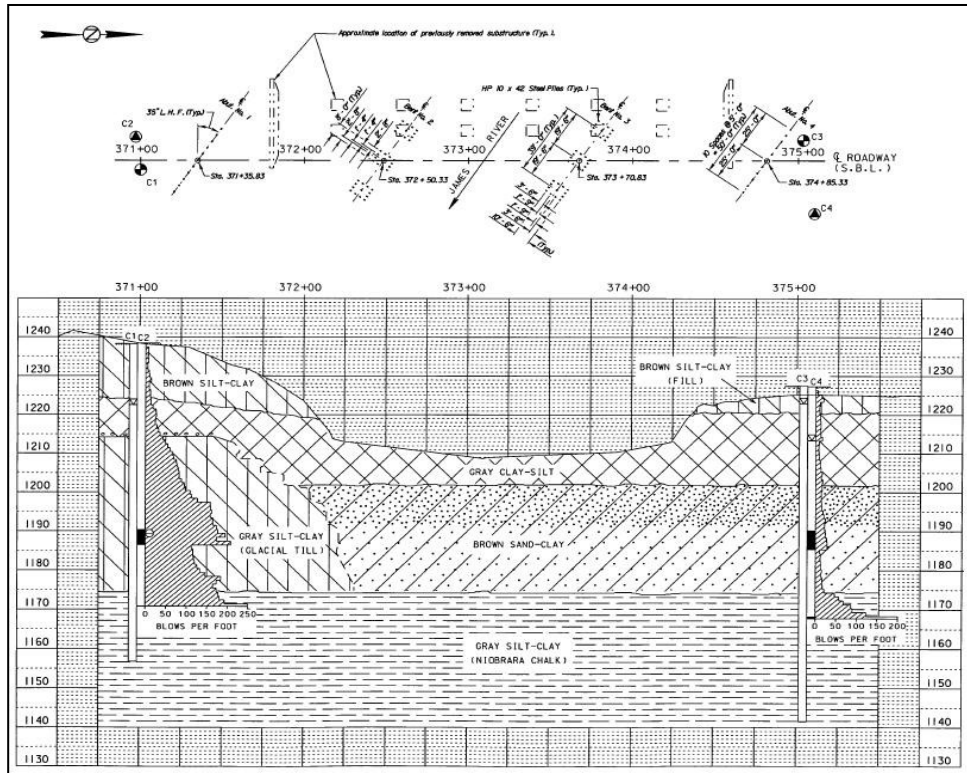
Figure 7.7 Subsurface profile from bridge plan in December 2000
(image courtesy of South Dakota Department of Transportation)

The site has experienced moderate scour over the years, with an estimated 5 ft of pier scour at one of the pier sets and 2 ft of contraction scour (Rossell and Ting, 2013). Figure 7.7 shows the subsurface profile at the time when the southbound bridge was built. More recent boring was completed below the north abutment between the northbound and southbound bridges on March 8, 2012, by the SDDOT. The soil materials that were observed during drilling included approximately 25 ft of clay and silt overlying 10 ft of silt and sand. Coarse sand and gravel were encountered at a depth of 35 ft. Two thin-wall tube samples were collected from the drill hole at depths of 24 to 26.5 ft and 29 to 31.5 ft. A third sample was collected by the researchers from SDSU near the left edge of water just upstream of the southbound bridge on November 17, 2011. This sample consisted primarily of a mildly cohesive clayey silt. EFA testing was conducted on the thin-walled tube samples. The test results for the mildly cohesive clayey silt are shown in the top plot of Figure 7.8. This sample has very high erosion rates. The test results for the high plasticity clay from the north abutment are shown in the bottom plot. The maximum fluid shear stress applied during the test was 24 N/m^2. Except for small pockets of sand that was rapidly washed away, the clay sample barely eroded during the EFA test.

74
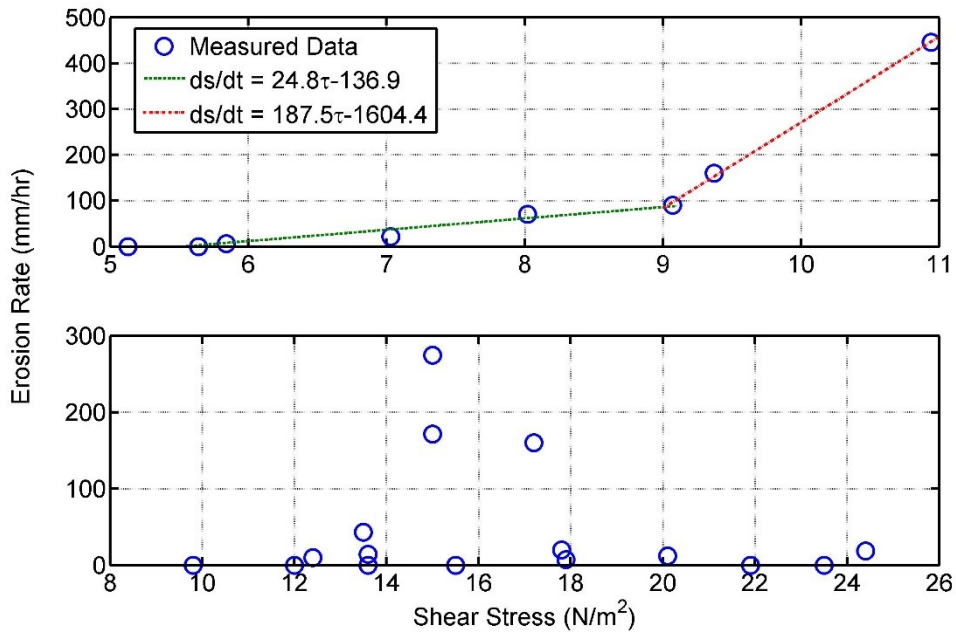
Figure 7.8 Variations of measured soil erosion rate with applied bed shear stress for mildly cohesive clayey silt (top plot) and high plasticity clay (bottom plot)

A 2D flow model of the bridge site was created in the Surface Water Modeling System (SMS) using the numerical model FESWMS. The floodplain topography in the 2D model was created using LiDAR data, and the bathymetry data were collected from a boat using a single-beam sounder. The 2D model was validated using flow measurements obtained during a 25-year flood. Details of the 2D flow model construction and validation can be found in Russell (2012) and Russell and Ting (2013). Figure 7.9 shows the variations of computed unit discharge and flow depth with flow discharge in the contracted section between the southbound and northbound bridges. The regression equations in Figure 7.9 were used with the energy method described in Section 5.5 to predict contraction scour. Table 7.1 summarizes the input parameters for the SRICOS simulations. The high plasticity clay collected from the foundation depth has very high critical shear stress (> 24 N/m^2). Therefore, no SRICOS simulations were conducted using the measured soil erosion function. SRICOS simulations were conducted using Eq. (5.2) with the soil parameters given in Table 5.1. Scour histories were computed using daily or hourly mean flows (whichever is available) from March 1, 1950, to May 16, 1998, and 15-minute flow data from May 17, 1998, to April 24, 2017. As with the SD13 bridge, scour histories were computed using all the available flow data, including those recorded before the bridges were built. The computed scour histories were used to determine the final scour depths and equivalent times of the maximum annual floods and the cumulative scour depth from 1950 to 2017.

Table 7.1 Input parameters for SRICOS simulations

Model input	Parameter value
Unit discharge q (ft^2/s)	Fig. 7.9
Initial flow depth y_i (ft)	Fig. 7.9
Manning's coefficient n	0.035
Fluid density ρ (kg/m^3)	998.2
Expansion loss coefficient C_e	0.5
Critical shear stress τ_c (N/m^2)	Table 5.1
Erosion rate constant a'	Table 5.1
Hydrograph	USGS streamflow data near Forestburg, SD
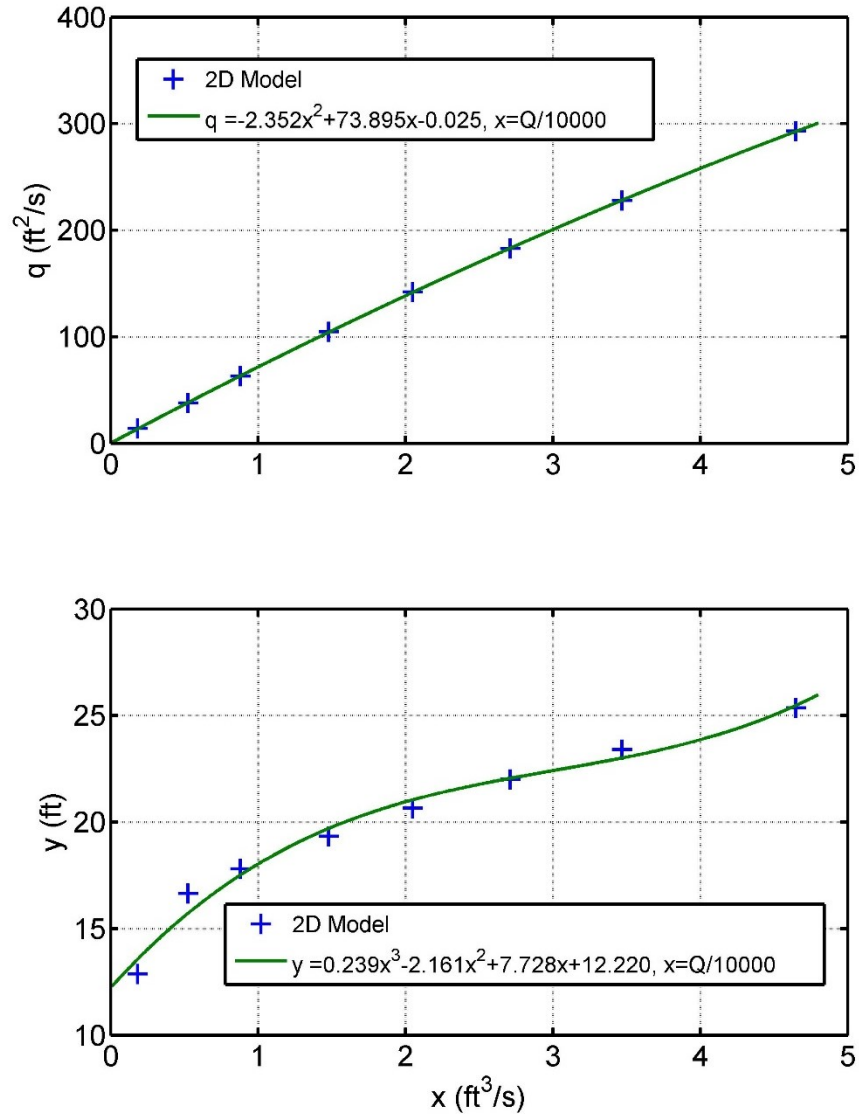
Figure 7.9 Variations of computed unit discharge (top plot) and flow depth (bottom plot) with flow discharge in contracted section

76

7.2 Scour History Analysis

Table 7.2 presents the results obtained using the erosion-rate-versus-shear-stress curve that separates soil regions III (medium erodibility) and IV (low erodibility) in Figure 5.3. The critical shear stress τ_c is 9.5 N/m^2 and the erosion rate constant a' is 1.62 (Table 5.1). As seen in Table 7.2, no floods smaller than the 10-year flood can produce any scour. The predicted final scour depths of the maximum annual floods are all very small (about 1 ft or less), and the initial soil erosion rates are very slow. This is the situation where use of the SRICOS method instead of the traditional HEC-18 method could produce significant reduction in the predicted final scour depth.

The return periods shown in Table 7.2 were obtained by fitting the Log Pearson Type III distribution to the measured annual peak flows from water years 1954 to 2016 using the Bulletin 17B method. The results are like those obtained by running the expected moment algorithm (EMA) without historic and regional information but are more conservative than the results of the EMA run with historic and regional information. The return periods obtained using different methods are compared in Chapter 12.

Figure 7.10 shows the results of SRICOS simulation from March 1950 to April 2017. From top to bottom, the individual plots represent the measured discharge, computed flow depth, computed bed shear stress, and predicted scour depth. The critical shear stress is shown as a dashed line in the computed bed shear stress plot. The predicted final scour depth produced by the complete hydrograph is 2.8 ft, compared with 2.7 ft when the maximum annual floods are used to compute the scour history. These results are very close because only a few large floods can produce scour due to the high soil critical shear stress. Figure 7.10 shows that large floods have occurred more frequently in the past two decades. Note that most of the predicted scour is produced by the three maximum annual floods in 1997, 2007, and 2011.

Table 7.2 shows that the maximum annual floods in 1997, 2010, and 2011 have long equivalent times compared with the other floods. This is due to the long duration of these floods. The results of SRICOS simulation for those three floods are presented in Figures 7.11–7.13. The computed bed shear stress exceeds the critical shear stress ($dz/dt > 0$) for over one month in the 1997 and 2011 floods, and for 29 days in the 2010 flood. The predicted final scour depths of these three floods are larger than those produced by the other maximum annual floods, even though the flood of May 2007 also has large peak discharge. Figure 7.14 shows the results of SRICOS simulation for the flood of May 2007. Note that this flood subsides quickly, and the bed shear stress is below the critical shear stress in less than one week from the beginning of the flood.

The capacity of a flood to produce scour may be measured by the ratio of the predicted final scour depth to the equilibrium scour depth $\frac{z_f}{z_{max}}$. Table 7.2 shows the $\frac{z_f}{z_{max}}$ ratios of all the maximum annual floods that can produce scour. They are very small (< 0.1), therefore the cumulative scour depth produced by a sequence of maximum annual floods is also small. The predicted cumulative scour depth from 1950 to 2017 is 2.8 ft (Figure 7.10). In contrast, the equilibrium scour depth of the largest recorded discharge (28,400 ft^3/s) is 20 ft (Table 7.2). The predicted cumulative scour depth is only about 14% of the equilibrium scour depth of the record flood. Hence, the predicted final scour is far from equilibrium condition.

Table 7.2 Summary of results from SRICOS simulations for all scouring maximum annual floods between 1950 and 2017

The results were obtained using the erosion-rate-versus-shear-stress curve that separates soil regions III and IV in Fig. 5.3. The critical discharge Q_c is 9,700 ft³/s.

Year	Peak Discharge Date	Peak Discharge Q_{max} (ft³/s)	Return Period (yr)	Final Scour Depth z_f (ft)	Initial Erosion Rate (ft/hr)	Equilibrium Scour Depth z_{max} (ft)	$\dfrac{z_f}{z_{max}} \times 100\%$
2011	3/25/2011	28,400	50.3	1.13	0.003866	20.01	5.6
1997	4/6/1997	25,600	41.4	0.98	0.003033	17.15	5.7
2007	5/8/2007	21,300	29.8	0.15	0.001970	12.62	1.2
2010	3/25/2010	19,800	26.3	0.64	0.001663	11.01	5.8
2001	4/10/2001	17,400	21.3	0.21	0.001236	8.42	2.5
1995	4/22/1995	13,800	14.8	0.1	0.000731	4.51	2.2
1969	4/9/1969	12,500	12.8	0.07	0.000554	2.76	2.5
1962	3/31/1962	12,000	12.1	0.01	0.000534	2.54	0.4

Year	Flow Duration Above Critical Discharge t_s (hr)	Equivalent Time t_e (hr)	t_{90} (hr)	$\dfrac{t_e}{t_{90}}$	$\dfrac{Q_{max}}{Q_c}$	$\dfrac{Q_{max} t_s}{3600 z_{max}^3}$
2011	1340.5	323.3	20,029	0.01614	2.93	1.32
1997	981	354.6	18,415	0.01926	2.64	1.38
2007	150	79	15,573	0.00507	2.20	0.44
2010	715.25	410.75	14,429	0.02847	2.04	2.95
2001	252.25	172	12,348	0.01393	1.79	2.04
1995	207	141.3	8,262	0.01710	1.42	8.65
1969	168	135.3	5,770	0.02345	1.29	27.75
1962	24	18.7	5,411	0.00346	1.24	4.88
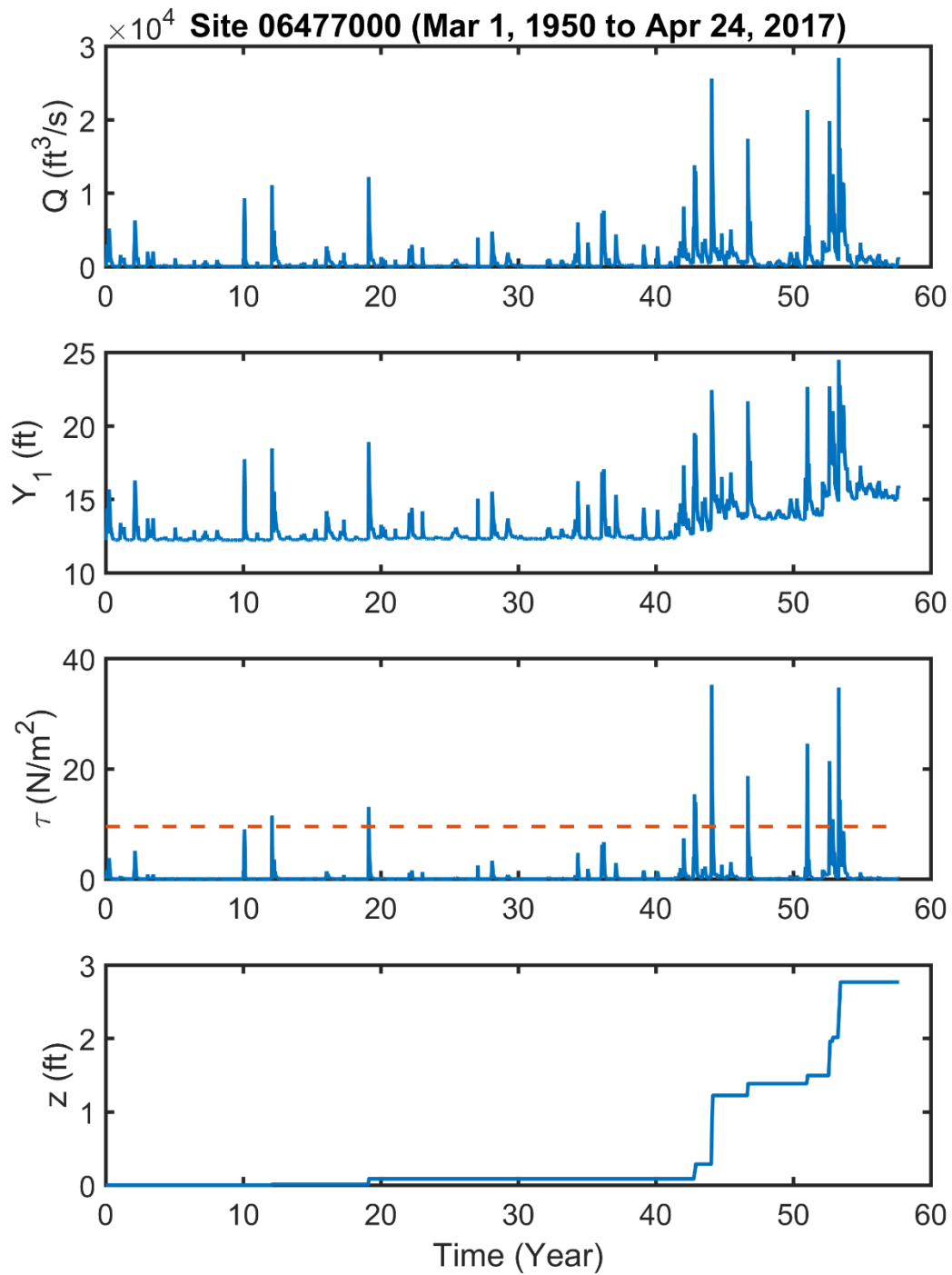
Figure 7.10 Computed history of contraction scour from March 1, 1950, to April 24, 2017, using the erosion-rate-versus-shear-stress curve that separates soil regions III and IV

The red dashed line represents the critical shear stress.
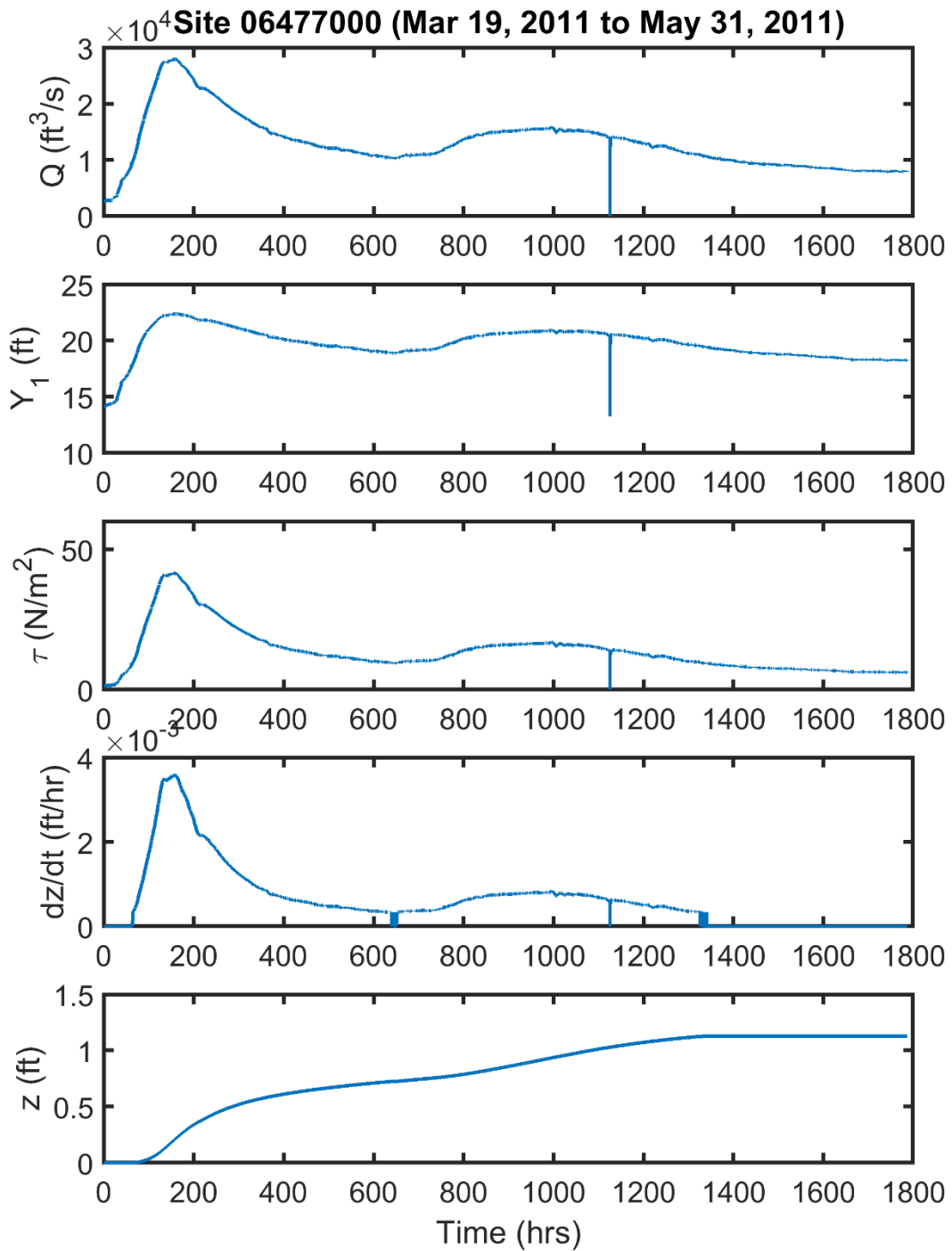
Figure 7.11 Computed history of contraction scour for the flood of March 2011
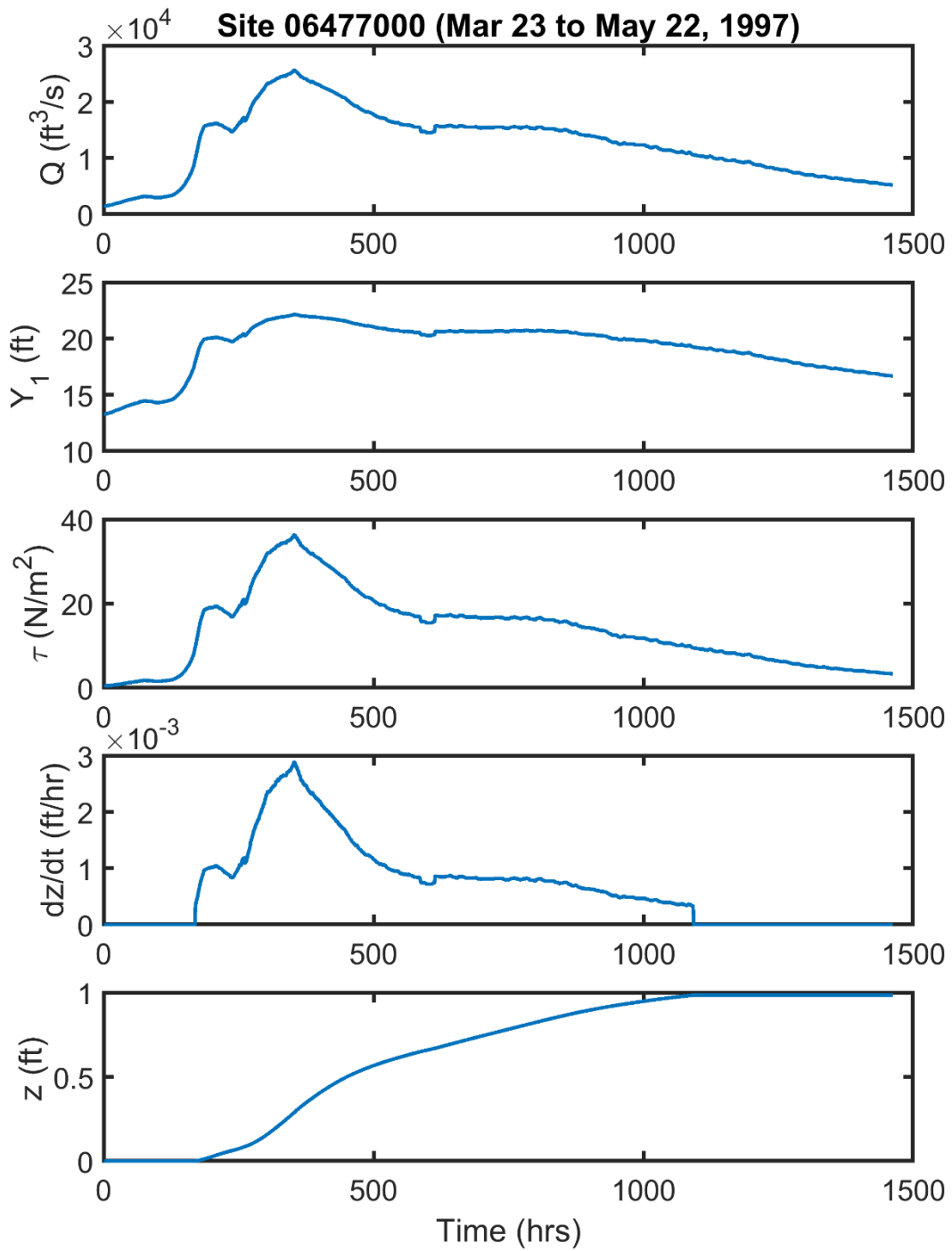
Figure 7.12 Computed history of contraction scour for the flood of April 1997
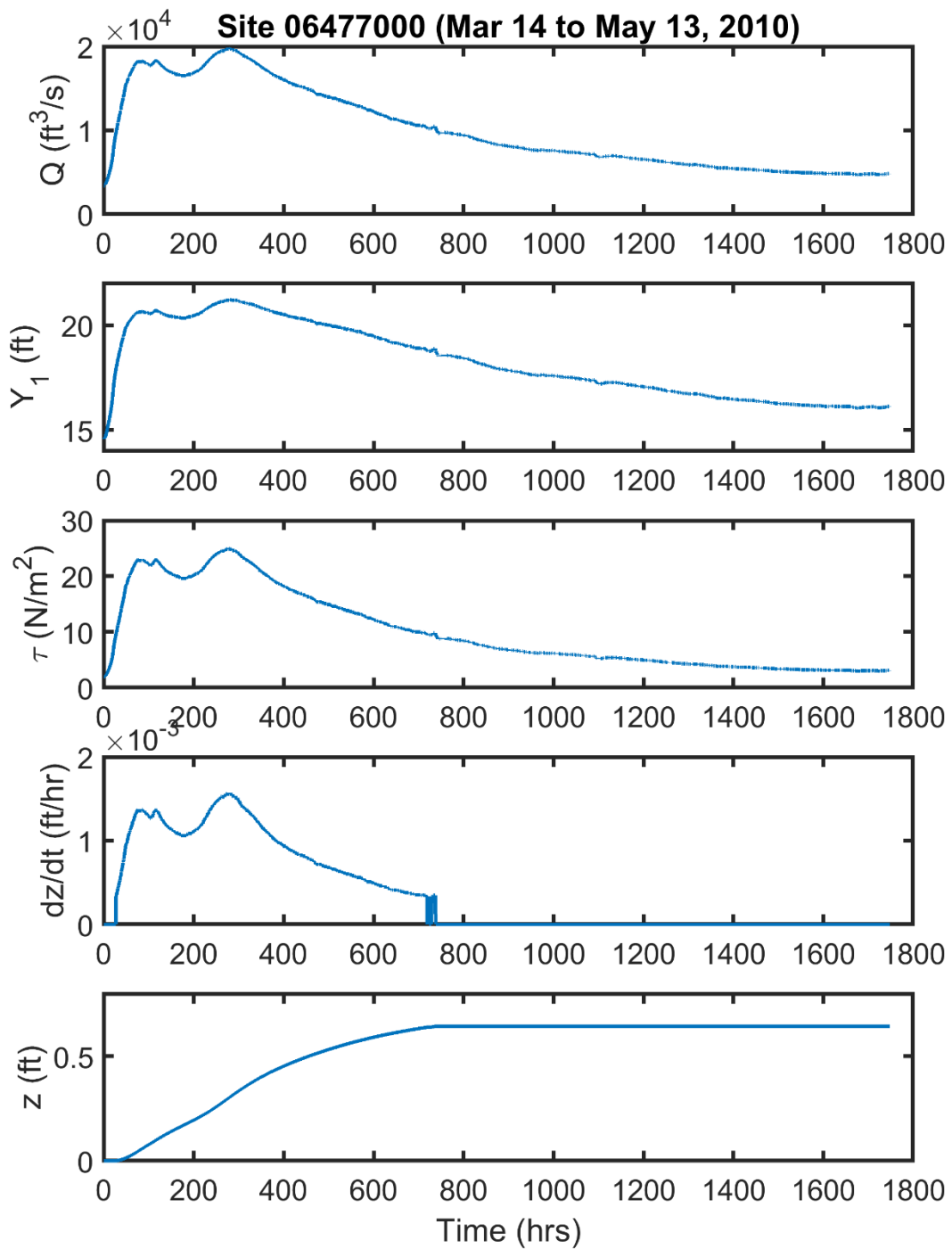
Figure 7.13 Computed history of contraction scour for the flood of March 2010
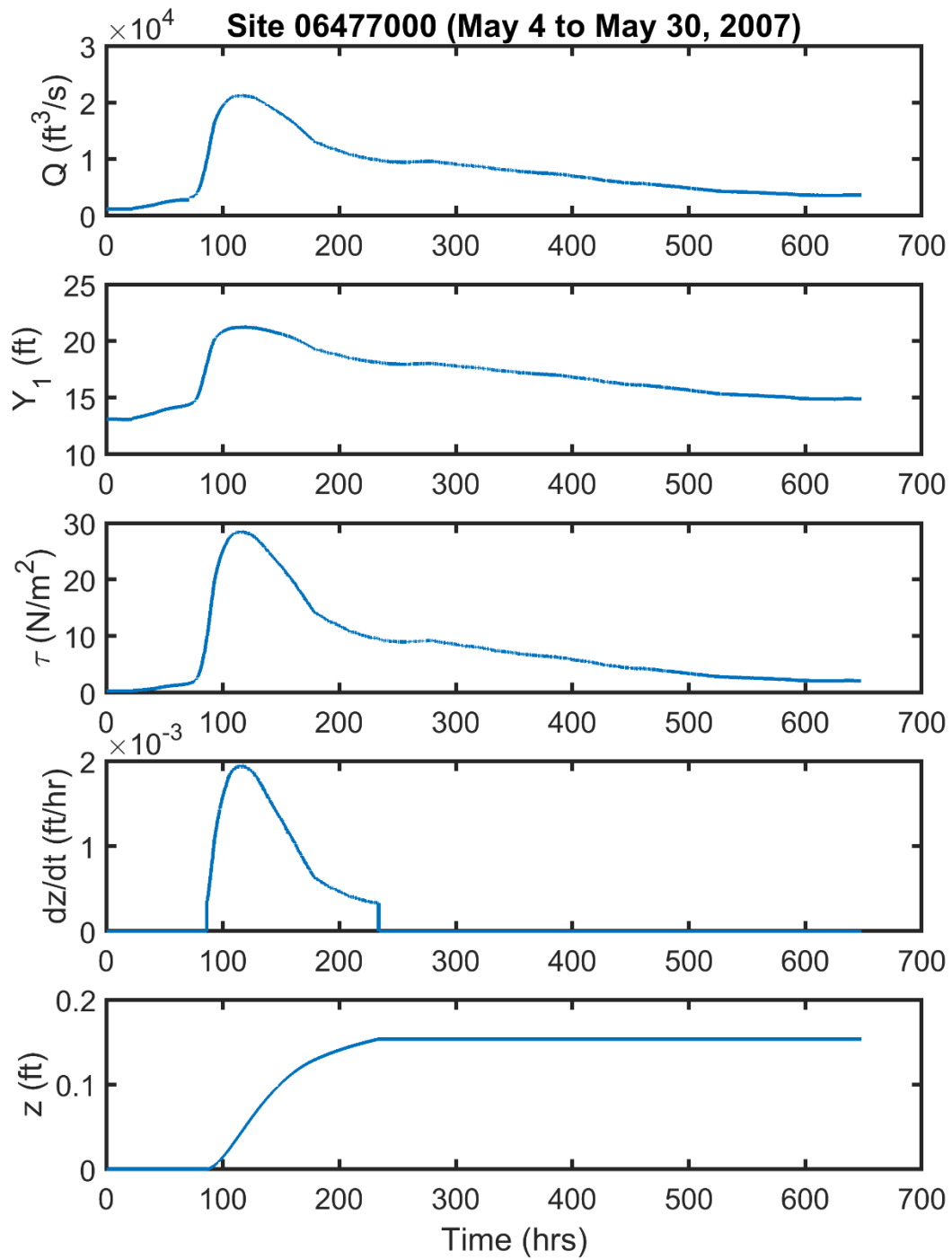
Figure 7.14 Computed history of contraction scour for the flood of May 2007

Table 7.3 presents the results obtained using the erosion-rate-versus-shear-stress curve that separates soil regions II (high erodibility) and III (medium erodibility) in Figure 5.3. The critical shear stress τ_c is 1.3 N/m^2 and the erosion constant a' is 2.5 (Table 5.1). The critical shear stress is much lower, and the soil erosion rates are much higher compared with the erosion-rate-versus-shear-stress curve that separates soil regions III and IV. For example, the initial rate of scour at the largest discharge (28,400 ft^3/s) is 2.2 ft/hr in Table 7.3 compared with 0.0039 ft/hr in Table 7.2. Due to the low critical shear stress and high erosion rates in this soil category, even floods below the 5-year flood can produce some scour. Nevertheless, the computed final scour depths of the maximum annual floods are still much smaller than their equilibrium scour depths. For example, the record flood in March 2011 has a predicted final scour depth of about 22 ft compared with the equilibrium scour depth of 76 ft. Hence, the computed scour depth is far from equilibrium condition. Figure 7.15 shows the results of SRICOS simulation from March 1950 to April 2017. The predicted final scour depth computed using the complete hydrograph is 28.5 ft, compared with 27.4 ft when the maximum annual floods are used to compute the scour history. The two predicted scour depths are very close. Therefore, the recorded hydrograph may be replaced by a sequence of maximum annual floods for the purpose of scour prediction. As in Figure 7.10, most of the predicted scour in Figure 7.15 is produced by the recent floods.

Table 7.3 shows that the equilibrium scour depth of the maximum annual flood in 2011 is 76 ft. It is unusual to see a bridge develop more than 10 ft of contraction scour during a single flooding event. The channel bed at a new bridge crossing may erode rapidly in the first few years after construction, and then scouring would slow as an equilibrium condition is established. In clear-water contraction scour, scouring would continue until the bed shear stress is reduced to the critical shear stress. Therefore, the final scour depth can be quite large if the soil critical shear stress is small. However, when the critical shear stress is small, live-bed scour may develop in the channel upstream. In live-bed scour, sediment transport from the upstream section would limit the contraction scour depth. The energy method described in Section 5.5 is only valid for clear-water scour. Clear-water scour may also apply if the sediment being transported from upstream stays in suspension through the contracted section. This mode of sediment transport is called suspended load transport and will generally require a value of $\frac{V_*}{\omega}$ much greater than 2, where V_* is the friction velocity in the contracted section and ω is fall velocity of the bed material being transported. The soil sample collected from the main channel upstream from the SD37 bridges consists primarily of a sandy clayey silt with a median diameter (d_{50}) of 0.035 mm (Figure 12.3). For sediment this fine, clear-water scour condition will likely occur at the bridge crossings (see Chapter 12).

The $\frac{z_f}{z_{max}}$ ratio is a measure of the capacity of a flood to produce scour. A large $\frac{z_f}{z_{max}}$ value means that the equilibrium scour depth can be achieved in a single flooding event, while a small $\frac{z_f}{z_{max}}$ value indicates that many floods would be required to develop the equilibrium scour depth. Table 7.3 shows that the values of $\frac{z_f}{z_{max}}$ ratio are between 0.11 and 0.32 for the floods greater than the 10-year flood. The cumulative scour depth produced by the recorded hydrograph from 1950 to 2017 is 28.5 ft (Figure 7.15), or about 38% of the equilibrium scour depth of the record flood (28,400 ft^3/s). This is considerably greater than the 14% predicted using the erosion-rate-versus-shear-stress curve that separates soil regions III and IV.

The results of SRICOS simulations for the maximum annual floods in 2007, 2010, and 2011 are presented in Figures 7.16 to 7.18. As seen in Table 7.3, the peak discharges in 2007 and 2010 are not significantly different, but the predicted final scour depth and equivalent time are both significantly larger for the 2010 flood. This is due to the long duration of this flood; the bed shear stress is above

the critical shear stress for about 10 weeks. The predicted $\frac{z_f}{z_{max}}$ ratio is 0.32, which is even greater than the value of 0.28 produced by the record flood in 2011.

The effect of soil erodibility on scour history development can be observed by comparing Figures 7.11 and 7.18 for the flood in March 2011. The SRICOS simulations were conducted using the erosion-rate-versus-shear-stress curves that separate soil region III from IV (Figure 7.11) and II from III (Figure 7.18). Note that the scour history produced by an actual hydrograph is very different from that produced by a constant discharge. In a steady flow, flow depth will increase and bed shear stress will decrease monotonically as scour depth increases with time. In an actual flood, the discharge increases gradually during the flood and does not reach the peak discharge until significant scour has already developed. Further increase in bed shear stress due to increase in discharge is then limited by the already large flow depth in the contracted section due to pre-existing scour. In Figure 7.18, the scour depth in the contracted section increases so rapidly that the bed shear stress starts to decrease before the peak flow arrives, although it is still greater than the critical shear stress, therefore scour depth continues to increase. The maximum scour depth is reached at about the same time as the peak discharge. The predicted final scour depth produced by the March 2011 flood is about 22 ft. The situation is different in Figure 7.11 when the soil erosion rates are much lower. The scour depth increases so slowly that the changes in flow depth and bed shear stress are determined primarily by the instantaneous discharge. A much higher maximum bed shear stress of 41.4 N/m^2 is developed in the contracted section. The scour depth continues to increase for several weeks after the flood has peaked, before reaching a predicted final scour depth of about 1 ft.

Table 7.3 Summary of results from SRICOS simulations for all scouring maximum annual floods between 1950 and 2017

The results were obtained using the erosion-rate-versus-shear-stress curve that separates soil regions II and III in Fig. 5.3. The critical discharge Q_c is 2,700 ft³/s.

Year	Peak Discharge Date	Peak Discharge Q_{max} (ft³/s)	Return Period (yr)	Final Scour Depth z_f (ft)	Initial Erosion Rate (ft/hr)	Equilibrium Scour Depth z_{max} (ft)	$\dfrac{z_f}{z_{max}}$ ×100%
2011	3/25/2011	28,400	50.3	21.52	2.232	76.19	28.2
1997	4/6/1997	25,600	41.4	20.66	1.527	68.97	30.0
2007	5/8/2007	21,300	29.8	10.8	0.779	57.44	18.8
2010	3/25/2010	19,800	26.3	16.98	0.598	53.29	31.9
2001	4/10/2001	17,400	21.3	10.92	0.376	46.52	23.5
1995	4/22/1995	13,800	14.8	7.91	0.166	36.06	21.9
1969	4/10/1969	12,500	12.8	6.52	0.117	31.27	20.3
1962	3/31/1962	12,000	12.1	3.39	0.101	30.67	11.1
1960	4/2/1960	10,900	10.6	3.33	0.072	27.31	12.2
1994	3/24/1994	8,180	7.3	2.89	0.026	18.8	15.4
1986	5/13/1986	7,740	6.8	4.05	0.021	17.38	23.3
1952	4/16/1952	6,290	5.4	2.31	0.0098	12.64	18.3
1984	6/25/1984	6,140	5.2	0.87	0.0090	12.14	7.2
1950	5/30/1950	5,180	4.4	1.32	0.0047	8.89	14.8
1999	5/22/1999	5,060	4.3	0.85	0.0043	8.48	10.0
1978	4/2/1978	4,830	4.1	0.73	0.0036	7.69	9.5
1998	5/24/1998	4,530	3.9	0.27	0.0028	6.65	4.1
1987	3/29/1987	4,530	3.9	0.32	0.0028	6.65	4.8
1977	3/15/1977	4,050	3.5	0.12	0.0018	4.95	2.4
1996	6/4/1996	3,790	3.3	0.3	0.0014	4.03	7.4
1993	8/4/1993	3,450	3	0.22	0.00092	2.79	7.9
1985	3/20/1985	3,300	2.9	0.12	0.00077	2.25	5.3
2013	6/29/2013	3,260	2.9	0.09	0.00073	2.10	4.3
1989	4/8/1989	3,080	2.7	0.06	0.00058	1.43	4.2
1972	5/31/1972	2,990	2.7	0.08	0.00051	1.1	7.3
1966	3/16/1966	2,800	2.6	0.02	0.00038	0.39	5.1
1991	6/10/1991	2,770	2.5	0.01	0.00037	0.27	3.7

Year	Flow Duration Above Critical Discharge t_s (hr)	Equivalent Time t_e (hr)	t_{90} (hr)	$\dfrac{t_e}{t_{90}}$	$\dfrac{Q_{max}}{Q_c}$	$\dfrac{Q_{max} t_s}{3600 z_{maz}^3}$
2011	1783.5	162.5	25,064	0.006483	10.52	0.0318
1997	1158	213.2	23,370	0.009123	9.48	0.0251
2007	588.25	65.9	20,640	0.003193	7.89	0.0184
2010	1747.5	313.1	19,646	0.015937	7.33	0.0635
2001	391.5	147.9	18,002	0.008216	6.44	0.0188
1995	1242	165.7	15,398	0.010761	5.11	0.1015
1969	1101	159.3	14,409	0.011055	4.63	0.1148
1962	408	57.9	14,022	0.004129	4.44	0.0471
1960	456	80	13,152	0.006083	4.04	0.0678
1994	835	185.1	10,881	0.017011	3.03	0.2855
1986	1056	393.5	10,491	0.037508	2.87	0.4325
1952	1032	359.2	9,126	0.039362	2.33	0.8929

Table 7.3 Summary of results from SRICOS simulations for all scouring maximum annual floods between 1950 and 2017

1984	336	113.6	8,974	0.012659	2.27	0.3203
1950	744	362.3	7,909	0.045807	1.92	1.5237
1999	530	232.2	7,760	0.029924	1.87	1.2216
1978	528	234.9	7,457	0.031501	1.79	1.5578
1998	237.75	102.6	7,021	0.014614	1.68	1.0173
1987	264	122.5	7,021	0.017448	1.68	1.1296
1977	96	69.1	6,170	0.011198	1.50	0.8904
1996	416	233.7	5,582	0.041866	1.40	6.6914
1993	356	251.2	4,575	0.054908	1.28	15.7092
1985	216	160.1	4,000	0.040029	1.22	17.3827
2013	165.25	125.6	3,828	0.032813	1.21	16.1584
1989	145	105.5	2,932	0.03598	1.14	42.4237
1972	192	160.1	2,392	0.066934	1.11	119.8097
1966	48	52.2	971	0.053759	1.04	629.3655
1991	25	23.9	703	0.033992	1.03	977.2957
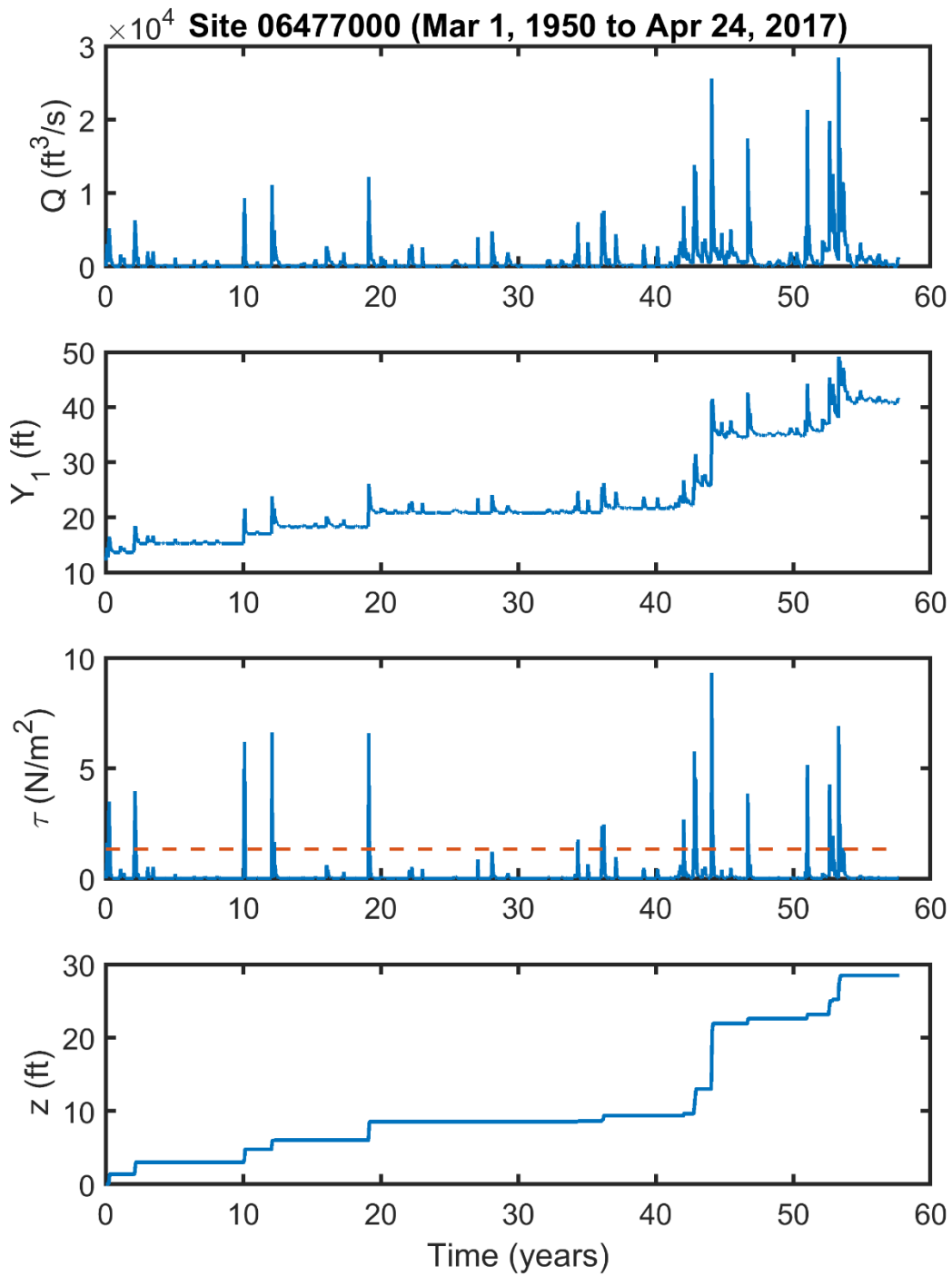
Figure 7.15 Computed history of contraction scour from March 1, 1950, to April 24, 2017, using the erosion-rate-versus-shear-stress curve that separates soil regions II and III

The red dashed line represents the critical shear stress.
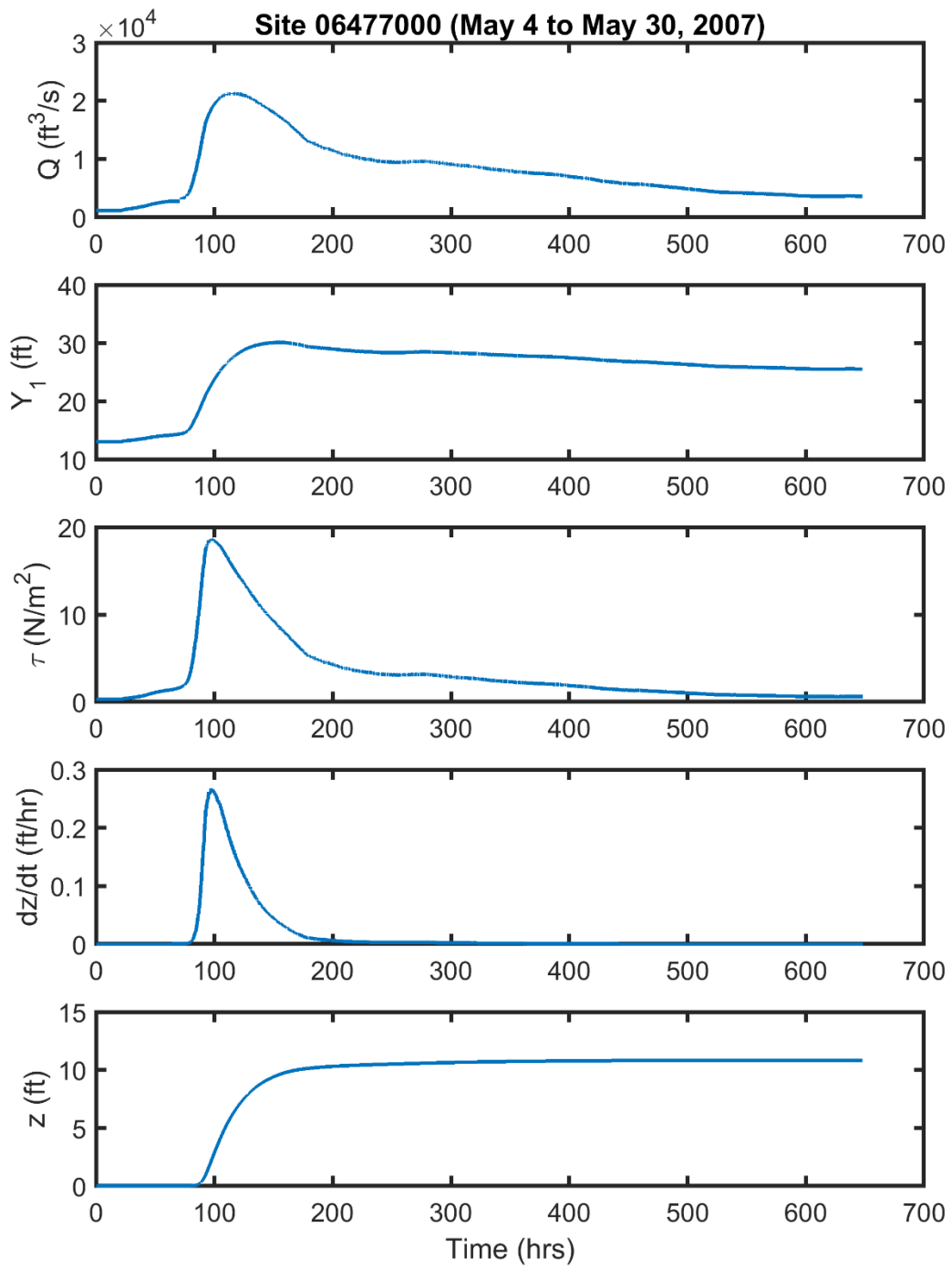
Figure 7.16 Computed history of contraction scour for the flood of May 2007
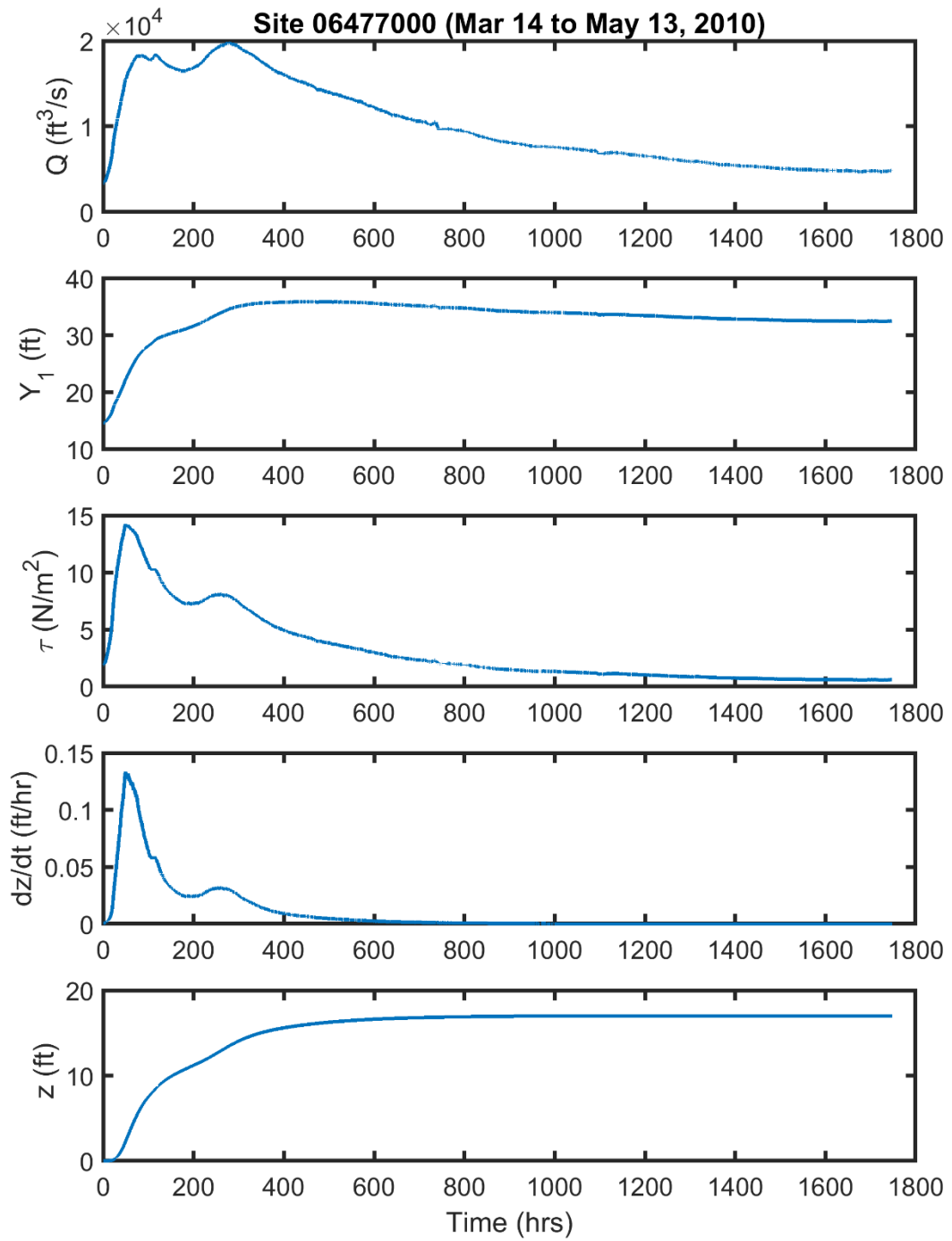
Figure 7.17 Computed history of contraction scour for the flood of March 2010
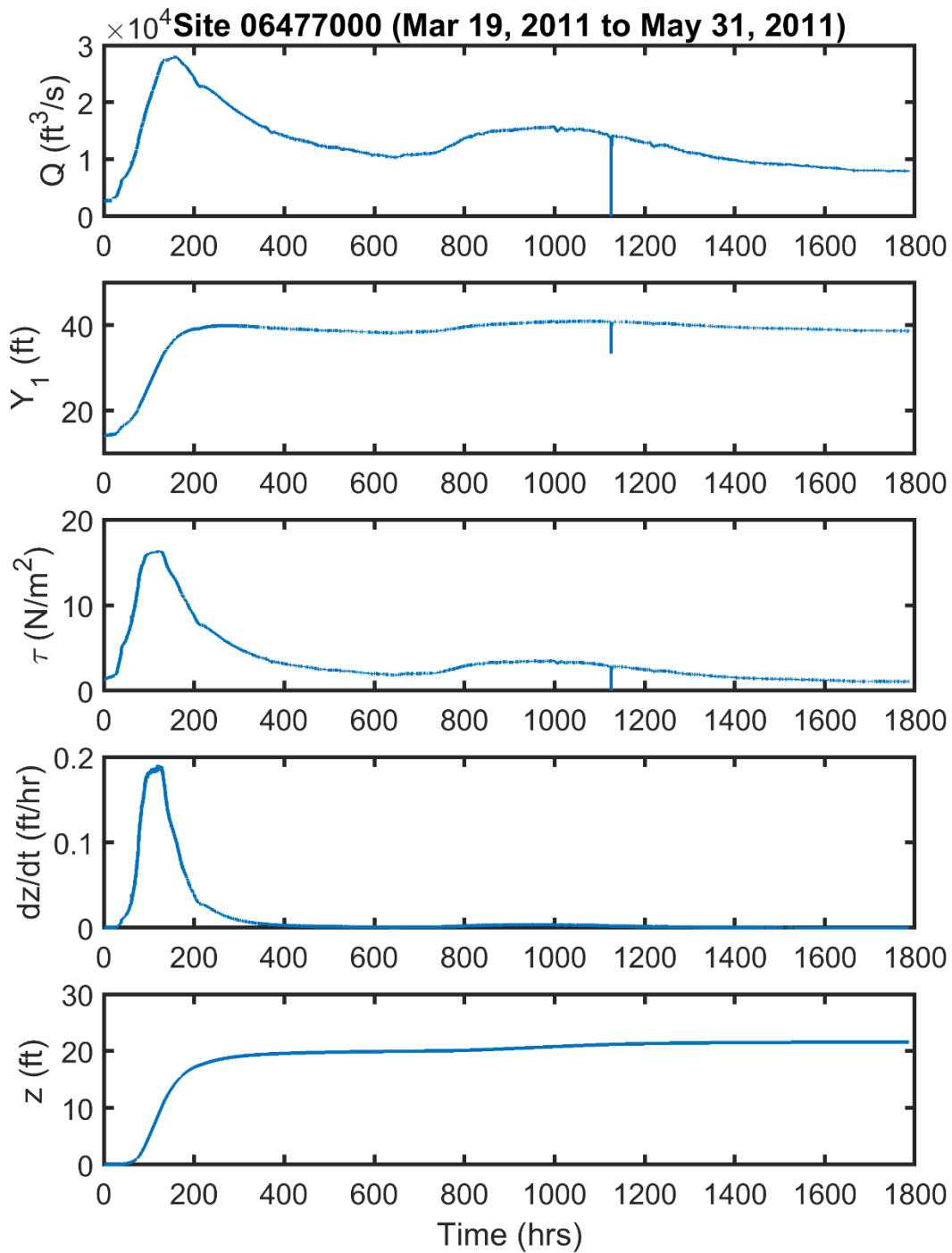
Figure 7.18 Computed history of contraction scour for the flood of March 2011

7.3   The t_e/t_{90} versus z_f/z_{max} Curve

In the energy method, the bed shear stress and rate of scour are adjusted in a stepwise procedure to predict the change in contraction scour depth with time. This approach does not require the computed scour history to follow a hyperbolic function. If the computed scour history follows the hyperbolic model, the computed $\frac{t_e}{t_{90}}$ ratios of the maximum annual floods shown in Tables 7.2 and 7.3 should be related to the $\frac{z_f}{z_{max}}$ ratio through Eq. (5.49). Figure 7.19 is a plot of the $\frac{t_e}{t_{90}}$ ratio computed using the energy method versus the $\frac{t_e}{t_{90}}$ ratio calculated using Eq. (5.49) with the $\frac{z_f}{z_{max}}$ values from the energy method. The agreement is poor, which suggests that a hyperbolic model may not describe the time history of contraction scour. Figure 7.19 shows that the hyperbolic model under-predicts the $\frac{t_e}{t_{90}}$ ratio (below the line of perfect agreement) when the initial rate of scour is smaller than 0.004 ft/hr. The latter includes all the maximum annual floods shown in Table 7.2 and those in Table 7.3 with return period less than about four years. On the other hand, the hyperbolic model over-predicts the $\frac{t_e}{t_{90}}$ ratio (above the line of perfect agreement) when the initial rate of scour is greater than 0.1 ft/hr. This includes all the maximum annual floods in Table 7.3 with return period greater than about 10 years.
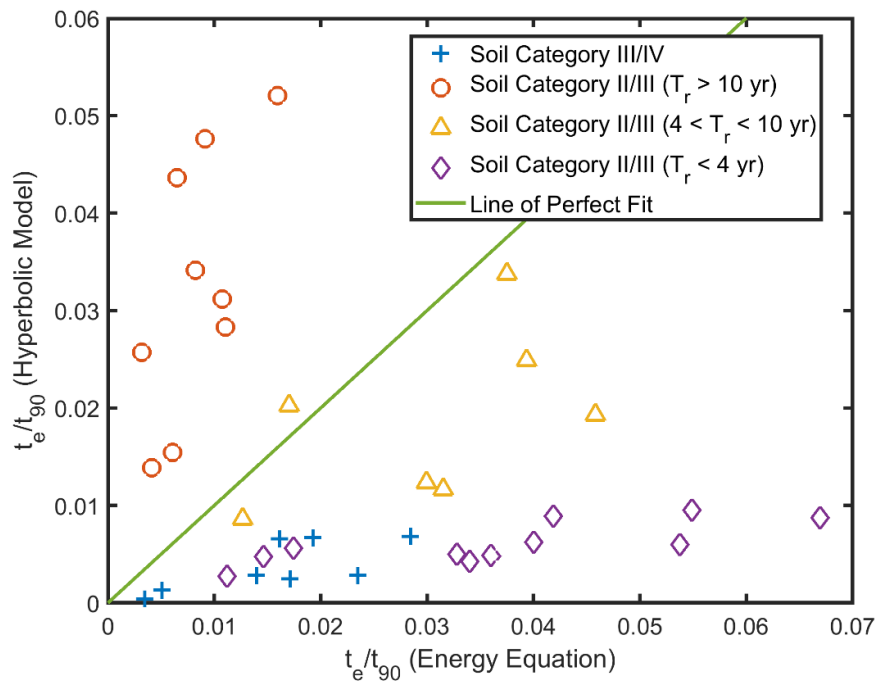
Figure 7.19 Comparison of the t_e/t_{90} ratios obtained using the energy method and hyperbolic model

To understand the significance of these results, we examine the computed scour histories produced by a constant discharge of 28,400 ft^3/s, which corresponds to the measured peak flow on March 25, 2011. Scour calculations are conducted for a time period of 100 hours using the erosion-rate-versus-shear-stress curve that separates soil regions III and IV, and for 125 hours using the erosion-rate-versus-shear-stress curve that separates soil regions II and III in Figure 5.3. Results of the SRICOS simulations are presented in Figures 7.20 and 7.21, respectively. The plots in both figures represent from top to bottom the time history of computed flow depth normalized by the maximum flow depth

at equilibrium condition $\frac{Y_1}{Y_{max}}$, computed bed shear stress normalized by the critical shear stress $\frac{\tau}{\tau_c}$, computed rate of scour normalized by the maximum rate of scour at the beginning of the flood $(\frac{dz}{dt})/(\frac{dz}{dt}_{max})$, and computed scour depth normalized by the equilibrium scour depth $\frac{z}{z_{max}}$.

Referring to Figure 7.20, the critical shear stress τ_c is 9.5 N/m^2, the equilibrium scour depth z_{max} is 20 ft, the initial rate of scour $\frac{dz}{dt}_{max}$ is 0.0039 ft/hr, and the time to reach 90% of the equilibrium scour depth is 20,029 hours (see $Q = 28,400$ ft^3/s in Table 7.2). The soil erosion rates are so slow that the final scour depth is far from equilibrium condition after the steady flow has been run for 100 hours (about four days). The flow depth in the contracted section has increased by only about 1% of the maximum flow depth at equilibrium condition. The bed shear stress has decreased from about 4.6 to 4.4 τ_c and the rate of scour by less than 7% of the initial rate of scour. The predicted final scour depth is 1.8% of the equilibrium scour depth ($z_f/z_{max} = 0.18$), and the equivalent time is 0.5% of the time it will take to reach 90% of the equilibrium scour depth ($t_e/t_{90} = 0.005$). For these flow conditions, the scour development with time does not follow the hyperbolic model. The variation of the $\frac{z_f}{z_{max}}$ ratio with the $\frac{t_e}{t_{90}}$ ratio computed using the energy method (blue line) is compared with the hyperbolic model given by Eq. (5.49) (red line) in the bottom plot. As seen, the hyperbolic model predicts that a $\frac{z_f}{z_{max}}$ ratio of 0.18 will be reached at about $\frac{t_e}{t_{90}} = 0.002$ instead of 0.005 as predicted by the energy method. Hence, the hyperbolic model under-predicts the $\frac{t_e}{t_{90}}$ ratio for a given $\frac{z_f}{z_{max}}$ ratio, or over-predicts the $\frac{z_f}{z_{max}}$ ratio for a given $\frac{t_e}{t_{90}}$ ratio.

A different trend is shown in Figure 7.21 for the results of SRICOS simulation conducted using the erosion-rate-versus-shear-stress curve that separates soil regions II and III. The critical shear stress τ_c is 1.33 N/m^2; the equilibrium scour depth z_{max} is 76.2 ft; the initial rate of scour $\frac{dz}{dt}_{max}$ is 2.2 ft/hr; and the time to reach 90% of the equilibrium scour depth is 25,064 hours (see $Q = 28,400$ ft^3/s in Table 7.3). The steady flow is run for 125 hours. The $\frac{Y_1}{Y_{max}}$ ratio increases from 0.23 to 0.43. The $\frac{\tau}{\tau_c}$ ratio decreases rapidly from 31.9 to 7.2, and the rate of scour from 2.2 ft/hr to 0.05 ft/hr. The computed final scour depth is 26% of the equilibrium scour depth ($z_f/z_{max} = 0.26$). The hyperbolic model, however, predicts that a $\frac{z_f}{z_{max}}$ ratio of 0.26 will be reached at $\frac{t_e}{t_{90}} = 0.039$ (red line, bottom plot) instead of 0.005 (blue line) by the energy method. Hence, the hyperbolic model over-predicts the $\frac{t_e}{t_{90}}$ ratio for a given $\frac{z_f}{z_{max}}$ ratio, or under-predicts the $\frac{z_f}{z_{max}}$ ratio for a given $\frac{t_e}{t_{90}}$ ratio.
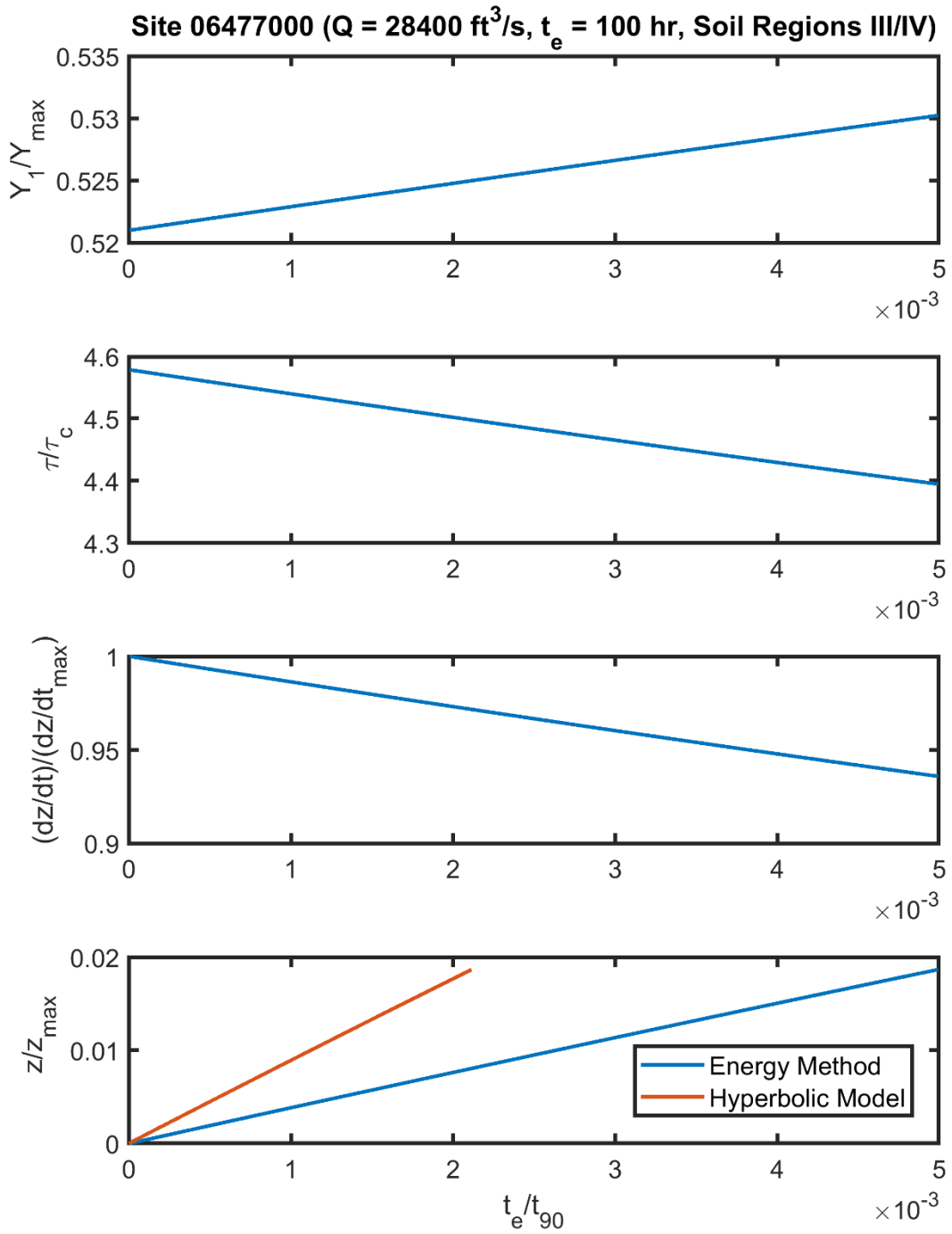
Figure 7.20 Computed history of contraction scour for a constant discharge of 28,400 ft³/s using the erosion-rate-versus-shear-stress curve that separates soil regions III and IV
The scour simulation is conducted for a time period of 100 hours.
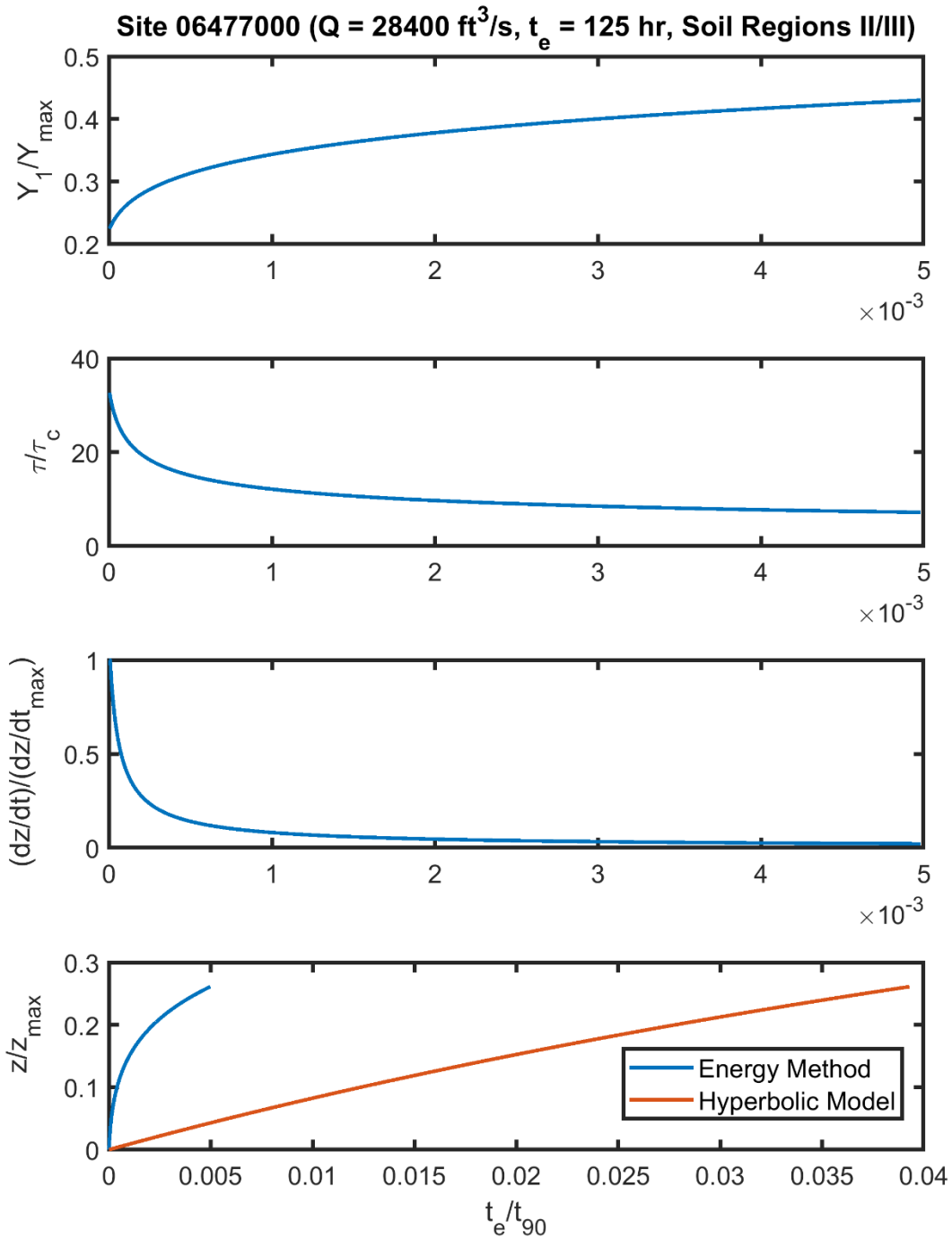
Figure 7.21 Computed history of contraction scour for a constant discharge of 28,400 ft³/s using the erosion-rate-versus-shear-stress curve that separates soil regions II and III
The scour simulation is conducted for a period of 125 hours.

The hyperbolic model (Eq. 5.22) is defined by two parameters, the initial rate of scour $\dot{z}_i$ and the equilibrium scour depth z_{max}. The model predicted that the $\frac{t_e}{t_{90}}$ and $\frac{z_f}{z_{max}}$ ratios are related by Eq. (5.49). Figure 7.22 shows the variation of the $\frac{z_f}{z_{max}}$ ratio with the $\frac{t_e}{t_{90}}$ ratio computed using the energy method for the maximum annual floods in Tables 7.2 and 7.3. The relationship predicted by the hyperbolic model (Eq. 5.49) is given by the green line. These results show that the $\frac{t_e}{t_{90}}$ and $\frac{z_f}{z_{max}}$ ratios are related but, unlike the hyperbolic model, the relationship depends on the soil erodibility. For a given $\frac{t_e}{t_{90}}$ ratio, the hyperbolic model over-predicts the $\frac{z_f}{z_{max}}$ ratio for soils with low rates of scour (see soil region III/IV) but under-predicts the $\frac{z_f}{z_{max}}$ ratio for soils with high rates of scour (see soil region II/III with $T_r > 10$ years). Thus, the hyperbolic model may not be flexible enough to represent the scour-depth-versus-time curve of contraction scour for all soil types.
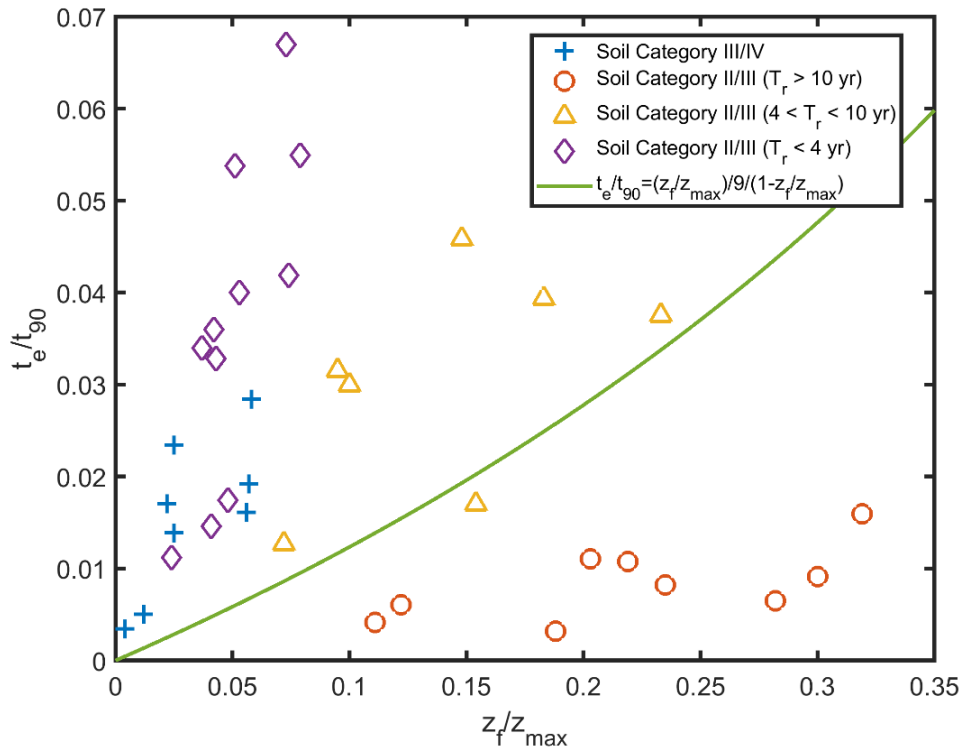
Figure 7.22 Variation of t_e/t_{90} ratio with z_f/z_{max} ratio computed using the energy method for the maximum annual floods in Tables 7.2 and 7.3

The hyperbolic model is represented by the solid green line.

7.4 Equivalent Time

The equivalent time computed using the erosion-rate-versus-shear-stress curve that separates soil regions III and IV is normalized by t_{90} and plotted against the normalized peak discharge $\frac{Q_{\max}}{Q_c}$ in Figure 7.23. There is much scatter in the data. The correlation between $\frac{t_e}{t_{90}}$ and $\frac{Q_{\max}}{Q_c}$ is poor; the R^2 value is 0.01463 and the root-mean-square error (RMSE) is 0.009095. Hence, the two parameters are essentially uncorrelated. The regression equation is given by:

$$\frac{t_e}{t_{90}} = 0.001636 \left[\frac{Q_{\max}}{Q_c} \right] + 0.01268 \tag{7.1}$$

The reason for the poor correlation can be seen in the computed scour histories shown in Figures 7.11 to 7.14. Scour depth increases so slowly that scouring continues long after the floods have peaked. Consequently, the peak discharge alone is not enough to predict the final scour depth and the equivalent time; flood duration is also an important parameter. The correlation of $\frac{t_e}{t_{90}}$ with $\frac{Q_{\max}t_s}{z_{\max}^3}$ is somewhat better (Figure 7.24); the R^2 value is 0.1293. However, the data are still very scattered and the RMSE (0.00855) is about the same as in Figure 7.23. The regression equation is given by:

$$\frac{t_e}{t_{90}} = 0.0003351 \left[\frac{Q_{\max}t_s}{z_{\max}^3} \right] + 0.01379 \tag{7.2}$$

When both $\frac{Q_{\max}}{Q_c}$ and $\frac{Q_{\max}t_s}{z_{\max}^3}$ are included as independent variables, the R^2 value increases significantly to 0.5957 and the RMSE decreases to 0.0064 (Figure 7.25). The multiple regression is given by the following equation:

$$\frac{t_e}{t_{90}} = 0.003011 \left[\frac{Q_{\max}}{Q_c} \right]^{1.703} \left[\frac{Q_{\max}t_s}{z_{\max}^3} \right]^{0.508} \tag{7.3}$$

Figure 7.26 compares the values of $\frac{t_e}{t_{90}}$ calculated using Eqs. (7.1) to (7.3) with the values from SRICOS simulations given in Table 7.2. The best agreement is obtained with Eq. (7.3). Both Eqs. (7.1) and (7.2) predict essentially a constant value of $\frac{t_e}{t_{90}}$ close to the mean value (≈ 0.016) of the different floods. Only Eq. (7.3) can predict the variations in $\frac{t_e}{t_{90}}$ ratio from flood to flood. The different predictions are also compared in Table 7.4. As seen, Eq. (7.3) in general does a better job in predicting the equivalent times of the different floods.
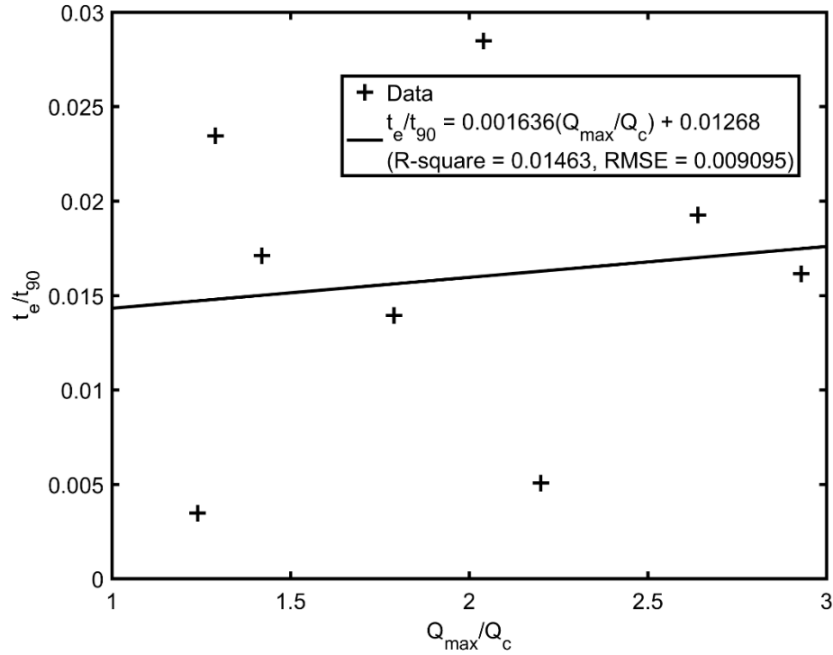
Figure 77.23 Normalized equivalent time versus normalized peak discharge
The results are computed using the erosion-rate-versus-shear-stress curve that separates soil regions III and IV.
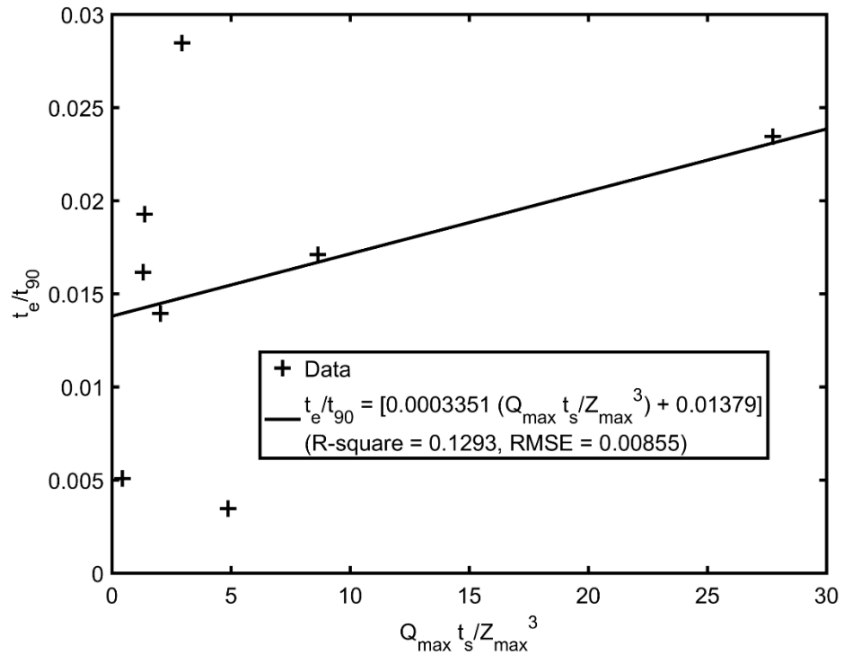
Figure 7.24 Normalized equivalent time versus normalized flood duration
The results are computed using the erosion-rate-versus-shear-stress curve that separates soil regions III and IV.
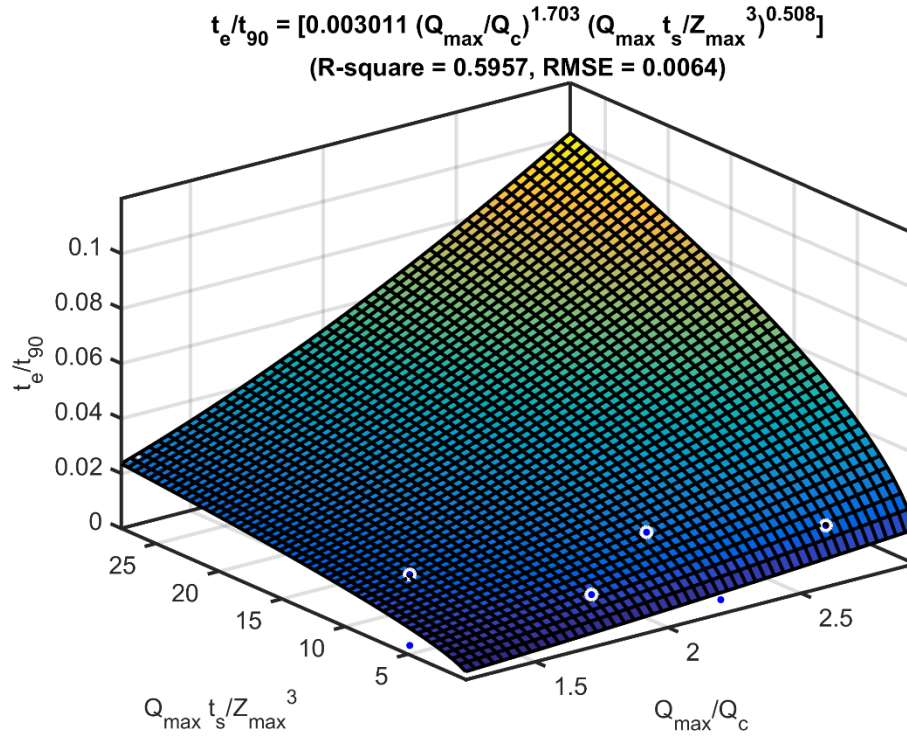
Figure 7.25 Normalized equivalent time versus normalized peak discharge and flood duration
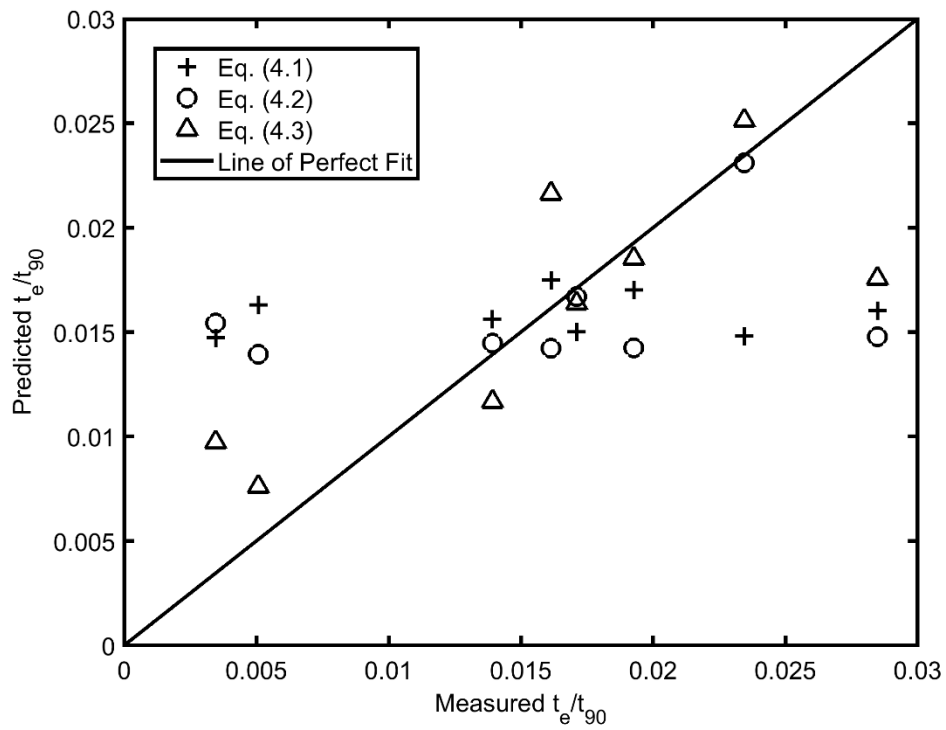
Figure 7.26 Comparison of different regression equations for predicting the t_e/t_{90} ratio

Table 7.4 Comparison of computed equivalent time from SRICOS simulations with predictions
of the different regression equations
*The results were obtained using the erosion-rate-versus-shear-stress curve that
separates soil regions III and IV.*

Year	$\dfrac{Q_{\max}}{Q_c}$	$\dfrac{Q_{\max}t_s}{3600z_{\max}^3}$	t_e, hr (Table 4.2)	t_e, hr (Eq. 4.1)	t_e, hr (Eq. 4.2)	t_e, hr (Eq. 4.3)
2011	2.93	1.32	333	350	285	433
1997	2.64	1.38	354.6	313	262	341
2007	2.20	0.44	79	254	217	118
2010	2.04	2.95	410.75	231	213	253
2001	1.79	2.04	172	193	179	144
1995	1.42	8.65	141.3	124	138	135
1969	1.29	27.75	135	85	133	145
1962	1.24	4.88	24	80	83	53

The results obtained using the erosion-rate-versus-shear-stress curve that separates soil regions II and III are presented in Figures 7.27 to 7.30. Only the maximum annual floods with return period greater than 10 years are included in the regression analysis. The regression equation for $\dfrac{t_e}{t_{90}}$ versus $\dfrac{Q_{\max}}{Q_c}$ is given by (Figure 7.27):

$$\frac{t_e}{t_{90}} = -0.000003993\left[\frac{Q_{\max}}{Q_c}\right] + 0.008358 \tag{7.4}$$

Figure 7.27 shows that $\dfrac{t_e}{t_{90}}$ and $\dfrac{Q_{\max}}{Q_c}$ are essentially uncorrelated; the R^2 value is close to zero and the RMSE is 0.004215. The latter is very large compared with the values of $\dfrac{t_e}{t_{90}}$. Inspection of Figures 7.16 to 7.18 shows that most of the increase in scour depth occurs after the peak flow arrives. Hence, the peak discharge alone is not enough to predict the final scour depth and equivalent time; the duration of the flood is also important. Figure 7.28 shows the regression equation for $\dfrac{t_e}{t_{90}}$ and $\dfrac{Q_{\max}t_s}{z_{\max}^3}$. The R^2 value is 0.2641 and the RMSE is 0.003659, which is somewhat better than Eq. (7.4). The regression equation is given by:

$$\frac{t_e}{t_{90}} = 0.055\left[\frac{Q_{\max}t_s}{z_{\max}^3}\right] + 0.005344 \tag{7.5}$$

A multiple regression involving both $\dfrac{Q_{\max}}{Q_c}$ and $\dfrac{Q_{\max}t_s}{z_{\max}^3}$ gives the following equation (Figure 4.29):

$$\frac{t_e}{t_{90}} = 0.01533\left[\frac{Q_{\max}}{Q_c}\right]^{0.9726}\left[\frac{Q_{\max}t_s}{z_{\max}^3}\right]^{0.8003} \tag{7.6}$$

The R^2 value is 0.5363 and the RMSE is 0.0031. The values of $\dfrac{t_e}{t_{90}}$ predicted by Eqs. (7.4) to (7.6) are compared with the results of SRICOS simulation in Figure 7.30, and the different predictions of t_e are presented in Table 7.5. As in Table 7.4, the regression equation developed using $\dfrac{Q_{\max}}{Q_c}$ as the independent variable [Eq. (7.4)] predicts essentially a constant value (≈ 0.0084) for the $\dfrac{t_e}{t_{90}}$ ratio. Including both $\dfrac{Q_{\max}}{Q_c}$ and $\dfrac{Q_{\max}t_s}{z_{\max}^3}$ as the independent variables improves the prediction of the $\dfrac{t_e}{t_{90}}$ ratio and its variation from flood to flood.
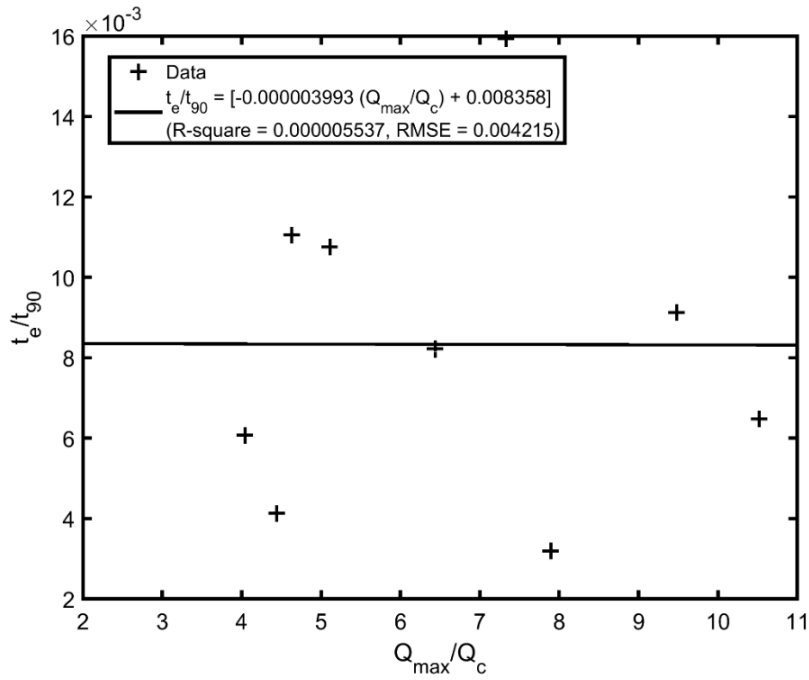
Figure 7.27 Normalized equivalent time versus normalized peak discharge
*The results are computed using the erosion-rate-versus-shear-stress curve
that separates soil regions II and III.*
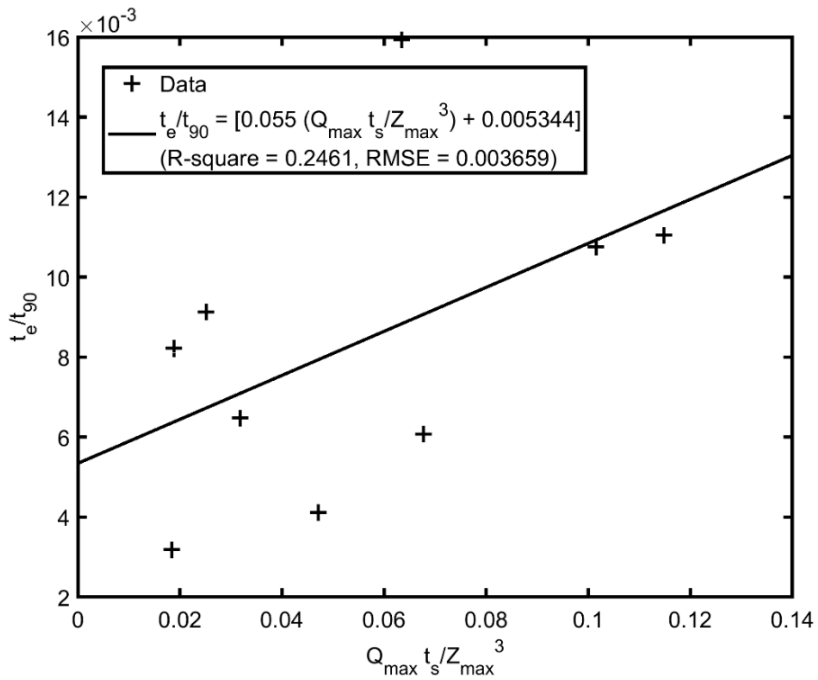
Figure 7.28 Normalized equivalent time versus normalized flood duration

$$t_e/t_{90} = [0.01533 \, (Q_{max}/Q_c)^{0.9726} \, (Q_{max} \, t_s/Z_{max}^3)^{0.8003}]$$
$$\text{(R-square = 0.5368, RMSE = 0.0031)}$$
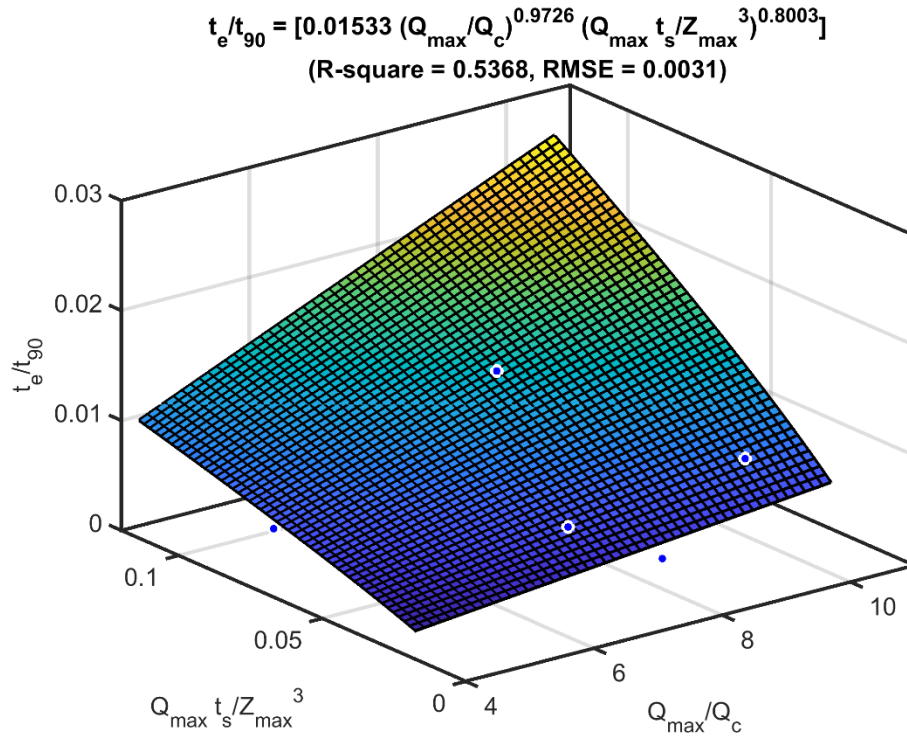
Figure 7.29 Normalized equivalent time versus normalized peak discharge and flood duration
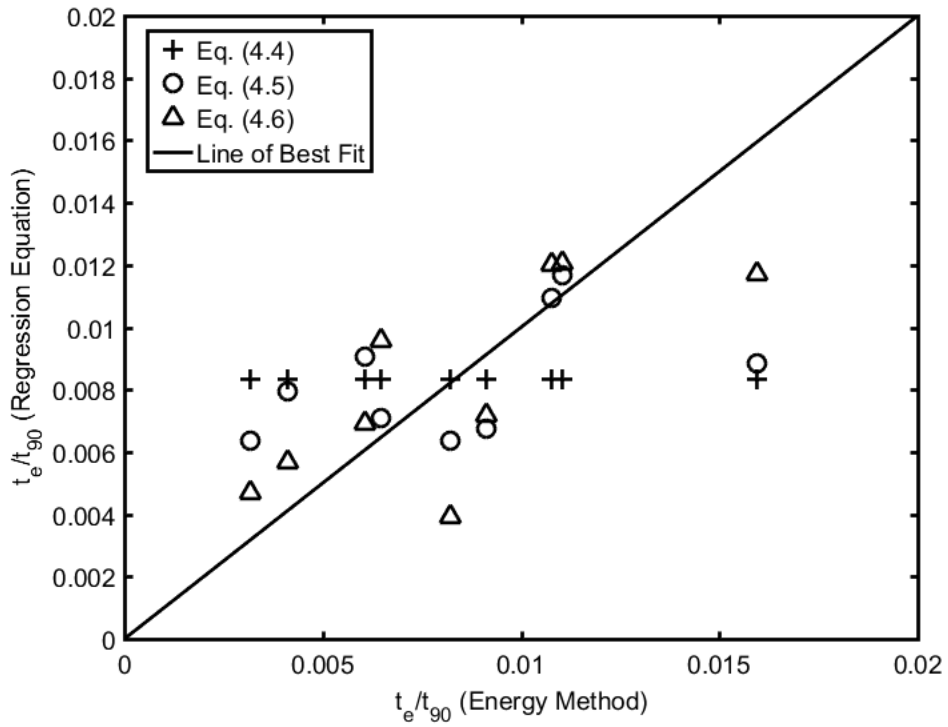
Figure 7.30 Comparison of different regression equations for predicting the t_e/t_{90} ratio

Table 7.5 Comparison of computed equivalent time from SRICOS simulations with predictions of the different regression equations

The results were obtained using the erosion-rate-versus-shear-stress curve that separates soil regions II and III.

Year	$\dfrac{Q_{max}}{Q_c}$	$\dfrac{Q_{max}t_s}{3600z_{max}^3}$	t_e, hr (Table 4.3)	t_e, hr (Fig. 4.4)	t_e, hr (Eq. 4.5)	t_e, hr (Eq. 4.6)
2011	10.52	0.0318	162.5	208	178	240
1997	9.48	0.0251	213.2	194	157	167
2007	7.89	0.0184	65.9	172	131	96
2010	7.33	0.0635	313.1	164	174	230
2001	6.44	0.0188	147.9	150	115	70
1995	5.11	0.1015	165.7	128	168	185
1969	4.63	0.1148	159.3	120	168	173
1962	4.44	0.0471	57.9	117	111	79
1960	4.04	0.0678	80	110	119	91

7.5 Generation of Future Hydrographs and Scour Risk Analysis

Although regression analysis has shown that the equivalent time of the maximum annual floods is a function of both peak discharge and flood duration, there is no reliable method to predict the duration of a flood; therefore, in practice Eq. (7.3) or (7.6) cannot be used to compute the $\dfrac{t_e}{t_{90}}$ ratio. However, Figures 7.23 and 7.27 can be used to select an envelope curve for the $\dfrac{t_e}{t_{90}}$ ratio. For example, Table 7.2 shows that the computed $\dfrac{t_e}{t_{90}}$ ratio is less than 0.02 except for the maximum annual flows in 1969 and 2010. Figure 7.31 shows the results of SRICOS simulation for a constructed series of 100 maximum annual floods obtained using a constant $\dfrac{t_e}{t_{90}}$ ratio of 0.02. The simulation is conducted using the erosion-rate-versus-shear-stress curve that separates soil regions III (medium erodibility) and IV (low erodibility). The soil critical shear stress τ_c is 9.5 N/m^2 and the erosion rate constant a' is 1.62. The critical discharge to produce scour is about 9,700 ft^3/s.

From top to bottom, the plots in Figure 7.31 represent the magnitude of annual peak flow Q, equivalent time t_e, flow depth Y_1, bed shear stress τ, initial rate of scour $\dfrac{dz}{dt}$, equilibrium scour depth z_{max}, and cumulative scour depth z. The largest flood in the constructed hydrograph has a discharge of 36,628 ft^3/s and an equivalent time of 483 hours. The return period is approximately 83 years. The predicted final scour depth for the entire series of 100 floods is 4.7 ft.

Table 7.6 presents the exceedance probabilities associated with different predicted final scour depths for the project lives of 50, 75, and 100 years. These statistics were computed using the results of 10,000 SRICOS simulations. The predicted final scour depths are much smaller than the equilibrium scour depths of the large floods (see the z_{max} plot in Table 7.2). For example, Table 7.6 shows that a contraction scour depth of 10 ft would have an exceedance probability of about 1% in a project life of 75 years. The flood of March 2011, which is about a 50-year flood, has an equilibrium scour depth of about 20 ft. Hence, accounting for the time rate of scour can significantly reduce the predicted scour depth for this soil category.

Table 7.6 Exceedance probabilities associated with predicted scour depths and project lives, with equivalent time given by $0.02t_{90}$

The soil critical shear stress τ_c and erosion rate constant a' are 9.5 N/m^2 and 1.62, respectively.

Contraction Scour Depth (ft)	4	5	6	7	8	9	10
Exceedance Probability (project life 50 yrs)	41%	24%	14%	7%	3%	<1%	<1%
Exceedance Probability (project life 75 yrs)	61%	44%	29%	18%	9%	4%	1%
Exceedance Probability (project life 100 yrs)	76%	63%	47%	32%	19%	10%	4%

Table 7.7 presents the results computed using a $\frac{t_e}{t_{90}}$ ratio of 0.03. This value provides an upper bound to the $\frac{t_e}{t_{90}}$ ratio for the maximum annual floods (see Figure 7.23). The exceedance probability for a predicted final scour depth of 10 ft in a project life of 75 years is increased to 10%. Although using a $\frac{t_e}{t_{90}}$ ratio of 0.03 would over-predict the equivalent time for most of the floods, the predicted final scour depth still represents a significant reduction from the equilibrium scour depth predicted using the HEC-18 method.
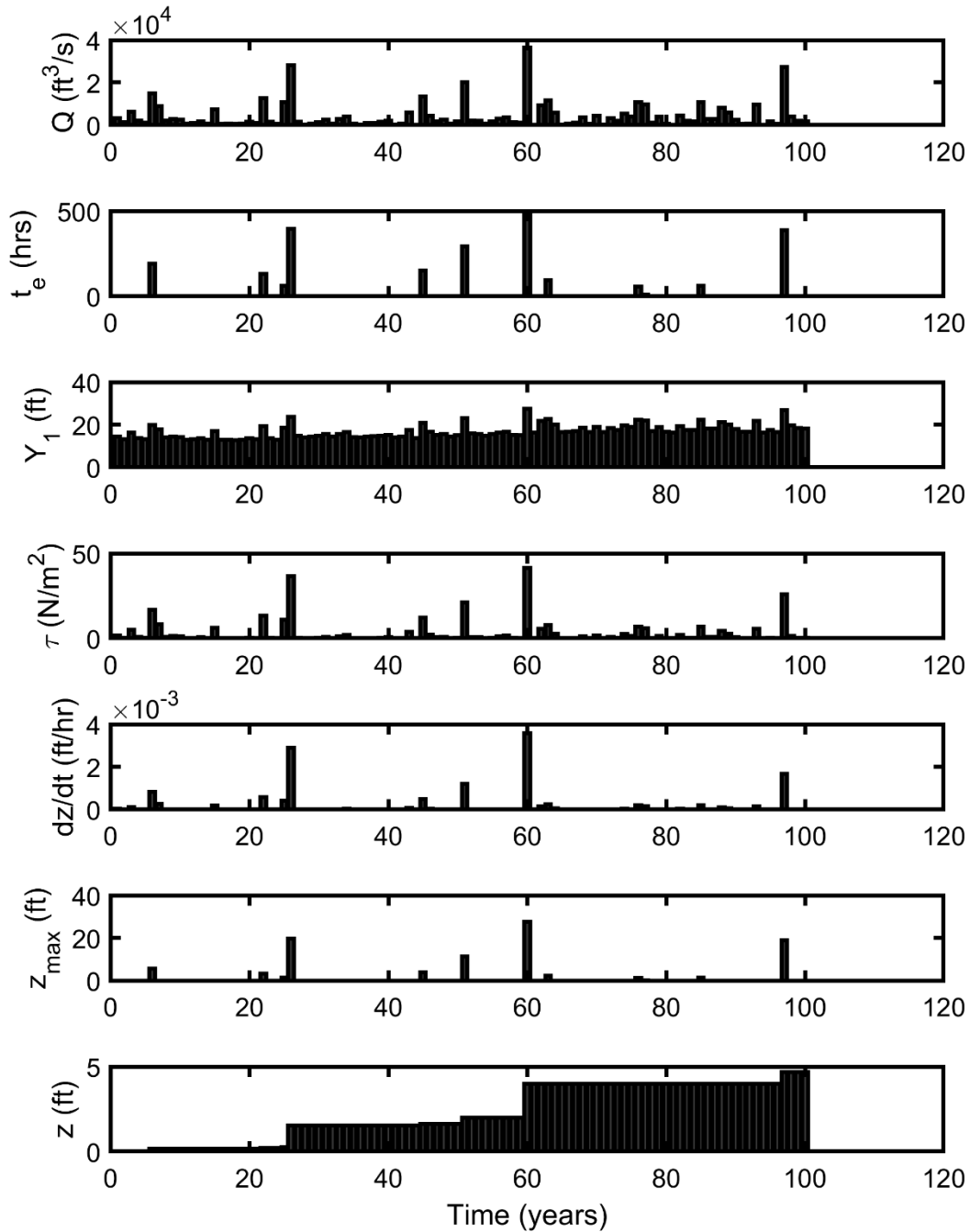
Figure 7.31 SRICOS simulation for a constructed series of 100 maximum annual floods
The soil critical shear stress τ_c and erosion rate constant a' are 9.5 N/m² and 1.62, respectively.

Table 7.7 Exceedance probabilities associated with predicted scour depths and project lives, with equivalent time given by $0.03t_{90}$

The soil critical shear stress τ_c and erosion rate constant a' are 9.5 N/m^2 and 1.62, respectively.

Contraction Scour Depth (ft)	4	5	6	7	8	9	10
Exceedance Probability (project life 50 yrs)	53%	45%	31%	20%	12%	7%	4%
Exceedance Probability (project life 75 yrs)	74%	65%	53%	39%	28%	18%	10%
Exceedance Probability (project life 100 yrs)	86%	79%	69%	57%	44%	32%	21%

Figure 7.32 presents the results of SRICOS simulation for a constructed series of 100 maximum annual floods conducted using the erosion-rate-versus-shear-stress curve that separates soil regions II (high erodibility) and III (medium erodibility). The soil critical shear stress τ_c is 1.33 N/m^2 and the erosion rate constant a' is 2.53. The critical discharge to produce scour is about 2,700 ft^3/s. The equivalent time is calculated using a $\frac{t_e}{t_{90}}$ ratio of 0.016. This value represents the upper limit of the $\frac{t_e}{t_{90}}$ ratio for the maximum annual floods with return period greater than 10 years (Figure 7.27). The largest flood in Figure 7.32 has a discharge of 36,317 ft^3/s and an equivalent time of 476 hours. The return period is approximately 82 years. The predicted final scour depth for the entire series of 100 floods is 40 ft. Table 7.8 presents the exceedance probabilities associated with different predicted final scour depths for the project lives of 50, 75, and 100 years. These results show that a predicted final scour depth of 50 ft would have an exceedance probability of 40% in a project life of 75 years. The predicted final scour depth is considerably higher compared with Table 7.7 for soil regions III and IV. However, when the critical shear stress is so low, the assumption of clear-water scour may not be valid. Sediment transport from the upstream section would limit the maximum scour depth that can be developed in the contracted section and the bridge site should be evaluated using the method for live-bed contraction scour.

Table 7.8 Exceedance probabilities associated with predicted scour depths and project lives

The soil critical shear stress τ_c and erosion rate constant a' are 1.33 N/m2 and 2.53, respectively. The equivalent time is given by $0.016t_{90}$.

Contraction Scour Depth (ft)	10	20	30	40	50	60
Exceedance Probability (project life 50 yrs)	98.8%	87%	65%	45%	28%	4%
Exceedance Probability (project life 75 yrs)	>99.9%	96%	81%	61%	40%	9%
Exceedance Probability (profile life 100 yrs)	>99.9%	>99.9%	90%	73%	51%	15%
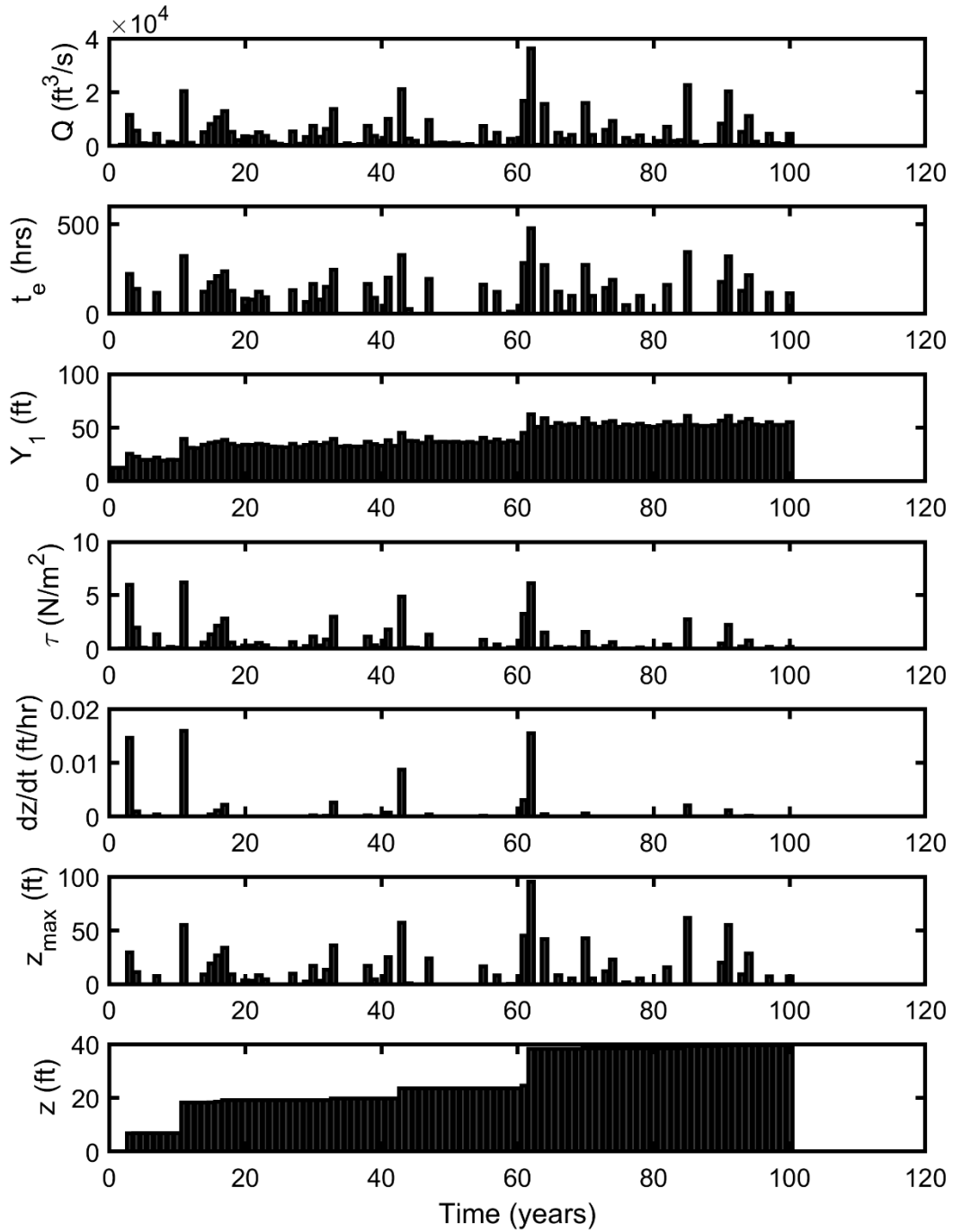
Figure 7.32 SRICOS simulation for a constructed series of 100 maximum annual floods
The soil critical shear stress τ_c and erosion rate constant α' are 1.33 N/m² and 2.53, respectively.

7.6 Comparison with Other Simplified SRICOS Methods

Table 7.9(a) and 7.9(b) presents the results of SRICOS simulations with the 100- and 200-peak flows run for five days. The results for the 500-year flood is not computed because the regression equations for the variations of unit discharge and flow depth shown in Figure 7.9 may not be valid for flow discharge much greater than 50,000 ft^3/s. The scour depths were computed using the erosion-rate-versus-shear-stress curves that separate soil regions III and IV in Table 7.9(a) and soil regions II and III in Table 7.9(b).

Referring to Table 7.9(a), the predicted final scour depth obtained by running the 100-year and 200-year peak flows for five days are 0.87 ft and 0.97 ft, respectively. These values are very close. In both cases, the computed scour depths are much smaller than the scour depths shown in Tables 7.6 and 7.7. Therefore, the exceedance probabilities of the computed scour depths are very high, and running the 100- or 200-year flood for five days would not be long enough to predict the final scour depth that may develop over the lifetime of the bridge.

When the 100-year and 200-year floods are run for five days with the erosion-rate-versus-shear stress curve that separates soil regions II and III, the predicted final scour depths are 28.3 ft and 34.1 ft, respectively [Table 7.9(b)]. The exceedance probability is about 80% for a project life of 75 years (Table 7.8), which is also very high. These results may be expected because the equivalent times of the maximum annual floods are all very long (see Table 7.3). Hence, multiple floods in an annual maximum series would contribute to the final scour depth.

If the S-SRICOS method is used to predict contraction scour, the equivalent time will be calculated using Eq. (5.43) with t_{hydro} taken to be the design life of the bridge, V_{max} the flow velocity produced by the design flood (e.g., the 100-year peak flow), and $\dot{z}_i$ the initial erosion rate at the maximum velocity. With $t_{hydro} = 75$ years, $V_{max} = \frac{q}{y_1} = 10.8$ ft/s and $\dot{z}_i = 0.0078 \frac{ft}{hr}$ [Table 7.9(a), soil categories III/IV], Eq. (5.43) yields a computed equivalent time of 1,108 hours (46 days). The computed final scour depth is 5.5 ft. From Table 7.7, the predicted scour depth has an exceedance probability of over 50%. For Table 7.9(b) we have $\dot{z}_i = 6.73 \frac{ft}{hr}$ for the 100-year flood and the computed equivalent time is 18,555 hours (773 days). The computed final scour depth is 24.3 ft and the exceedance probability is close to 90% (Table 7.8).

Table 7.9 Results of SRICOS simulations with the 100- or 200-year peak flows run for 5 days
(a) τ_c = 9.5 N/m^2, a' = 1.62, and (b) τ_c = 1.33 N/m^2, a' = 2.53

(a)

T_r (yr)	Q (ft^3/s)	q (ft^2/s)	Y_1 (ft)	Initial τ (N/ m^2)	Y_{max} (ft)	z_{max} (ft)	$\dot{z}_i$ (ft/hr)	z_f (ft)
100	40,025	258.1	23.9	67.2	55.2	30.6	0.0078	0.87
200	54,901	334.8	29.1	71.3	69	39.1	0.0086	0.97

(b)

T_r (yr)	Q (ft^3/s)	q (ft^2/s)	Y_1 (ft)	Initial τ (N/ m^2)	Y_{max} (ft)	z_{max} (ft)	$\dot{z}_i$ (ft/hr)	z_f (ft)
100	40,025	258.1	23.9	67.2	128.5	103.4	6.73	28.3
200	54,901	334.8	29.1	71.3	160.2	130.1	7.82	34.1

7.7 Summary

SRICOS simulations of contraction scour show that for the erosion-rate-versus-shear-stress curve that separate soil regions III (medium erodibility) and IV (low erodibility), there are significant reductions in the predicted final scour depths compared with the equilibrium scour depths of the large floods over a period of several decades when time rate of scour is considered. Soils that fall into this category include high plasticity clay and coarse gravel. For soils with very low critical shear stress, live-bed scour may occur, and the maximum scour depth is then limited by sediment transport from the upstream section. The relationships between equivalent time, peak discharge, and flood duration were obtained by multiple regression analysis. It was found that the equivalent times of the large floods are not predicted well using the peak discharge alone. Nevertheless, these results can be used to select an upper bound for the $\frac{t_e}{t_{90}}$ ratio to obtain conservative estimates for the equivalent time for floods of different return periods. Because of the long equivalent times of some floods, multiple floods in a hydrograph will contribute to scour and a single design flood will not be enough to predict the final scour depth developed over the lifetime of the bridge. It was also found that the predicted scour histories generally do not follow a hyperbolic function. Specifically, the relationship between the $\frac{t_e}{t_{90}}$ ratio and $\frac{z_f}{z_{max}}$ ratio varies with soil erodibility. The hyperbolic model over-predicts the rates of scour for soils with high critical shear stress and low erosion rates but under-predicts the rates of scour for soils with low critical shear stress and high erosion rates.

8. PIER SCOUR ANALYSIS – INTERSTATE 90 BRIDGES OVER SPLIT ROCK CREEK NEAR BRANDON, SOUTH DAKOTA

8.1 Site Description

The Interstate 90 bridges (Structures # 50-284-165 & 50-284-166) over Split Rock Creek are located on Interstate 90 westbound and eastbound, respectively, about 2,000 ft east of the Brandon/Corson exit in southeast South Dakota (Figure 8.1). The parallel bridges were rebuilt in 2017 and the lengths of the new bridges are both 378'–5½", with four spans. The bridge piers are consisted of groups of 3-ft-diameter columns pier sets (four columns per set for the eastbound bridge, and three columns per set for the westbound bridge) supported on spread footings. The pier sets and abutments are skewed at 30 degrees parallel to the flow. The low-flow channel runs under both bridges between bent 3 and bent 4. The bridge openings are classified as a spill-through abutment protected by riprap with two horizontal to one vertical side slope extending to the toe of the berms. The bed material of the stream is predominantly silt and clay. Before the bridges were rebuilt, river bottom profiles and streamflow measurements were collected by the USGS on the upstream and downstream sides of the bridge crossings on July 2, 1992 (1,420 ft^3/s), March 29, 1993 (4,600 ft^3/s), and May 8, 1993 (14,700 ft^3/s), as part of a scour assessment program conducted in South Dakota (Niehus, 1996). The measured channel profiles show 2 ft to 3 ft of pier scour in the low-flow channel and less than 1 ft of contraction scour. A gauging station (06482610) is located less than one mile upstream from the bridge site, but it operated only as a crest-stage partial-record gauging station from 1990 to 2001. The largest flood from 1966 to 2017 was recorded on May 8, 1993, and has a peak discharge of 18,900 ft^3/s. The estimated drainage areas at the gauging station and bridge site are 464 mi^2 and 466 mi^2, respectively.

A flood frequency analysis was conducted by fitting the Log Pearson Type III distribution to the recorded annual peak flows at the Corson station from water years 1966 to 2017. Table 8.1 shows the computed peak discharges and their return periods. The estimated 2-year, 100-year, and 500-year peak discharges are 2,373, 30,203, and 58,138 ft^3/s, respectively. A hydraulic analysis of the bridge site was conducted by HR Green in 2015 using the Hydrologic Engineering Center's River Analysis System HEC-RAS. Figures 8.2 and 8.3 show the variations of computed flow depth and flow velocity, respectively, with discharge. These results are taken from river station 8.333 located 128 ft upstream of the westbound bridge. The flow depth and flow velocity are the maximum values from the flow distribution output computed for a given discharge. Since HEC-RAS distributes flow by conveyance, these flow depths and velocities would generally represent the flow conditions in the low-flow channel where the flow is the deepest.

Figure 8.1 Aerial photograph of Interstate 90 bridges over the Split Rock Creek near Brandon, South Dakota

(Map data ©2018 Google)

Table 8.1 Estimated peak discharges for different return periods at Interstate 90 bridges over Split Rock Creek

Recurrence Interval (Years)	Peak Discharge (ft³/s)
2	2,372
5	5,721
10	9,230
25	15,581
50	22,017
100	30,203
200	40,509
500	58,138
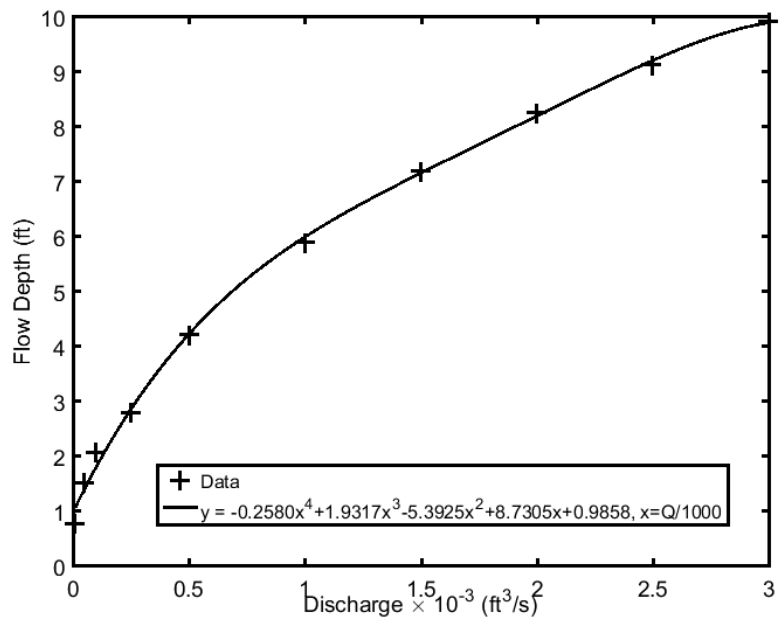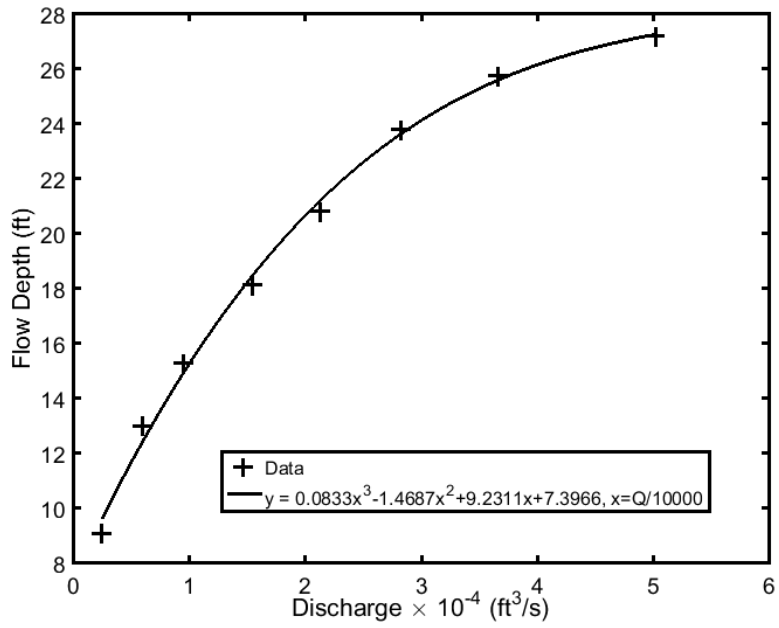
Figure 8.2 Computed flow depth versus flow discharge; high flow (top plot), and low flow (bottom plot)
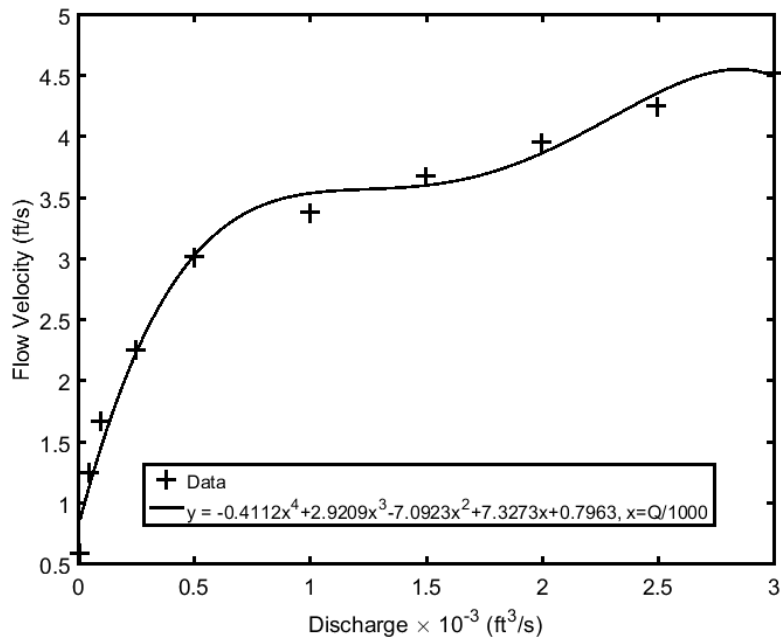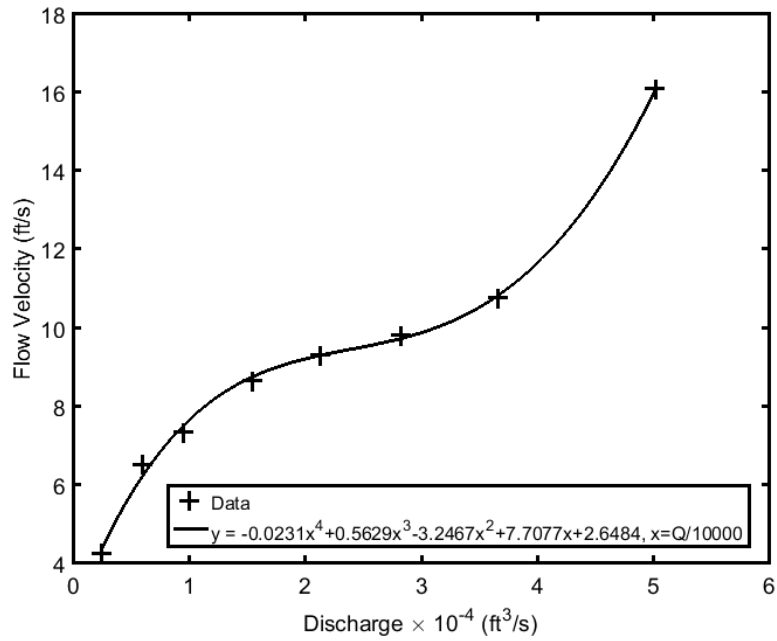
Figure 8.3 Computed flow velocity versus flow discharge; high flow (top plot) and low flow (bottom plot)

Table 8.2 Summary of input parameters for SRICOS simulations

Pier geometry	Pier width $a = 3$ ft, pier length $L = 9$ ft (# of piers $\cdot$ a), pier shape cylindrical ($K_1 = 1.0$)
Channel geometry	Number of bents $N = 3$, pier spacing $S = 85$ ft, angle coefficient $K_2 = 1.0$, bed condition coefficient $K_3 = 1.1$
Flow parameters	Figs. 8.2 and 8.3
Fluid parameters (20° C)	Density $\rho = 998.2$ kg/m^3, kinematic viscosity $v = 1.004 \times 10^{-6}$ m^2/s
Soil parameters	Table 5.1
Hydrograph	USGS streamflow data at Corson, South Dakota

8.2 Streamflow Analysis

Recorded hydrographs from the streamflow gauging station at Corson and the soil erosion rate chart in Figure 5.3 (see also Table 5.1) were used with the SRICOS method to compute scour histories from 2001 to 2017. Table 8.2 shows the values of the input parameters used in the SRICOS simulations. The Split Rock Creek at Corson station was operated as a continuous-record streamflow station from October 1, 1965, to September 30, 1989, and from October 1, 2002, to the present. The station was operated as a crest-stage partial-record station from October 1, 1989, to September 30, 2001. Daily mean flow data are available from 1965 to 1989 and 15-minute flow data from 2001 to the present. The daily-to-hourly disaggregation method described in Straub and Over (2010) was used to interpolate hourly mean flows from daily mean flows. The method computes a set of flow values that are assumed to apply at noon each day, with intermediate flow values represented by straight line segments. Figure 8.4 shows a comparison of the interpolated flows (dashed line) with the recorded daily mean flows (solid line) for the recorded maximum annual flood in 1969. A peak discharge of 17,800 ft^3/s was recorded on April 8, 1969, compared with an interpolated peak flow of 18,310 ft^3/s. These values are very close. However, this is not the case for most floods. Figure 8.5 shows the results for the maximum annual flood in 1979. The disaggregation method interpolates a peak flow of 9,098 ft^3/s compared with a recorded peak flow of 10,500 ft^3/s. Table 8.3 shows a comparison of the recorded and interpolated peak flow values for the large floods between 1966 and 1989. Flash floods often occur in the Split Rock Creek. The flow durations may not be long enough for accurate daily-to-hourly streamflow disaggregation in some cases. This may be why the peak discharge was under-estimated for many of the larger floods.

Table 8.3 Comparison of recorded peak flows and interpolated peak flows from streamflow disaggregation

Year	1969	1974	1978	1979	1982	1983	1984	1985	1986
Measured Peak Flow (ft^3/s)	17,800	5,240	3,250	10,500	3,090	4,500	9,020	4,100	7,920
Interpolated Peak Flow (ft^3/s)	18,310	2,214	3,337	9,098	1,440	3,793	8,036	2,864	7,406
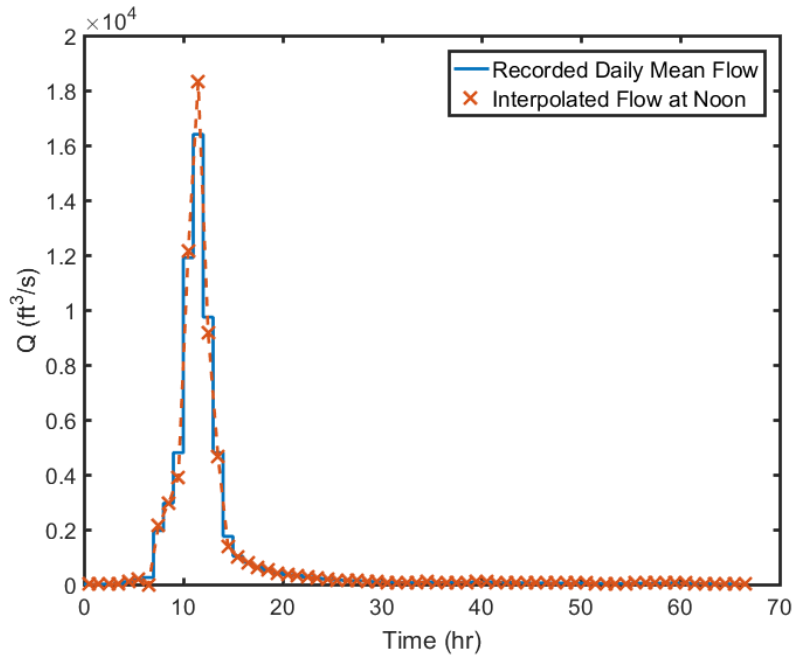
Figure 8.4 Daily-to-hourly streamflow disaggregation for the maximum annual flood
on April 8, 1969
*The interpolated peak flow magnitude is 18,310 ft³/s, which is comparable to the recorded
peak flow of 17,800 ft³/s.*
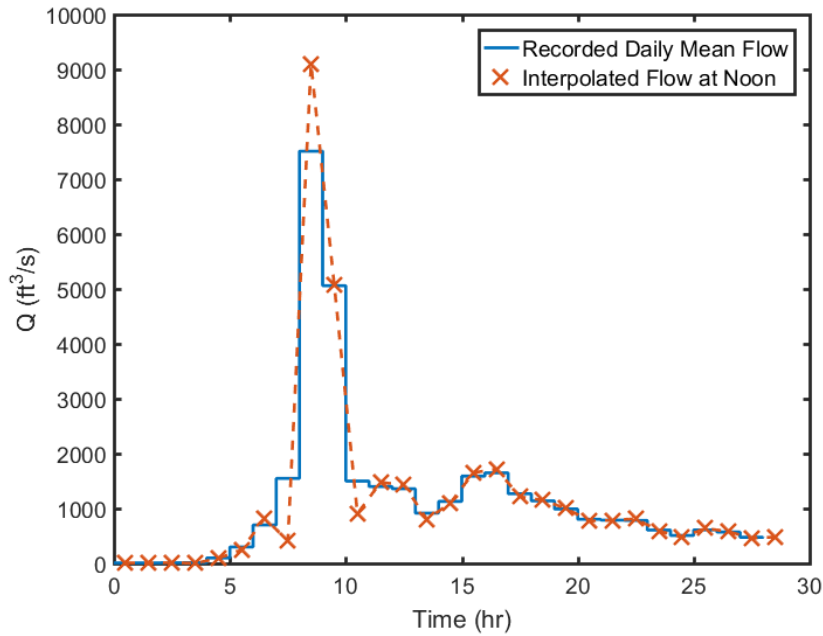
Figure 8.5 Daily-to-hourly streamflow disaggregation for the maximum annual flood
on March 22, 1979
*The interpolated peak flow magnitude is 9,098 ft³/s, which is significantly less than the
recorded peak flow of 10,500 ft³/s.*

When continuous record is not available, daily streamflow data may be transferred from a gauging station (the donor) on another stream to the ungauged stream using the QPPQ method (Archfield et al., 2013). The discharge time series at the Split Rock Creek at Corson gauging station from October 1, 1989, to September 30, 2001, was estimated using the QPPQ method using the Skunk Creek station at Sioux Falls (06481500) as an index station. The Skunk Creek station has an estimated drainage area of 622 mi^2 and the drainage basin characteristics are like the Split Rock Creek. Two overlapping periods (October 1, 1965, to September 30, 1989, and October 1, 2003, to September 30, 2016) were used to compute flow-duration curves (FDCs) for the two stations, and the QPPQ method was used to estimate the discharge time series for the period from October 1, 1989, to September 30, 2001, when continuous flow record is not available at the Split Rock Creek at Corson station.

A detailed description of the procedure to compute FDCs and estimate discharge time series using the QPPQ method can be found in Straub and Over (2010). A flow-duration curve is a cumulative frequency curve that shows the percent of time during which specified discharges were equaled or exceeded in a given period. FDCs are computed by sorting observed daily mean flow values in ascending order and assigning exceedance probability $P(Q_i)$ to each flow value (Q_i, $i = 1, 2, \ldots n$) by using the following plotting formula:

$$P(Q_i) = 1 - \frac{i - a}{n + 1 - 2a} \tag{8.1}$$

where n is the number of days in the record and the parameter a (not to be confused with the pier width) depends on the distribution with a value of 0.40 suggested for situations in which the exact distribution is unknown (Bedient and Huber, 1992). Figure 8.6 shows the computed FDCs at Skunk Creek (base gage) and Split Rock Creek (extension gage) for the overlapping period. To give an example, the figure shows that the daily mean flow was at least 100 ft^3/s for about 19% (FDC Percentile = 0.19) of the time at Skunk Creek and about 24% (FDC Percentile = 0.24) at Split Rock Creek.
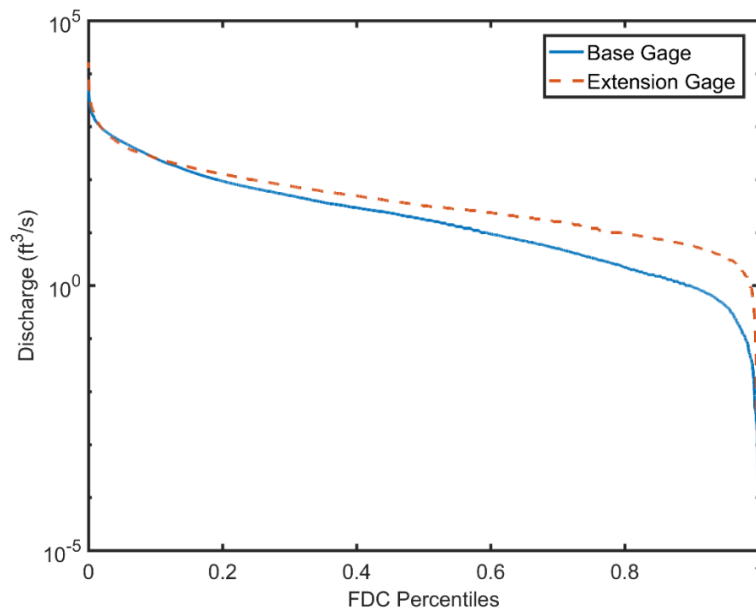
Figure 8.6 Flow-duration curves (FDCs) at the base (Skunk Creek) and extension (Split Rock Creek) gages during the overlapping period (10/1/1965 to 9/30/1989 and 10/1/2003 to 9/30/2016)

In the QPPQ method, it is assumed that the time history of exceedance probabilities of the flows at the base and extension gages are identical. Figure 8.7 shows a scatter plot of the computed FDC percentiles for the observed flows at Skunk Creek and Split Rock Creek during the overlapping period. Although there is high correlation (R value = 0.9155) between the two records, considerable discrepancies exist for some flows. Specifically, flow rates with similar exceedance probabilities were found to occur at different times at the two sites, not at the same time as the method has assumed. This can happen in two watersheds with similar basin characteristics due to different storm paths and spatial variability in precipitation during the storm.
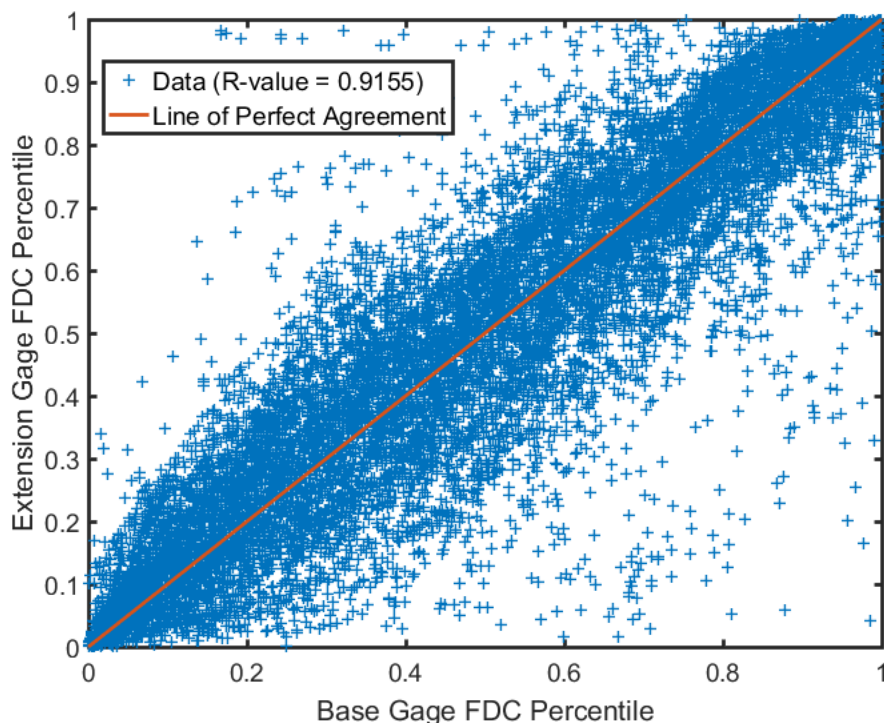
Figure 8.7 Scatter plot of FDC percentiles for Skunk Creek (base gage) and Split Rock Creek (extension gage) during the overlapping period (10/1/1965 to 9/30/1989 and 10/1/2003 to 9/30/2016)

Figure 8.8 shows the time series of recorded discharges at Skunk Creek (top plot) and the estimated discharges at Split Rock Creek (bottom plot) during the extension period. To illustrate the procedure of the QPPQ method, the observed daily mean flow at Skunk Creek on July 11, 1993 (day 1,380 of the extension period), is 7,610 ft³/s and the measured peak discharge is 8,640 ft³/s. This is also the maximum daily mean flow at the Skunk Creek station in 1993. From the computed flow-duration curve for Skunk Creek shown in Figure 8.6, the observed discharge has an exceedance probability of 0.00004418. The QPPQ method assumes that the time history of exceedance probabilities is identical at the base and extension gages. The corresponding discharge (16,850 ft³/s) is interpolated (or extrapolated) from the computed flow-duration curve for Split Rock Creek. Based on the assumption of the QPPA method, the maximum daily mean flow at Split Rock Creek would also occur on July 11, 1993. This is not true. In 1993, the maximum annual flood in Split Rock Creek occurred on May 8 with a measured peak discharge of 18,900 ft³/s.
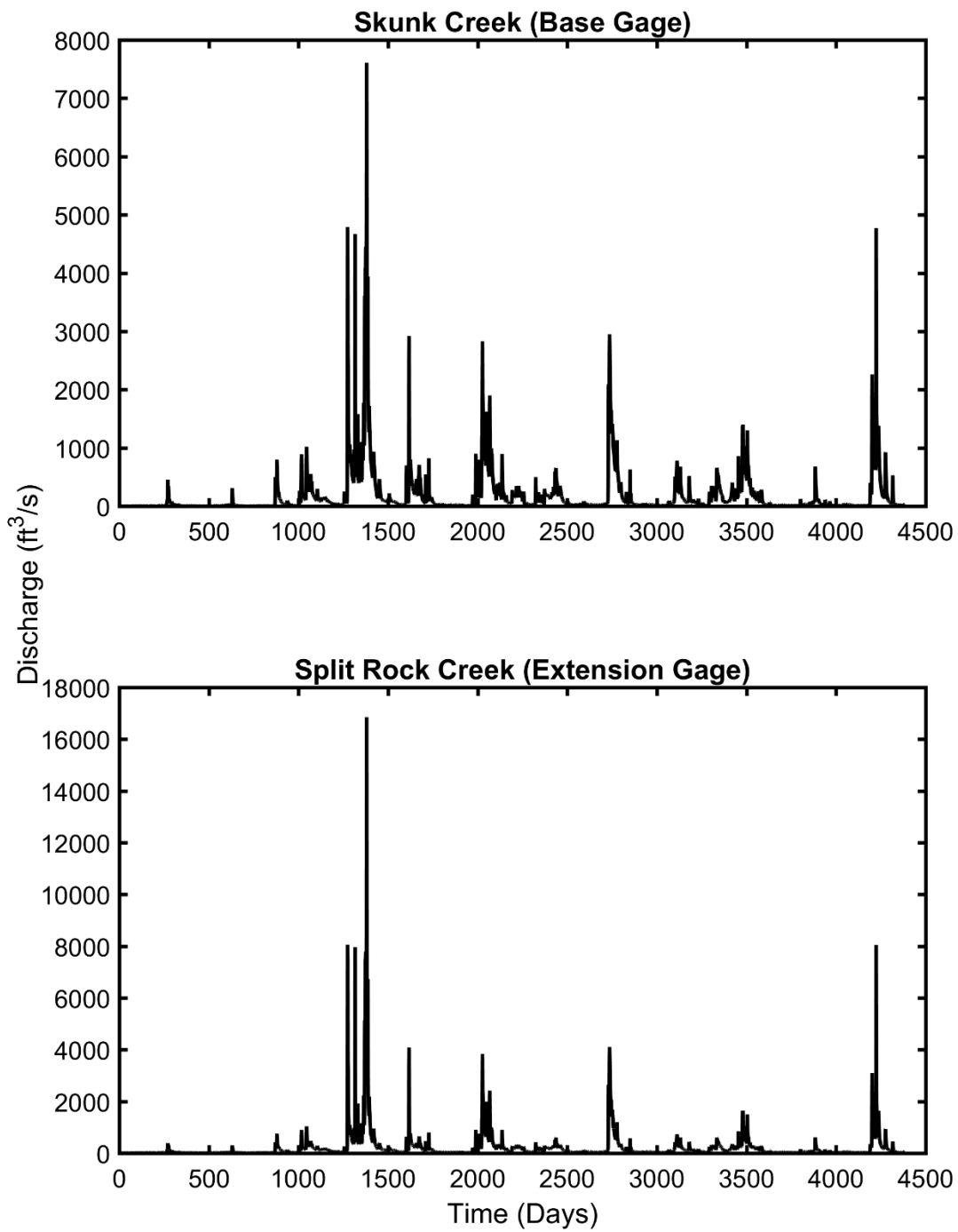
Figure 8.8 Time series of recorded discharges at Skunk Creek (top plot) and estimated discharges at Split Rock Creek (bottom plot) during the extension period (October 1,1989, to September 30, 2001)

The Split Rock Creek at Corson gauging station operated as a crest-stage partial-record station during the extension period. The recorded annual peak flows can be used to check the estimated discharges obtained using the QPPQ method. Table 8.4 lists the observed annual peak flows for three large floods during the extension period together with the daily mean flows estimated using the QPPQ method and the disaggregated hourly mean flows. These results show that the disaggregated hourly mean flows are significantly lower than the observed peak flows. Comparison of the streamflow records at the two stations during the overlapping period shows that observed peak flows did not always occur on the same day at the two stations, thus violating the basic assumption of the QPPQ method.

Table 8.4 Observed peak flows in selected years during the extension period and estimated daily and hourly mean flow values at the Split Rock Creek at Corson streamflow gauging station

Day of Observed Peak Streamflow	5/8/93	4/19/95	3/28/97
Observed Peak Flow Value (ft^3/s)	18,900	5,820	8,290
Estimated Daily Mean Flow by QPPQ method (ft^3/s)	7,962	3,834	4,103
Interpolated Hourly Mean Flow (ft^3/s)	10,420	4,320	4,234

8.3   Scour History Analysis

SRICOS simulations were conducted from 2001 to 2017 when 15-minute flow data are available. Table 8.5 shows the results for the maximum annual floods with return period greater than two years. The pier scour simulations were conducted using the erosion-rate-versus-shear-stress curve that separates soil regions III and IV in Figure 5.3. All the predicted final scour depths are very small (less than 0.2 ft). This is the situation where using the SRICOS method instead of the traditional HEC-18 method could result in significant reduction in the predicted scour depth. The predicted final scour depth obtained using the recorded hydrograph from October 1, 2001, to November 18, 2017, is 0.57 ft (Figure 8.9). For comparison, the equilibrium scour depth of the 100-year peak flow (30,203 ft^3/s) is 8.8 ft. Figure 8.10 presents the results of SRICOS simulation for the maximum annual flood in 2010. This flood has a recorded peak discharge of 13,100 ft^3/s. The critical shear stress is 9.5 N/m^2 (red dashed line in the bed-shear-stress-versus-time plot). Scouring ceases at the end of the flood when the measured discharge falls below the critical discharge. The duration of the flood t_s, defined as the time period when the measured discharge exceeds the critical discharge, is about five days.

The flood durations of the maximum annual floods in Table 8.5 range from one to six days and generally increase with discharge. All the maximum annual floods have $\frac{z_f}{z_{max}}$ values much less than unity. This ratio is a measure of the capacity of a flood to produce scour. A large $\frac{z_f}{z_{max}}$ ratio indicates that a flood would be able to produce a final scour depth close to its equilibrium scour depth. The $\frac{t_e}{t_{90}}$ ratio is another parameter for measuring the rate of scour. Introduced in Chapter 5, the equivalent time t_e is the time that will take for the peak discharge in a recorded hydrograph to produce the same final scour depth as the actual hydrograph, and t_{90} is the time it will take to reach 90% of the equilibrium scour depth for the peak discharge. A small $\frac{t_e}{t_{90}}$ ratio means that the equivalent duration of the flood t_e is much shorter than the time required to reach the equilibrium scour depth, and thus the final scour depth produced by the flood will be small compared with the equilibrium scour depth. This is the situation where using the SRICOS method to predict scour instead of the traditional HEC-18 method may be beneficial. As seen in Table 8.5, the $\frac{t_e}{t_{90}}$ ratios of the maximum annual floods are all close to zero. This is consistent with the small predicted final scour depth produced by the recorded hydrograph from 2001 to 2017 (Figure 8.9).

Table 8.5 Summary of results of SRICOS simulations for the maximum annual floods between 2001 and 2017 that can produce scour

The SRICOS simulations were conducted using the erosion-rate-versus-shear-stress curve that separates soil regions III and IV in Fig. 5.3. The critical discharge is 1,580 ft^3/s.

Year	Peak Discharge Date	Peak Discharge Q_{max} (ft^3/s)	Return Period (yr)	Final Scour Depth z_f (ft)	Initial Erosion Rate (ft/hr)	Equilibrium Scour Depth z_{max} (ft)	$\dfrac{z_f}{z_{max}} \times 100\%$
2010	9/24/2010	13,100	18.1	0.17	0.003392	7.79	2.2
2014	6/17/2014	13,100	18.1	0.14	0.003392	7.79	1.8
2006	4/7/2006	8,020	8	0.04	0.002024	7.03	0.57
2011	7/15/2011	4,730	3.9	0.06	0.001054	6.22	0.96
2012	5/7/2012	4,730	3.9	0.04	0.001054	6.22	0.64
2007	3/13/2007	4,050	3.3	0.05	0.000871	6.01	0.83
2004	5/30/2004	3,400	2.7	0.01	0.000708	5.79	0.17
2015	7/7/2015	2,510	2.1	0.01	0.000507	5.46	0.18

Year	Flow Duration Exceeding Critical Discharge t_s (hr)	Equivalent Time t_e (hr)	t_{90} (hr)	$\dfrac{t_e}{t_{90}} \times 1000$	$\dfrac{Q_{max}}{Q_c}$	$\dfrac{Q_{max}t_s}{z_{maz}^3}$
2010	114.25	50.78	20,681.74	2.4553	8.2911	3166.03
2014	131.75	41.96	20,681.74	2.0288	8.2911	3650.98
2006	49.25	21.69	31,242.31	0.6943	5.0759	1136.88
2011	100	57.55	53,121.75	1.0834	2.9937	1965.58
2012	76.75	39.46	53,121.75	0.7428	2.9937	1508.58
2007	90.25	59.1	62,081.36	0.952	2.5633	1683.75
2004	36.25	19.53	73,617.70	0.2653	2.1519	634.97
2015	21.75	18.45	97,014.91	0.1902	1.5886	335.39
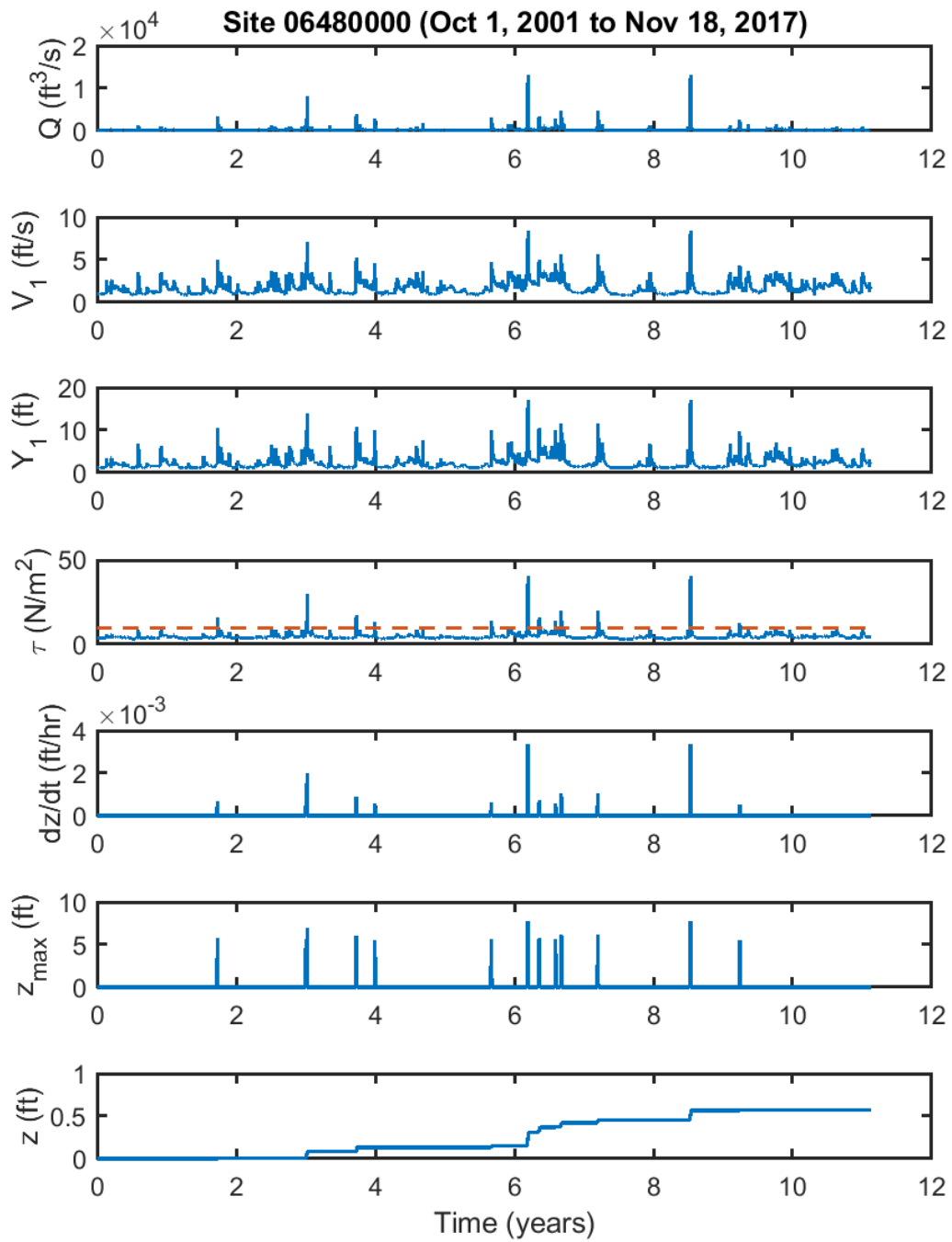
Figure 8.9 Computed scour history from October 1, 2001, to November 18, 2017, using the erosion-rate-versus-shear-stress curve that separates soil regions III and IV
The red dashed line represents the critical shear stress.
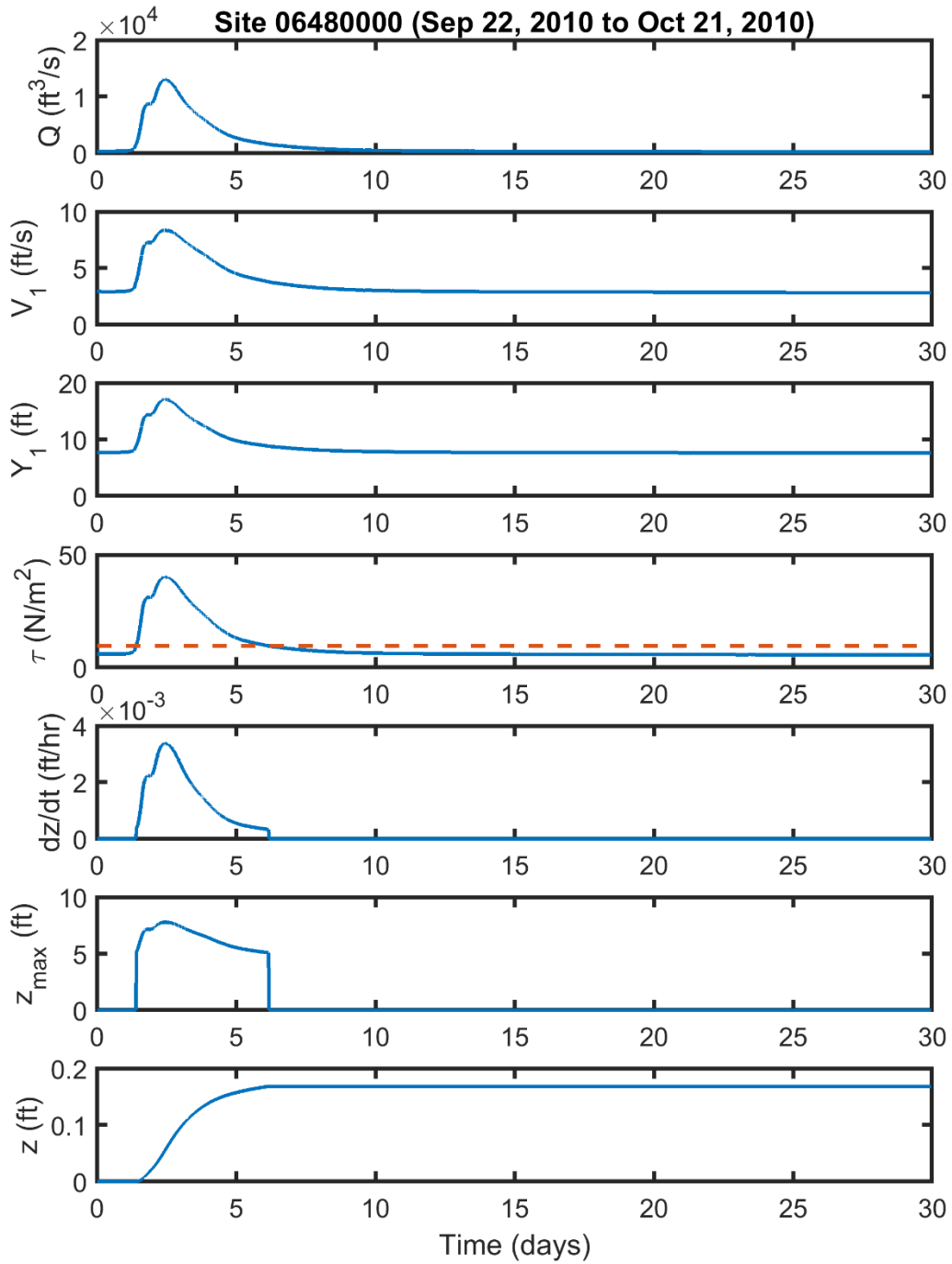
Figure 8.10 Computed scour history for the maximum annual flood in 2010 using the erosion-rate-versus-shear-stress curve that separates soil regions III and IV
The red dashed line represents the critical shear stress.

Table 8.6 show the results obtained using the erosion-rate-versus-shear-stress curve that separates soil regions II and III. The critical shear stress is 1.33 N/m^2. The critical discharge is extremely low (< 1 ft^3/s). Consequently, all the maximum annual floods produce some scour. Furthermore, the soil erosion rates of the large floods are quite high. The predicted final scour depth obtained using the recorded hydrograph from October 1, 2001, to November 18, 2017, is 7 ft (Figure 8.11), which is not much smaller than the equilibrium scour depth of the 100-year peak flow (8.8 ft). Hence, accounting for the time rate of scour would not produce significant reduction in the predicted final scour depth in this case. Figure 8.12 shows the results of SRICOS simulation for the maximum annual flood in 2010. The bottom plot shows that the soil erosion rates are so high that the final scour depth is reached at the same time as the peak discharge and scouring ceases as soon as the discharge decreases.

Compared with Table 8.5, the $\frac{z_f}{z_{max}}$ and $\frac{t_e}{t_{90}}$ ratios of the maximum annual floods are much larger in Table 8.6. The $\frac{z_f}{z_{max}}$ ratio is around 0.8 and the $\frac{t_e}{t_{90}}$ ratio is about 0.6 and 0.4 for the maximum annual floods in 2010 and 2014, respectively. Both are about a 20-year flood. When a flood can produce a final scour depth close to the equilibrium scour depth, a sequence of such floods would produce a final scour depth close to the equilibrium scour depth of the largest flood in the hydrograph. Hence, accounting for the time rate of scour would not result in significant reduction in the predicted final scour depth in this situation. Figure 8.13 is a plot of the variations of $\frac{t_e}{t_{90}}$ ratio with $\frac{z_f}{z_{max}}$ ratio for the maximum annual floods in Tables 8.5 and 8.6. Since the computed scour history is assumed to follow a hyperbolic function, all the data points fall on a solid line represented by Eq. (5.49). Thus, this plot provides a concise summary of the stages of scour produced by different floods in different soil categories.

SRICOS simulations were also conducted using the erosion-rate-versus-shear-stress curve that separates soil regions I and II. The results (not shown) show that the equilibrium scour depth is reached by all the maximum annual floods and the computed equivalent times are less than one hour. Hence, the equilibrium scour depth can be reached in a single flooding event and there are no benefits in accounting for the time rate of scour.

Table 8.6 Summary of results from SRICOS simulations for all the maximum annual floods between 2001 and 2017 with peak discharge greater than 1,000 ft^3/s

The SRICOS simulations were conducted using the erosion-rate-versus-shear-stress curve that separates soil regions II and III in Fig. 5.3.

Year	Peak Discharge Date	Peak Discharge Q_{max} (ft^3/s)	Return Period (yr)	Final Scour Depth z_f (ft)	Initial Erosion Rate (ft/hr)	Equilibrium Scour Depth z_{max} (ft)	$\dfrac{z_f}{z_{max}} \times 100\%$
2010	9/24/2010	13,100	18.1	6.63	1.8190	7.79	85.1
2014	6/17/2014	13,100	18.1	6.14	1.8190	7.79	78.8
2006	4/7/2006	8,020	8	4.22	0.8121	7.03	60.0
2011	7/15/2011	4,730	3.9	4.18	0.2932	6.22	67.2
2012	5/7/2012	4,730	3.9	3.64	0.2932	6.22	58.5
2007	3/13/2007	4,050	3.3	3.68	0.2179	6.01	61.2
2004	5/30/2004	3,400	2.7	2.75	0.1576	5.79	47.5
2015	7/7/2015	2,510	2.1	2.54	0.0934	5.46	46.5
2008	7/19/2008	1,710	1.6	1.31	0.0415	4.9	26.7
2016	5/1/2016	1,480	1.5	3.01	0.0378	4.82	62.4
2013	6/24/2013	1,340	1.4	2.44	0.0369	4.78	51.0
2002	8/21/2002	1,320	1.4	1.7	0.0368	4.77	35.6
2005	6/22/2005	1,180	1.3	2.06	0.0364	4.73	43.6
2003	4/20/2003	1,130	1.3	2.55	0.0362	4.72	54.0

Year	Critical Discharge (ft^3/s)	Flow Duration Exceeding Critical Discharge t_s (hr)	Equivalent Time t_e (hr)	t_{90} (hr)	$\dfrac{t_e}{t_{90}}$	$\dfrac{Q_{max}}{Q_c}$
2010	<1	NA	24.4	38.57	0.6326	NA
2014	<1	NA	15.94	38.57	0.4133	NA
2006	<1	NA	13.02	77.86	0.1672	NA
2011	<1	NA	43.49	190.95	0.2278	NA
2012	<1	NA	29.84	190.95	0.1563	NA
2007	<1	NA	43.45	248.3	0.1750	NA
2004	<1	NA	33.34	330.82	0.1008	NA
2015	<1	NA	50.75	526.16	0.0965	NA
2008	<1	NA	43.06	1,064.07	0.0405	NA
2016	<1	NA	212.28	1,147.59	0.1850	NA
2013	<1	NA	135.69	1,165.50	0.1164	NA
2002	<1	NA	71.84	1,166.67	0.0616	NA
2005	<1	NA	100.19	1,171.29	0.0855	NA
2003	<1	NA	153.45	1,173.66	0.1307	NA
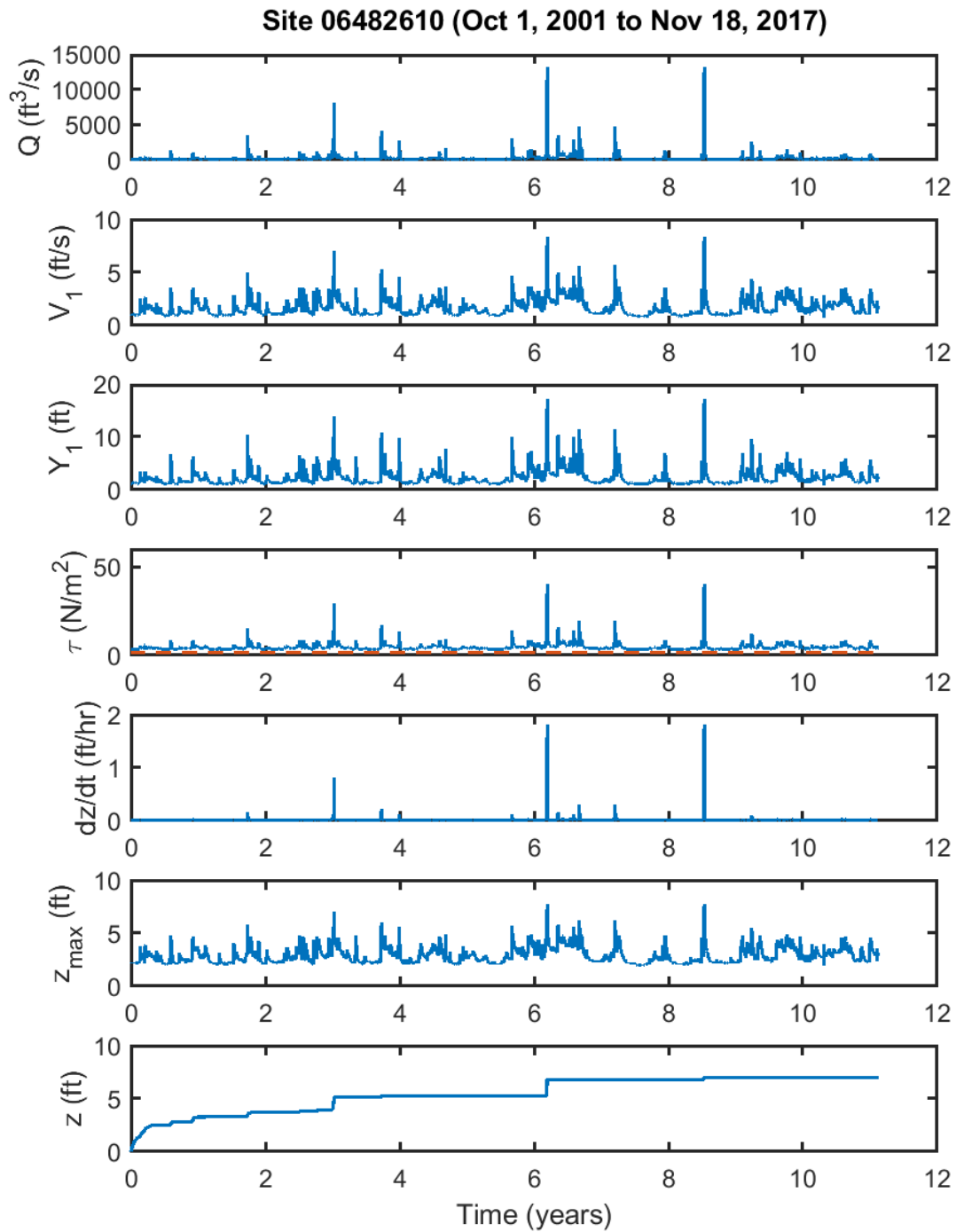
Figure 8.11 Computed scour history from October 1, 2001, to November 18, 2017, using the erosion-rate-versus-shear-stress curve that separates soil regions II and III
The red dashed line represents the critical shear stress.
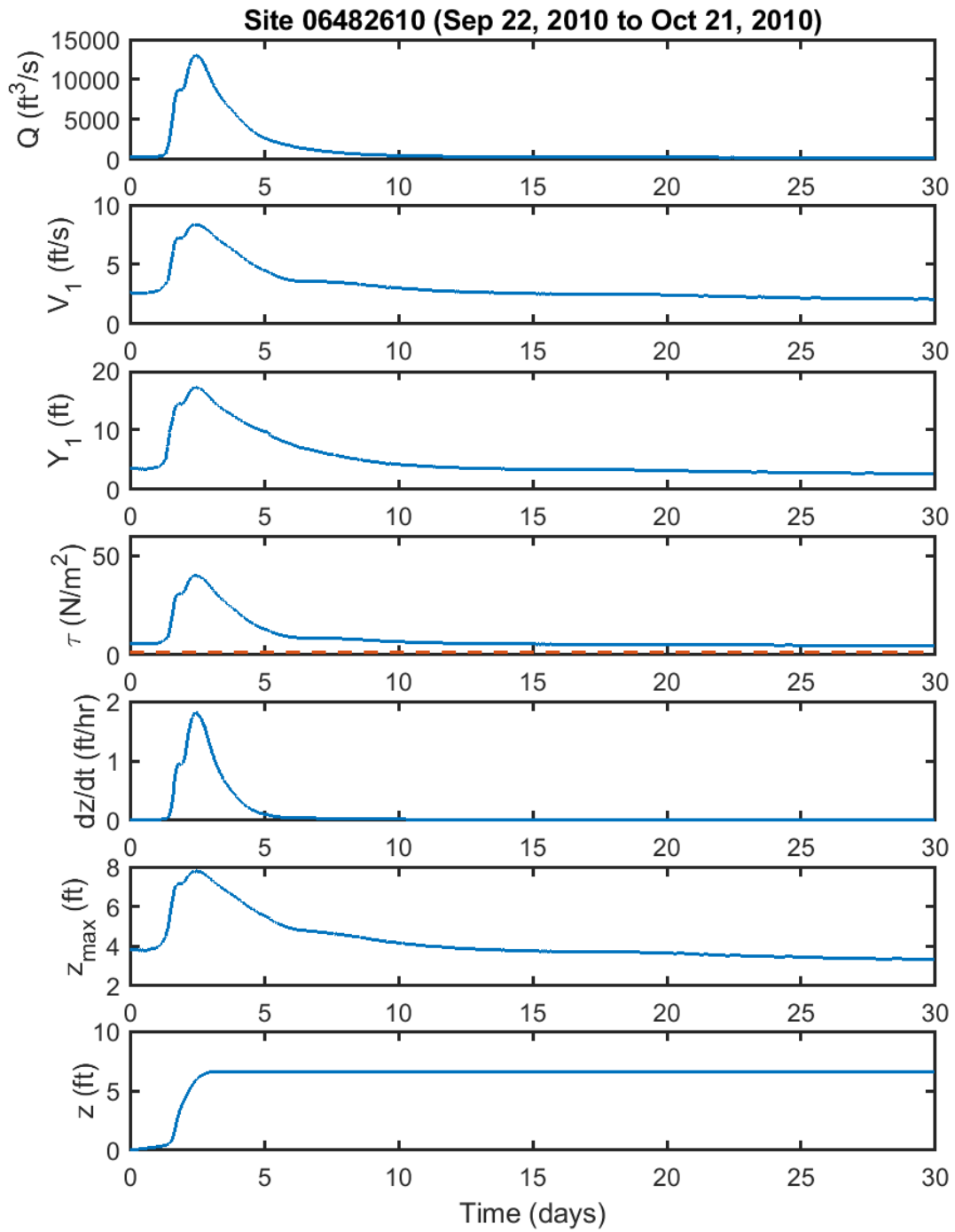
Figure 8.12 Computed scour history for the maximum annual flood in 2010 using the erosion-rate-versus-shear-stress curve that separates soil regions II and III
The red dashed line represents the critical shear stress.
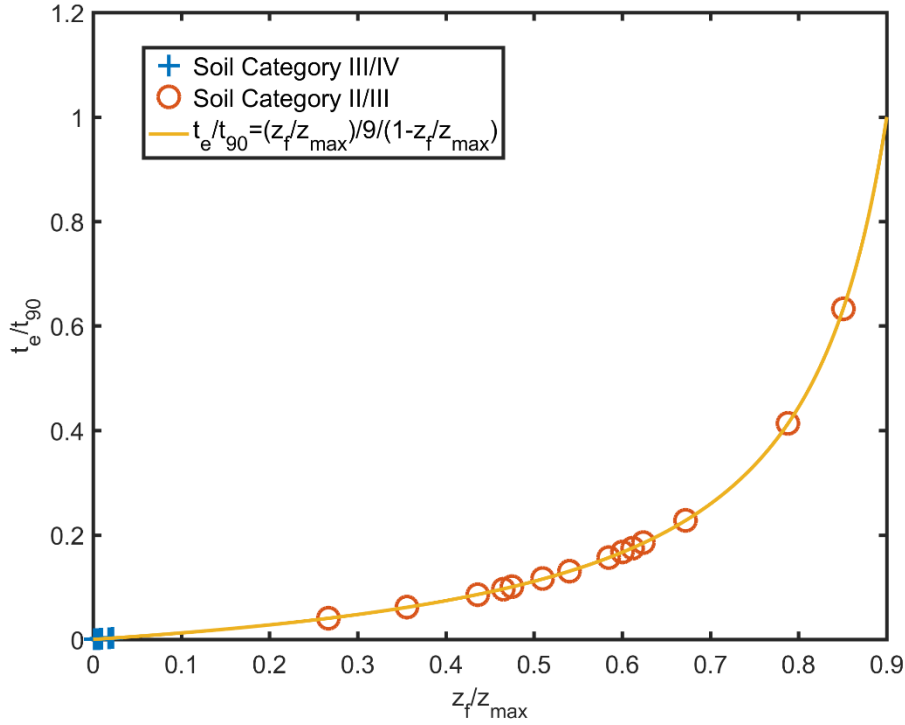
Figure 8.13 Variations of t_e/t_{90} ratio with z_f/z_{max} ratio for the maximum annual floods in Tables 8.5 and 8.6

8.4 Equivalent Time

Also presented in Tables 8.5 and 8.6 is the equivalent time t_e required for the peak discharge of each flood to produce the same predicted final scour depth as the one produced by the recorded hydrograph. Referring to Table 8.5, the value of t_e for the maximum annual floods ranges from about 20 to 50 hours (one to two days). Also shown are the flow duration t_s when the calculated bed shear stress exceeds the critical shear stress and the time t_{90} for the peak discharge to produce a final scour depth equal to 90% of its equilibrium scour depth. The equivalent time t_e is normalized by t_{90} and correlated to the normalized peak discharge $\frac{Q_{max}}{Q_c}$ and normalized flood duration $\frac{Q_{max}t_s}{z_{max}^3}$, where Q_c is the discharge corresponding to the critical shear stress and z_{max} is the equilibrium scour depth at peak discharge. The results are presented in Figures 8.14 to 8.16. The regression equations are given by:

$$\frac{t_e}{t_{90}} = \left[0.2796\left(\frac{Q_{max}}{Q_c}\right) - 0.1522\right] \times 10^{-3} \tag{8.2}$$

$$\frac{t_e}{t_{90}} = \left[0.6526\left(\frac{Q_{max}t_s}{z_{max}^3}\right) - 86.57\right] \times 10^{-6} \tag{8.3}$$

$$\frac{t_e}{t_{90}} = \left[1.409\left(\frac{Q_{max}}{Q_c}\right)^{0.2934}\left(\frac{Q_{max}t_s}{z_{max}^3}\right)^{0.828}\right] \times 10^{-6} \tag{8.4}$$

Figure 8.17 compares the three regression equations for predicting the $\frac{t_e}{t_{90}}$ ratio. The best correlation is obtained with the normalized flood duration $\frac{Q_{max}t_s}{z_{max}^3}$ (Figure 8.15 and Eq. 8.3); the R^2 value is 0.9354 and the RMSE is 0.0002249. Including the normalized discharge $\frac{Q_{max}}{Q_c}$ as an additional parameter

(Figure 8.16 and Eq. 8.4) does not produce any significant improvement; the changes in R^2 value and RMSE are minimal. Figure 8.14 shows that the $\frac{t_e}{t_{90}}$ ratio is also well correlated with $\frac{Q_{max}}{Q_c}$ (the R^2 value is 0.853 and the RMSE is 0.0003392), although the correlation is not as good as with $\frac{Q_{max}t_S}{Z_{max}^3}$. Since it is difficult to estimate the flood duration t_s, Eq. (8.2) will be used to estimate the $\frac{t_e}{t_{90}}$ ratio for generating future hydrographs.
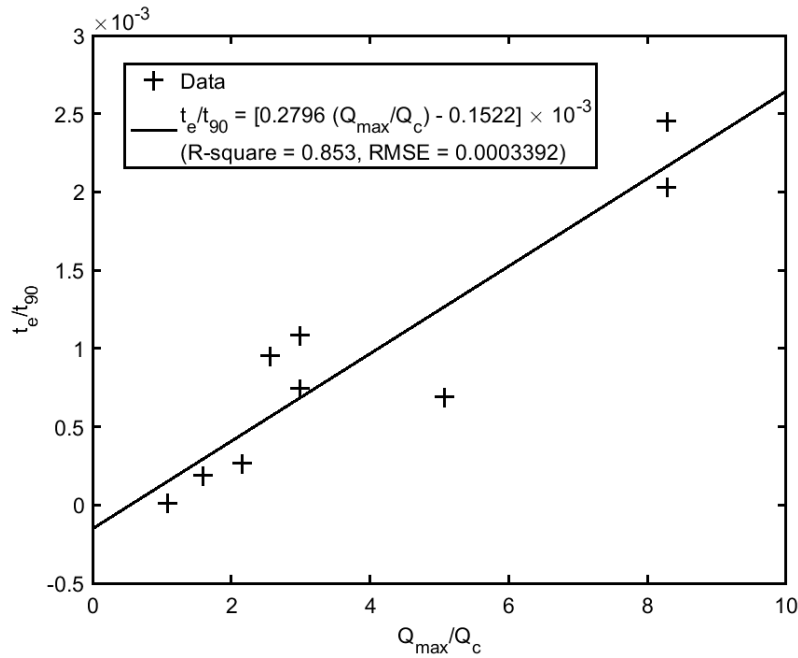
Figure 8.14 Normalized equivalent time versus normalized peak discharge for the erosion-rate-versus-shear-stress curve that separates soil regions III and IV
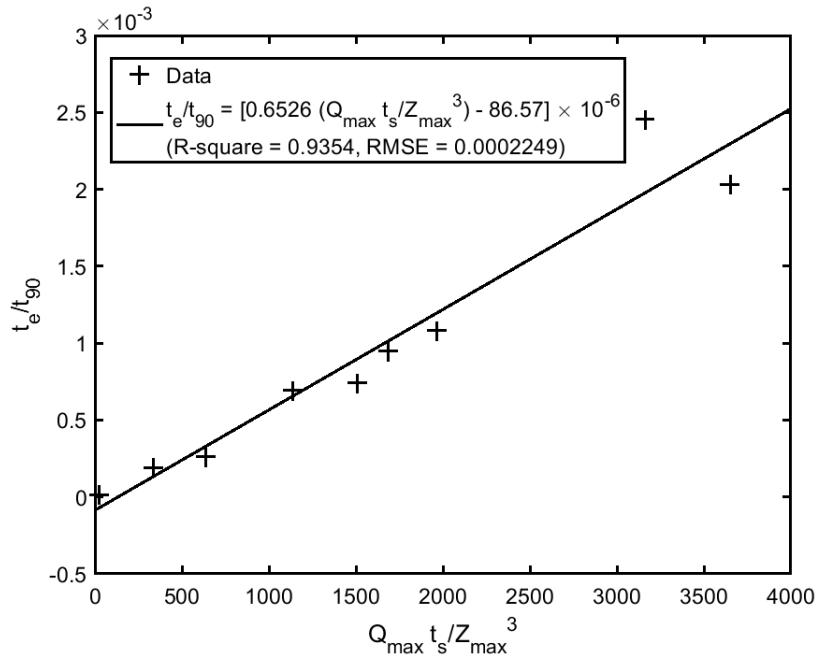
Figure 8.15 Normalized equivalent time versus normalized flood duration for the erosion-rate-versus-shear-stress curve that separates soil regions III and IV

$$t_e/t_{90} = [1.409\,(Q_{max}/Q_c)^{0.2934}\,(Q_{max}\,t_s/Z_{max}^3)^{0.828}] \times 10^{-6}$$
$$(\text{R-square} = 0.9339, \text{RMSE} = 0.0002128)$$
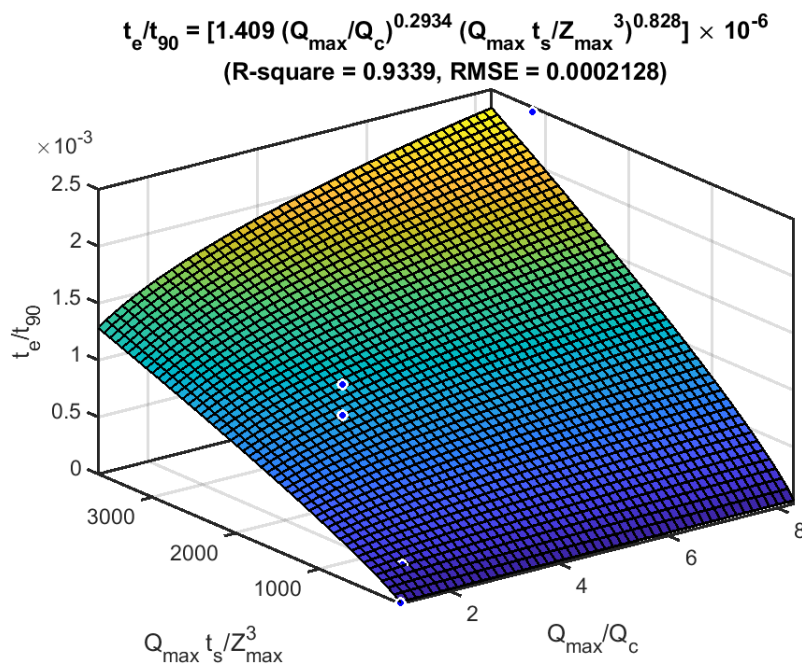
Figure 8.16 Normalized equivalent time versus normalized peak discharge and flood duration for the erosion-rate-versus-shear-stress curve that separates soil regions III and IV
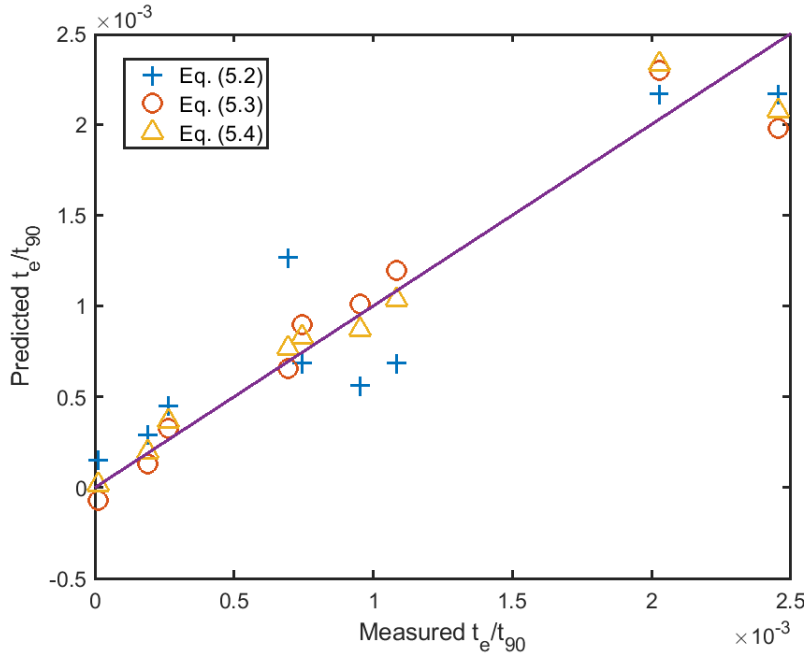
Figure 8.17 Comparison of different regression equations for predicting the t_e/t_{90} ratio
The solid line is the line of perfect agreement.

Figure 8.18 shows the relationship between $\frac{t_e}{t_{90}}$ and $\frac{Q_{max}}{Q_c}$ when the erosion-rate-versus-shear-stress curve that separates soil categories II and III is used to conduct the SRICOS simulations. The critical discharge Q_c is very low and is taken to be 1 ft³/s. Note that Q_c is only a normalization factor. Its value does not affect the equivalent time if the flow duration greater than Q_c is not included in the regression equation. The best-fit-line between $\frac{t_e}{t_{90}}$ and $\frac{Q_{max}}{Q_c}$ ($R^2 = 0.7818$) is given by:

$$\frac{t_e}{t_{90}} = \left[3.356\left(\frac{Q_{max}}{Q_c}\right) + 3682\right] \times 10^{-5} \tag{8.5}$$

8.5   Generation of Future Hydrographs and Scour Risk Analysis

Figure 8.19 shows the results of SRICOS simulation for one constructed series of 100 maximum annual floods. The simulation is conducted using the erosion-rate-versus-shear-stress curve that separates soil regions III (medium erodibility) and IV (low erodibility). The soil critical shear stress τ_c is 9.5 N/m² and the erosion rate constant a' is 1.62. The critical discharge to produce scour is about 1,580 ft³/s. From top to bottom, the plots represent the magnitude of annual peak flow Q, equivalent time t_e, approach flow velocity V_1, approach flow depth Y_1, initial bed shear stress τ, initial rate of scour $\frac{dz}{dt}$, equilibrium scour depth z_{max}, and cumulative scour depth z. The equivalent time is computed using Eq. (8.2). The largest flood in Figure 8.19 has a magnitude of 35,997 ft³/s and an equivalent time of 73 hours. The return period is approximately 150 years. The predicted final scour depth for the entire series of 100 floods is 2.7 ft.
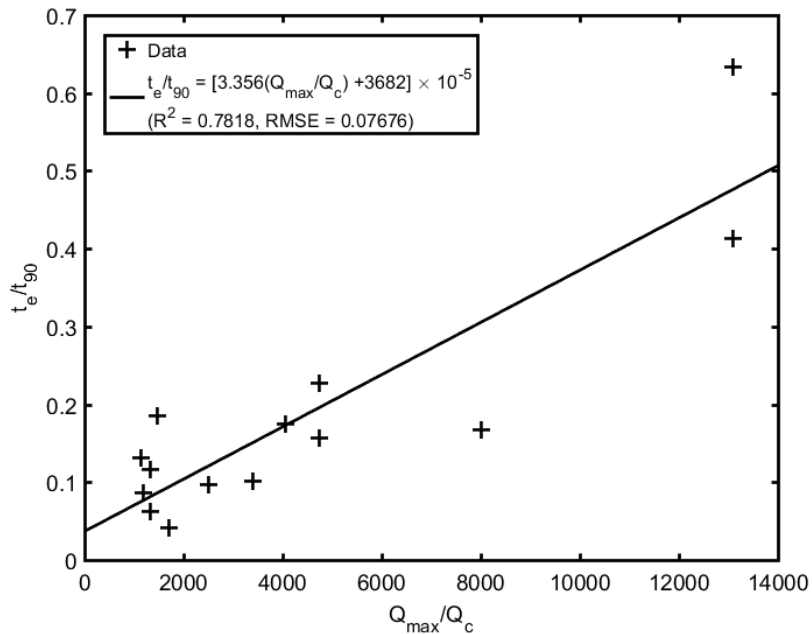
Figure 8.18 Normalized equivalent time versus normalized peak discharge for the erosion-rate-versus-shear-stress curve that separates soil categories II and III
The critical discharge Q_c is taken to be 1 ft³/s.

Table 8.7 shows the exceedance probabilities associated with different predicted scour depths for the project lives of 50, 75, and 100 years. These statistics are computed based on 20,000 SRICOS simulations. These results show that the predicted final scour depths are very small for this soil category. For example, the exceedance probability for a scour depth of 3 ft is only about 5% in a project life of 75 years. The small scour depth is due to the high soil critical shear stress and slow rates of scour.

Table 8.7 Exceedance probabilities associated with predicted scour depths and project lives
The soil critical shear stress τ_c and erosion rate constant α' are 9.5 N/m² and 1.62, respectively. The equivalent time is computed using Eq. (8.2).

Scour Depth (ft)	2.0	2.5	3.0	3.5	4.0	4.5	5.0
Exceedance Probability (project life 50 yrs)	15%	4%	2%	<1%	<1%	<1%	<1%
Exceedance Probability (project life 75 yrs)	54%	18%	5%	<1%	<1%	<1%	<1%
Exceedance Probability (project life 100 yrs)	91%	52%	18%	5%	2%	<1%	<1%
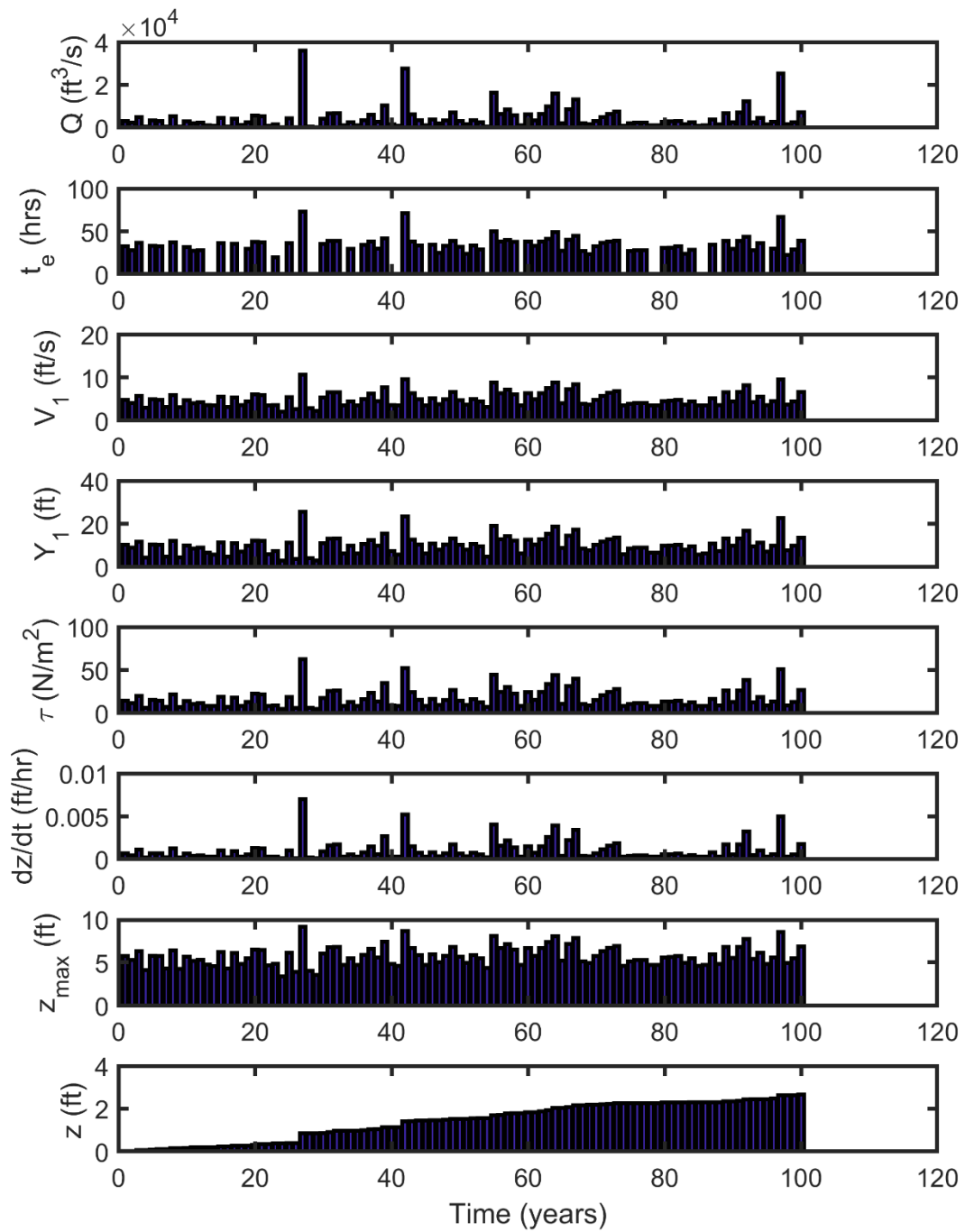
Figure 8.19 SRICOS simulation for a constructed series of 100 maximum annual floods
The soil critical shear stress τ_c and erosion rate constant α' are 9.5 N/m² and 1.62, respectively. The equivalent time is computed using Eq. (8.2).

Figure 8.20 presents the simulation results for a constructed series of 100 maximum annual floods conducted using the erosion-rate-versus-shear-stress curve that separates soil regions II (high erodibility) and III (medium erodibility). The soil critical shear stress τ_c is 1.33 N/m^2 and the erosion rate constant a' is 2.53. The critical discharge to produce scour is less than 1 ft^3/s. The predicted final scour depth is 8.5 ft, which is very close to the equilibrium scour depth of 8.8 ft for the 100-year flood. In fact, the rates of scour are so high that most of the scour occurs in the first few years. Due to pre-existing scour, the subsequent floods produce almost no additional scour. The largest flood in Figure 8.20 has a magnitude of 35,314 ft^3/s and an equivalent time of 19 hours; the return period is approximately 145 years. This flood occurs in the sixth year and the predicted scour depth after the flood is 8.4 ft compared with 8.5 ft for the predicted final scour depth. Before this flood, two smaller floods (peak flow magnitude 2,493 and 11,532 ft^3/s) together have already produced a cumulative scour depth of 6.2 ft.

Table 8.8 shows the exceedance probabilities associated with different predicted scour depths for the project lives of 50, 75, and 100 years. These results show that there is about a 32% chance that the equilibrium scour depth of the 100-year flood (8.8 ft) will be exceeded during a project life of 75 years. The exceedance probability increases to 72% for a predicted final scour depth of 8 ft. For non-cohesive soils, it is assumed that the equilibrium scour depth can be reached in the course of a single design flood. If the design life of a bridge is 75 years and the design flood has a return period of 100 years, there is a 53% chance that the design flood will be exceeded at least once during the design life of the bridge (Table 6.8). Hence, the SRICOS method produces no significant reduction in the predicted final scour depth compared with the traditional HEC-18 method for this soil category.

Table 8.8 Exceedance probabilities associated with predicted scour depths and project lives
The soil critical shear stress τ_c and erosion rate constant a' are 1.33 N/m^2 and 2.53, respectively. The equivalent time is computed using Eq. (8.5).

Scour Depth (ft)	7	8	9	10	11	12
Exceedance Probability (project life 50 yrs)	96%	53%	22%	15%	4%	2%
Exceedance Probability (project life 75 yrs)	99.6%	72%	32%	22%	6%	2%
Exceedance Probability (project life 100 yrs)	99.9%	85%	41%	28%	8%	3%
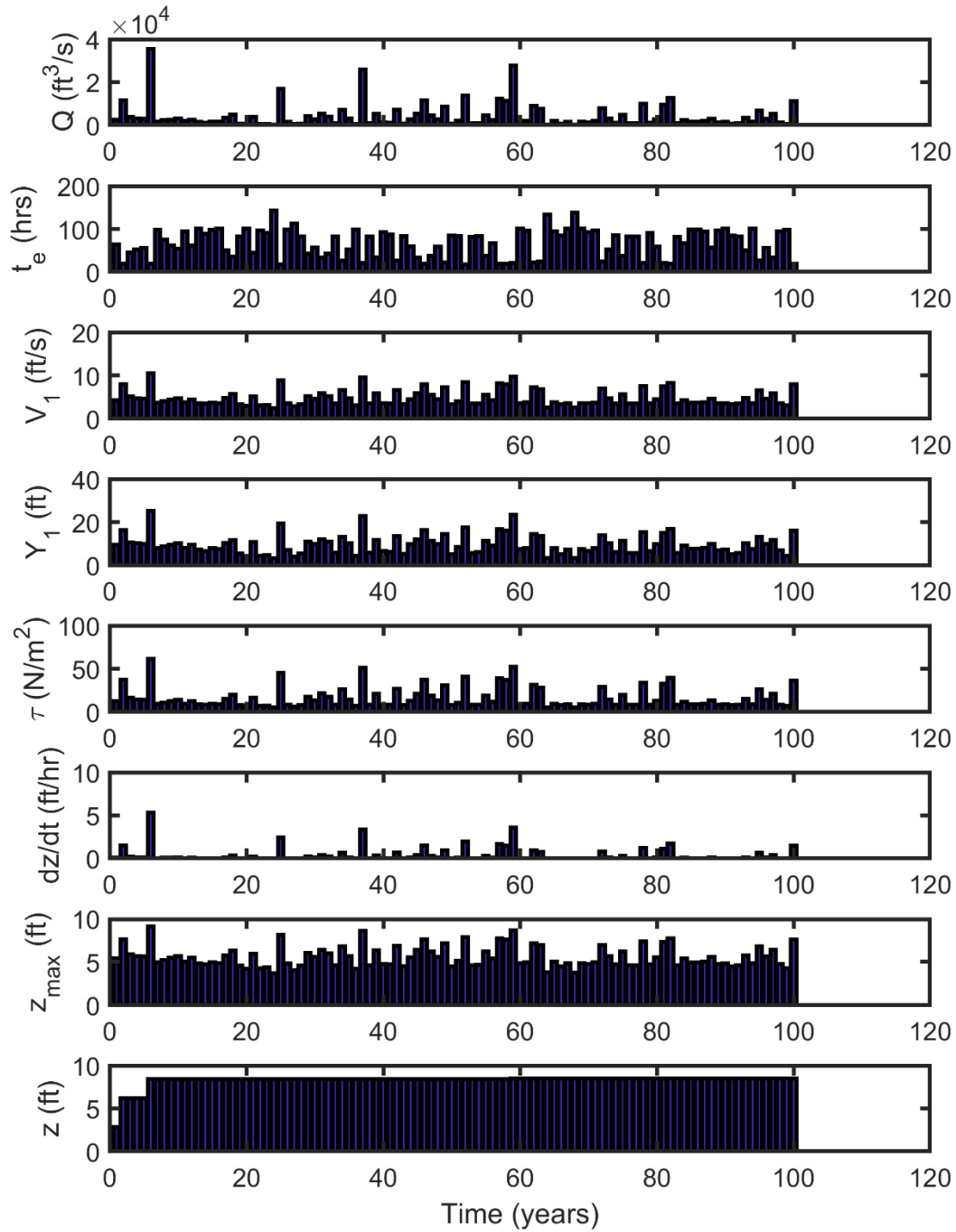
Figure 8.20 SRICOS simulation for a constructed series of 100 maximum annual floods

The soil critical shear stress τ_c and erosion rate constant a' are 1.33 N/m² and 2.53, respectively. The equivalent time is computed using Eq. (8.5).

8.6   Comparison with Other Simplified SRICOS Methods

Table 8.9 presents the results of SRICOS simulations with the 100- and 500-peak discharges running for five days. The soil critical shear stress τ_c and erosion rate constant a' are for the erosion-rate-versus-shear-stress curve that separates soil regions III and IV. The equilibrium scour depth was computed using the HEC-18 equation for pier scour (Eq. 5.9) in Table 8.9(a) and the equation developed for cohesive soils (Eq. 5.14) in Table 8.9(b). As with the SD13 bridge, Eq. (5.14) predicts a much larger equilibrium scour depth for both the 100- and 500-year floods than Eq. (5.9), which is not realistic. Therefore, Eq. (5.9) has been used to compute the equilibrium scour depth for pier scour in this study.

Table 8.9(a) shows that the predicted final scour depth obtained by running the 500-year peak discharge for five days is about 2 ft. This is much smaller than the equilibrium scour depth of the 500-year flood, which is about 11 ft. From Table 8.7, the exceedance probabilities for the predicted final scour depth are 15%, 54%, and 91% for the project live of 50, 75, and 100 years, respectively. These risk values are quite high; therefore, running the 500-year flood for five days is not long enough to safely predict the scour depth that would develop over the lifetime of the bridge.

As a rule of thumb, the HEC-18 document recommends that the maximum scour depth for round nose piers aligned with the flow should not be greater than 2.4 times the pier width for Froude number ≤0.8, or 7.2 ft for a 3-ft diameter circular pier. This will be the maximum scour depth used for design in non-cohesive soils. Table 8.7 shows that the exceedance probability for a predicted final scour depth of 3.5 ft is less than 1% for a project life of 75 years. Therefore, the SRICOS method can produce a small reduction in scour depth for this soil category.

If the S-SRICOS method is used to predict future scour, the equivalent time will be calculated using Eq. (5.42) with t_{hydro} taken to be the design life of the bridge, V_{max} the flow velocity produced by the design flood (e.g., the 100-year peak flow), and $\dot{z}_i$ the initial erosion rate for the maximum velocity. With $t_{hydro} = 75$ years, $V_{max} = 9.9$ ft/s and $\dot{z}_i = 0.0055 \frac{ft}{hr}$ (Table 8.9), the computed equivalent time is 746 hours. The final scour depth computed using Eq. (5.22) is 3 ft, which has an exceedance probability of about 5 % (Table 8.7).

The same analysis was repeated with the soil critical shear stress τ_c and erosion rate constant a' given by the erosion-rate-versus-shear-stress curve that separates soil categories II and III. The rates of scour are so high that it takes only 28 hours to reach 90% of the equilibrium scour depth for the 100-year discharge and four hours for the 500-year discharge. Hence, there are no benefits in using the SRICOS method to predict the final scour depth for this soil category.

Table 8.9 Results of SRICOS simulations with the 100- and 500-year peak flows run for 5 days and z_{max}

Computed using: (a) HEC-18 equation for pier scour (Eq. 5.9) and (b) equilibrium scour depth for cohesive soils (Eq. 5.14). The soil critical shear stress τ_c and erosion rate constant α' are 9.5 N/m² and 1.62, respectively.

(a)									
T_r (yr)	Q (ft³/s)	V_1 (ft/s)	y_1 (ft)	α (°)	Initial τ (N/m²)	V_c (ft/s)	z_{max} (ft)	$\dot{z}_i$ (ft/hr)	z_f (ft)
100	30,203	9.9	24.2	0	54.3	4.6	8.8	0.0055	0.62
500	58,138	16.1	28.7	0	131.2	5.0	11.1	0.0232	2.22
(b)									
T_r (yr)	Q (ft³/s)	V_1 (ft/s)	y_1 (ft)	α (°)	Initial τ (N/m²)	V_c (ft/s)	z_{max} (ft)	$\dot{z}_i$ (ft/hr)	z_f (ft)
100	30,203	9.9	24.2	0	54.3	4.6	11.3	0.0055	0.63
500	58,138	16.1	28.7	0	131.2	5.0	16.7	0.0232	2.39

8.7   Summary

As with the SD13 bridge over the Big Sioux River, SRICOS simulations show that, except for the erosion-rate-versus-shear-stress curve that separates soil regions III (medium erodibility) and IV (low erodibility), there is no significant reduction in the predicted final scour depth at the Interstate 90 bridges when compared with the equilibrium scour depth of the 100-year flood. The HEC-18 method would predict a maximum design scour depth of 7.2 ft (2.4 × pier diameter) for this site. The results of Monte Carlo simulations indicate that a predicted final scour depth of 3.5 ft would have a probability of exceedance of less than 1% for a project life of 75 years if the time rate of scour is considered. Hence, there is a small scour depth reduction in using the SRICOS method for this soil category. However, the reduction in scour depth is relatively small because the equilibrium scour depth is not large anyway. It was found that running the 500-year peak flow for five days does not produce a predicted final scour depth that would have an acceptable risk level, therefore the simplified method is not recommended. The potential of a flood to produce scour can be assessed using the $\frac{z_f}{z_{max}}$ and $\frac{t_e}{t_{90}}$ ratios. A small $\frac{z_f}{z_{max}}$ ratio means that the scour depth produced by the flood will be small compared to the equilibrium scour depth. Similarly, a small $\frac{t_e}{t_{90}}$ ratio means that the equivalent duration of the flood is much shorter than the time required to reach the equilibrium scour depth. In both cases, the contribution of the flood to the final scour depth in a sequence of floods would be small. On the other hand, a series of floods with large $\frac{z_f}{z_{max}}$ and $\frac{t_e}{t_{90}}$ ratios would likely produce a cumulative scour depth close to the equilibrium scour depth of the largest flood in the hydrograph.

9. NATIONAL SURVEY

9.1 Introduction

A national survey on evaluating bridge scour in cohesive soils and methods for hydrograph generation was conducted through the AASHTO Research Advisory Council (RAC). The survey questionnaire prepared by the research team is presented in Section 9.2. A summary of the survey results is attached in Appendix I. The survey results are discussed in Section 9.3.

9.2 Questionnaire

1. From your experience, what are the most important scour issues related to cohesive soils (check all that apply)?

   ☐ Critical shear stress

   ☐ Soil erosion rate

   ☐ Equilibrium scour depth

   ☐ Other (please describe)

2. What method does your agency use to measure or determine soil erodibility (check all that apply)?

   ☐ My agency does **not** measure or determine soil erodibility

   ☐ Erosion Function Apparatus (EFA)

   ☐ Jet Erosion Test (JET)

   ☐ Flume

   ☐ Empirical formulae

   ☐ Other (please describe)

3. What method does your agency use to predict bridge scour in cohesive soils (check all that apply)?

   ☐ My agency does **not** predict scour in cohesive soils

   ☐ Traditional HEC-18 method for non-cohesive soils

   ☐ Apply engineering judgement to the HEC-18 method

   ☐ Scour Rate in Cohesive Soils (SRICOS) method

   ☐ Other (please describe)

4. How does your agency decide to use the SRICOS method instead of the traditional HEC-18 method, which does not account for the time rate of scour (check all that apply)?

☐ My agency does **not** use the SRICOS method for scour analysis

☐ Soil erodibility

☐ Soil type

☐ Scour critical bridges

☐ Other (please describe)

```
┌─────────────────────────────────────────────────────────┐
│                                                         │
│                                                         │
│                                                         │
└─────────────────────────────────────────────────────────┘
```

5. Has your agency used time series of streamflow to predict scour?

☐ Yes

☐ No

6. If your agency has estimated streamflow for an ungauged stream, please identify which methods you have used (check all that apply):

☐ My agency has **not** estimated streamflow time series for an ungauged stream

☐ Drainage-area ratio

☐ Nonlinear spatial interpolation

☐ Scaling by the at-site mean variance

☐ QPPQ method based on flow-duration curves and an index stream gage

☐ Other (please describe)

```
┌─────────────────────────────────────────────────────────┐
│                                                         │
│                                                         │
│                                                         │
└─────────────────────────────────────────────────────────┘
```

7. If your agency has used synthetic streamflow data in scour analysis, please identify how you constructed the synthetic hydrograph (check all that apply):

☐ My agency has **not** used synthetic streamflow data

☐ Snyder's synthetic unit hydrograph

☐ Natural Resources Conservation Service (NRCS) synthetic unit hydrograph

☐ US Bureau of Reclamation (USBR) synthetic unit hydrograph

☐ General dimensionless unit hydrograph (GDUH)

☐ Other (please specify and describe)

```
┌─────────────────────────────────────────────────────────┐
│                                                         │
│                                                         │
│                                                         │
└─────────────────────────────────────────────────────────┘
```

8. Please describe the type of situations where your agency has used flood duration in scour analysis, if any:

☐   My agency has **not** used flood duration in scour analysis

☐   My agency has used flood duration in scour analysis of these types of situations:

> (text box)

9. How has your agency estimated flood duration for scour analysis (check all that apply)?

☐   My agency has **not** estimated flood duration for scour analysis

☐   Discharge-duration-frequency (QdF) analysis

☐   Peak-volume analysis

☐   Volume over threshold analysis

☐   Other (please specify and describe)

> (text box)

10. What forecasting models have your agency used to predict flood time series (check all that apply)?

☐   My agency has **not** used models to predict flood time series

☐   Autoregressive (AR) model

☐   Moving average (MA) model

☐   Autoregressive integrated moving average (ARIMA) model

☐   Other (please specify and describe)

> (text box)

9.3 Survey Summary

Twenty-one (21) responses were received from the survey. Regarding questions related to evaluating bridge scour in cohesive soils, critical shear stress, soil erosion rate, and equilibrium scour depth are listed as the most important scour issues. However, most agencies surveyed do not measure or determine soil erodibility, which is a critical input parameter to the SRICOS method. An erosion function apparatus (EFA) is available commercially, but it has been used primarily in research projects. Reliability of the test results is the main concern for not using the apparatus. Most agencies use the traditional HEC-18 method developed for non-cohesive soils to evaluate bridge scour in cohesive soils, then apply engineering judgment to the results of the HEC-18 method. TxDOT includes SRICOS as an optional method for cohesive and layered soil. MDDOT uses an in-house program called ABSCOUR that incorporates the guidance in HEC-18.

On the questions related to hydrograph generation, the USGS regional regression equations (now incorporated in StreamStats) and drainage-area ratio are the two methods most commonly used to estimate peak discharge in ungauged streams. Most of the agencies surveyed have not used synthetic streamflow data. The Snyder and NRCS unit hydrographs have been used only in rare occasions. All but two of the agencies responding to the survey reported that they have not used flood duration in scour analysis. Flood duration is considered only if bridges are on rivers controlled by the outflow of dams and lakes. TxDOT has used the National Water Model (NWM) to forecast stream flow, but most of the agencies surveyed have not used hydrologic models to predict flood time series for scour prediction.

Although the SRICOS method is included in HEC-18 as an alternative approach for predicting scour at bridges founded on cohesive soils, most DOTs only use the traditional HEC-18 method. The SRICOS method requires a higher level of expertise in relation to subsurface exploration, laboratory testing, and hydraulic and hydrologic analysis in order to ensure reliable results. This research project is motivated by the need to develop a practical procedure for applying the SRICOS method, particularly regarding hydrograph generation. The approach adopted in this project is outlined below.

1. The SRICOS method will be applied to only a small percentage of bridges built over waterways. A simple screening tool is needed to identify bridge sites where the SRICOS method may be more appropriate than the traditional HEC-18 method.

2. The time rate of scour is the main difference in determining the final scour depth in cohesive and non-cohesive soils. Although empirical equations have been developed to calculate the equilibrium scour depth in cohesive soils. These equations may not be applied to soils other than those used to develop the equations. The scour equations in HEC-18 already have a built-in factor of safety for design. The equations developed for non-cohesive soils in HEC-18 are used to predict the equilibrium scour depth in cohesive soils in this study. Therefore, any reductions in the computed scour depth in the SRICOS simulations are due to the time effect of scour. The scour evaluation procedure developed in this project is an extension of the HEC-18 procedure.

3. Due to pre-existing scour, only a small number of floods in a continuous hydrograph would contribute to scour. A major task in this project is to verify this assumption for pier and contraction scour using two bridge sites with long streamflow records. At each site, the final scour depth computed using the complete streamflow record was compared with the final scour depth obtained using the maximum annual floods. Scour histories were computed using soil erosion functions representing a range of cohesive and non-cohesive soils.

4. The hydrograph generation method proposed in this study is consistent with the USGS's method for flood frequency analysis, which is also employed in the HEC-18 method to determine the return period of the design flood. The hydrograph generation method employs a series of maximum annual floods sampled randomly from the Log Pearson Type III distribution. Many equally probable annual maximum series are generated and used with the SRICOS method to predict the distribution of final scour depth and exceedance probabilities associated with different predicted scour depths and project lives.

10.   DECISION TOOL AND SCREENING PROCEDURE

10.1 Introduction

This chapter outlines a screening procedure to determine when conducting a full SRICOS-EFA analysis may be useful in evaluating bridges for scour. Only pier and contraction scour in clear-water scour condition is addressed in this report. The decision process involves scour analysis at three different levels of increasing complexity. In the Level I analysis, information on soil types and/or the results of EFA testing are used with simple calculations to eliminate bridge sites where use of the SRICOS method is not recommended. A hydraulic analysis is required to provide flow data for the scour analysis. In the Level II analysis, recorded hydrographs or hydrographs transferred from gauging stations nearby are used with the SRICOS method to compute the scour histories of selected historical floods. The results are used to assess whether time rate of scour may be an important factor in predicting scour at the bridge site and to determine the equivalent times for floods of different return periods. In the Level III analysis, maximum annual floods are generated from an assumed peak flow distribution such as the Log Pearson Type III distribution. Each of the floods in the annual maximum series is a rectangular hydrograph represented by a constant discharge and an equivalent time. Many annual maximum series are generated and used with the SRICOS method to compute the final scour depth. The risk values associated with different predicted scour depths and project lives are then determined. Details of the procedure are described in Sections 10.2 and 10.3 for pier scour and contraction scour, respectively. Specific issues related to ungauged sites are discussed in Section 10.4.

10.2 Pier Scour

For round nose piers aligned with the flow, the HEC-18 document recommends that the maximum pier scour depth to pier width ratio be taken as 2.4 for Froude numbers less than or equal to 0.8 and 3.0 for larger Froude numbers. For smaller bridges, these guidelines essentially limit the design scour depth to a few feet. Due to the uncertainties inherent in predicting flood magnitudes and in measuring the soil critical shear stress and erosion rates, it would not be safe or cost-effective to reduce the design scour depth in such cases even if a smaller scour depth is predicted by the SRICOS method. Thus, the SRICOS method is most useful when the equilibrium scour depth is large and the design life of the bridge is short in relation to the expected rate of scour. An example of this situation is given by the SD13 bridge over the Big Sioux River. The bridge has 30-ft-long piers, and high flow angle of attack produces equilibrium scour depth close to 20 ft for a wide range of flow rates. SRICOS simulations, however, predict that the final scour depth produced by a 150-year flood is only about 0.5 ft if the erosion-rate-versus-shear-stress curve that separates regions III and IV in the soil erodibility chart proposed by Briaud et al. (2011) is used to predict the critical shear stress and soil erosion rates. Risk analysis conducted using Monte Carlo simulation further confirms there is only about a 1% probability that a final scour depth of 7 ft would be exceeded in a 75-year project life. In this case, accounting for the slower rates of scour in cohesive soils could significantly reduce the design scour depth. However, if the erosion-rate-versus-shear-stress curve that separates regions II and III is used for the SRICOS simulations, the predicted final scour depths of the large floods are all close to their equilibrium scour depths, and the probability that the equilibrium scour depth of the largest recorded flood will be exceeded at least once in 75 years increases to about 70%. Similar conclusions were reached when SRICOS simulations were conducted using the measured soil erosion function. In the last two situations, it would not be safe to reduce the scour depth obtained using the HEC-18 method in the design of the bridge foundation.

In another case study, the Interstate 90 bridges over Split Rock Creek have 3-ft diameter cylindrical pier sets that are skewed parallel to the flow. Based on the recommendation of the HEC-18 document, the maximum pier scour depth should not be taken to be greater than 7.2 ft. SRICOS simulation for an 18-year flood, which is the largest flood with 15-minute flow record at this site, predicts a final scour depth of only 0.2 ft if the erosion-rate-versus-shear stress curve that separates regions III and IV in the soil erodibility chart is used to predict scour. Risk analyses predict there is less than a 1% chance that the final scour depth will exceed 3.5 ft in a 75-year project life. Although these results suggest that the design scour depth may be reduced, in view of the relatively small equilibrium scour depth, other considerations such as high traffic volume and long design life for the interstate bridges may lead the engineer to adopt the equilibrium scour depth for design instead of a smaller scour depth predicted by the SRICOS method.

When the erosion-rate-versus-shear-stress curve that separates regions II and III is used to predict pier scour at the Interstate 90 bridges, the predicted final scour depths of the maximum annual floods are all close to their equilibrium scour depths. In addition, risk analyses predict a greater than 70% chance that the equilibrium scour depth will be exceeded during the design life of the bridges. For both the SD13 bridge and Interstate 90 bridges, it was found that running the 500-year flood for five days would not provide a safe margin for choosing the design scour depth. At both sites, there is a greater than 50% chance that the predicted final scour depth produced by a 500-year flood will be exceeded at least once in a 75-year project life in soil category IV (low erodibility). Due to the slow rates of scour, a longer flow duration is needed to reproduce the effect of a continuous hydrograph over the project life.

Using the soil erosion rate chart proposed by Briaud et al. (2011), the results of SRICOS analysis for the two bridge sites show that, over a period of several decades, the predicted final scour depths in soil category IV (low erodibility) would be significantly less than the equilibrium scour depths, while soil categories I (very high erodibility) and II (high erodibility) would produce final scour depths equal or close to the equilibrium scour depths. The region of uncertainty is soil category III (medium erodibility) where additional analysis will be required to determine whether predicted final scour depths would be substantially less than the equilibrium scour depths. This can be done by computing the final scour depths of selected maximum annual floods and plotting the results on a $\frac{z_f}{z_{max}}$ versus $\frac{t_e}{t_{90}}$ curve as shown in Figure 6.11 for the SD13 Bridge, which is reproduced here in Figure 10.1.

The SRICOS method assumes that the scour-depth-versus-time curve follows a hyperbolic function. A hyperbolic function is defined by two parameters, the initial rate of scour $\dot{z}_i$ and the equilibrium scour z_{max} (Eq. 5.22). In the hyperbolic model, the time required to reach 90% of the equilibrium scour depth t_{90} is given by $\frac{9z_{max}}{\dot{z}_i}$. This parameter is a measure of the time required to reach the equilibrium scour depth for a given discharge. For the purpose of scour prediction, an actual hydrograph may be replaced by an equivalent rectangular flood represented by the peak discharge and an equivalent time. The latter is the time it will take for the peak discharge to produce the same final scour depth as that created by the actual hydrograph. For the hyperbolic model, the $\frac{z_f}{z_{max}}$ and $\frac{t_e}{t_{90}}$ ratios are related through Eq. (5.49), which is reproduced below as Eq. (10.1):
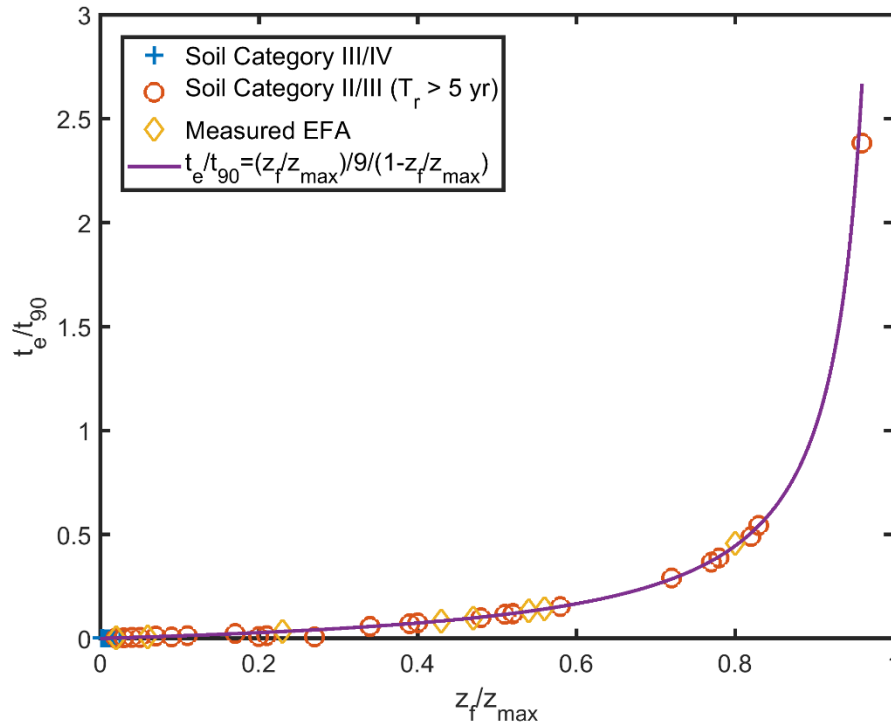
Figure 10.1 Variations of t_e/t_{90} ratio with z_f/z_{max} ratio for the maximum annual floods, SD13 bridge over the Big Sioux River
The hyperbolic model is represented by the solid line.

$$\frac{t_e}{t_{90}} = \frac{\dfrac{z_f}{z_{max}}}{9\left(1 - \dfrac{z_f}{z_{max}}\right)} \tag{10.1}$$

Equation (10.1) is plotted as a solid line in Figure 10.1. Also shown on the plot are the final scour depths and equivalent times for the maximum annual floods computed using the measured erosion function and the erosion-rate-versus-shear-stress curves that separate soil region III from IV, and region II from III in Figure 5.3. All the data points fall on the same line. Thus, Figure 10.1 provides a concise summary of the final scour depths produced by different floods compared with the equilibrium condition. For both the measured soil erosion function and the erosion-rate-versus-shear-stress curve that separates soil regions II and III, the large floods have relatively large $\frac{z_f}{z_{max}}$ ratios, which means that a sequence of maximum annual floods occurring over a period of several decades would likely produce a final scour depth comparable to the equilibrium scour depth. Only in soil region IV are the computed $\frac{z_f}{z_{max}}$ and $\frac{t_e}{t_{90}}$ ratios of all the maximum annual floods close to zero, which indicates that the final scour depth produced by a series of such floods would also be small. Based on these research findings, it is recommended that pier scour evaluation in cohesive soils be divided into three levels:

1. In the Level 1 analysis, the HEC-18 method is used to predict the equilibrium scour depth for the 100-year flood. Soil samples may be collected from the bridge site to determine the critical shear stress and initial erosion rate and classify the soil types. The SRICOS method is run with the 100-year peak flow for five days. If the soil type falls into either soil category I or II and/or the computed scour depth is close to the equilibrium scour depth, the maximum scour depth can be reached during a single flooding event and no reduction should be applied to the design

scour depth obtained using the HEC-18 method. The engineer may also adopt the equilibrium scour depth for design if it is judged to be reasonable or other considerations (e.g., high traffic volume, long design life) dictate a more conservative approach.

2. In the Level II analysis, the final scour depths and equivalent times of selected recorded maximum annual floods are computed using the measured soil erosion function. The results are plotted on a $\frac{z_f}{z_{max}}$ versus $\frac{t_e}{t_{90}}$ curve to assess the rates of scour produced by the large floods. A decision is made to adopt the scour depth calculated using the HEC-18 method or proceed to a full SRICOS-EFA analysis in the Level III analysis.

3. In the Level III analysis, the computed equivalent times of the maximum annual floods are normalized by t_{90} and correlated to the peak discharges and/or flood durations to develop regression equations for the equivalent time. Alternatively, the computed results may be used to select an envelope curve for the $\frac{t_e}{t_{90}}$ ratio. The Log Pearson Type III or another suitable probability distribution is used to generate the distribution of peak flow magnitude, and the equivalent times for different peak discharges are calculated using the regression equations for the $\frac{t_e}{t_{90}}$ ratio. Many annual maximum series are generated by Monto Carlo simulation and used with the SRICOS method to determine the distribution of final scour depth. A design scour depth is chosen by considering the risk values associated with different project lives.

The screening procedure is demonstrated for pier scour using the SD13 bridge over the Big Sioux River near Flandreau in Chapter 11.

10.3 Contraction Scour

The maximum flow depth in a contracted section in clear-water scour can be calculated as:

$$y_{max} = \left(\frac{\rho g n^2 q^2}{\tau_c}\right)^{\frac{3}{7}}$$

(10.2)

where n is Manning's coefficient, q is discharge per unit width, and τ_c is critical shear stress. With clear-water scour, the scour depth in the contracted section will continue to increase until the bed shear stress falls below the critical shear stress. Therefore, the equilibrium scour depth can be quite large if the critical shear stress is small, unless live-bed scour occurs in the channel upstream. In the latter case, sediment transport into the contracted section from upstream would limit the contraction scour depth and the equations for live-bed scour in HEC-18 should be used instead of Eq. (10.2) to predict the equilibrium scour depth.

Note that using the SRICOS method to predict contraction scour does not reduce the equilibrium scour depth, but by accounting for the slower rates of scour in cohesive soils, the method can predict the change in channel bed elevation over time due to the construction of a new bridge or modification of an existing bridge. Channel erosion is often observed at new bridges because the channel bed is not in equilibrium with the flow conditions. Figure 10.2 shows the channel cross sections measured at different times at the SD37 southbound bridge over the James River. The bridge was completed in the fall of 2002, but 2 to 3 ft (0.6 to 0.9 m) of contraction scour had already developed at the bridge crossing by the summer of 2004, even though no significant floods occurred in 2003 and 2004; the measured maximum annual flows were 751 and 931 ft³/s, respectively. It is also probable that the bridge site was backfilled with unconsolidated materials that were more erodible, and thus the high erosion rates for the low flow rates. The first major flood after the southbound bridge was built occurred on May 8, 2007, with a measured peak discharge of 21,300 ft³/s. This flood followed by an even larger flood in March 2011 (peak discharge 28,400 ft³/s) produced no additional contraction

scour. These observations are consistent with the high plasticity clay found at the foundation depth, which has a very high critical shear stress (> 24 N/m^2) (see Figure 7.8).
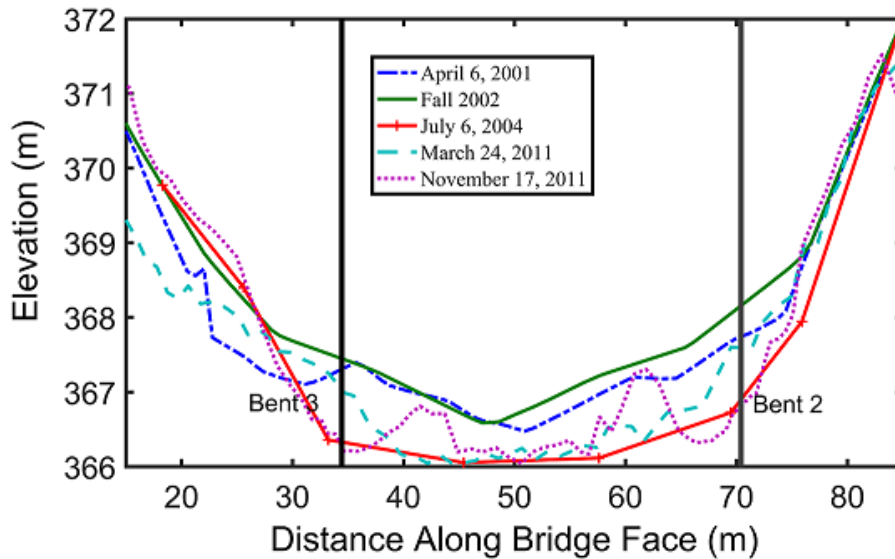
Figure 10.2 Measured channel cross sections at downstream face of SD37 southbound bridge over the James River *(from Rossell and Ting, 2013)*

The procedure for applying the SRICOS method to predict contraction scour at a bridge site follows a similar procedure in pier scour and can be divided into three levels:

1. In the Level I analysis, the HEC-18 method is used to determine whether live-bed or clear-water contraction scour would occur at the bridge site. If live-bed contraction scour occurs, the SRICOS method is not applicable, and the contraction scour depth should be calculated using the live-bed contraction scour equations in HEC-18. If clear-water contraction scour occurs, the equilibrium scour depth in the contracted section is predicted using Eq. (10.2), which is valid for both cohesive and non-cohesive soils. For non-cohesive soils, the critical shear stress can be estimated using the Shields diagram. For cohesive soils, the critical shear stress should be measured. Unlike pier scour, the equilibrium scour depth in contraction scour is very sensitive to the value of the critical shear stress. Using a measured soil erosion function, the SRICOS method is run with the 100-year peak flow for five days. If the soil type falls into either soil region I or II and/or the computed scour depth is close to the equilibrium scour depth, the maximum scour depth can be reached during a single flooding event and no reduction should be applied to the scour depth obtained using the HEC-18 method.

2. In the Level II analysis, the final scour depths and equivalent times of selected historical floods are computed using the measured soil erosion function. The results are plotted on a $\frac{z_f}{z_{max}}$ versus $\frac{t_e}{t_{90}}$ curve similar that shown in Figure 10.3 for the SD37 bridges. As discussed in Chapter 4, in this case, the computed data points will not generally fall on the solid line represented by a hyperbolic function. For contraction scour, it was found that the hyperbolic model over-predicts the $\frac{z_f}{z_{max}}$ ratio at low rates of scour but under-predicts the $\frac{z_f}{z_{max}}$ ratio at high rates of scour (see Figure 10.3). Nevertheless, by examining the distribution of $\frac{z_f}{z_{max}}$ ratios produced by the historical floods, the engineer can obtain a good idea whether the equilibrium scour depth would be reached during the design life of the project. The engineer can then

145

proceed to the Level III analysis if the final scour depth is expected to be significantly less than the equilibrium scour depth.

3. In the Level III analysis, the computed equivalent times of the maximum annual floods are normalized by t_{90} and correlated to the measured peak discharges and/or flood durations to develop regression equations to compute the equivalent times for floods of different return periods. However, we have seen in Chapter 7 that for the SD37 bridges the $\frac{t_e}{t_{90}}$ ratio is poorly correlated to the peak discharge, and currently there are no reliable methods to predict the duration of an individual flood. The latter is a complicated function of the hydrologic characteristics of the drainage basin and climatic conditions. Thus, flood duration can vary significantly from year to year even for floods with similar return periods. The best solution at the present time may be to use the computed $\frac{t_e}{t_{90}}$ ratios of the historical floods and engineering judgment to select an envelope curve for the $\frac{t_e}{t_{90}}$ ratio. The computed scour depth would be conservative, but it could still be significantly less than the equilibrium scour depth if the time rates of scour are slow. The Log Pearson Type III or another flood frequency distribution can then be used with Monte Carlo simulation to generate many equally probable annual maximum series to compute the distribution of final scour depth using the SRICOS method. The risk values can then be determined for different project lives to select a design scour depth.

The screening procedure is demonstrated for contraction scour using the SD37 bridges over the James River near Mitchell in Chapter 12.
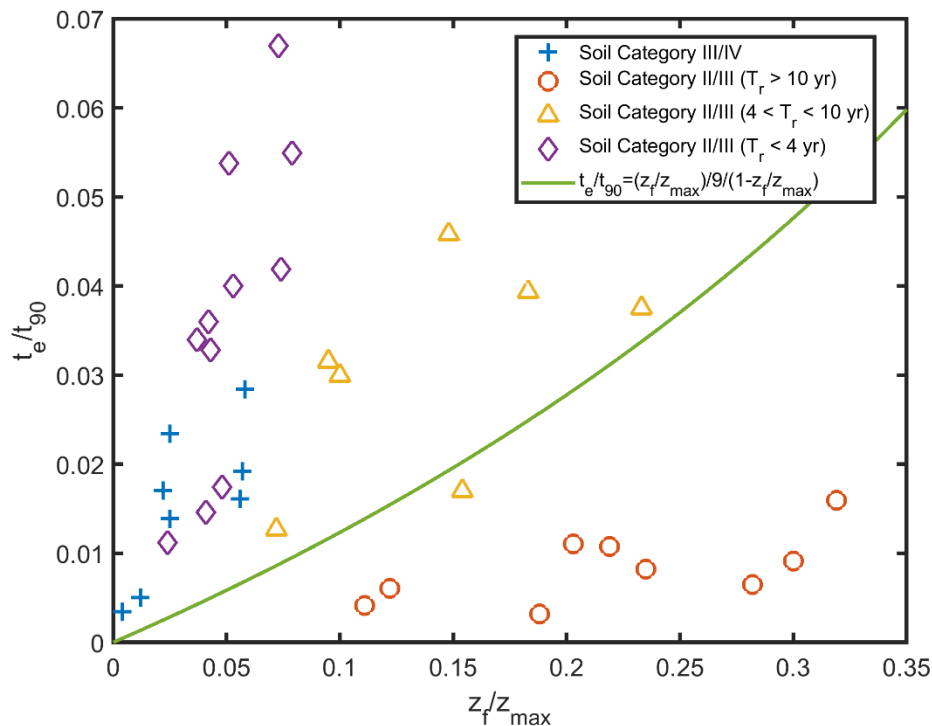
Figure 10.3 Variations of t_e/t_{90} ratio with z_f/z_{max} ratio for the maximum annual floods, SD37 bridges over the James River
The hyperbolic model is represented by the solid line.

146

10.4 Application of SRICOS Method to Ungauged Streams

If no gauging station exists at a bridge site, a discharge-versus-time curve for the historical flows will have to be estimated before one can compute the scour histories and determine the magnitudes and equivalent times of the individual floods. The drainage-area ratio method may be used to transfer streamflow data from a nearby gauging station or stations to an ungauged location on the same stream. For an ungauged stream, daily mean flow data may be transferred from a gauging station (the donor) on another stream to the ungauged stream using the QPPQ method (Archfield et al., 2013). The QPPQ method is described in detail in Chapter 8 and demonstrated using the Split Rock Creek by employing the Skunk Creek station at Sioux Falls (06481500) as an index station. In this case, the Split Rock Creek at Corson gauging station has continuous streamflow records from 1965 to 1989 and from 2001 to the present. The QPPQ method was used to estimate the discharge time series for the period from 1989 to 2001 when continuous flow record is not available. Streamflow records from the overlapping period (1965 to 1989 and 2003 to 2016) were used to compute flow-duration-curves (FDCs) for the two stations (Figure 8.6). A flow-duration curve is a cumulative frequency curve that shows the percent of time during which specified discharges were equaled or exceeded within a given period. The recorded hydrograph at the Skunk Creek station was transferred to the Split Rock Creek station assuming that the time histories of exceedance probabilities are identical at the two locations. Thus, a required criterion of the QPPQ method is that stream flows at the ungauged site and donor gauge are highly correlated.

The procedure will have to be modified if no flow data exist at the ungauged site. In this scenario, the FDC at the donor gauge can still be constructed using observed streamflow data, but the FDC at the ungauged site will have to be generated by other means. Like peak-flow magnitude, regional regression equations can be developed for estimating flow-duration curve exceedance probabilities for ungauged streams. Exceedance-probability quantiles are related to basin characteristics and physical measurements such as drainage area, land cover such as percent area consisting of cultivated land, and soil parameters such as hydraulic conductivity of the saturated soils. Ziegeweid et al. (2015) developed a total of 115 regression equations to calculate flow-duration curves and low-flow frequency statistics for small streams in Minnesota. To our knowledge, similar information is not available in South Dakota.

The Level I and Level III analyses are similar for gauged and ungauged sites. For an ungauged site, the procedure differs primarily in the Level II analysis, which requires the equivalent times to be determined for floods of different return periods from the computed scour histories. If a site has no flow data at all, scour histories would have to be estimated using synthetic hydrographs. As an example, the NRCS unit triangular hydrograph is shown in Figure 10.4. It is defined by the peak discharge Q_p and time to peak t_p. The length of the recession limb is assumed to be $1.67t_p$ so that the total duration of the hydrograph is $2.67t_p$. Other synthetic unit hydrographs commonly used in flood routing includes the Snyder unit hydrograph and Espey unit hydrograph (Bedient and Huber, 1992). Regional regression equations for estimating peak flow magnitude and frequency relations for South Dakota streams are published in Sando (1998). These regression equations can be used to estimate the peak flow magnitudes for selected recurrence intervals based on basin and climatic characteristics. Various empirical equations also exist to estimate the flood duration of a synthetic hydrograph. For the NRCS triangular hydrograph, t_p is related to the time of concentration t_c by $t_p = 0.67t_c$. Understandably, using synthetic hydrographs in SRICOS simulations will introduce additional uncertainties. Therefore, the results obtained must be treated with caution. The procedure is demonstrated using a worked example in Chapter 13.
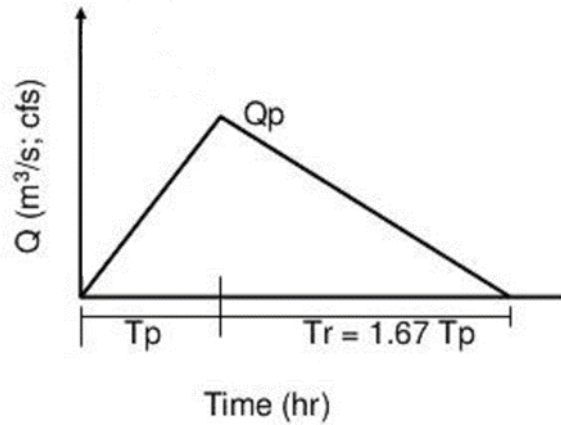
Figure 10.4 NRCS synthetic unit triangular hydrograph

10.5 Summary

A procedure for incorporating the influence of time in evaluating bridges for pier and contraction scour was developed. The complete process includes three levels of analysis in increasing order of complexity. The Level I analysis involves computing the equilibrium scour depth using the traditional HEC-18 method, assessing soil erodibility using a generalized soil erosion rate chart and USCS soil classification or a measured soil erosion function, running the SRICOS method with the 100-year peak flow for five days, and assessing the results using engineering judgment to determine whether it would be beneficial to apply the SRICOS method. The Level II analysis involves computing the scour histories of selected historical floods and using the results to predict the final scour depths and equivalent times of the individual floods. These results are then plotted on a $\frac{z_f}{z_{max}}$ versus $\frac{t_e}{t_{90}}$ chart to examine the time rates of scour for floods of different return periods. In the Level III analysis, a stochastic approach and Monte Carlo simulation is used to generate many annual maximum series for scour prediction using the SRICOS method. The distribution of computed final scour depth is used to determine the risk values associated with different project lives. Several approaches to applying the above procedure to ungauged streams or sites with inadequate streamflow data are also discussed.

11. WORKED EXAMPLE – PIER SCOUR

11.1 Site Description

This chapter demonstrates the use of the decision tool and hydrograph generation method for pier scour outlined in Section 10.2. The site is the SD13 bridge over the Big Sioux River near Flandreau. The steel-girder bridge has three pier sets with webs, each 3-ft wide and 30-ft long. The bridge crossing is located immediately downstream of a 90-degree bend. Compound channel flows produce large flow angle of attack and equilibrium scour depth at bent 2 over a wide range of flow discharges. A description of the bridge site can be found in Section 6.1 where an aerial photograph of the site is shown in Figure 6.1, a photograph of the bridge crossing in Figure 6.2, the subsurface profile in Figure 6.3, and the measured soil erosion function in Figure 6.4. Details of the hydraulic analysis using 1D and 2D flow models can be found in Larsen et al. (2011) and Ting et al. (2017).

11.2 MATLAB Scripts

Table 11.1 is a list of the MATLAB scripts used in this example. The scripts are included as supplementary files to the final report.

Table 11.1 MATLAB scripts used in worked-out example
The section where each file is used is listed with the filename.

Filename	Description
ReturnPeriod_FloodMagnitude (Section 11.5.1)	Fit a Log-Pearson Type III distribution to the measured annual peak flows and compute the flood magnitude for a given return period
SRICOS_ConstantQ (Sections 11.5.3 – 11.5.6)	Compute the final scour depth produced by a constant discharge using the SRICOS method
SRICOS_RecordedHydrograph (Section 11.6.1)	Compute the scour history using a recorded hydrograph and determine the equivalent duration
SRICOS_FutureHydrograph_Single (Section 11.7.2)	Generate a single future hydrograph using the Log Pearson Type III distribution and compute the scour history using the SRICOS method
SRICOS_FutureHydrograph_Multiple (Section 11.7.2)	Generate multiple realizations of the future hydrograph and compute the distribution of final scour depth and risk value

11.3 Bridge Parameters

Pier width a = 3 ft (0.9144 m)

Pier length L = 30 ft (9.144 m)

Pier shape = octagonal pier sets with webs

Channel width W_1 = 436 ft (132.9 m)

Number of pier sets N = 3

Pier spacing S = 120 ft (36.6 m)

11.4 Fluid Parameters

Density of water $\rho = 998.2$ kg/m^3(1.94 slug/ft^3) @ 20°C

Kinematic viscosity of water $\nu = 1.004 \times 10^{-6}$ m^2/s (1.081×10^{-5} ft^2/s) @ 20°C

Acceleration of gravity $g = 9.81$m/s^2 (32.2 ft/s^2)

11.5 Level I Assessment

The Level I assessment includes a basic hydrologic, hydraulic, and scour analysis like the bridge scour evaluation documented in HEC-18. The procedure involves estimating the 100-year and 500-year recurrence interval peak discharges, computing the hydraulic conditions resulting from each discharge, and calculating the equilibrium scour depths using the pier scour equation in HEC-18. Borehole data are used to delineate the soil stratigraphy, and thin-walled tube samples may be collected and tested in an erosion function apparatus (EFA) to obtain the soil erosion function. Alternatively, the soil classification may be used with Figure 5.3 to estimate the critical shear stress and soil erosion rates. The SRICOS method is run with the estimated 100-year peak discharge for five days. If the soil type falls into category I or II and/or the computed final scour depth is close to the equilibrium scour depth, the maximum scour depth can be reached during a single design flood and no reduction to the scour depth obtained using the HEC-18 method is recommended. The engineer may also adopt the equilibrium scour depth for design if the scour depth computed using the HEC-18 method is judged to be reasonable or other considerations (e.g., high traffic volume, long design life) dictate a more conservative approach.

11.5.1 Flood Frequency Analysis

The Log Pearson Type III distribution was fitted to the annual peak flows recorded at the Big Sioux River near Brookings gauging station (06480000) to estimate the flood magnitudes for different return periods. The algorithm is implemented in the MATLAB script "ReturnPeriod_FloodMagnitude.m." The relationship between the peak discharge and exceedance probability is shown in Figure 11.1, and the estimated discharges for selected return periods are presented in Table 11.2. In Table 11.2, a drainage area ratio adjustment of 1.025 has been applied to transfer the discharges at the Brookings station to the bridge site.

Table 11.3 shows the results of flood frequency analysis conducted by the USGS office in South Dakota using the expected moments algorithm (EMA) in PeakFQ. Results are presented for runs without historic analysis and regional information, and with historic analysis and regional information. The results obtained without historic analysis and regional information are like those obtained using the Bulletin 17B method shown in Table 11.2 and are more conservative than the results obtained with historic analysis and regional information. The output from the EMA run with historic analysis is included in Appendix III.

Table 11.2 Peak flow estimates for different return periods at Brookings streamflow gauging station and SD13 bridge

The discharge values were obtained by fitting the Log Pearson Type III distribution to the recorded annual peak flows from water year 1954 to 2016 using the Bulletin 17B method.

Exceedance Probability	Return Period (Years)	Peak Flow at Brookings Station (ft³/s)	Peak Flow at SD13 Bridge (ft³/s)
0.995	1	103.4	106
0.5	2	2,572	2,636
0.2	5	6,512	6,675
0.1	10	10,353	10,612
0.04	25	16,689	17,106
0.02	50	22,513	23,076
0.01	100	29,293	30,025
0.005	200	37,090	38,017
0.002	500	49,063	50,290

Table 11.3 Peak flow estimates at Brookings streamflow gauging station using the expected moments algorithm in Bulletin 17C

Exceedance Probability	Return Period (Years)	Peak Flow without Historic Analysis and Regional Information (ft³/s)	Peak Flow with Historic Analysis and Regional Information (ft³/s)
0.995	1	103.6	95.9
0.5	2	2,572	2,584
0.2	5	6,515	6,370
0.1	10	10,350	9,886
0.04	25	16,680	15,420
0.02	50	22,500	20,290
0.01	100	29,260	25,760
0.005	200	37,030	31,820
0.002	500	48,960	40,740
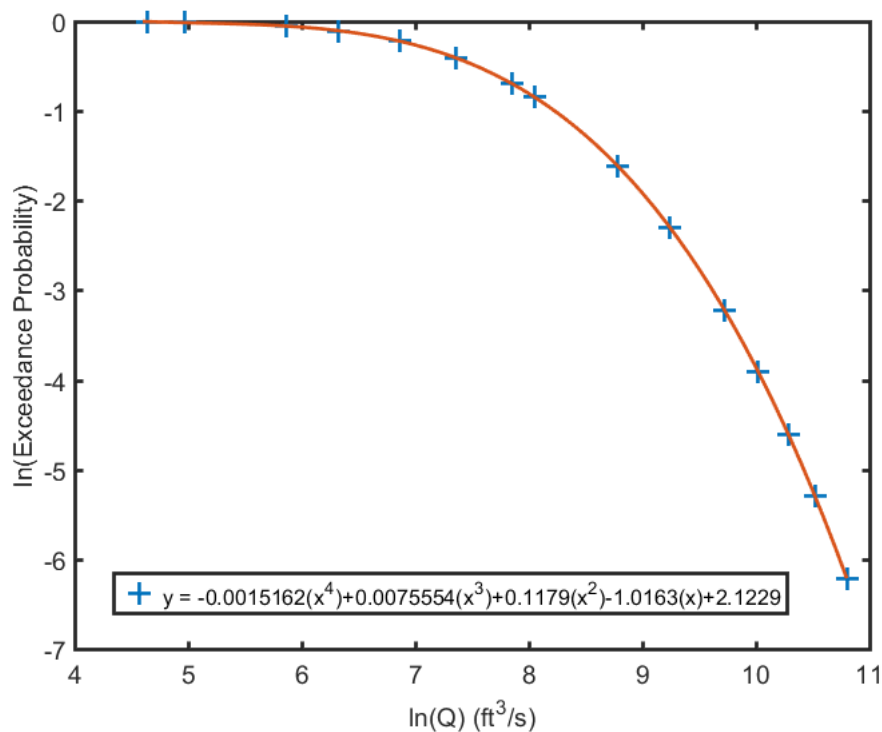
Figure 11.1 Relationship between peak discharge and exceedance probability at Brookings streamflow gauging station obtained using the Log Pearson Type III distribution following the Bulletin 17B method
The red line is the best-fit line.

11.5.2 Hydraulic Analysis

Tables 11.4 to 11.6 show the results of hydraulic analysis for bents 2, 3 and 4, respectively, obtained using the 2D flow model FESWMS in the Surface Water Modeling System (SMS).

Table 11.4 Computed results for bent 2 from 2D flow model

Discharge Q (ft³/s)	Velocity V_1(ft/s)	Flow Angle of Attack α (degrees)	Flow Depth y_1(ft)
1,000	0.56	47.2	3.84
1,624	0.98	44.9	4.26
3,500	0.98	42.7	5.14
4,346	2.98	43.5	5.46
7,500	4.19	41.1	5.92
7,774	4.11	39.5	6.13
9,090	4.42	36.3	6.90
10,000	4.73	34.1	7.20
12,500	5.28	30.6	7.92
15,000	5.66	27.8	8.61
17,500	6.17	26.0	9.21
20,000	7.17	25.6	9.63
30,000	8.52	17.0	11.32
31,300	8.69	16.5	11.55
35,000	9.34	15.8	12.01
40,000	10.12	15.1	12.57

Table 11.5 Computed results for bent 3 from 2D flow model

Discharge Q (ft³/s)	Velocity V_1(ft/s)	Flow Angle of Attack α (degrees)	Flow Depth y_1 (ft)
1,000	0.81	39.1	11.45
1,624	1.24	38.6	11.88
3,500	1.24	38.6	12.80
4,346	2.89	38.8	13.14
7,500	4.29	35.9	13.57
7,774	4.19	33.9	13.77
9,090	4.22	30.8	14.50
10,000	4.35	29.2	14.81
12,500	4.70	25.8	15.54
15,000	5.06	23.4	16.25
17,500	5.42	21.6	16.88
20,000	5.48	20.1	17.35
30,000	7.11	16.4	19.22
31,300	7.14	16.2	19.49
35,000	7.61	15.5	20.02
40,000	8.26	14.7	20.70

Table 11.6 Computed results for bent 4 from 2D flow model

Discharge Q (ft³/s)	Velocity V_1(ft/s)	Flow Angle of Attack α (degrees)	Flow Depth y_1 (ft)
1,000	0.50	4.6	2.46
1,624	0.60	6.4	2.89
3,500	0.54	16.6	3.83
4,346	0.42	24.7	4.17
7,500	2.15	13.3	4.65
7,774	2.29	11.5	4.80
9,090	2.43	10.6	5.49
10,000	2.54	10.2	5.78
12,500	3.35	2.7	6.43
15,000	3.92	4.6	7.09
17,500	4.50	5.1	7.65
20,000	4.72	7.3	8.02
30,000	7.07	9.1	9.72
31,300	7.27	8.2	9.99
35,000	7.98	8.9	10.46
40,000	8.93	9.7	11.05

11.5.3 Compute Equilibrium Scour Depth for 100-Year Discharge (Q_{100} = 30,025 ft³/s)

Compute the equilibrium scour depth at bent 2

The peak flow used for this example is taken from Table 11.2. The value of Q_{100} after adjusting for drainage area is 30,025 ft³/s, which is very close to the discharge of 30,000 ft³/s shown in Tables 11.4 to 11.6. For ease of reference, we shall use the computed flow depth and flow velocity for 30,000 ft³/s in the scour calculations for the 100-year flood.

Flow depth $y_1 = 11.32$ ft (3.45 m)

Approach flow velocity $V_1 = 8.52$ ft/s (2.6 m/s)

Flow angle of attack $\alpha = 17.0$ degrees

It is shown in Section 5.2 that Eq. (5.14), which was proposed for computing the equilibrium scour depth in cohesive soils by Briaud et al. (2009), would generally produce a larger scour depth than the HEC-18 equation [Eq. (5.9)]. Therefore, the HEC-18 equation is used to compute the equilibrium scour depth in this example (see also Section 11.5.5).

$$\frac{z_{max}}{a} = 2.0 K_1 K_2 K_3 \left(\frac{y_1}{a}\right)^{0.35} \left(\frac{V_1}{\sqrt{gy_1}}\right)^{0.43} \qquad \text{(Eq. 5.9)}$$

$K_1 = 1.0$

$$K_2 = \left(\cos\alpha + \frac{L}{a}\sin\alpha\right)^{0.65} = \left(\cos 17.0° + \frac{30}{3}\sin 17.0°\right)^{0.65} = 2.41$$

$K_3 = 1.1$

$$\frac{V_1}{\sqrt{gy_1}} = \frac{8.52}{\sqrt{(32.2)(11.32)}} = 0.45$$

$$\frac{z_{max}}{a} = 2.0 \times 1.0 \times 2.41 \times 1.1 \times \left(\frac{11.32}{3}\right)^{0.35} (0.45)^{0.43} = 5.99$$

$z_{max} = 5.99 \times 3 = 18.0$ ft

Compute the equilibrium scour depth at bent 3

Flow depth $y_1 = 19.22$ ft (5.86 m)

Approach flow velocity $V_1 = 7.11$ ft/s (2.17 m/s)

Flow angle of attack $\alpha = 16.4$ degrees

$$\frac{z_{max}}{a} = 2.0 K_1 K_2 K_3 \left(\frac{y_1}{a}\right)^{0.35} \left(\frac{V_1}{\sqrt{gy_1}}\right)^{0.43}$$

$K_1 = 1.0$

$$K_2 = \left(\cos\alpha + \frac{L}{a}\sin\alpha\right)^{0.65} = \left(\cos 16.4° + \frac{30}{3}\sin 16.4°\right)^{0.65} = 2.37$$

$K_3 = 1.1$

$$\frac{V_1}{\sqrt{gy_1}} = \frac{7.11}{\sqrt{(32.2)(19.22)}} = 0.29$$

$$\frac{z_{max}}{a} = 2.0 \times 1.0 \times 2.37 \times 1.1 \times \left(\frac{19.22}{3}\right)^{0.35} (0.29)^{0.43} = 5.87$$

$z_{max} = 5.87 \times 3 = 17.6$ ft

Compute the equilibrium scour depth at bent 4

Flow depth $y_1 = 9.72$ ft (2.96 m)

Approach flow velocity $V_1 = 7.07$ ft/s (2.15 m/s)

Flow angle of attack $\alpha = 9.1$ degrees

$$\frac{z_{max}}{a} = 2.0 K_1 K_2 K_3 \left(\frac{y_1}{a}\right)^{0.35} \left(\frac{V_1}{\sqrt{g y_1}}\right)^{0.43}$$

$K_1 = 1.0$

$$K_2 = \left(\cos\alpha + \frac{L}{a}\sin\alpha\right)^{0.65} = \left(\cos 9.1° + \frac{30}{3}\sin 9.1°\right)^{0.65} = 1.85$$

$K_3 = 1.1$

$$\frac{V_1}{\sqrt{g y_1}} = \frac{7.07}{\sqrt{(32.2)(9.72)}} = 0.4$$

$$\frac{z_{max}}{a} = 2.0 \times 1.0 \times 1.85 \times 1.1 \times \left(\frac{9.72}{3}\right)^{0.35} (0.4)^{0.43} = 4.14$$

$$Z_{max} = 4.14 \times 3 = 12.4 \text{ ft}$$

Bent 2 is used in the following analysis since it has the largest equilibrium scour depth.

11.5.4 Compute Equilibrium Scour Depth for 500-Year Discharge (Q_{500} = 50,290 ft³/s)

The value of Q_{500} after adjusting for drainage area is 50,290 ft³/s (see Table 11.2). The flow depth, approach flow velocity, and flow angle of attack for the 500-year peak flow were extrapolated from the computed results for bent 2 in Table 11.4:

Flow depth $y_1 = 13.56$ ft (4.13 m)

Approach flow velocity $V_1 = 11.66$ ft/s (3.55 m/s)

Flow angle of attack $\alpha = 13.5$ degrees

$$\frac{z_{max}}{a} = 2.0 K_1 K_2 K_3 \left(\frac{y_1}{a}\right)^{0.35} \left(\frac{V_1}{\sqrt{g y_1}}\right)^{0.43}$$

$K_1 = 1.0$

$$K_2 = \left(\cos\alpha + \frac{L}{a}\sin\alpha\right)^{0.65} = \left(\cos 13.5° + \frac{30}{3}\sin 13.5°\right)^{0.65} = 2.18$$

$K_3 = 1.1$

$$\frac{V_1}{\sqrt{g y_1}} = \frac{11.66}{\sqrt{(32.2)(13.56)}} = 0.56$$

$$\frac{z_{max}}{a} = 2.0 \times 1.0 \times 2.18 \times 1.1 \times \left(\frac{13.56}{3}\right)^{0.35} (0.56)^{0.43} = 6.34$$

$$z_{max} = 6.34 \times 3 = 19.0 \text{ ft}$$

The computed equilibrium scour depth is about the same as that of the 100-year flood.

11.5.5 Compute Equilibrium Scour Depth using Eq. 5.14 and Measured Soil Critical Shear Stress

The equilibrium scour depths computed using Eq. (5.9) and Eq. (5.14) are compared in this section. The soil at the foundation depth on the north abutment adjacent to bent 2 is classified as very silty fine sand. The percentage by weight of sample finer than the No. 200 sieve (0.074 mm) is 30%. The measured critical shear stress τ_c is 18.6 N/m^2 (Figure 6.4). The Manning's n value is taken to be 0.035. The critical velocity V_c is found using Eq. (5.15).

100-Year Flood

Flow depth $y_1 = 11.32$ ft (3.45 m)

Approach flow velocity $V_1 = 8.52$ ft/s (2.6 m/s)

Flow angle of attack $\alpha = 17.0$ degrees

$K_1 = 1.0$
$K_2 = 2.41$

$$V_c = \sqrt{\frac{\tau_c y_1^{\frac{1}{3}}}{\rho g n^2}} = \sqrt{\frac{(18.6)(3.45)^{\frac{1}{3}}}{(998.2)(9.81)(0.035)^2}} = 1.53\,\frac{m}{s}\left(5.02\,\frac{ft}{s}\right)$$

$$z_{max} = 2.2 K_1 K_2 a \left(\frac{2.6 V_1}{\sqrt{ga}} - \frac{V_c}{\sqrt{ga}}\right)^{0.7} = 2.2 \times 1.0 \times 2.41 \times 3 \times \left(\frac{(2.6)(8.52)}{\sqrt{(32.2)(3)}} - \frac{5.02}{\sqrt{(32.2)(3)}}\right)^{0.7} = 23.5\text{ ft}$$

500-Year Flood

Flow depth $y_1 = 13.56$ ft (4.13 m)

Approach flow velocity $V_1 = 11.66$ ft/s (3.55 m/s)

Flow angle of attack $\alpha = 13.5$ degrees

$K_1 = 1.0$
$K_2 = 2.18$

$$V_c = \sqrt{\frac{\tau_c y_1^{\frac{1}{3}}}{\rho g n^2}} = \sqrt{\frac{(18.6)(4.13)^{\frac{1}{3}}}{(998.2)(9.81)(0.035)^2}} = 1.58\,\frac{m}{s}\left(5.17\,\frac{ft}{s}\right)$$

$$z_{max} = 2.2 K_1 K_2 a \left(\frac{2.6 V_1}{\sqrt{ga}} - \frac{V_c}{\sqrt{ga}}\right)^{0.7} = 2.2 \times 1.0 \times 2.18 \times 3 \times \left(\frac{(2.6)(11.66)}{\sqrt{(32.2)(3)}} - \frac{5.17}{\sqrt{(32.2)(3)}}\right)^{0.7} = 27.8\text{ ft}$$

The equilibrium scour depths for the 100- and 500-year peak flows computed using Eq. (5.14) are much greater than the corresponding equilibrium scour depths computed using the HEC-18 equation. Therefore, the equilibrium scour depths computed using the HEC-18 equation have been used in the SRICOS simulations. The equilibrium scour depth in non-cohesive soil is used to limit the maximum scour depth that can be developed at the bridge site.

11.5.6 Compute Maximum Bed Shear Stress and Initial Rate of Scour around Bent 2 and Run 100-Year Peak Discharge for 5 Days:

Flow depth $y_1 = 11.32$ ft (3.45 m)

Approach flow velocity $V_1 = 8.52$ ft/s (2.6 m/s)

Flow angle of attack $\alpha = 17.0$ degrees

Critical shear stress $\tau_c = 18.6$ N/m^2 (Fig. 6.4)

Erosion function constant $a' = 7.49$ mm/h/(N/m^2) (Fig. 6.4)

Erosion function exponent $b' = 1$ (Fig. 6.4)

Eq. (5.17) – Eq. (5.21):

$$k_w = 1 + 16e^{\frac{-4y_1}{a}} = 1 + 16e^{\frac{-4(11.32)}{3}} = 1$$

$$k_{sp} = 1 + 5e^{\frac{-1.1S}{a}} = 1 + 5e^{\frac{-1.1(120)}{3}} = 1$$

$$k_{sh} = 1.15 + 7e^{\frac{-4L}{a}} = 1.15 + 7e^{\frac{-4(30)}{3}} = 1.15$$

$$k_\alpha = 1 + 1.5 \left(\frac{\alpha}{90°}\right)^{0.57} = 1 + 1.5 \left(\frac{17.0°}{90°}\right)^{0.57} = 1.58$$

$$\tau_{max} = k_w k_{sp} k_{sh} k_\alpha \times 0.094\rho V_1^2 \left[\frac{1}{\log\left(\frac{aV_1}{\nu}\right)} - \frac{1}{10}\right]$$

$$= 1 \times 1 \times 1.15 \times 1.58 \times 0.094 \times 998.2 \times 2.6^2 \times \left[\frac{1}{\log\left(\frac{(0.9144)(2.6)}{1.004\times10^{-6}}\right)} - \frac{1}{10}\right] = 65.6 \text{ N/m}^2$$

Eq. (5.3):

$$\dot{z}_i = a'(\tau - \tau_c)^{b'} = 7.49(65.6 - 18.6)^1 = 352 \text{ mm/h (1.15 ft/h)}$$

Eq. (5.22):

$$z = \frac{t}{\frac{1}{\dot{z}_i} + \frac{t}{z_{max}}} = \frac{5(24)}{\frac{1}{1.15} + \frac{(5)(24)}{18}} = 15.9 \text{ ft}$$

The computed final scour depth is close to the equilibrium scour depth of the 100-year flood. The equilibrium scour depth can be reached during a single design flood. Therefore, the SRICOS method would produce no significant reduction in the predicted final scour depth.

To illustrate the procedures for the Level II and Level III assessment, we consider a hypothetical case where the soil erosion function is given by the solid line that separates geo-material categories III and IV in Figure 5.3. From Table 5.1,

Critical shear stress $\tau_c = 9.5$ N/m^2

Erosion rate constant $a' = 1.62$

Eq. (5.2):

$$\dot{z}_i = 0.1 \left(\frac{\tau}{\tau_c}\right)^{a'} = 0.1 \left(\frac{65.6}{9.5}\right)^{1.62} = 2.3 \frac{\text{mm}}{\text{h}} \left(0.0075 \frac{\text{ft}}{\text{h}}\right)$$

Eq. (5.22):

$$z = \frac{t}{\frac{1}{\dot{z}_i} + \frac{t}{z_{max}}} = \frac{5(24)}{\frac{1}{0.0075} + \frac{(5)(24)}{18}} = 0.86 \text{ ft}$$

The computed final scour depth is considerably less than the equilibrium scour depth. Level II assessment is recommended.

11.6 Level II Assessment

11.6.1 Compute the t_e/t_{90} and z_f/z_{max} Ratios of Maximum Annual Floods

The MATLAB script "SRICOS_RecordedHydrograph.m" was used with the recorded hydrographs transferred from the Brookings station to compute the scour histories of the maximum annual floods that can produce scour ($Q_{max} > Q_c$). The results for the 2010 flood are shown below and in Figure 11.2. The complete results for all the scouring maximum annual floods can be found in Table 6.3.

Peak discharge Q_{max}= 20,295 ft³/s

Critical discharge Q_c = 4,581 ft³/s

Flow duration above critical discharge t_s = 126.5 h

Predicted final scour depth z_f = 0.21 ft

Equilibrium scour depth at peak discharge z_{max}= 18.5 ft

Initial rate of scour at peak discharge $\dot{z}_i$ = 0.00444 ft/s

Equivalent time t_e = 47.84 h

Time to reach 90% of equilibrium scour depth t_{90} = 37,594 h

The values of the $\frac{Q_{max}}{Q_c}$, $\frac{t_e}{t_{90}}$ and $\frac{z_f}{z_{max}}$ ratios are 4.43, 0.00127 and 0.011, respectively. Table 11.7 summarizes the results for all the maximum annual floods with return period greater than or equal to five years. The computed $\frac{z_f}{z_{max}}$ and $\frac{t_e}{t_{90}}$ ratios are plotted in Figure 11.3. All the values are close to zero, which means that the scour depths produced by the recorded floods are far from the equilibrium condition. Therefore, the time rate of scour is an important factor in determining the final scour depth.

Table 11.7 Computed t_e/t_{90} and z_f/z_{max} ratios for the maximum annual floods with return period greater than or equal to 5 years (*see also Table 6.3*)

Year	$\dfrac{Q_{max}}{Q_c}$	Return Period (year)	$\dfrac{z_f}{z_{max}}$	$\dfrac{t_e}{t_{90}}$
1969	7.59	152	0.028	0.00320
2010	4.43	36.7	0.011	0.00127
2011	3.45	21.1	0.025	0.00289
1984	3.07	16.7	0.010	0.00112
1993	2.98	15.7	0.008	0.00095
1997	2.46	11.1	0.019	0.00218
1962	2.37	10.4	0.005	0.00054
1960	2.15	8.9	0.002	0.00018
1985	1.89	7.2	0.004	0.00050
1965	1.72	6.3	0.003	0.00032
1995	1.55	5.4	0.004	0.00046
1986	1.50	5.2	0.002	0.00026
2001	1.49	5.2	0.015	0.00167
2007	1.46	5	0.002	0.00027
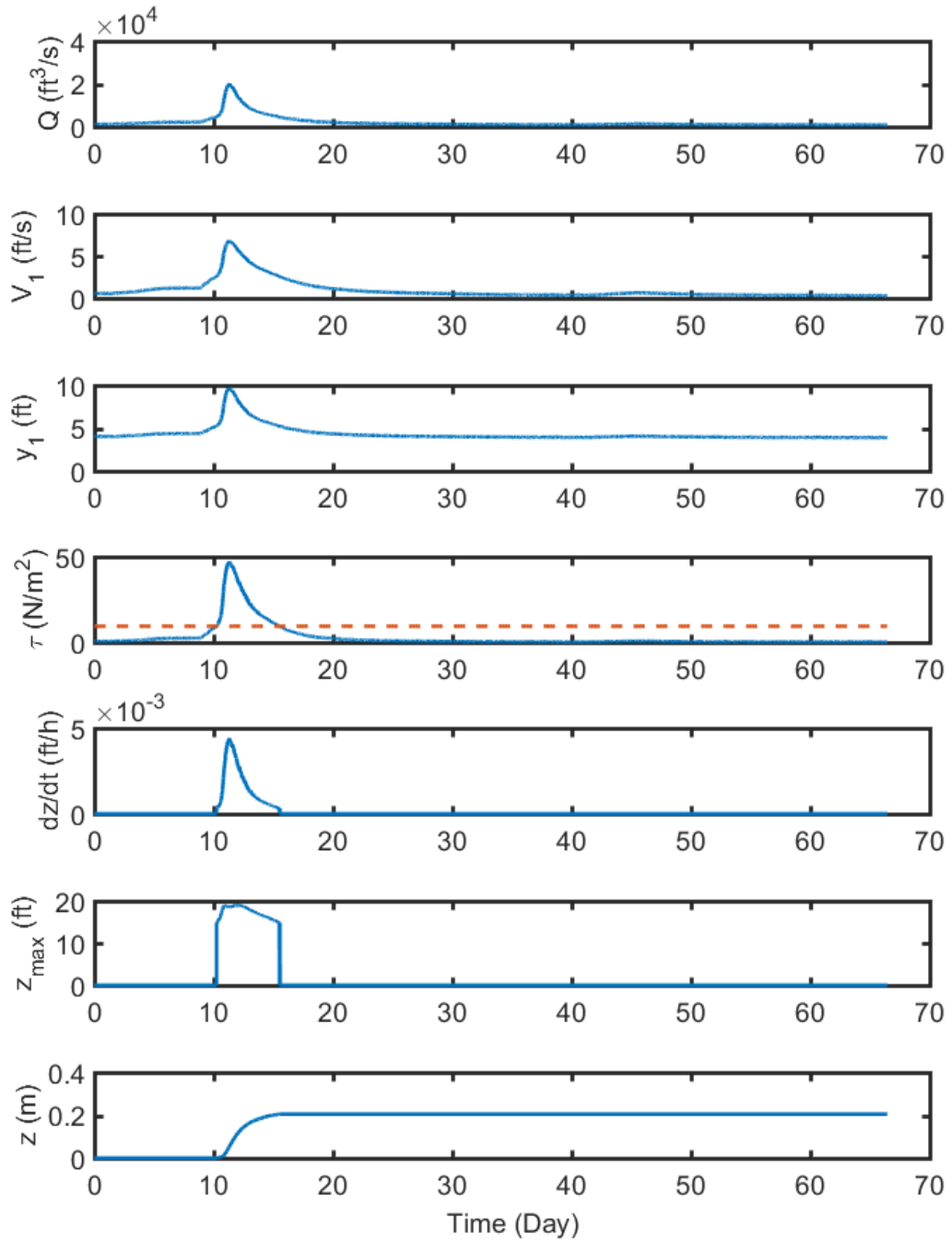
Figure 11.2 SRICOS simulation for bent 2 from September 4 to November 19, 2010

160
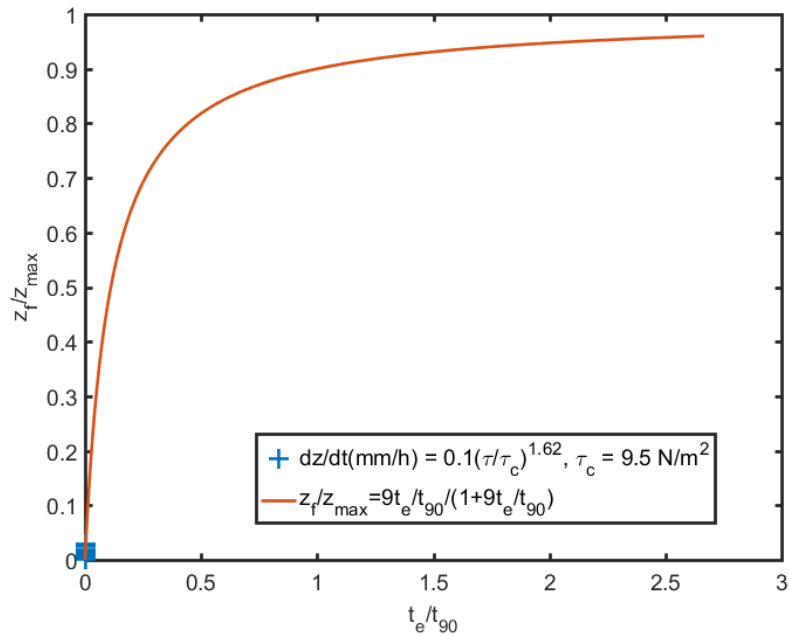
Figure 11.3 Variation of z_f/z_{max} ratio with t_e/t_{90} ratio for the maximum annual floods shown in Table 11.7

11.7 Level III Assessment

11.7.1 Relate t_e/t_{90} Ratio to Q_{max}/Q_c Ratio

The $\dfrac{t_e}{t_{90}}$ ratio is plotted against the $\dfrac{Q_{max}}{Q_c}$ ratio in Figure 11.4 to show the relationship between the dimensionless equivalent time and dimensionless discharge. There is a linear relationship between the two parameters except for three floods (1997, 2001, and 2011), which have large equivalent time due to the very long recession times of these floods. One approach is to treat the three floods as outliers and estimate the $\dfrac{t_e}{t_{90}}$ ratio using the solid line in Figure 11.4. A conservative approach is to estimate the $\dfrac{t_e}{t_{90}}$ ratio using the dashed line, which will increase the equivalent times for all the floods in the SRICOS simulations.
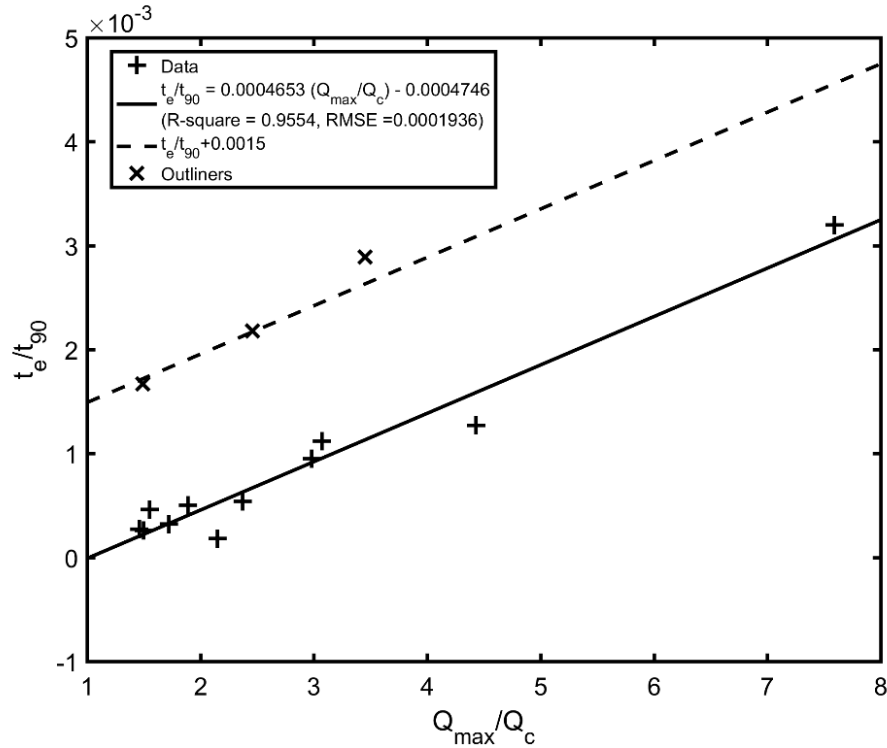
Figure 11.4 Variation of t_e/t_{90} ratio with Q_{max}/Q_c ratio for the maximum annual floods

11.7.2 Generate Future Hydrographs and Compute Scour Histories Using the SRICOS Method

The MATLAB script "SRICOS_FutureHydrograph_Single.m" can be used to generate a single future hydrograph and compute the corresponding scour history using the SRICOS method. Figure 11.5 shows an example for one constructed series of 75 maximum annual floods. The largest flood in Figure 11.5 has a magnitude of 29,970 ft^3/s, which is approximately a 100-year flood. The predicted final scour depth for the entire series of 75 floods is 2.1 ft. The main computation steps are demonstrated in this section.

The MATLAB script first computes the values of the parameters of the Log Pearson Type III (LP-III) distribution using 63 years (water years 1954 to 2016) of recorded annual peak discharges at the Big Sioux River gauging station (06480000). The base 10 logarithm of each of 63 discharge values in Table 11.8 are computed and substituted into Eq. (5.53) to obtain the mean μ_y, standard deviation σ_y, and skew coefficient C_y of $\log Q$:

$$\mu_y = 3.3924, \sigma_y = 0.4957, C_y = -0.2161$$
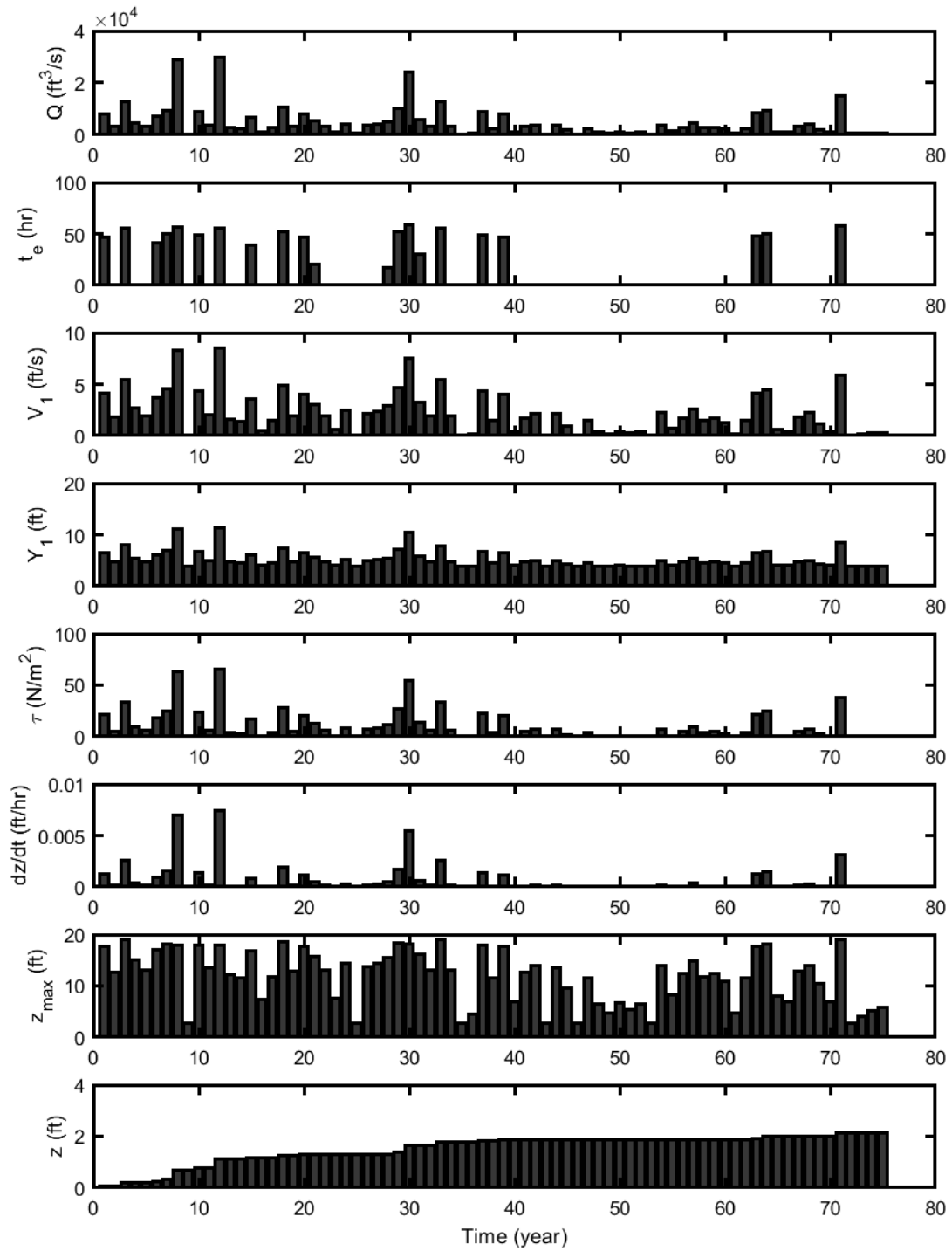
Figure 11.5 SRICOS simulation for a constructed series of 75 maximum annual floods

Table 11.8 Recorded annual peak discharges at USGS streamflow gauging station near Brookings from water years 1954 to 2016

Year	Q_{max} (ft³/s)	Year	Q_{max} (ft³/s)	Year	Q_{max} (ft³/s)
1954	1,970	1975	696	1996	2,990
1955	1,180	1976	1,080	1997	11,000
1956	287	1977	1,750	1998	2,180
1957	5,320	1978	5,960	1999	1,870
1958	382	1979	4,720	2000	683
1959	240	1980	3,820	2001	6,680
1960	9,620	1981	143	2002	2,340
1961	1,340	1982	718	2003	965
1962	10,600	1983	3,300	2004	521
1963	1,880	1984	13,700	2005	1,020
1964	952	1985	8,440	2006	2,790
1965	7,700	1986	6,690	2007	6,520
1966	4,560	1987	2,400	2008	2,780
1967	1,880	1988	950	2009	3,740
1968	230	1989	1,900	2010	19,800
1969	33,900	1990	1,990	2011	15,400
1970	3,350	1991	1,430	2012	2,520
1971	2,100	1992	5,760	2013	3,480
1972	5,060	1993	13,300	2014	1,840
1973	3,010	1994	5,660	2015	1,320
1974	950	1995	6,910	2016	1,020

The MATLAB function *rand* is used to generate a sequence of uniformly distributed random numbers with values between 0 and 1. For example, the largest flood in Figure 11.5 occurs in Year 12 and is given a random number of 0.98995, which corresponds to an exceedance probability of $P_{12} = 1 - 0.98995 = 0.01005$. The standard normal variate z is computed using Eq. (5.57) and the frequency factor K using Eq. (5.56). The computed frequency factor is substituted into Eq. (5.54) to obtain the value of $\log Q$. A drainage area ratio adjustment of 1.025 is then applied to give the discharge at the bridge site. Thus, we have

Eq. (5.57):

$$w = \sqrt{\ln\left(\frac{1}{P^2}\right)} = \sqrt{\ln\left(\frac{1}{0.01005^2}\right)} = 3.0332$$

$$z = w - \frac{2.515517 + 0.802853w + 0.010328w^2}{1 + 1.432788w + 0.189269w^2 + 0.001308w^3}$$

$$= 3.03 - \frac{2.515517 + 0.802853(3.0332) + 0.010328(3.0332)^2}{1 + 1.432788(3.0332) + 0.189269(3.0332)^2 + 0.001308(3.0332)^3}$$

$$= 2.3249$$

Eq. (5.56):

$$K \approx z + (z^2 - 1)\left(\frac{C_y}{6}\right) + \frac{1}{3}(z^3 - 6z)\left(\frac{C_y}{6}\right)^2 - (z^2 - 1)\left(\frac{C_y}{6}\right)^3 + z\left(\frac{C_y}{6}\right)^4 + \frac{1}{3}\left(\frac{C_y}{6}\right)^5$$

$$= 2.3249 - (2.3249^2 - 1)\left(\frac{-0.2161}{6}\right) + \frac{1}{3}(2.3249^3 - 6(2.3249))\left(\frac{-0.2161}{6}\right)^2$$

$$- (2.3249^2 - 1)\left(\frac{-0.2161}{6}\right)^3 + 2.3249\left(\frac{-0.2161}{6}\right)^4 + \frac{1}{3}\left(\frac{-0.2161}{6}\right)^5 = 2.1659$$

Eq. (5.54):

$$y = \mu_y + K \cdot \sigma_y = 3.3924 + (2.1659)(0.4957) = 4.466$$

$$Q_{\text{Brookings}} = \log^{-1}Q = \log^{-1}(4.466) = 29{,}242\,\frac{\text{ft}^3}{\text{s}}$$

$$Q_{\text{Bridge}} = (1.025)(29242) = 29{,}973\,\frac{\text{ft}^3}{\text{s}}$$

The hydraulic results from Section 11.5.2 are used with the pier scour equations in the SRICOS method to compute the initial rate of scour (see Section 11.5.6) and equilibrium scour depth for Q_{Bridge} (see Section 11.5.3). The time to reach 90% of the equilibrium scour depth is then computed using Eq. (5.48) and the equivalent duration of the flood using the regression equation in Figure 11.4. Thus, we have

$$\dot{z}_i = 0.0074 \text{ ft/h}$$

$$z_{\text{max}} = 17.99 \text{ ft}$$

$$t_{90} = \frac{9z_{\text{max}}}{\dot{z}_i} = \frac{9(17.99)}{0.0074} = 21{,}880 \text{ h}$$

$$\frac{t_{e,12}}{t_{90,12}} = 0.0004653\frac{Q_{\text{max},12}}{Q_c} - 0.0004746 = 0.0004653\frac{29973}{4581} - 0.0004746 = 0.0025698$$

$$t_{e,12} = 0.0025698(21880) = 56.2 \text{ h}$$

From Figure 11.5, the pre-existing scour depth before Year 12 is 0.7522 ft. The equivalent time t^* to produce this scour depth by flood 12 is computed using Eq. (5.25).

$$t^* = \frac{z}{\dot{z}_{12}\left(1 - \frac{z}{z_{\text{max},12}}\right)} = \frac{0.7522}{(0.0074)\left(1 - \frac{0.7522}{17.99}\right)} = 106.1 \text{ h}$$

The cumulative scour depth produced by flood 12 and all previous 11 floods is computed using Eq. (5.24):

$$z = \frac{t^* + t_{12}}{\dfrac{1}{\dot{z}_{12}} + \dfrac{t^* + t_{12}}{z_{max,12}}} = \frac{106.1 + 56.2}{\dfrac{1}{0.0074} + \dfrac{106.1 + 56.2}{17.99}} = 1.13 \text{ ft}$$

This scour depth becomes the pre-existing scour depth for the next flood. The above procedure is repeated for all the floods in the annual maximum series to yield the final scour depth of 2.1 ft.

The MATLAB script "SRICOS_FutureHydrograph_Multiple.m" implements this procedure in a FOR loop to generate multiple realizations of the annual maximum series, which are then used with the SRICOS method to compute the distribution of final scour depth and determine the exceedance probability (risk value) associated with different predicted scour depths and project lives. Figure 11.6 shows the cumulative probability of predicted final scour depth for the project lives of 50, 75, and 100 years. Each curve is compiled from 20,000 SRICOS simulations.
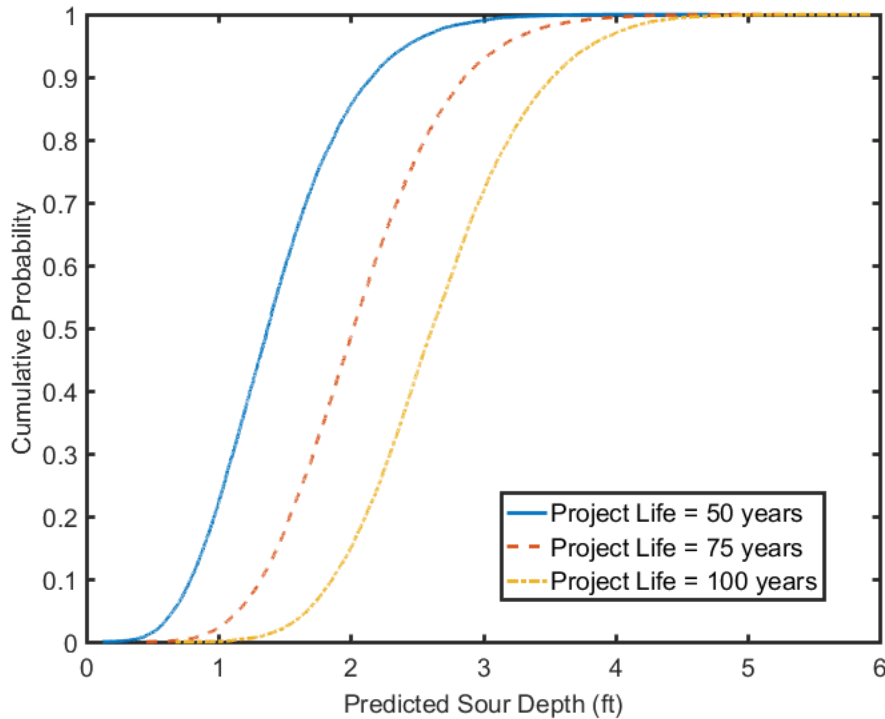
Figure 11.6 Cumulative probability of predicted scour depth for different project lives

Table 11.9 shows selected results from the SRICOS simulations. The probability that a final scour depth of 7 ft will be exceeded in a 75-year project life is less than 1% if the equivalent durations of the maximum annual floods are computed using the regression equation given by the solid line in Figure 11.4, and increases to about 33% if the dashed line is used to estimate the equivalent duration (Table 11.10).

Table 11.9 Exceedance probabilities associated with predicted scour depths and project lives
The equivalent durations of the maximum annual floods are computed using the solid line in Figure 11.4.

Scour Depth (ft)	2	3	4	5	6	7
Exceedance Probability (project life 50 yrs)	14%	1%	<1%	<1%	<1%	<1%
Exceedance Probability (project life 75 yrs)	51%	7%	<1%	<1%	<1%	<1%
Exceedance Probability (project life 100 yrs)	85%	28%	3%	<1%	<1%	<1%

Table 11.10 Exceedance probabilities associated with predicted scour depths and project lives
The equivalent durations of the maximum annual floods are computed using the dashed line in Figure 11.4.

Scour Depth (ft)	6	7	8	9
Exceedance Probability (project life 50 yrs)	10%	<1%	<1%	<1%
Exceedance Probability (project life 75 yrs)	96%	33%	<1%	<1%
Exceedance Probability (project life 100 yrs)	>99.99%	97%	40%	<1%

11.7.3 Flood Frequency Analysis Using PeakFQ

The MATLAB script "ReturnPeriod_FloodMagnitude.m" fits the Log-Pearson Type III distribution to the recorded annual peak flows (Table 11.8) using the Bulletin 17B method to determine the values of the mean, standard deviation, and skew coefficient, which are given in Section 11.7.2 by:

$$\mu_y = 3.3924, \sigma_y = 0.4957, \ C_y = -0.2161$$

The values computed using EMA with historic analysis and regional information are given by (see Appendix III):

$$\mu_y = 3.3866, \sigma_y = 0.4894, \ C_y = -0.3150$$

These values were also used to generate future hydrographs for scour prediction. Table 11.11 shows the results obtained with the equivalent durations of the maximum annual floods computed using the dashed line in Figure 11.4. Compared with Table 11.l0, the exceedance probabilities of the predicted scour depths are slightly lower due to the lower peak flow estimates (see Table 11.3).

Table 11.11 Exceedance probabilities associated with predicted scour depths and project lives

The parameters of the LP-III distribution are computed using EMA with historic analysis and regional information. The equivalent durations of the maximum annual floods are computed using the dashed line in Figure 11.4.

Scour Depth (ft)	6	7	8	9
Exceedance Probability (project life 50 yrs)	6%	<1%	<1%	<1%
Exceedance Probability (project life 75 yrs)	94%	25%	<1%	<1%
Exceedance Probability (project life 100 yrs)	>99.9%	97%	30%	<1%

11.8 Summary

The screening tool and hydrograph generation method are demonstrated using the measured soil erosion function in Figure 6.4 and the soil-erosion-rate-versus-shear-stress curve that separates geo-material regions III and IV in Figure 5.3 to predict pier scour at the SD13 bridge. In the Level I assessment, the SRICOS method is run with the 100-year peak discharge for five days. For the measured EFA curve, the predicted final scour depth is close to the equilibrium depth obtained using the HEC-18 method and a full SRICOS analysis is not recommended. In the second case, the predicted final scour depth is much smaller than the equilibrium scour depth. A Level II assessment was carried out to determine the values of the $\frac{t_e}{t_{90}}$ and $\frac{z_f}{z_{max}}$ ratios for all the maximum annual floods recorded between 1953 and 2016. These results confirm that the predicted scour depths are far from equilibrium conditions. A Level III assessment was conducted to determine the relationship between the dimensionless equivalent times and dimensionless peak discharges for the maximum annual floods. The regression equation was used to assign equivalent times to the individual floods in the constructed hydrographs. The hydrograph generation method employs the Log Pearson Type III distribution. A MATLAB script is provided, which uses the Bulletin 17B method to compute the mean, standard deviation, and skew coefficient of the distribution. Historical and regional flood information can be incorporated by running the USGS PeakFQ, which uses the expected moment algorithm (EMA) recommended in Bulletin 17C for flood frequency analysis. The LP-III distribution was sampled randomly to create a set of 20,000 annual maximum series to predict the distribution of final scour depth using the SRICOS method. The risk values were computed for different scour depths and project lives. It was found that even with very conservative estimates for the equivalent times, the predicted final scour depth can be reduced by 50% for a risk value of <1% in a 75 years project life. The latter is much less than the 53% probability that a 100-year flood would be exceeded at least once in 75 years.

12. WORKED EXAMPLE – CONTRACTION SCOUR

12.1 Site Description

This chapter demonstrates the use of the decision tool and hydrograph generation method for contraction scour outlined in Section 10.3. The site is the James River bridges on SD37 northbound and southbound located about 20 miles north of Mitchell. Each of the parallel bridges has two pier sets with three 3.75-ft diameter cylindrical piers per set and spill-through abutment with two horizontal to one vertical slope embankment. Both the pier sets and abutments are skewed at an angle of 35° parallel to the general direction of the flow. Because all the floodplain flow must pass through the bridge openings, the site has a high potential for contraction scour. A detailed description of the bridge site can be found in Section 7.1 where an aerial photograph of the site is shown in Figure 7.1, the main dimensions and layout of the bridge waterway in Figure 7.2, photographs of the bridge crossings in Figures 7.3 to 7.6, subsurface profile in Figure 7.7, and measured soil erosion functions in Figure 7.8. Details of the hydraulic analysis conducted using 1D and 2D flow models can be found in Rossell and Ting (2013) and Ting et al. (2017). Additional information, including grain size distributions of soil samples collected from the bridge site, can be found in Wagner et al. (2006).

12.2 MATLAB Scripts

Table 12.1 is a list of the MATLAB scripts used in this example. The MATLAB scripts are included as supplementary files to the final report.

Table 12.1 MATLAB scripts used in worked-out example
The section where each file is used is listed with the filename.

Filename	Description
ReturnPeriod_FloodMagnitude (Section 12.5.1)	Fit a Log-Pearson Type III distribution to the measured annual peak flows and compute the flood magnitude for a given return period
SRICOS_ ConstantQ Section 12.5.3	Compute the final scour depth produced by a constant discharge using the energy method
SRICOS_RecordedHydrograph (Section 12.6.1)	Compute the scour history using a recorded hydrograph and determine the equivalent duration
SRICOS_FutureHydrograph_Single (Section 12.7.2)	Generate a single future hydrograph using the Log Pearson Type III distribution and compute the scour history using the energy method
SRICOS_FutureHydrograph_Multiple (Section 12.7.2)	Generate multiple realizations of the future hydrograph and compute the distribution of final scour depth and risk value

12.3 Bridge Parameters

Pier diameter a = 3.75 ft

Pier shape = group of three cylindrical piers

Number of pier sets N = 2

Pier set spacing S = 98.7 ft

12.4 Fluid Parameters

Density of water $\rho = 998.2$ kg/m^3 (1.94 slug/ft^3) @ 20ºC

Kinematic viscosity of water $\nu = 1.004 \times 10^{-6}$ m^2/s (1.081×10^{-5} ft^2/s) @ 20ºC

Acceleration of gravity $g = 9.81$m/s^2 (32.2 ft/s^2)

12.5 Level I Assessment

The Level I assessment includes a basic hydrologic, hydraulic, and scour analysis like the bridge scour evaluation documented in HEC-18. The ratio of the friction velocity V^* in the contracted section to the fall velocity ω of the D_{50} of the bed material being transported from the upstream reach is calculated. If this ratio is much larger than 2, the bed material would be transported mostly as suspended load and the site is evaluated for clear-water scour (Arneson et al., 2012). If live-bed scour occurs, the SRICOS method is not applicable, and the contraction scour depth should be calculated using the procedure for evaluating live-bed scour in HEC-18. For clear-water scour, the flow depth in the contracted section at equilibrium condition can be calculated using Eq. (5.31), which reduces to Eq. (5.32) for non-cohesive soils. The equilibrium scour depth can then be calculated using Eq. (5.35). The critical shear stress and soil erosion rate are either measured by performing an EFA test on soil samples collected from the bridge site, or they can be estimated using Figure 5.3 based on the USCS soil classification. The SRICOS method is then run with the 100-year peak discharge for five days. If the soil type falls into soil category I or II and/or the computed scour depth is close to the equilibrium scour depth, the maximum scour depth may be reached during a single flooding event. If the predicted final scour depth is much smaller than the equilibrium scour depth, the effect of time on scour development may be significant, and this is confirmed by performing the Level II assessment. In the Level III assessment, a full SRICOS analysis is conducted with generation of future hydrographs.

12.5.1 Flood Frequency Analysis

Annual peak discharges from water years 1950 to 2017 at the James River near Forestburg streamflow gauging station (06477000) were used with the Log Pearson Type III distribution to estimate the flood magnitudes for different return periods. The algorithm following the Bulletin 17B method is implemented in the MATLAB script "ReturnPeriod_FloodMagnitude.m." Figure 12.1 shows the relationship between peak discharge and exceedance probability. The data are presented in Table 12.2. Table 12.3 shows the results of flood frequency analysis conducted by the USGS in South Dakota using the expected moments algorithm (EMA) in PeakFQ. Results are presented for EMA runs without historic analysis and regional information, and with historic analysis and regional information. The results obtained without historic analysis and regional information are like the results from the Bulletin 17B method shown in Table 12.2, and they are much more conservative than the results of the EMA run with historic analysis and regional information. The output from the PeakFQ run with historic analysis is included in Appendix IV.
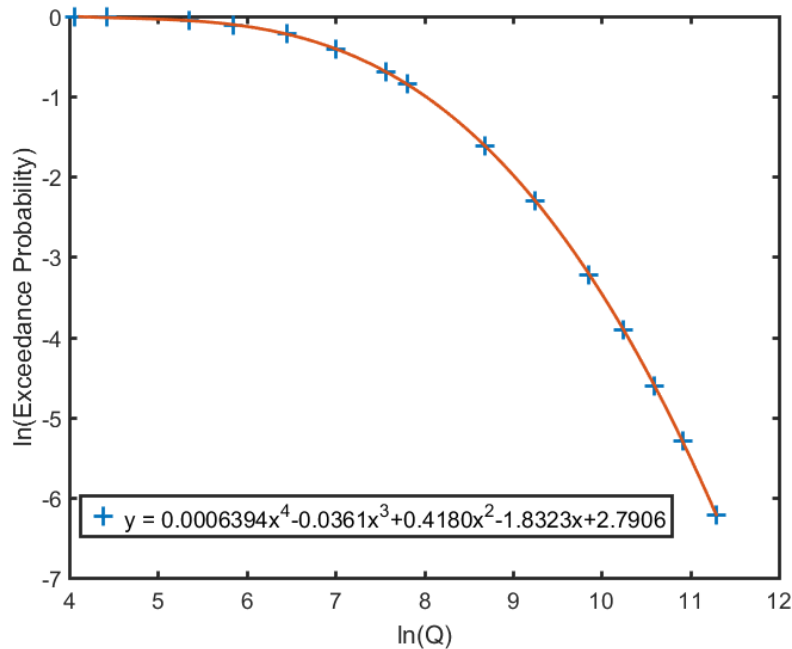
Figure 12.1 Relationship between peak discharge and exceedance probability at James River near Forestburg streamflow gauging station obtained using the Log Pearson Type III distribution

Table 12.2 Peak flow estimates for different return periods at the James River near Forestburg streamflow gauging station
The values are computed by fitting the Log Pearson Type III distribution to the measured annual peak flows from water years 1950 to 2017 following the Bulletin 17B method.

Exceedance Probability	Return Period (Years)	Peak Flow from LP-III (ft³/s)
0.995	1	58
0.5	2	1,948
0.2	5	5,904
0.1	10	10,472
0.04	25	19,188
0.02	50	28,287
0.01	100	40,025
0.005	200	54,901
0.002	500	80,351

12.5.2 Hydraulic Analysis

Figure 12.2 shows the variations of unit discharge and flow depth in the contracted section between the southbound and northbound bridge with the flow discharge computed using the 2D flow model FESWMS. The northbound bridge was built in 1992 and the southbound bridge in 2002. The 2D flow simulations were conducted up to a discharge of 46,500 ft³/s when the highway north of the bridge crossings is overtopped.

Table 12.3 Peak flow estimates at James River near Forestburg streamflow gauging station using the expected moments algorithm

Exceedance Probability	Return Period (Years)	Peak Flow without Historic Analysis and Regional Information (ft³/s)	Peak Flow with Historic Analysis and Regional Information (ft³/s)
0.995	1	56.5	52.5
0.5	2	1,965	1,919
0.2	5	5,990	9,379
0.1	10	10,630	9,886
0.04	25	19,480	16,230
0.02	50	28,710	22,920
0.01	100	40,580	31,070
0.005	200	55,600	40,840
0.002	500	81,230	56,540
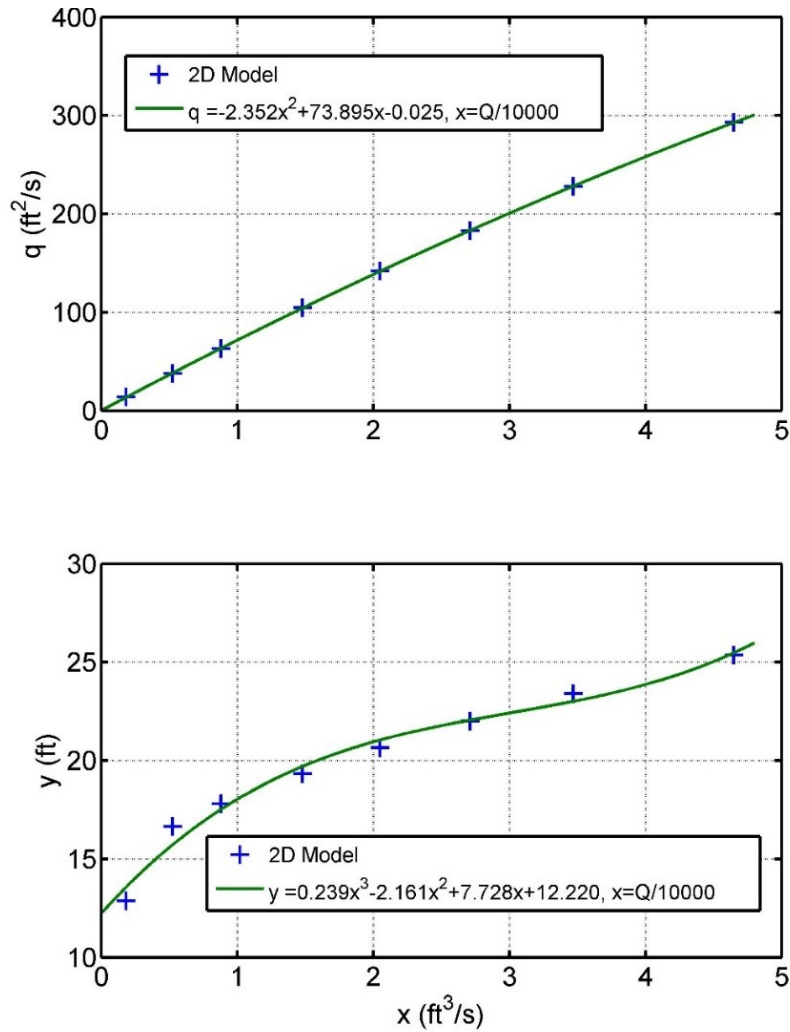
Figure 12.2 Variations of computed unit discharge (top plot) and flow depth (bottom plot) with flow discharge in the contracted section
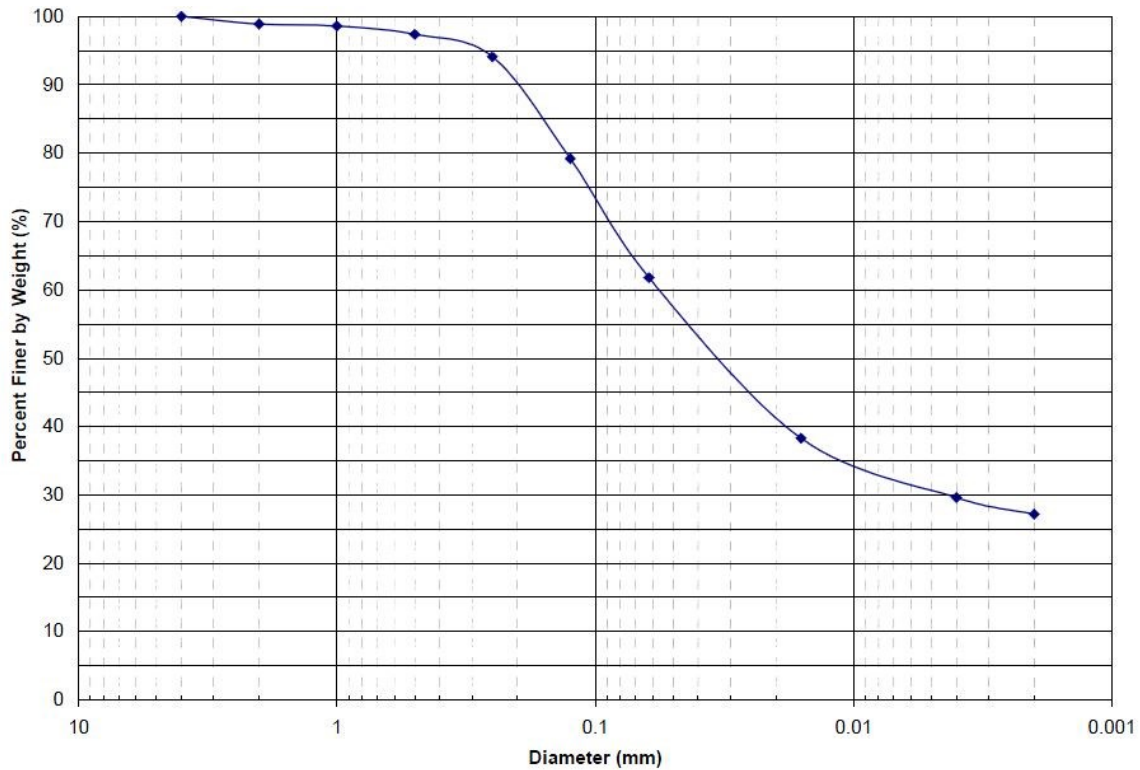
Figure 12.3 Grain size distribution for bed material sample collected in the main channel 150 ft upstream of the northbound bridge (*from Wagner et al., 2006*)

12.5.3 Scour History Analysis

Determine the mode of bed material transport:

Contraction scour calculations were performed for a discharge of 40,025 ft³/s, the 100-year peak flow shown in Table 12.2. This discharge is approximately a 200-year flood for the EMA run with historic analysis and regional information (Table 12.3). The grain size distribution for the soil sample collected in the main channel 150 ft upstream of the northbound bridge is shown in Figure 12.3. The sample consists primarily of a sandy clayey silt and has a D_{50} of about 0.035 mm.

Discharge for 100-year peak flow $Q_{100} = 40,025$ ft³/s   (Table 12.2)

Flow depth $y_i = 23.87$ ft (7.28 m)   (Figure 12.2)

Unit discharge $q = 258.06$ ft²/s (23.98 m²/s)   (Figure 12.2)

Median grain diameter $D_{50} = 0.035$ mm   (Figure 12.3)

Acceleration of gravity $g = 32.2$ ft/s² $\left(9.81 \text{ m/s}^2\right)$

Manning coefficient $n = 0.035$

Initial bed shear stress in the contracted sections:

$$\tau = \frac{\rho g n^2 q^2}{y_i^{\frac{7}{3}}} = \frac{(998.2)(9.81)(0.035)^2(23.98)^2}{(7.28)^{\frac{7}{3}}} = 67.2 \text{ N/m}^2 \quad \text{(Eq. 5.37)}$$

$$V^* = \sqrt{\frac{\tau}{\rho}} = \sqrt{\frac{67.2}{998.2}} = 0.26 \text{ m/s}$$

$$\omega = 0.0015 \text{ m/s (for } D_{50} = 0.035 \text{ mm)}$$

$$\frac{V^*}{\omega} = \frac{0.26}{0.0015} = 173 \gg 2.0 \text{ (clear-water scour)}$$

Compute the equilibrium scour depth:

The thin-walled tube sample of high plasticity clay collected from the bridge foundation depth did not erode for applied bed shear stress up to about 24 N/m² (Figure 7.8, bottom plot). Scour analysis was conducted using the erosion-rate-versus-shear-stress curve given by the solid line separating geo-material regions III (medium erodibility) and IV (low erodibility) in Figure 5.3. We have

Critical shear stress $\tau_c = 9.5$ N/m²   (Table 5.1)

Erosion rate constant $a' = 1.62$ (Table 5.1)

Expansion loss coefficient $C_e = 0.5$

Initial rate of scour:

$$\dot{z}_i = 0.1\left(\frac{\tau}{\tau_c}\right)^{a'} = 0.1\left(\frac{67.2}{9.5}\right)^{1.62} = 2.4\frac{\text{mm}}{\text{h}}\left(0.0078\frac{\text{ft}}{\text{h}}\right) \quad \text{(Eq. 5.2)}$$

Flow depth at equilibrium condition:

$$y_{\text{max}} = \left(\frac{\rho g n^2 q^2}{\tau_c}\right)^{\frac{3}{7}} = \left(\frac{998.2 \times 9.81 \times 0.035^2 \times 23.98^2}{9.5}\right)^{\frac{3}{7}} = 16.8 \text{ m (55.2 ft)} \quad \text{(Eq. 5.31)}$$

Equilibrium scour depth:

$$z_{\text{max}} = y_{\text{max}} + (1 - C_e)\frac{q^2}{2gy_{\text{max}}^2} - \left[y_i + (1 - C_e)\frac{q^2}{2gy_i^2}\right] \quad \text{(Eq. 5.35)}$$

$$= 16.8 + (1 - 0.5)\frac{23.98^2}{2(9.81)(16.8)^2} - \left[7.28 + (1 - 0.5)\frac{23.98^2}{2(9.81)(7.28)^2}\right]$$

$$= 9.3 \text{ m (30.5 ft)}$$

Compute the final scour depth for the 100-year flood for a duration of five days:

Since the scour depth history of contraction scour may not follow the hyperbolic model, the final scour depth should be determined by the direct step method (see Section 5.5). The first two time steps of the recursive scheme is demonstrated below using a time step Δt of 24 h.

Time = 0 to 24 h:

$$\left(\frac{dy_{BR}}{dt}\right)_{t=0} = \frac{(dz/dt)_{t=0}}{\left[1 - \frac{(1-C_e)q^2}{gy_{BR,0}^3}\right]} = \frac{2.4}{[1-(1-0.5)(23.98)^2/((9.81)(7.28)^3]}$$

$$= 2.6 \text{ mm/h } (0.0085 \text{ ft/h})$$

$$y_{BR,24} = y_{BR,0} + \left(\frac{dy_{BR}}{dt}\right)_{t=0} \Delta t = 7.28 + \frac{2.6}{1000}(24) = 7.34 \text{ m } (24.08 \text{ ft})$$

$$z_{t=24} = z_{t=0} + \left(\frac{dz}{dt}\right)_{t=0} \Delta t = 0 + \left(\frac{2.4}{1000}\right)(24) = 0.0576 \text{ m } (0.19 \text{ ft})$$

Time = 24 to 48 h:

$$\tau_{t=24} = \frac{\rho g n^2 q^2}{y_{BR,24}^{\frac{7}{3}}} = \frac{(998.2)(9.81)(0.035)^2(23.98)^2}{(7.34)^{\frac{7}{3}}} = 65.9 \text{ N/m}^2$$

$$\left(\frac{dz}{dt}\right)_{t=24} = 0.1\left(\frac{\tau}{\tau_c}\right)^{a'} = 0.1\left(\frac{65.9}{9.5}\right)^{1.62} = 2.3\frac{\text{mm}}{\text{h}}\left(0.0075\frac{\text{ft}}{\text{h}}\right)$$

$$\left(\frac{dy_{BR}}{dt}\right)_{t=24} = \frac{(dz/dt)_{t=24}}{\left[1 - \frac{(1-C_e)q^2}{gy_{BR,24}^3}\right]} = \frac{2.3}{[1-(1-0.5)(23.98)^2/((9.81)(7.34)^3]}$$

$$= 2.48 \text{ mm/h } (0.0081 \text{ ft/h})$$

$$y_{BR,48} = y_{BR,24} + \left(\frac{dy_{BR}}{dt}\right)_{t=24} \Delta t = 7.34 + \frac{2.48}{1000}(24) = 7.4 \text{ m } (24.28 \text{ ft})$$

$$z_{t=48} = z_{t=24} + \left(\frac{dz}{dt}\right)_{t=24} \Delta t = 0.0576 + \left(\frac{2.3}{1000}\right)(24) = 0.113 \text{ m } (0.37 \text{ ft})$$

The algorithm is implemented in the MATLAB script "SRICOS_ConstantQ.m." The final scour depth after five days computed using a time step of 0.1 h is 0.265 m or 0.87 ft, which is much smaller than the equilibrium scour depth of 9.3 m or 30.5 ft.

To simplify the procedure for hand calculations, the hyperbolic function may be used to estimate the final scour depth in preliminary analysis and the result compared with the equilibrium scour depth to determine whether time rate of scour is an important factor in scour development. We have

$$z = \frac{t}{\dfrac{1}{\dot{z}_i} + \dfrac{t}{z_{max}}} = \frac{120}{\dfrac{1}{\dfrac{2.4}{1000}} + \dfrac{120}{9.3}} = 0.279 \text{ m } (0.92 \text{ ft})$$

As discussed in Sections 7.3 and 10.3, the hyperbolic model over-predicts the final scour depth for soils with high critical shear stress and low erosion rates. Nevertheless, the differences computed for five days are small, and the predicted final scour depth is much smaller than the equilibrium scour depth.

12.6 Level II Assessment

12.6.1 Compute the t_e/t_{90} and z_f/z_{max} Ratios of Maximum Annual Floods

The MATLAB script "SRICOS_RecordedHydrograph.m" was used with the recorded hydrographs to compute the scour histories of the maximum annual floods that can produce scour ($Q_{max} > Q_c$). An example output for the maximum annual flood in 2010 is shown below. The recorded flow history and computed scour history can be seen in the top and bottom plots of Figure 12.4 (see also Table 7.2).

Peak discharge Q_{max}= 19,800 ft^3/s

Critical discharge Q_c = 9,700 ft^3/s

Flow duration above critical discharge t_s = 715.25 h (29.8 days)

Predicted final scour depth z_f = 0.64 ft

Equilibrium scour depth at peak discharge z_{max}= 11.01 ft

Initial rate of scour at peak discharge $\dot{z}_i = 0.001663$ ft/s

Equivalent time $t_e = 411$ h

Time to reach 90% of equilibrium scour depth $t_{90} = 14{,}429$ h (601.2 days)

The corresponding values of the $\frac{Q_{max}}{Q_c}$, $\frac{t_e}{t_{90}}$ and $\frac{z_f}{z_{max}}$ ratios are 2.04, 0.02847, and 0.058, respectively. Table 12.4 summarizes the results for all the maximum annual floods that can produce scour. The computed $\frac{z_f}{z_{max}}$ and $\frac{t_e}{t_{90}}$ ratios are plotted in Figure 12.5. All the computed values are close to zero, which means that the scour depths produced by the recorded floods are far from equilibrium condition. Therefore, the time rate of scour is an important factor in determining the final scour depth.
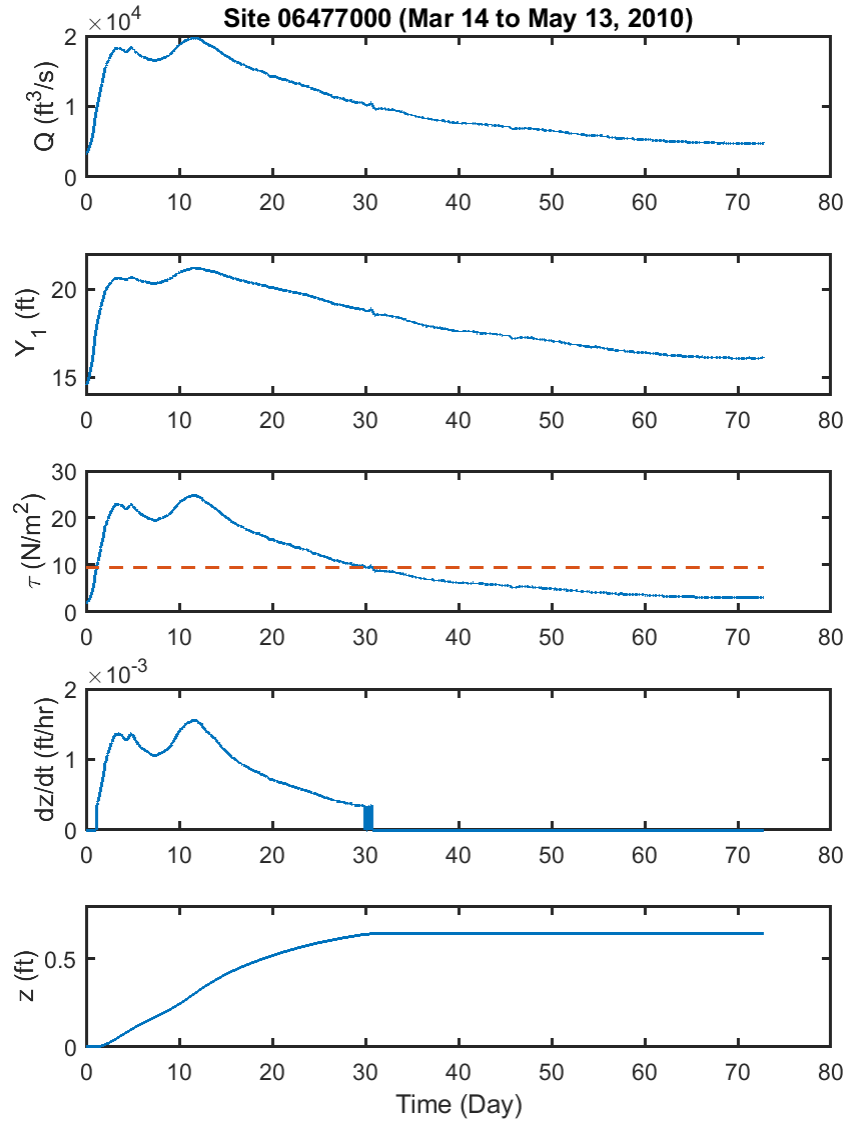
Figure 12.4 Computed history of contraction scour for the maximum annual flood in 2010. *The red dashed line represents the critical shear stress*

Table 12.4 Computed t_e/t_{90} and z_f/z_{max} ratios for the maximum annual floods that can produce scour *(see also Table 7.2)*

Year	$\dfrac{Q_{max}}{Q_c}$	Return Period (year)	$\dfrac{z_f}{z_{max}}$	$\dfrac{t_e}{t_{90}}$	$\dfrac{t_e}{t_{90}}^*$
2011	2.93	50.3	0.056	0.01614	0.00694
1997	2.64	41.4	0.057	0.01926	0.00694
2007	2.20	29.8	0.012	0.00507	0.00137
2010	2.04	26.3	0.058	0.02847	0.00689
2001	1.79	21.3	0.025	0.01393	0.00281
1995	1.42	14.8	0.022	0.01710	0.00254
1969	1.29	12.8	0.025	0.02345	0.00333
1962	1.24	12.1	0.004	0.00346	0.00302
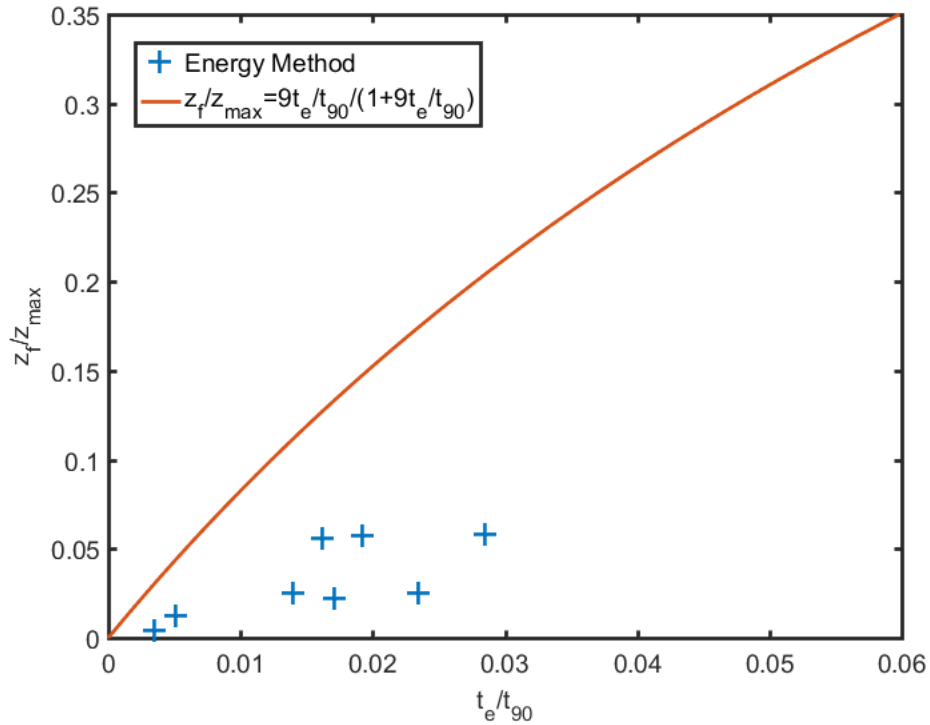
Figure 12.5 Variation of z_f/z_{max} ratio with t_e/t_{90} ratio for the maximum annual floods shown in Table 12.4

12.7 Level III Assessment

12.7.1 Relate t_e/t_{90} Ratio to Q_{max}/Q_c Ratio

The computed $\frac{t_e}{t_{90}}$ ratio is plotted against the $\frac{Q_{max}}{Q_c}$ ratio in Figure 12.6. There is essentially no correlation between the two parameters. In Chapter 7, a $\frac{t_e}{t_{90}}$ ratio of 0.03 was used as an upper bound to compute the equivalent time for scour prediction using the SRICOS method. This approach requires the t_{90} value to be calculated by a direct step method for every discharge value, which is computationally intensive when many annual maximum series must be generated for scour risk analysis. A simpler method is to normalize the equivalent time by the t_{90} value from the hyperbolic model (denoted by $t_{90}{}^*$), which is also a measure of the time required to reach equilibrium condition. For the maximum annual flood in 2010, we have

$$t_{90}{}^* = \frac{9z_{max}}{\dot{z}_i} = \frac{9(11.01)}{0.001663} = 59{,}585 \text{ h}$$

$$\frac{t_e}{t_{90}{}^*} = \frac{411}{59{,}585} = 0.0069$$

The results are included in the last column in Table 12.4 and plotted against $\frac{Q_{max}}{Q_c}$ ratio in Figure 12.7.

178

There is a stronger correlation between $\frac{t_e}{t_{90}^*}$ and $\frac{Q_{max}}{Q_c}$ compared with $\frac{t_e}{t_{90}}$ and $\frac{Q_{max}}{Q_c}$. The regression equation given by the dashed line in Figure 12.7 was used to compute the equivalent time in the SRICOS simulations.
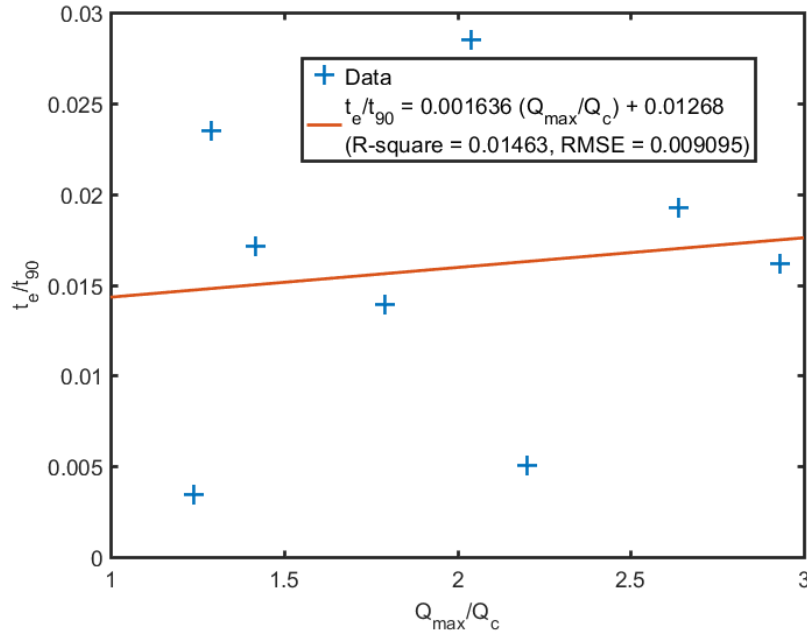
Figure 12.6 Variation of t_e/t_{90} ratio with Q_{max}/Q_c ratio for the maximum annual floods in Table 12.4
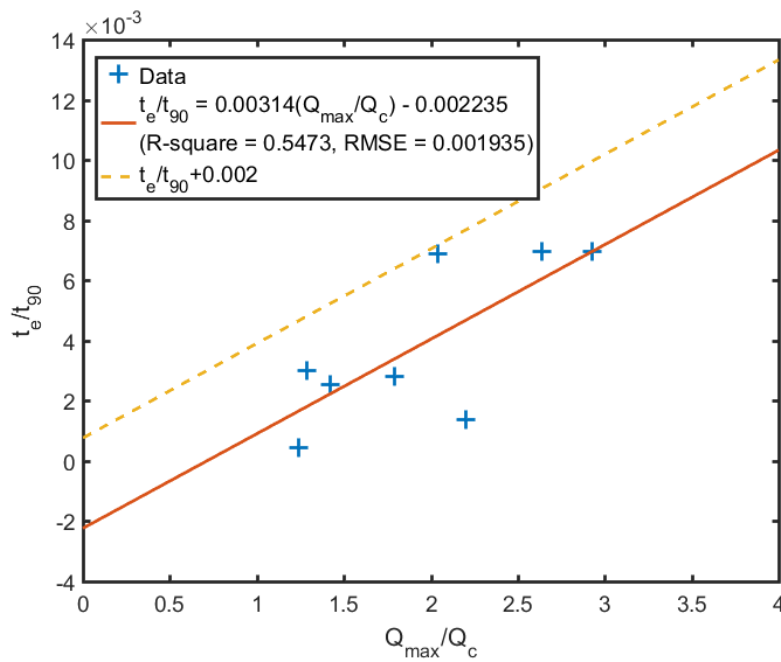
Figure 12.7 Variation of t_e/t_{90} ratio with Q_{max}/Q_c ratio for the maximum annual floods in Table 12.4 with t_{90} computed using the hyperbolic model

12.7.2 Generate Future Hydrographs and Compute Scour Histories using the SRICOS Method

The MATLAB script "SRICOS_FutureHydrograph_Single.m" can be used to generate a single future hydrograph for computing the scour history using the SRICOS method. Figure 12.8 shows an example for one constructed series of 75 maximum annual floods. The largest flood in Figure 12.8 has a magnitude of 39,931 ft³/s, which is approximately a 100-year flood. The predicted final scour depth for the entire series of 75 floods is 5.6 ft.

The hydrograph generation method follows the same procedure as in pier scour. The MATLAB script first computes the values of the parameters of the Log Pearson Type III (LP-III) distribution using 68 years (water years 1950 to 2017) of recorded annual peak flows at the James River near Forestburg gauging station (06477000). The base 10 logarithm of each of the peak flow values in Table 12.5 is computed and the results are substituted into Eq. (5.53) to calculate the mean μ_y, standard deviation σ_y, and skew coefficient C_y of $\log Q$.

$$\mu_y = 3.2841, \sigma_y = 0.5770, C_y = -0.0574$$

Table 12.5 Recorded annual peak flows at James River near Forestburg streamflow gauging station from water years 1950 to 2017

Year	Q_{max} (ft³/s)	Year	Q_{max} (ft³/s)	Year	Q_{max} (ft³/s)
1950	5,180	1973	2,770	1996	3,790
1951	1,600	1974	280	1997	25,600
1952	6,290	1975	1,040	1998	4,530
1953	2,080	1976	308	1999	5,060
1954	332	1977	4,050	2000	911
1955	1,210	1978	4,830	2001	17,400
1956	920	1979	1,920	2002	428
1957	864	1980	336	2003	751
1958	924	1981	63	2004	931
1959	80	1982	1,050	2005	1,920
1960	10,900	1983	925	2006	2,010
1961	702	1984	6,140	2007	21,300
1962	12,000	1985	3,330	2008	965
1963	599	1986	7,740	2009	9,400
1964	561	1987	4,530	2010	19,800
1965	1,010	1988	415	2011	28,400
1966	2,800	1989	3,080	2012	1,790
1967	1,910	1990	260	2013	3,260
1968	372	1991	2,520	2014	1,520
1969	12,500	1992	743	2015	1,720
1970	1,320	1993	3,450	2016	968
1971	980	1994	8,180	2017	1,320
1972	2,990	1995	13,000		
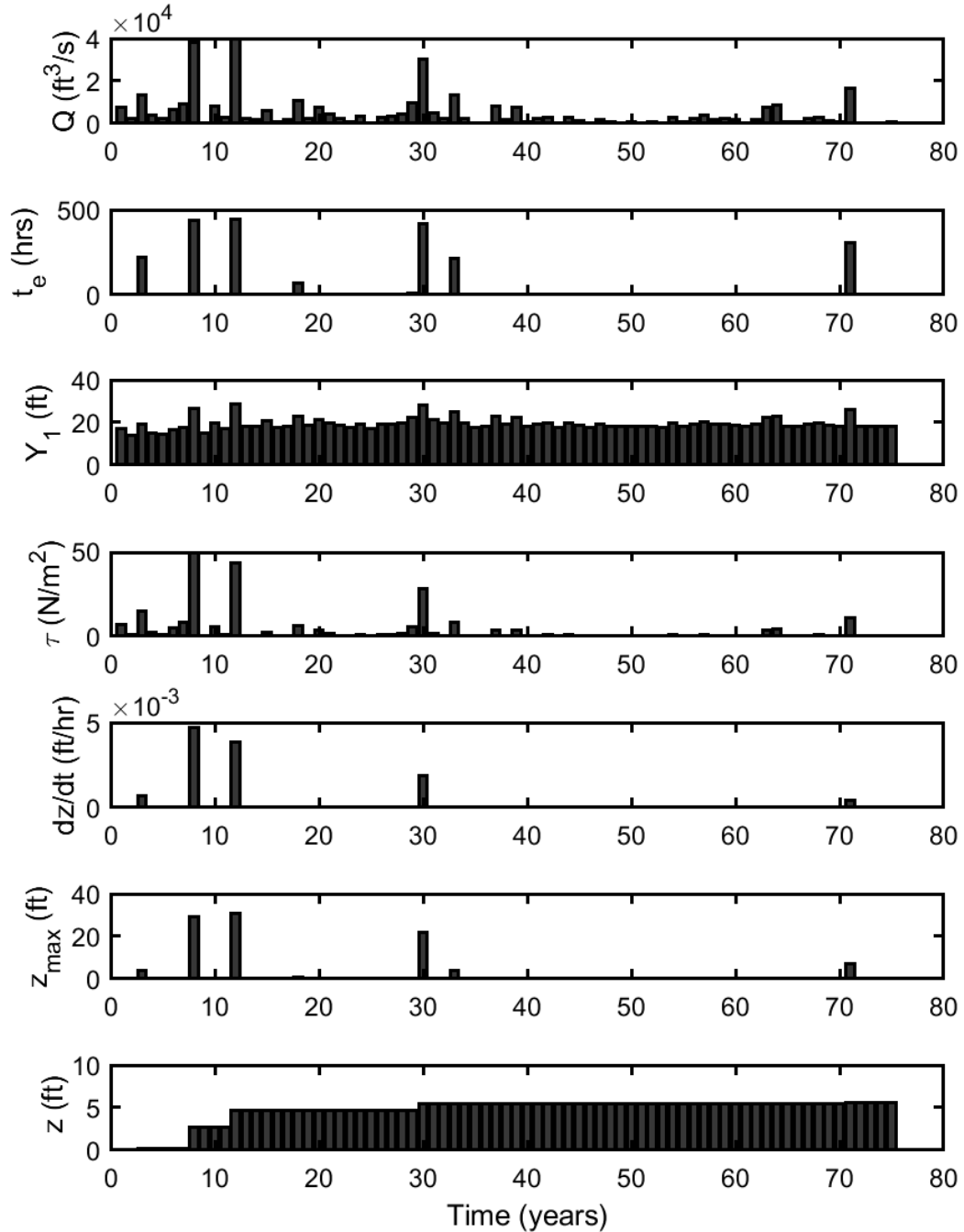
Figure 12.8 SRICOS simulation for a constructed series of 75 maximum annual floods

The MATLAB function *rand* is used to generate a sequence of uniformly distributed random numbers with values between 0 and 1. Example of an annual maximum series is shown in the top plot of Figure 12.8. The largest flood in Figure 12.8 occurs in Year 12 and is given a random number of 0.99, which corresponds to an exceedance probability of $P_{12} = 1 - 0.99 = 0.01$. The standard normal variate z is computed using Eq. (5.57) and the frequency factor K using Eq. (5.56). The computed frequency factor is substituted into Eq. (5.54) to obtain the value of $\log Q$. Thus, we have:

$$w = \sqrt{\ln\left(\frac{1}{P^2}\right)} = \sqrt{\ln\left(\frac{1}{0.01^2}\right)} = 3.0349$$

$$z = w - \frac{2.515517 + 0.802853w + 0.010328w^2}{1 + 1.432788w + 0.189269w^2 + 0.001308w^3}$$

$$= 3.0349 - \frac{2.515517 + 0.802853(3.0349) + 0.010328(3.0349)^2}{1 + 1.432788(3.0349) + 0.189269(3.0349)^2 + 0.001308(3.0349)^3}$$

$$= 2.3268$$

$$K \approx z + (z^2 - 1)\left(\frac{C_y}{6}\right) + \frac{1}{3}(z^3 - 6z)\left(\frac{C_y}{6}\right)^2 - (z^2 - 1)\left(\frac{C_y}{6}\right)^3 + z\left(\frac{C_y}{6}\right)^4 + \frac{1}{3}\left(\frac{C_y}{6}\right)^5$$

$$= 2.3268 - (2.3268^2 - 1)\left(\frac{-0.0574}{6}\right) + \frac{1}{3}(2.3268^3 - 6(2.3268))\left(\frac{-0.0574}{6}\right)^2$$

$$- (2.3268^2 - 1)\left(\frac{-0.0574}{6}\right)^3 + 2.3268\left(\frac{-0.0574}{6}\right)^4 + \frac{1}{3}\left(\frac{-0.0574}{6}\right)^5 = 2.2845$$

$$y = \mu_y + K \cdot \sigma_y = 3.2841 + (2.2814)(0.5770) = 4.60046$$

$$Q = \log^{-1}y = \log^{-1}(4.60046) = 39{,}853\frac{\text{ft}^3}{\text{s}}$$

The computed Q value is used with the regression equations in Figure 12.2 to calculate the flow depth and unit discharge in the contracted section (see below).

$$x = \frac{Q}{10000} = \frac{39853}{10000} = 3.9853$$

$$q = -2.352x^2 + 73.895x - 0.025 = -2.352(3.9853)^2 + 73.895(3.9853) - 0.025$$

$$= 257.11 \text{ ft}^2/\text{s} \ (23.89 \text{ m}^2/\text{s})$$

$$y_i = 0.239x^3 - 2.161x^2 + 7.728x + 12.220$$

$$= 0.239(3.9853)^3 - 2.161(3.9853)^2 + 7.728(3.9853) + 12.220$$

$$= 23.82 \text{ ft} \ (7.26 \text{ m})$$

The flow depth of 23.82 ft is the flow depth without pre-existing scour. This flow depth is used to compute the initial rate of scour and equilibrium scour depth for the discharge of 39,853 ft³/s, and the time to reach 90% of the equilibrium scour depth t_{90} and equivalent time t_e. We have

$$\tau = \frac{\rho g n^2 q^2}{y_i^{\frac{7}{3}}} = \frac{(998.2)(9.81)(0.035)^2(23.89)^2}{(7.26)^{\frac{7}{3}}} = 67.08 \text{ N/m}^2$$

$$\dot{z}_i = 0.1\left(\frac{\tau}{\tau_c}\right)^{a'} = 0.1\left(\frac{67.08}{9.5}\right)^{1.62} = 2.37\frac{\text{mm}}{\text{h}}\left(0.0078\frac{\text{ft}}{\text{h}}\right)$$

$$y_{max} = \left(\frac{\rho g n^2 q^2}{\tau_c}\right)^{\frac{3}{7}} = \left(\frac{998.2 \times 9.81 \times 0.035^2 \times 23.89^2}{9.5}\right)^{\frac{3}{7}} = 16.78 \text{ m (55.0 ft)}$$

$$z_{max} = y_{max} + (1 - C_e)\frac{q^2}{2gy_{max}^2} - \left[y_i + (1 - C_e)\frac{q^2}{2gy_i^2}\right]$$

$$= 16.78 + (1 - 0.5)\frac{23.89^2}{2(9.81)(16.78)^2} - \left[7.26 + (1 - 0.5)\frac{23.89^2}{2(9.81)(7.26)^2}\right]$$

$$= 9.3 \text{ m (30.5 ft)}$$

$$t_{90} = \frac{9z_{max}}{\dot{z}_i} = \frac{9(30.5)}{0.0078} = 35,192 \text{h}$$

$$\frac{t_{e,12}}{t_{90,12}} = \left(0.00314\frac{Q_{max,12}}{Q_c} - 0.002235\right) + 0.002 = \left(0.00314\frac{39853}{9700} - 0.002235\right) + 0.002$$

$$= 0.01267$$

$$t_{e,12} = 0.01267(35192) = 446 \text{ h}$$

The maximum annual flood in Year 12 is represented by an equivalent flood with a constant discharge of $39,853\frac{\text{ft}^3}{\text{s}}$ and a duration of 446 h. From Figure 12.8, the pre-existing scour depth before Year 12 is 2.64 ft. The flow depth at the beginning of Year 12 is obtained by solving Eq. (5.40) where $y_{BR,WI}$ is the flow depth without the pre-existing scour depth. The flow depth with pre-existing scour depth y_{BR} is approximated by $y_{BR,WI} + z$, where z is the pre-existing scour depth, and substituted into the right-hand side of Eq. (5.40) to revise y_{BR} once. Thus, we have

$$y_{BR} \approx y_{BR,WI} + z = 23.82 + 2.64 = 26.46 \text{ ft}$$

$$y_{BR} = y_{BR,WI} + z + (1 - C_e)\frac{q^2}{2g}\left(\frac{1}{y_{BR,WI}^2} - \frac{1}{y_{BR}^2}\right)$$

$$= 23.82 + 2.64 + (1 - 0.5)\frac{(257.11)^2}{2(32.2)}\left(\frac{1}{23.82^2} - \frac{1}{26.46^2}\right) = 26.63 \text{ ft}$$

The flow depth of 26.63 ft is the flow depth at the beginning of Year 12. This flow depth and the unit discharge of 257.11 ft²/s are used to compute the scour depth at the end of the time step following the procedure demonstrated in Section 12.5.3. The new scour depth after the flood is 4.62 ft. This procedure is repeated for all the floods in the annual maximum series to yield the final scour depth of 5.6 ft.

The MATLAB script "SRICOS_FutureHydrograph_Multiple.m" implements a FOR loop to generate multiple realizations of the annual maximum series, which are used with the procedure described above to compute the distribution of final scour depth and exceedance probability (risk value) associated with different predicted scour depths and project lives. Figure 12.9 shows the cumulative probability of predicted final scour depth for the project lives of 50, 75, and 100 years. Each curve is the results of 20,000 SRICOS simulations with the equivalent duration of each flood computed using the solid line in Figure 12.7.
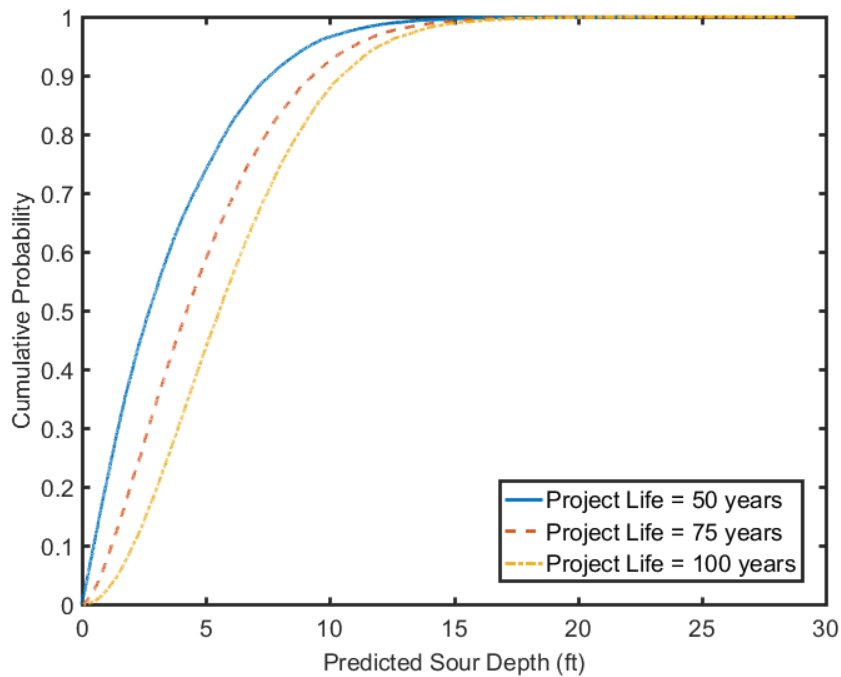
Figure 12.9 Cumulative probability of predicted scour depth for different project lives
The equivalent time is computed using the solid line in Figure 12.7.

Tables 12.6 and 12.7 show the exceedance probabilities for different predicted scour depths and project lives. For example, the probability that a final scour depth of 10 ft will be exceeded in a 75-year project life is about 7% if the equivalent durations of the maximum annual floods are computed using the regression equation given by solid line in Figure 12.7 and increases slightly to around 9% for the dashed line.

Table 12.6 Exceedance probabilities associated with predicted scour depths and project lives
The equivalent durations of the floods are computed using the regression equation represented by the solid line in Figure 12.7.

Scour Depth (ft)	4	6	8	10	12	14
Exceedance Probability (project life 50 yrs)	35%	18%	8%	3%	1%	<1%
Exceedance Probability (project life 75 yrs)	53%	32%	16%	7%	3%	1%
Exceedance Probability (project life 100 yrs)	68%	45%	25%	12%	5%	2%

Table 12.7 Exceedance probabilities associated with predicted scour depths and project lives
The equivalent durations of the floods are computed using the regression equation represented by the dashed line in Figure 12.7.

Scour Depth (ft)	4	6	8	10	12	14
Exceedance Probability (project life 50 yrs)	41%	23%	11%	5%	2%	<1%
Exceedance Probability (project life 75 yrs)	62%	39%	21%	9%	4%	2%
Exceedance Probability (project life 100 yrs)	78%	54%	33%	16%	7%	3%

12.7.3 Flood Frequency Analysis Using PeakFQ

The MATLAB script "ReturnPeriod_FloodMagnitude.m" fits the Log-Pearson Type III distribution to the recorded annual peak flows (Table 12.5) using the Bulletin 17B method to determine the values of the mean, standard deviation, and skew coefficient, which are given in Section 12.7.2 by:

$$\mu_y = 3.2841, \sigma_y = 0.5770, C_y = -0.0574$$

The parameter values obtained from the EMA run with historic analysis and regional information are given by (see Appendix IV):

$$\mu_y = 3.2648, \sigma_y = 0.5612, C_y = -0.1890$$

These estimates were also used to generate future hydrographs for scour prediction. Table 12.8 shows the results obtained with the equivalent durations of the maximum annual floods computed using the dashed line in Figure 12.7. Compared with Table 12.7, the exceedance probabilities of the predicted scour depths are considerably smaller due to the much lower annual peak flow estimates (see Table 12.3).

Table 12.8 Exceedance probabilities associated with predicted scour depths and project lives
The equivalent durations of the maximum annual floods are computed using the dashed line in Figure 12.7.

Scour Depth (ft)	4	6	8	10	12	14
Exceedance Probability (project life 50 yrs)	23%	9%	3%	1%	<1%	<1%
Exceedance Probability (project life 75 yrs)	38%	18%	6%	2%	<1%	<1%
Exceedance Probability (project life 100 yrs)	54%	28%	12%	4%	1%	<1%

12.8 Summary

The screening tool and hydrograph generation method are demonstrated for clear-water contraction scour at the SD37 bridges over the James River near Mitchell using the soil-erosion-rate-versus-shear-stress curve that separates geo-material regions III and IV in Figure 5.3. In the Level I assessment, the SRICOS method was run with the 100-year peak flow for five days. The predicted final scour depth is much smaller than the equilibrium scour depth. A Level II assessment was carried out to determine the

values of the $\frac{t_e}{t_{90}}$ and $\frac{z_f}{z_{max}}$ ratios for all the maximum annual floods recorded between 1950 and 2017 that can produce scour. These results confirm that all the predicted scour depths are far from equilibrium condition. A Level III assessment was conducted to determine the relationship between the dimensionless equivalent times of the maximum annual floods and the dimensionless peak discharges. The regression equations were used to assign flood durations to annual peak flows of different return periods. A faster algorithm was developed by normalizing the equivalent times of the maximum annual floods by the t_{90} computed using the hyperbolic model. The Log Pearson Type III distribution was sampled randomly to create 20,000 annual maximum series to predict the distribution of final scour depth using the energy method. The risk values were computed for different scour depths and project lives. Future hydrographs were generated with the parameters of the LP-III distribution estimated using both the Bulletin 17B method and the EMA run with historic analysis and regional information. Even with the more conservative flood estimates from the Bulletin 17B method, the predicted final scour depth can be reduced by more than 50% and still maintains a risk value of less than 5% in a 75 years project life.

13. WORKED EXAMPLE – UNGAUGED STREAMS

13.1 Site Description

This chapter demonstrates the application of the SRICOS method at ungauged streams. The site is the Interstate 90 bridges over the Split Rock Creek near Brandon. The parallel bridges have 3-ft diameter cylindrical pier sets supported on spread footings with spill-through abutments. Both the pier sets and abutments are skewed at an angle of 30° parallel to the general direction of the flow. A detailed description of the bridge site can be found in Section 8.1 where an aerial photograph of the site is shown in Figure 8.1, the results of flood frequency analysis in Table 8.1, and the results of hydraulic analysis in Figures 8.2 and 8.3.

The Split Rock Creek at Corson streamflow gauging station (06482610) is located less than one mile upstream from the bridge site. This station has been operated from October 1, 1965, to September 29, 1989, and from October 1, 2001, to the present as a continuous-record streamflow gauging station. The station was operated from 1990 to 2001 as a crest-stage partial-record gauging station. In Chapter 8, the QPPQ method was used with the recorded daily mean flow from the Skunk Creek streamflow gauging station at Sioux Falls to estimate the missing flow record at Split Rock Creek. The estimated daily mean flows were disaggregated to hourly values using the method by Straub and Over (2010). The QPPQ method is applicable only when the flow histories at the base and extension gages are highly correlated. The interpolated hourly mean flows at Split Rock Creek were found to be greatly under-estimated for some floods (Table 8.4).

Implementation of the SRICOS method at an ungauged site differs from a gauged site primarily in the Level II assessment, which requires the equivalent times to be determined for floods of different return periods from historical flow records. For ungauged sites, the hydrographs of the historical floods will have to be estimated. Historical floods are modeled using the NRCS unit triangular hydrograph in this example.

13.2 MATLAB Scripts

Table 13.1 is a list of the MATLAB scripts used in this example. The MATLAB scripts are included as supplementary files to the final report.

Table 13.1 MATLAB scripts used in example
The section where each file is used is listed with the filename.

Filename	Description
ReturnPeriod_FloodMagnitude (Section 13.3)	Fit a Log-Pearson Type III distribution to the measured annual peak flows and compute the flood magnitude for a given return period using the Bulletin 17B method
SRICOS_NRCS_Triangular_Hydrograph (Section 13.5)	Compute the scour history using the NRCS unit triangular hydrograph and determine the equivalent duration
SRICOS_FutureHydrograph_Multiple (Section 13.5)	Generate multiple realizations of the future hydrograph and compute the distribution of final scour depth and risk value

13.3 Flood Frequency Analysis

Table 13.2 shows the recorded annual peak flows at the Split Rock Creek at Corson streamflow gauging station (06482610) from water years 1966 to 2017. The flow data were used with the Log Pearson Type III distribution to estimate the peak discharges for floods of different return periods. The

algorithm is implemented in the MATLAB script "ReturnPeriod_FloodMagnitude.m." The results are plotted in Figure 13.1 and summarized in Table 13.3.

Table 13.2 Recorded annual peak flows at Split Rock Creek streamflow gauging station at Corson from water years 1966 to 2017

Year	Q_{max} (ft^3/s)	Year	Q_{max} (ft^3/s)	Year	Q_{max} (ft^3/s)
1966	550	1984	9,020	2002	1,320
1967	925	1985	4,100	2003	1,130
1968	1,850	1986	7,920	2004	3,400
1969	17,800	1987	1.840	2005	1,180
1970	2,500	1988	491	2006	8,020
1971	1,300	1989	1,200	2007	4,050
1972	1,900	1990	1,150	2008	1,710
1973	840	1991	500	2009	400
1974	5,240	1992	4,800	2010	13,100
1975	446	1993	18,900	2011	4,730
1976	900	1994	4,700	2012	4,730
1977	2,470	1995	5,820	2013	1,340
1978	3,250	1996	956	2014	13,100
1979	10,500	1997	8,290	2015	2,510
1980	2,230	1998	No Data	2016	1,480
1981	1,110	1999	No Data	2017	946
1982	3,090	2000	No Data		
1983	4,500	2001	No Data		
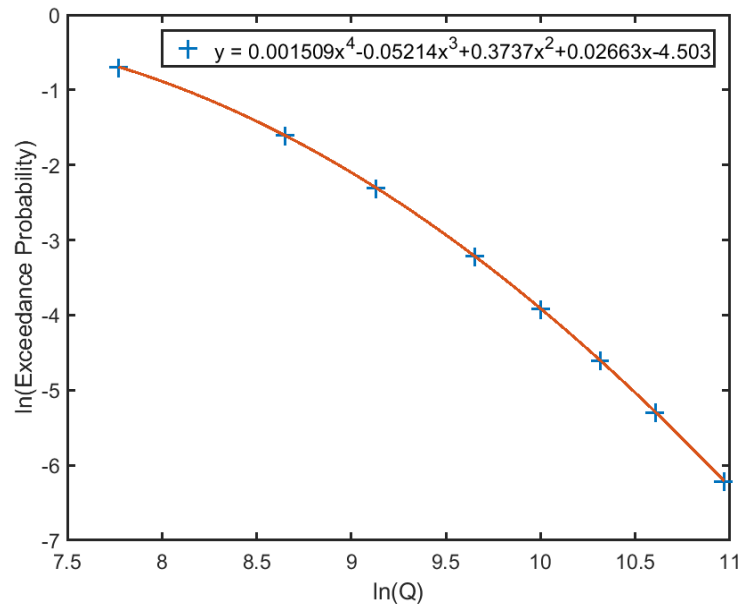
Figure 13.1 Relationship between peak discharge and exceedance probability at Split Rock Creek near Corson streamflow gauging station for the Log Pearson Type III distribution

Table 13.3 Peak flow estimates for different return periods at Split Rock Creek near Corson streamflow gauging station

The values are computed by fitting the Log Pearson Type III distribution to the measured annual peak flows from water years 1966 to 2017 following the Bulletin 17B method.

Exceedance Probability	Return Period (Years)	Peak Flow from LP-III (ft³/s)
0.5	2	2,373
0.2	5	5,721
0.1	10	9,230
0.04	25	15,581
0.02	50	22,017
0.01	100	30,203
0.005	200	40,509
0.002	500	58,138

Table 13.4 shows the results of flood frequency analysis conducted by the USGS in South Dakota using the expected moments algorithm (EMA) in PeakFQ. Results are presented for EMA runs conducted without historic analysis, and with and without regional information. The results from the Bulletin 17B method shown in Table 13.3 are more conservative than the results of the EMA runs. The output from PeakFQ is included in Appendix V.

Table 13.4 Peak flow estimates at Split Rock Creek near Corson streamflow gauging station using the expected moments algorithm conducted without historic analysis

Exceedance Probability	Return Period (Years)	Peak Flow without Regional Information (ft³/s)	Peak Flow with Regional Information (ft³/s)
0.5	2	2,373	2,429
0.2	5	5,722	5,778
0.1	10	9,153	9,055
0.04	25	15,220	14,580
0.02	50	21,220	19,800
0.01	100	28,700	26,050
0.005	200	37,910	33,460
0.002	500	53,290	45,270

13.4 Hydraulic Analysis

Figure 13.2 shows the variations of computed maximum flow velocity and the corresponding flow depth with discharge in the approach flow just upstream from the westbound bridge (see also Figures 8.2 and 8.3). This information is used with the NRCS unit triangular hydrograph to compute the equivalent times for floods of different return periods.

13.5 NRCS Unit Triangular Hydrograph

The NRCS unit triangular hydrograph (Figure 10.4) is defined by the peak discharge Q_p, time to peak T_p, and recess time T_r, where T_p and T_r are related to the time of concentration T_c by:

$$T_p = 0.67 T_c, \qquad T_r = 1.67 T_p \qquad\qquad (13.1)$$

The time of concentration is the time required for a water particle to flow from the hydraulically most distant point of the watershed to the point in question. It consists of travel time under sheet flow, shallow concentrated flow, and channel flow. The time of concentration is a function of rainfall distribution and drainage basin characteristics. Many empirical formulae have been proposed for estimating the value of T_c for small watersheds (e.g., Bedient and Huber, 1992).

For ungauged streams, the peak discharge Q_{max} may be estimated using regional regression equations (Sando, 1998). For South Dakota, this information has been incorporated into the USGS StreamStats tool (https://streamstats.usgs.gov). Measured annual peak discharges at the Interstate 90 bridges are available from the streamflow gauging station at Corson from water year 1966 so the recorded annual peak flows are used in this example instead. StreamStats can delineate the drainage basin (Figure 13.3) and compute various basin characteristics. Table 13.5 shows the output from StreamStats. The length of the longest flow path at the bridge site is about 100 miles and the mean slope along the main channel is 4.29 ft per mile. These values may be used in conjunction with other information (e.g., NRCS curve number) to estimate the time of concentration. Assuming a major portion of the flow path is channel flow (see Figure 13.3), the time of concentration may be calculated as:

$$T_c(h) = \frac{L}{3600V} \qquad\qquad (13.2)$$

where L is flow length in ft and V is channel velocity in ft/s. Taking V as the bank full velocity with a range of 3 to 5 ft/s from the output of HEC-RAS analysis, we get:

$$T_c = \frac{(100 \text{ miles})(5280 \text{ ft/mile})}{(3600 \text{ s/h})(3 \text{ to } 5 \text{ ft/s})} \approx 30 \text{ to } 50 \text{ h}$$

$$T_p = 0.67(30 \text{ to } 50 \text{ h}) \approx 20 \text{ to } 33 \text{ h}$$

$$T_r = 1.67(20 \text{ to } 33 \text{ h}) \approx 33 \text{ to } 55 \text{ h}$$

Table 13.6 shows the values of T_p determined from the recorded hydrographs for the maximum annual floods in Table 8.5 that have only one dominant peak. An example of the recorded hydrograph can be found in Figure 8.10. The values of T_p range from 12 to 26 hours (about 1/2 day to 1 day). Note that small floods may not affect the entire drainage basin, whereas the range of values obtained using Eq. (13.2) are based on the longest flow path and thus are more representative of large floods.

Table 13.7 shows the values of T_p that would produce the same final scour depths in Table 13.6 if the measured peak discharges are used with the NRCS triangular hydrograph and the erosion-rate-versus-shear-stress curve that separates soil erosions III and IV in Figure 5.3 to predict the scour history using the SRICOS method. The range of T_p values is about one to two days, which are between one to two times greater than the values obtained using the recorded hydrographs.
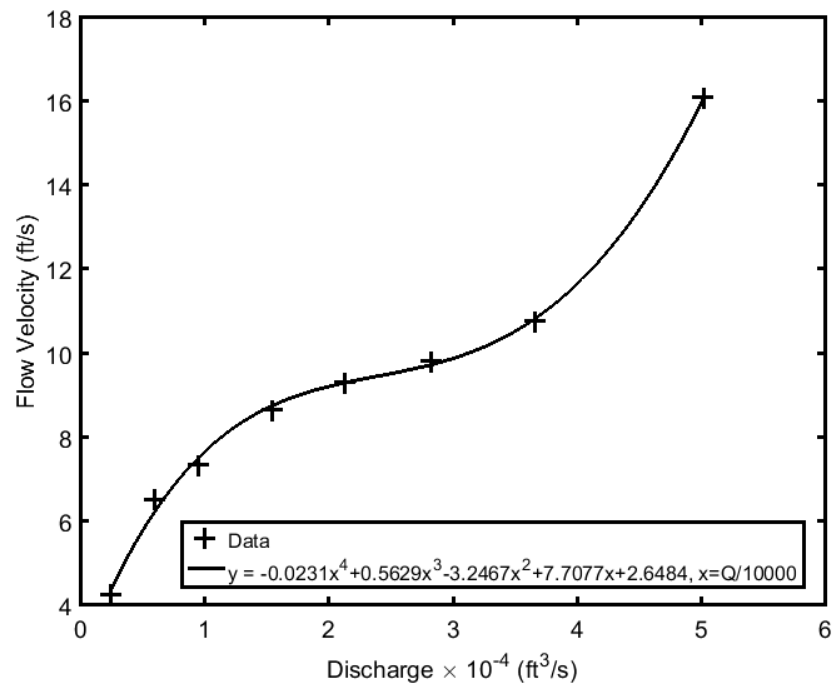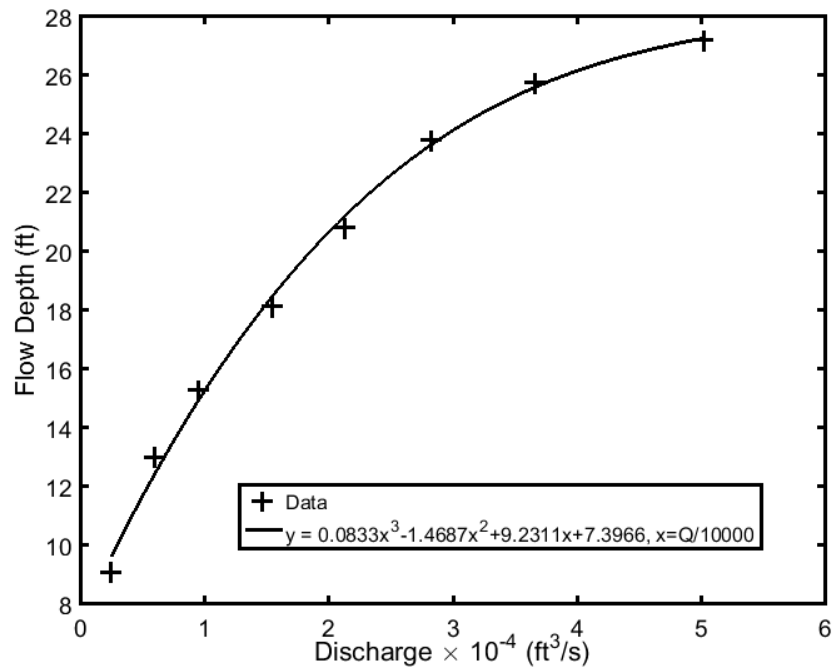
Figure 13.2 Computed maximum flow depth (top plot) and flow velocity (bottom plot) versus flow discharge in the low-flow channel
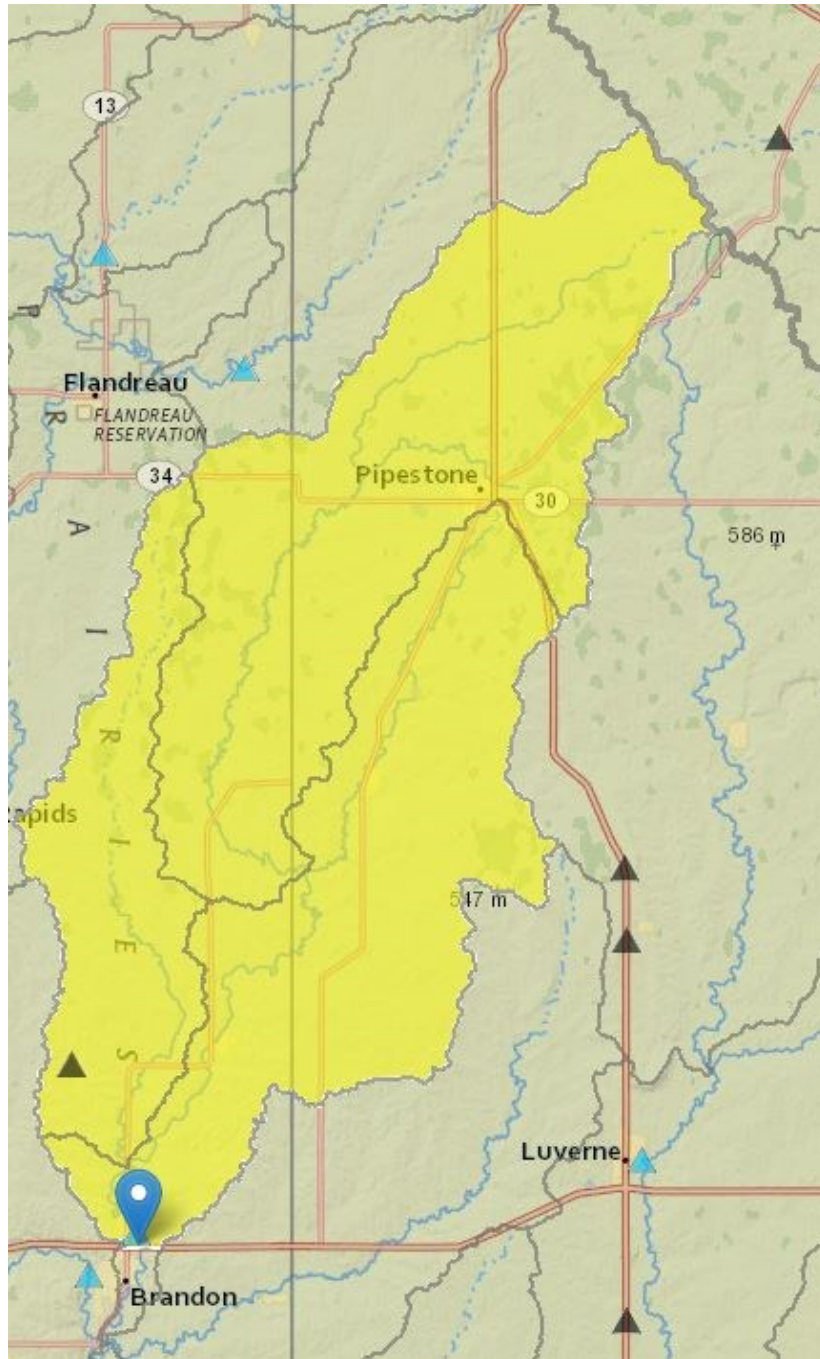
Figure 13.3 Drainage basin for Interstate 90 bridges over Split Rock Creek

Table 13.5 Drainage basin characteristics for Interstate 90 bridges over Split Rock Creek

Parameter Code	Parameter Description	Value Unit
BSLDEM10M	Mean basin slope computed from 10 m DEM	2.3 percent
COMPRAT	A measure of basin shape related to basin perimeter and drainage area	2.19 dimensionless
CONTOA	Area that contributes flow to a point on a stream	484.34 square miles
CSL10_85	Change in elevation divided by length between points 10 and 85 percent of distance along main channel to basin divide - main channel method not known	4.29 feet per mile
DRNAREA	Area that drains to a point on a stream	484.34 square miles
ELEV	Mean Basin Elevation	1630 feet
ELEVMAX	Maximum basin elevation	1980 feet
LFPLENGTH	Length of longest flow path	100.6 miles
MINBELEV	Minimum basin elevation	1306 feet
NONCONTDA	Area covered by noncontributing drainage area	0 square miles
OUTLETELEV	Elevation of the stream outlet in thousands of feet above NAV088	1306 feet
BASINPERIM	Perimeter of the drainage basin as defined In SIR 2004-5262	170.95 miles
LAKESNWI	Percent lakes and ponds as determined from the National Wetlands Inventory (2001)	0.153 percent
LC11DEV	Percentage of developed (urban) land from NLCD 2011 classes 21-24	5.94 percent
LC11IMP	Average percentage of impervious area determined from NLCD 2011 Impervious dataset	0.64 percent
LIME	Percentage of area of limestone geology	0 percent
PII_SD	Maximum 24-hour precipitation that occurs on average once in 2 years minus 1.5 inches	1.19 inches
RELIEF	Maximum - minimum elevation	678 feet
RELRELF	Basin relief divided by basin perimeter	3.97 feet per mile
SD_AS	Percent Artesian Spring from Sando and others (2008)	0 percent
SD_ASLZ	Percent Loss Zone/ Artesian Spring from Sando and others (2008)	0 percent
SD_BHEXT	Percent Black Hills Exterior from Sando and others (2008)	0 percent
SD_CC	Percent Crystalline Co1e from Sando and others (2008)	0 percent
SD_LSTHW	Percent Limestone Headwaters from Sando and others (2008)	0 percent
SD_LSTLZ	Percent Limestone Loss Zone from Sando and others (2008)	0 percent
SD_SNDHLS	Percent Sand Hills setting from Sando and others (2008)	0 percent
SLOPERAT	Slope ratio computed as longest flow path (10-85) slope divided by basin slope	1.84 dimensionless
STORNWI	Percentage of storage (combined water bodies and wetlands) from the National Wetlands Inventory	1.345 percent
WETLNDNWI	Percent wetlands as determined from the National Wetlands Inventory (2001)	1.192 percent

Table 13.6 Time to peak for the maximum annual floods with return period greater than 2 years
See also Table 8.5. The SRICOS simulations were conducted using the erosion-rate-versus-shear-stress curve that separates soil regions III and IV in Figure 5.3. Floods that have one dominant peak in the recorded hydrographs are highlighted in red.

Year	Peak Discharge Q_{max} (ft^3/s)	Flow Duration Exceeding Critical Discharge t_s (hr)	Final Scour Depth z_f (ft)	Equilibrium Scour Depth z_{max} (ft)	Equivalent Time t_e (hr)	Time To Peak T_p (hr)
2010	13,100	114.25	0.17	7.79	50.78	26
2014	13,100	131.75	0.14	7.79	41.96	Multiple Peaks
2006	8,020	49.25	0.04	7.03	21.69	12
2011	4,730	100	0.06	6.22	57.55	24
2012	4,730	76.75	0.04	6.22	39.46	Multiple Peaks
2007	4,050	90.25	0.05	6.01	59.1	Multiple Peaks
2004	3,400	36.25	0.01	5.79	19.53	Multiple Peaks
2015	2,510	21.75	0.01	5.46	18.45	26

Table 13.7 Time to peak needed to produce the same predicted final scour depths in Table 13.6 using the NRCS unit triangular hydrograph
Floods that have one dominant peak in the recorded hydrographs are highlighted in red.

Year	Peak Discharge (ft^3/s)	Flow Duration Exceeding Critical Discharge t_s (hr)	Final Scour Depth z_f (ft)	Equilibrium Scour Depth z_{max} (ft)	Equivalent Time t_e (hr)	Time to Peak T_p (hr)
2010	13,100	94	0.17	7.79	50.56	40
2014	13,100	78	0.14	7.79	41.67	33
2006	8,020	39	0.04	7.03	21.16	18
2011	4,730	92	0.06	6.22	58.07	50
2012	4,730	63	0.04	6.22	39.95	36
2007	4,050	87	0.05	6.01	58.28	54
2004	3,400	28	0.01	5.79	20.17	20
2015	2,510	23	0.01	5.46	18.76	23

The NRCS unit triangular hydrograph was used with a time to peak T_p value of 24 hours to compute the scour histories of the maximum annual floods. The results are used to determine the $\frac{t_e}{t_{90}}$ ratios (Table 13.8). Compared with Table 8.5, the $\frac{t_e}{t_{90}}$ ratios obtained using the NRCS triangular hydrograph are generally smaller. Consequently, the computed $\frac{z_f}{z_{max}}$ ratios are also smaller. Table 13.9 shows the corresponding results obtained using a T_p value of 48 hours. The computed $\frac{t_e}{t_{90}}$ and $\frac{z_f}{z_{max}}$ ratios are closer to those shown in Table 8.5.

The computed $\frac{t_e}{t_{90}}$ ratio is plotted against the $\frac{Q_{max}}{Q_c}$ ratio for $T_p = 24$ h in the top plot and for $T_p = 48$ h in the lower plot of Figure 13.4. These regression curves were used to compute the equivalent times for floods of different return periods for hydrograph generation. The exceedance probabilities for different predicted final scour depths and project lives are presented for $T_p = 24$ h in Table 13.10 and for $T_p = 48$ h in Table 13.11. The exceedance probabilities were computed using 20,000 SRICOS simulations. These results may be compared with Table 8.7, where the relationship between the $\frac{t_e}{t_{90}}$ ratio and $\frac{Q_{max}}{Q_c}$ ratio was determined using recorded hydrographs. The exceedance probabilities are lower if the NRCS triangular hydrograph is used with a T_p value of 24 h to predict scour, but higher for a T_p value of 48 h. The differences are substantial for the small scour depths because their exceedance probabilities are large. The differences are not so significant for the large scour depths because their exceedance probabilities are small anyway. For example, the exceedance probability for a predicted final scour depth of 5 ft is less than 1% in a project life of 75 years in all three tables. Since the design scour depth should have a small exceedance probability (e.g., <1%), a highly accurate T_c value may not be critical.

Table 13.8 Summary of results of SRICOS simulations for the maximum annual floods between 2001 and 2017 that can produce scour

The SRICOS simulations were conducted using the erosion-rate-versus-shear-stress curve that separates soil regions III and IV in Figure 5.3 and the NRCS unit triangular hydrograph with a time to peak T_p of 24 hours. The critical discharge is 1,580 ft³/s.

Year	Peak Discharge Date	Peak Discharge Q_{max} (ft³/s)	Return Period (yr)	Final Scour Depth z_f (ft)	Initial Erosion Rate (ft/hr)	Equilibrium Scour Depth z_{max} (ft)	$\frac{z_f}{z_{max}} \times 100\%$
2010	9/24/2010	13,100	18.1	0.10	0.003392	7.79	1.3
2014	6/17/2014	13,100	18.1	0.10	0.003392	7.79	1.3
2006	4/7/2006	8,020	8	0.06	0.002024	7.03	0.85
2011	7/15/2011	4,730	3.9	0.03	0.001054	6.22	0.48
2012	5/7/2012	4,730	3.9	0.03	0.001054	6.22	0.48
2007	3/13/2007	4,050	3.3	0.02	0.000871	6.01	0.33
2004	5/30/2004	3,400	2.7	0.02	0.000708	5.79	0.35
2015	7/7/2015	2,510	2.1	0.01	0.000507	5.46	0.18

Year	Flow Duration Exceeding Critical Discharge t_s (hr)	Equivalent Time t_e (hr)	t_{90} (hr)	$\frac{t_e}{t_{90}} \times 1000$	$\frac{Q_{max}}{Q_c}$	$\frac{Q_{max} t_s}{z_{maz}^3}$
2010	57	30.35	20,681.74	1.4675	8.2911	1579.55
2014	57	30.35	20,681.74	1.4675	8.2911	1579.55
2006	52	28.20	31,242.31	0.9026	5.0759	1200.36
2011	42	26.64	53,121.75	0.5015	2.9937	825.54
2012	42	26.64	53,121.75	0.5015	2.9937	825.54
2007	39	26.04	62,081.36	0.4194	2.5633	727.61
2004	34	24.44	73,617.70	0.3320	2.1519	595.56
2015	23	18.94	97,014.91	0.1952	1.5886	354.67

Table 13.9 As in Table 10.8, but for T_p of 48 hours

Year	Peak Discharge Date	Peak Discharge Q_{max} (ft³/s)	Return Period (yr)	Final Scour Depth z_f (ft)	Initial Erosion Rate (ft/hr)	Equilibrium Scour Depth z_{max} (ft)	$\frac{z_f}{z_{max}} \times 100\%$
2010	9/24/2010	13,100	18.1	0.20	0.003392	7.79	2.6
2014	6/17/2014	13,100	18.1	0.20	0.003392	7.79	2.6
2006	4/7/2006	8,020	8	0.11	0.002024	7.03	1.6
2011	7/15/2011	4,730	3.9	0.06	0.001054	6.22	0.96
2012	5/7/2012	4,730	3.9	0.06	0.001054	6.22	0.96
2007	3/13/2007	4,050	3.3	0.05	0.000871	6.01	0.83
2004	5/30/2004	3,400	2.7	0.03	0.000708	5.79	0.52
2015	7/7/2015	2,510	2.1	0.02	0.000507	5.46	0.37

Year	Flow Duration Exceeding Critical Discharge t_s (hr)	Equivalent Time t_e (hr)	t_{90} (hr)	$\frac{t_e}{t_{90}} \times 1000$	$\frac{Q_{max}}{Q_c}$	$\frac{Q_{max} t_s}{z_{maz}^3}$
2010	113	60.51	20,681.74	2.9258	8.2911	3131.39
2014	113	60.51	20,681.74	2.9288	8.2911	3131.39
2006	103	56.19	31,242.31	1.7985	5.0759	2377.64
2011	85	53.57	53,121.75	1.0084	2.9937	1670.74
2012	85	53.57	53,121.75	1.0084	2.9937	1670.74
2007	78	52.06	62,081.36	0.8386	2.5633	1455.21
2004	68	48.87	73,617.70	0.7072	2.1519	1191.11
2015	47	38.53	97,014.91	0.3972	1.5886	724.76
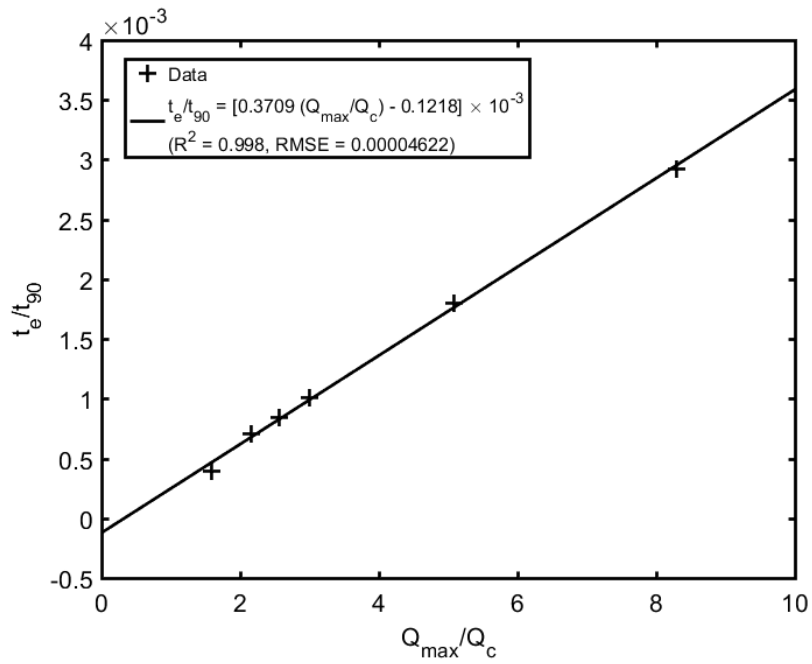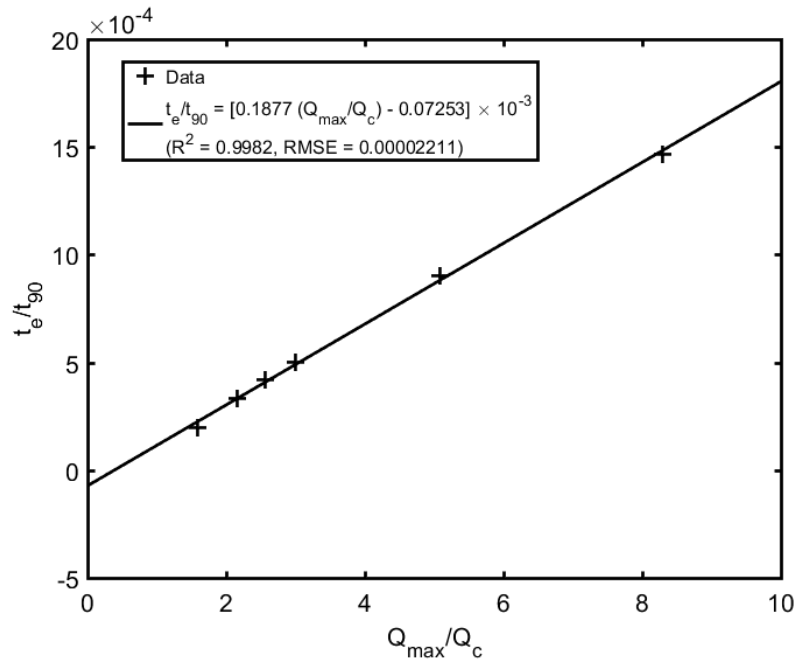
Figure 13.4 Normalized equivalent time versus normalized peak discharge; $T_p = 24$ h (top plot) and 48 h (bottom plot)

Table 13.10 Exceedance probabilities associated with predicted scour depths and project lives

The soil critical shear stress τ_c and erosion rate constant a' are 9.5 N/m² and 1.62, respectively. The equivalent time is computed using the regression curve in the top plot of Figure 13.4.

Scour Depth (ft)	2.0	2.5	3.0	3.5	4.0	4.5	5.0
Exceedance Probability (project life 50 yrs)	3%	1%	<1%	<1%	<1%	<1%	<1%
Exceedance Probability (project life 75 yrs)	15%	4%	1%	<1%	<1%	<1%	<1%
Exceedance Probability (project life 100 yrs)	47%	12%	3%	1%	<1%	<1%	<1%

Table 13.11 As in Table 13.10, but the equivalent time is computed using the regression curve in the bottom plot of Figure 13.4.

Scour Depth (ft)	2.0	2.5	3.0	3.5	4.0	4.5	5.0
Exceedance Probability (project life 50 yrs)	42%	15%	5%	2%	1%	<1%	<1%
Exceedance Probability (project life 75 yrs)	92%	56%	22%	7%	3%	1%	<1%
Exceedance Probability (project life 100 yrs)	>99%	92%	58%	22%	8%	3%	1%

13.6 Summary

A simple method for estimating the equivalent times of maximum annual floods at ungauged streams is tested using the Interstate 90 bridges over the Split Rock Creek. The hydrograph of the maximum annual floods is modeled by the NRCS unit triangular hydrograph, which is defined by the peak discharge Q_p and time to peak T_p. The latter is related to the time of concentration T_c, which may be estimated using empirical equations and drainage basin characteristics, or open-channel flow equation if a major portion of the flow path is channel flow. The peak flows for floods of different return periods can be estimated using regional regression equations. It was found that the T_p values used in the NRCS unit triangular hydrograph need to be much larger than the observed values in order to produce similar predicted scour depths as those obtained using the equivalent times derived from recorded hydrographs. Further investigation to refine the hydrograph generation method for ungauged stream is needed.

14.   FINDINGS AND CONCLUSIONS

14.1 Scour History Analysis

The relationship between time rate of scour, soil erodibility and time sequence of flow was investigated for pier scour at the SD13 bridge over the Big Sioux River and Interstate 90 bridges over Split Rock Creek, and for contraction scour at the SD37 bridges over the James River. SRICOS simulations of recorded floods from the 1950s to 2017 were conducted using the erosion-rate-versus-shear-stress curves of different geo-materials classified as low, medium, or high erodibility. Significant reduction in the predicted final scour depth was found only in regions III (medium erodibility) and IV (low erodibility) of the soil erodibility chart. Cohesive soils that fall into this category include high plasticity silt and clay. When a measured EFA curve for silty fine sand was used to compute scour history at the SD13 bridge, over 50% of the equilibrium scour depth was developed in a single flooding event.

The equivalent times of the maximum annual floods were determined using the recorded hydrographs. This parameter is defined as the time required for the maximum discharge in a hydrograph to create the same predicted final scour depth as the one created by the complete hydrograph. The relationships between equivalent time, peak discharge, and flood duration were obtained by multiple regression analysis. For pier scour, the equivalent time depends primarily on peak discharge and secondly on the flood duration above the critical discharge, and there is a strong correlation between the $\frac{t_e}{t_{90}}$ ratio and $\frac{Q_{max}}{Q_c}$ ratio where t_e is equivalent time, t_{90} is time to reach 90% of equilibrium scour depth, Q_{max} is maximum discharge, and Q_c is critical discharge at initiation of scour. The relationships between flow histories, computed scour histories, and soil erodibility can be concisely summarized on a dimensionless plot of $\frac{t_e}{t_{90}}$ ratio versus $\frac{z_f}{z_{max}}$ ratio, where z_f is predicted final scour depth and z_{max} is equilibrium scour depth. This dimensionless plot can be used as a screening tool to assess the effect of time on scour at a bridge site.

For contraction scour, it was found that the predicted scour history generally does not follow a hyperbolic function. The relationship between the $\frac{t_e}{t_{90}}$ ratio and $\frac{z_f}{z_{max}}$ ratio varies with soil erodibility. The hyperbolic model over-predicts the rate of scour for soils with high critical shear stress and low erosion rates but under-predicts the rates of scour for soils with low critical shear stress and high erosion rates. The computed $\frac{t_e}{t_{90}}$ ratio is also poorly correlated to the $\frac{Q_{max}}{Q_c}$ ratio. A stronger correlation was found between the $\frac{t_e}{t_{90}^*}$ ratio and $\frac{Q_{max}}{Q_c}$ ratio, where t_{90}^* is related to the equilibrium scour depth z_{max} and initial rate of scour $\dot{z}_i$ by $\frac{9z_{max}}{\dot{z}_i}$. This latter may be used as an alternative time scale for contraction scour.

14.2 Hydrograph Generation and Scour Prediction

SRICOS simulations conducted using streamflow records spanning several decades at the three bridge sites show that a continuous hydrograph may be replaced by a sequence of maximum annual floods for the purpose of scour prediction. The basic framework for hydrograph generation proposed in this study is an annual maximum series. The advantage of working with maximum annual floods is that the peak discharge in one year may be assumed to be independent from the peak discharge in another year. Therefore, an annual maximum series can be generated by sampling from a suitable distribution such as the Log Pearson Type III (LP-III) distribution, which is commonly used for flood frequency

analysis in the United States. The proposed hydrograph generation method takes advantage of recent advances in statistical methods described in Bulletin 17C. The parameters of the LP-III distribution can be computed by running the USGS program PeakFQ (https://water.usgs.gov/software/PeakFQ/). A stochastic approach is adopted where many equally probable annual maximum series are generated by Monte Carlo simulation and used with the SRICOS method to compute the distribution of predicted scour depth and risk values. This approach is site-specific in that it allows the temporal distribution of floods to be varied in an annual maximum series but assumes that the flood's flow history of a given return period will repeat itself at the same site.

14.3 Screening Tool

Based on these research findings, three levels of assessment in increasing order of complexity are proposed for evaluating pier and contraction scour in cohesive soils:

The Level I assessment will be a basic hydrologic, hydraulic, geotechnical, and scour analysis like the procedure for scour evaluation in HEC-18. A flood frequency analysis is conducted to determine the moments of the LP-III distribution and peak flow magnitudes for floods of different return periods. A bridge hydraulic analysis is performed using a one-dimensional (1D) or two-dimensional (2D) flow model. Borehole data are obtained to delineate the soil stratigraphy and for geotechnical testing, and thin-walled tube samples may be collected and tested in an erosion function apparatus (EFA) to measure the erosion-rate-versus-shear-stress curve. Alternatively, USCS soil classification may be used with Figure 5.3 to estimate the critical shear stress τ_c and erosion rate constant a'. Equation (5.22) is then run with the estimated 100-year peak discharge for five days. If the soil type falls into category I or II and/or the computed final scour depth is close to the equilibrium scour depth, the maximum scour depth can be reached during a single flooding event and no reduction to the predicted scour depth from the HEC-18 method is recommended. The engineer may also adopt the equilibrium scour depth for design if the scour depth predicted by the HEC-18 method is judged to be reasonable or other considerations (e.g., high traffic volume, long design life) dictate a more conservative approach.

In the Level II assessment, scour histories of past floods are computed using a measured soil erosion function to determine the final scour depths and equivalent times. The results are plotted on a $\frac{t_e}{t_{90}}$ versus $\frac{z_f}{z_{max}}$ curve to assess the potential of floods of different return periods to produce scour. A decision is made to adopt the scour depth predicted using the HEC-18 method or proceed to a full SRICOS analysis.

In the Level III assessment, the equivalent times of past floods are normalized by their t_{90} (for pier scour) or t_{90}^* (for contraction scour) values and correlated to the $\frac{Q_{max}}{Q_c}$ ratio. The LP-III distribution is used to generate a sequence of annual peak flows, and the equivalent times are calculated using a regression equation developed for the $\frac{t_e}{t_{90}}$ or $\frac{t_e}{t_{90}^*}$ ratio. Many annual maximum series are generated and used with the SRICOS method to predict the exceedance probability of final scour depth. A design scour depth is selected based on the risk values associated with different project lives.

15.   IMPLEMENTATION RECOMMENDATIONS

15.1 Recommendation 1: Evaluating Scour in Cohesive Soils

Recommendation 1. For bridge sites with cohesive soils where scour is a controlling factor in bridge design, include an additional check in the current SDDOT bridge design process to determine whether time effect of scour may be an important factor in predicting the final scour depth.

The Level I assessment described in Section 14.3 applies procedures normally required for bridge scour evaluation described in HEC-18. The only addition is running a SRICOS simulation for the 100-year peak flow for five days, which can be done using a measured soil erosion function or selecting an erosion rate curve from Figure 5.3 based on the USCS soil classification. The latter is usually performed as part of the foundation investigation. The SRICOS simulation for a constant discharge can be performed easily by hand calculations or using the MATLAB scripts provided with this report as demonstrated by the worked examples in Chapters 11 and 12 for pier scour and contraction scour, respectively. Therefore, the Level I assessment would not take much more than what would be needed for the conventional bridge scour evaluation at a typical bridge site.

It is recommended that the HEC-18 equation for predicting pier scour in non-cohesive soils (Eq. 5.9) should also be used to compute the equilibrium scour depth in cohesive soils. It is shown that Eq. (5.14) would generally predict a larger equilibrium scour depth than Eq. (5.9), which is not supported by available observed data. Furthermore, empirical equations developed for predicting the equilibrium scour depth in cohesive soils may not be applied to soils other than those used to develop the equations. The equilibrium scour depth in contraction scour is directly related to the soil critical shear stress (see Eq. 5.31). For bridge sites with large, predicted contraction scour depths, the critical shear stress should be measured instead of estimated based on grain sizes. The latter would require additional equipment such as the EFA (see Section 15.2).

The Level II and III assessment is only intended to be applied to a very small percentage of bridge sites (e.g., scour critical bridges). The Level II assessment involves computing the scour histories produced by the maximum annual floods. Daily or sub-daily streamflow data are needed, in addition to a measured soil erosion function. The SRICOS simulations for unsteady flows can be conducted by modifying the MATLAB scripts provided with this report. In this project, the scour history analysis was conducted for all the maximum annual floods that can produce scour. In practice, a smaller number of representative floods may be analyzed to evaluate the time effect of scour for the large floods and to develop regression equations for computing their equivalent times. The scour history analysis can be completed within one day by a hydraulic engineer. Each EFA test would also require one to two days to perform depending on the measured soil erosion rates.

The level III assessment involves generating many annual maximum series by Monte Carlo simulation and computing the distribution of predicted final scour depth. The hydrograph generation method requires the mean, standard deviation and skew coefficient of the logarithm of annual peak flows as input. These parameters are already determined during the flood frequency analysis conducted as part of the hydrologic analysis in a conventional bridge scour evaluation. SDDOT may also request assistance from the USGS Office in South Dakota to conduct the flood frequency analysis using PeakFQ. After the Level II assessment, the hydrograph generation and scour risk analysis can be performed quickly using the MATLAB scripts provided with this report.

15.2 Recommendation 2: Soil Erosion Rate Testing

Recommendation 2. Monitor current and future research to observe new improvements to the erosion function apparatus (EFA) and acquire the capability to conduct soil erosion rate testing.

The major impediment to successful implementation of this project will be an apparatus to measure the soil erosion function. The soil erosion tests can take up to several days, depending on the number of soil samples needed to be tested and their erosion rates. Thin-walled tube samples will need to be collected from the bridge site, which can be performed during the geotechnical investigation. Presently, the Fluid Mechanics Laboratory at South Dakota State University (SDSU) can measure soil erosion rates of thin-walled tube samples in a tilting flume up to a maximum applied bed shear stress of about 25 N/m^2. A research project (MPC-596) is underway at SDSU to measure the turbulent flow characteristics and fluid shear stresses induced over a soil sample in an EFA type facility. The expected outcome of this project will be an improved experimental setup and laboratory testing procedure to more accurately measure the critical shear stress and erosion rates of cohesive soils. The Federal Highway Administration (FHWA) is conducting a research project (FHWA-PROJ-11-0177) to develop an in-situ scour and erosion testing device to measure soil erosion rates in the field. It is recommended that SDDOT monitors these and other current and future research to observe new improvements to the SRICOS/EFA method and acquire the capability to conduct soil erosion rate testing.

15.3 Recommendation 3: Training

Recommendation 3. Conduct training on scour evaluation using the SRICOS method.

Training of SDDOT personnel will be required to implement the findings of this project. The principal investigator can organize a workshop on hydrograph generation and perform scour evaluation using the SRICOS method. The MATLAB scripts and project data developed in this project are already included with this report as supplementary files.

15.4 Recommendation 4: Suggested Research

Recommendation 4. Conduct additional research to improve the hydrograph generation methods for using the SRICOS method.

The Level II assessment requires scour histories of past floods to be computed. For an ungauged site, the drainage-area ratio method may be used to transfer streamflow data from a nearby gauging station. If the stream is ungauged, daily mean flow may be transferred from an adjacent watershed using the QPPQ method. The QPPQ method was demonstrated for the Interstate 90 bridges over Split Rock Creek using the Skunk Creek near Sioux Falls station as the donor. If no suitable donor is available, synthetic hydrographs would have to be used. The method was explored in Chapter 13 using the NRCS unit triangular hydrograph, but more in-depth studies are needed. Regional regression equations for estimating flow-duration curve exceedance probabilities for ungauged streams will be extremely useful for applying for the QPPQ method. They are not available in South Dakota and should be investigated.

Maximum annual floods are used in this project to generate future hydrographs with durations of several decades to predict long-term scour. Hydrograph generation methods that can be applied to short time periods of up to a few years will be useful for evaluating scour at temporary bridges. Time series methods are widely used to produce short- or intermediate-range forecasts in economic analysis.

Advanced models can include seasonality and long-term correlation observed in streamflow data. Time series models should be explored for hydrograph generation for use with the SRICOS method in future research.

The equivalent times of historical floods were predicted based on the peak discharges in this project. Large equivalent times were found for floods with long recession times. It was observed that this effect can be important for soils with very slow erosion rates. Research to better understand the effect of long recession time on the development of scour in cohesive soils will be useful for improving the SRICOS method.

Large floods are occurring more frequently in South Dakota. An example is seen at the SD37 bridges over the James River (Figure 7.10). The hydrograph generation method developed in this project assumes that the parameters of the constructed hydrographs do not change with time. Research on the trends of flooding in South Dakota streams will be beneficial to the design of bridges over waterways and resilience of transportation infrastructure in the state in the age of climate change.

16.   RESEARCH BENEFITS

The method currently used by SDDOT for designing bridge foundations assumes that the bed material is sand and designs for a single (worst-case) flood event such as the 100-year or 500-year flood using the peak flow magnitude. This approach is generally regarded as conservative because the duration of flooding events in many watersheds in South Dakota is not long enough to generate equilibrium scour, and the bed material is more likely to be cohesive. Since silts and clays scour more slowly than sands, using the traditional methods for evaluating scour at bridges may over-predict the extent of scour. This could result in over-design of new bridge foundations or installation of unnecessary scour countermeasures at existing bridges. Furthermore, bridges that are classified as scour critical may in fact be safe.

The immediate benefits of this project will be an alternative approach to evaluating bridge scour in cohesive soils. The SRICOS method will be most useful when the design life of the bridge is short compared with the expected duration of the scouring floods, and for sites with slow rates of scour. Potential situations may include:

- Bridges scheduled to be replaced in a few years
- Bridges over ephemeral streams
- Scour critical bridges, which may be safe if the slower rates of scour in cohesive soils are considered
- Bridges on low volume roads that can be closed temporarily during severe floods

The results of this research are directly applicable to practice, first by giving the design engineer a screening tool to identify bridge sites where the SRICOS method may be beneficial or more appropriate than the traditional HEC-18 method, and second, by providing a step-by-step procedure to generate flood hydrographs for scour prediction using the SRICOS method and assessing the scour risk. When use of the SRICOS method is advisable, substantial savings in foundation costs and scour countermeasures may result and this can be measured by the dollars saved in SDDOT projects.

The bridge scour evaluation procedure developed in this project may be considered an extension of the HEC-18 method, first, by including the time effect of scour and, second, by using a stochastic approach to predict the probability of exceedance of the predicted scour depth. The new procedure can be used to assess the susceptibility of bridges to scour damages by large floods more realistically, where the bridges would probably be classified as unsafe based on the traditional HEC-18 method. A broader impact of this project will be a new tool that can be incorporated into a statewide hazard assessment program to identify flood vulnerable bridges in South Dakota, which would have considerable benefits to the resiliency of the state's transportation system. The suggested research outlined in Section 5.4 will contribute to this goal by further improving the SRICOS/EFA/hydrograph generation method.

REFERENCES

Akan, A. O. (2010). *Open Channel Hydraulics*. Butterworth-Heinemann, Burlington, Massachusetts.

Archfield, S. A., Steeves, P. A., Guthrie, J. D., and Ries III, K. G. (2013). "Towards a publicly available, map-based regional software tool to estimate unregulated daily streamflow at ungauged rivers." *Geoscientific Model Developmen*t, Vol. 6, pp. 101-115.

Arneson, L. A., Zevenbergen, L. W., Lagasse, P. F., and Clopper, P. E. (2012). "Evaluating scour at bridges." Publication No. FHWA-HIF-12-003, Hydraulic Engineering Circular No. 18, Federal Highway Administration, Washington, DC.

Bedient, P. B., and Huber, W. C. (1992). *Hydrology and Floodplain Analysis*. Addison-Wesley, Reading, Massachusetts.

Briaud, J.-L., Chen, H. C., Kwak, K. W., Han, S. W., and Ting, F. C. K. (2001b). "Multiflood and multilayer method for scour rate prediction at bridge piers." *J. Geotechnical and Geoenvironmental Eng.*, ASCE, Vol. 127, No. 2, pp. 114-125.

Briaud, J.-L., Chen, H. C., Li, Y., Nurtjahyo, P., and Wang, J. (2004). "Pier and contraction scour in cohesive soils." NCHRP Report 516, Transportation Research Board, Washington, DC.

Briaud, J.-L., Ting, F. C. K., Chen, H. C., Cao, Y., Han, S. W., and Kwak, K. W. (2001a). "Erosion function apparatus for scour rate predictions." *J. Geotechnical and Geoenvironmental Eng.*, ASCE, Vol. 127, No. 2, pp. 105-113.

Briaud, J.-L., Ting, F. C. K., Chen, H. C., Gudavalli, R., Perugu, S., and Wei, G. (1999). "SRICOS: Prediction of scour rate in cohesive soils at bridge piers." *J. Geotechnical and Geoenvironmental Eng.*, ASCE, Vol. 125, No. 4, pp. 237-246.

Briaud, J.-L., Chen, H.-C.., Chang, K.-A., Oh, S. J., Chen, S., Wang J, Li, Y., Kwak, K., Nartjaho, P., Gudaralli, R., Wei, W. Pergu, S., Cao, Y. W., and Ting, F. (2011). "The SRICOS-EFA method." Summary Report, Texas A&M University, College Station, Texas.

Briaud, J.-L, Govindasamy, A. V., Kim, D., Gardoni, P., Olivera, F., Chen, H. C., Mathewson, C., and Elsbury, K. (2009). "Simplified methods for estimating scour at bridges." Report No. FHWA/TX-09/0-5505-1, Texas Department of Transportation.

Brubaker, K. L., Ghelardi, V., Goodings, D., Guy, L., and Pathak, P. (2004). "Estimation of long-term scour at Maryland Bridges using EFA/SRICOS." Report No. MD-04-SP107B4E, Maryland Department of Transportation.

Chow, V. T., Maidment, D. R., and Mays, L. W. (1988). *Applied Hydrology*: New York, McGraw-Hill Publishing Company.

Curry, J. E., Crim, Jr. S. H., Güven, O., Melville, J. G., and Santamaria, S. (2003). "Scour evaluations of two bridge sites in Alabama with cohesive soils." Final report for Alabama Department of Transportation Research Project 930-490R.

Debnath, K., and Chaudhuri, S. (2010). "Bridge pier scour in clay-sand mixed sediments at near-threshold velocity for sand." *J. Hydraulic Eng.*, 10.1061/(ASCE)HY.1943-7900.0000221.

England, J. F., Jr., Cohn, T. A., Faber, B. A., Stedinger, J. R., Thomas, W. O., Jr., Veilleux, A. G., Kiang, J. E., and Mason, R. R., Jr. (2018). "Guidelines for determining flood flow frequency – Bulletin 17C: U.S. Geological Survey Techniques and Methods," book 4, chap. B5, 148 p., https://doi.org/10.3133/tm4B5.

Ettema, R., Melville, B. W., and Barkdoll, B. (1998). "Scale effect in pier scour experiments." *J. Hydraulic Eng.*, ASCE, Vol. 124, No. 6, pp. 639-642.

Ghelardi, V. M. (2004). "Estimation of long term bridge pier scour in cohesive soils at Maryland bridges using EFA/SRICOS." M.S. thesis, Department of Civil Engineering, University of Maryland, College Park, Maryland.

Güven, O., Melville, J. G., and Curry, J. E. (2002). "Analysis of clear water scour at bridge contractions in cohesive soils." TRB Paper No. 02-2127, Transportation Research Record, National Research Council, Washington DC.

Harris, J. M., and Whitehouse, R. J. S. (2017). "Scour development around large-diameter monopiles in cohesive soils: evidence from the field." *J. Waterways, Port, Coastal, and Ocean Eng.,* ASCE, Vol. 143, No. 5, 04017002.

Kite, G.W. (1977) *Frequency and Risk Analyses in Hydrology*. Water Resources Publications, Fort Collins, Colorado, USA.

Kothyari, U. C., Kumar, A., and Jain, R. K. (2014). "Influence of cohesion on river bed scour in the wake region of piers." *J. Hydraulic Eng.*, ASCE, Vol. 140, No. 1, pp. 1-13.

Larsen, R. J., Ting, F. C. K., and Jones, A. L. (2011). "Flow velocity and pier scour prediction in a compound channel: Big Sioux River Bridge at Flandreau, South Dakota." *J. Hydraulic Eng.*, ASCE, Vol. 137, No. 5, pp. 595-605.

Molinas, A., and Hosny, M. M. (1999). "Experimental study on scour around circular piers in cohesive soil." Publication No. FHWA-RD-99-186, Federal Highway Administration, U.S. Department of Transportation, McLean, VA.

Munson, B. R., Okiishi, T. H., Huebsch, W. W., and Rothmayer, A. P. (2013). *Fundamentals of Fluid Mechanics*, Seventh Edition, John Wiley & Sons.

Niehus, C. A. (1996). "Scour assessments and sediment-transport simulation for selected bridge sites in South Dakota." USGS Water-Resources Investigations Report 96-4075.

Oh, S. J. (2009). "Experimental study of bridge scour in cohesive soil." Ph.D. Dissertation, Texas A&M University, College Station, Texas.

Roberson, J. A., Cassidy, J. J., and Chaudhry, M. H. (1998). *Hydraulic Engineering*, John Wiley & Sons.

Rossell, R. P. (2012). "Two-dimensional flow modeling of the James River at the SD37 Bridge crossing north of Mitchell, South Dakota." M.S. thesis, Department of Civil and Environmental Engineering, South Dakota State University, Brookings, South Dakota.

Rossell, R. P., and Ting, F. C. K. (2013). "Hydraulic and contraction scour analysis of a meandering channel: James River Bridges near Mitchell, South Dakota." *J. Hydraulic Eng.*, ASCE, Vol. 139, No. 12, pp. 1286-1296.

Sando, S. K. (1998). "Techniques for estimating peak-flow magnitude and frequency relations for South Dakota Streams." U.S. Geological Survey Scientific Investigations Report 98-4055.

Sando, S. K., Driscoll, D. G., and Parrett, C. (2008). "Peak-flow frequency estimates based on data through water year 2001 for selected streamflow-gaging stations in South Dakota." U.S. Geological Survey Scientific Investigations Report 2008-5104.

Shan, H., Shen, J., Kilgore, R., and Kerenyi, K. (2015). "Scour in cohesive soils." Report No. FHWA-HRT-15-033, Federal Highway Administration, McLean, Virginia.

Straub, T. D., and Over, T. M. (2010). "Pier and contraction scour prediction in cohesive soils at selected bridges in Illinois." Research Report ICT-R27-19, Illinois Department of Transportation.

Ting, F. C. K., Jones, A. L., and Larsen, R. J. (2010). "Evaluation of SRICOS method on cohesive soils in South Dakota." MPC-08-195, North Dakota State University – Upper Great Plains Transportation Institute, Fargo: Mountain-Plains Consortium.

Ting, F. C. K., Larsen, R. J., and Rossell, R. P. (2017). "Analysis of compound channel flow with two-dimensional models." MPC-17-336, North Dakota State University – Upper Great Plains Transportation Institute, Fargo: Mountain-Plains Consortium.

Ting, F. C. K., Briaud, J.-L, Chen, H. C., Gudavalli, R., Perugu, S., and Wei, G. (2001). "Flume tests for scour in clay at circular piers." *J. Hydraulic Eng.*, ASCE, Vol. 127, No. 11, pp. 969-978.

Tucker-Kulesza, S., and Karim, M. Z. (2017). "Characterizing soil erosion potential using electrical resistivity imaging." Report No. K-TRAN: KSU-15-4, Final Report, Kansas State University, Topeka, Kansas.

U.S. Interagency Advisory Committee on Water Data (1982). "Guidelines for determining flood flow frequency." Bulletin 17B, U.S. Department of the Interior, Geological Survey, Office of Water Data, Reston, Virginia.

Wagner, C. R., Mueller, D. S., Parola, A. C., Hagerty, D. J., and Benedict, S. T. (2006). "Scour at contracted bridges." Final Report for NCHRP Project 24-14, Transportation Research Board, Washington, D.C.

Wang, J. (2004). "The SRICOS-EFA Method for complex pier and contraction scour." Ph.D. Dissertation, Department of Civil Engineering, Texas A&M University, College Station, Texas.

Wilson, E. B., and Hiferty, M. M. (1931). "The distribution of chi-square." Proceedings of the National Academy of Sciences of the United States of America, 17, 684-688.

Ziegeweid, J. R., Lorenz, D. L., Sanocki, C. A., and Czuba, C. R. (2015). "Methods for estimating flow-duration curve and low-flow frequency statistics for ungaged locations on small streams in Minnesota." U.S. Geological Survey Scientific Investigations Report 2015-5170.

APPENDIX I SUMMARY OF RESULTS FROM NATIONAL SURVEY

SDDOT Scour Rate In Cohesive Soils (SRICOS) Survey

Q1 Please provide your contact information:

Answered: 21   Skipped: 0

ANSWER CHOICES	RESPONSES	
Name	100.00%	21
Agency	100.00%	21
Address	0.00%	0
Address 2	0.00%	0
City/Town	0.00%	0
State	100.00%	21
ZIP/Postal Code	0.00%	0
Country	0.00%	0
Email Address	100.00%	21
Phone Number	100.00%	21

#	NAME	DATE
1	Neil VanBebber	8/23/2018 7:36 AM
2	John Delphia	8/10/2018 6:29 PM
3	Tom Flournoy	8/10/2018 3:44 PM
4	Dale Heft	8/10/2018 1:04 PM
5	Thomas Birnbrich	8/9/2018 8:11 AM
6	Larry Tolfa	8/6/2018 11:23 AM
7	Kevin Marton	8/6/2018 9:25 AM
8	Herbert McDowell	8/6/2018 8:31 AM
9	Erik Carlson	8/3/2018 9:33 PM
10	Andrzej ("Andy") J. Kosicki	8/3/2018 9:46 AM
11	Michael Menghini	8/2/2018 2:47 PM
12	Brian Radakovic	8/2/2018 12:51 PM
13	Tingzong Guo	8/2/2018 12:50 PM
14	Brad Pfeifer	8/2/2018 12:47 PM
15	Dale Henderson	8/2/2018 12:33 PM
16	Petra DeWall	8/2/2018 9:49 AM
17	Michael Orth	8/2/2018 8:56 AM
18	Saul Nuccitelli	8/2/2018 8:23 AM
19	Leslie Lewis	8/2/2018 8:11 AM
20	Ted Barber	8/2/2018 8:04 AM
21	Dave Claman	8/2/2018 7:09 AM
#	AGENCY	DATE

1 / 16

1	Illinois Department of Transportation	8/23/2018 7:36 AM
2	Texas Department of Transportation - Bridge Division Geotechnical Branch	8/10/2018 6:29 PM
3	ALDOT	8/10/2018 3:44 PM
4	ArDOT	8/10/2018 1:04 PM
5	Ohio DOT	8/9/2018 8:11 AM
6	NYSDOT	8/6/2018 11:23 AM
7	SDDOT	8/6/2018 9:25 AM
8	Idaho Transportation Department	8/6/2018 8:31 AM
9	Michigan Dept. of Transportation	8/3/2018 9:33 PM
10	MDOT SHA	8/3/2018 9:46 AM
11	Wyoming DOT	8/2/2018 2:47 PM
12	NCDOT	8/2/2018 12:51 PM
13	LA DOTD	8/2/2018 12:50 PM
14	NDDOT	8/2/2018 12:47 PM
15	Missouri DOT	8/2/2018 12:33 PM
16	MnDOT	8/2/2018 9:49 AM
17	Kansas DOT	8/2/2018 8:56 AM
18	TxDOT	8/2/2018 8:23 AM
19	Oklahoma Department of Transportation	8/2/2018 8:11 AM
20	New Mexico Dept. of Transportation	8/2/2018 8:04 AM
21	Iowa DOT	8/2/2018 7:09 AM

#	ADDRESS	DATE
	There are no responses.	

#	ADDRESS 2	DATE
	There are no responses.	

#	CITY/TOWN	DATE
	There are no responses.	

#	STATE	DATE
1	IL	8/23/2018 7:36 AM
2	TX	8/10/2018 6:29 PM
3	AL	8/10/2018 3:44 PM
4	AR	8/10/2018 1:04 PM
5	OH	8/9/2018 8:11 AM
6	NY	8/6/2018 11:23 AM
7	SD	8/6/2018 9:25 AM
8	ID	8/6/2018 8:31 AM
9	MI	8/3/2018 9:33 PM
10	MD	8/3/2018 9:46 AM
11	WY	8/2/2018 2:47 PM
12	NC	8/2/2018 12:51 PM
13	LA	8/2/2018 12:50 PM

2 / 16

#		DATE
14	ND	8/2/2018 12:47 PM
15	MO	8/2/2018 12:33 PM
16	MN	8/2/2018 9:49 AM
17	KS	8/2/2018 8:56 AM
18	TX	8/2/2018 8:23 AM
19	OK	8/2/2018 8:11 AM
20	NM	8/2/2018 8:04 AM
21	IA	8/2/2018 7:09 AM

#	ZIP/POSTAL CODE	DATE
	There are no responses.	

#	COUNTRY	DATE
	There are no responses.	

#	EMAIL ADDRESS	DATE
1	neil.vanbebber@illinois.gov	8/23/2018 7:36 AM
2	John.Delphia@txdot.gov	8/10/2018 6:29 PM
3	flournoyg@dot.state.al.us	8/10/2018 3:44 PM
4	dale.heft@ardot.gov	8/10/2018 1:04 PM
5	tom.birnbrich@dot.ohio.gov	8/9/2018 8:11 AM
6	larry.tolfa@dot.ny.gov	8/6/2018 11:23 AM
7	kevin.marton@state.sd.us	8/6/2018 9:25 AM
8	herbert.mcdowell@itd.idaho.gov	8/6/2018 8:31 AM
9	carlsone2@michigan.gov	8/3/2018 9:33 PM
10	akosicki@sha.state.md.us	8/3/2018 9:46 AM
11	michael.menghini@wyo.gov	8/2/2018 2:47 PM
12	bmradakovic@ncdot.gov	8/2/2018 12:51 PM
13	tingzong.guo@la.gov	8/2/2018 12:50 PM
14	bpfeifer@nd.gov	8/2/2018 12:47 PM
15	dale.henderson@modot.mo.gov	8/2/2018 12:33 PM
16	petra.dewall@state.mn.us	8/2/2018 9:49 AM
17	mike.orth@ks.gov	8/2/2018 8:56 AM
18	saul.nuccitelli@txdot.gov	8/2/2018 8:23 AM
19	llewis@odot.org	8/2/2018 8:11 AM
20	ted.barber@state.nm.us	8/2/2018 8:04 AM
21	david.claman@iowadot.us	8/2/2018 7:09 AM

#	PHONE NUMBER	DATE
1	217-785-2917	8/23/2018 7:36 AM
2	512-416-2359	8/10/2018 6:29 PM
3	334-242-6598	8/10/2018 3:44 PM
4	501-569-2062	8/10/2018 1:04 PM
5	614-752-2974	8/9/2018 8:11 AM
6	518-485-7265	8/6/2018 11:23 AM

3 / 16

7	(605) 773-4995	8/6/2018 9:25 AM
8	2083348540	8/6/2018 8:31 AM
9	517-335-1919	8/3/2018 9:33 PM
10	410-545-8340	8/3/2018 9:46 AM
11	307-777-4427	8/2/2018 2:47 PM
12	919-707-6747	8/2/2018 12:51 PM
13	225-379-1342	8/2/2018 12:50 PM
14	701-328-1213	8/2/2018 12:47 PM
15	(573) 522-5016	8/2/2018 12:33 PM
16	651-366-4473	8/2/2018 9:49 AM
17	785-296-0419	8/2/2018 8:56 AM
18	5124162219	8/2/2018 8:23 AM
19	405-521-6500	8/2/2018 8:11 AM
20	505-827-5449	8/2/2018 8:04 AM
21	515-239-1487	8/2/2018 7:09 AM

4 / 16

Q2 Would you like to receive results of this survey?

Answered: 21   Skipped: 0
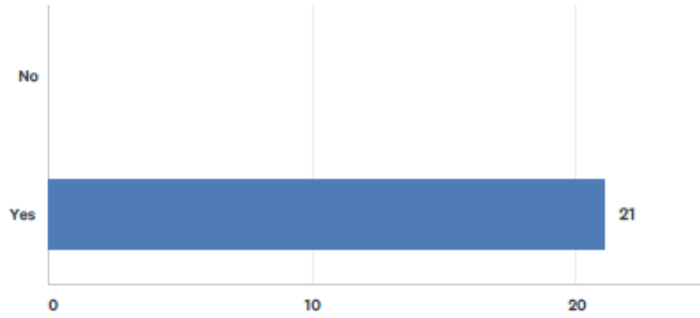
ANSWER CHOICES	RESPONSES	
No	0.00%	0
Yes	100.00%	21
TOTAL		21

Q3 From your experience, what are the most important scour issues related to cohesive soils (check all that apply)?

Answered: 21   Skipped: 0
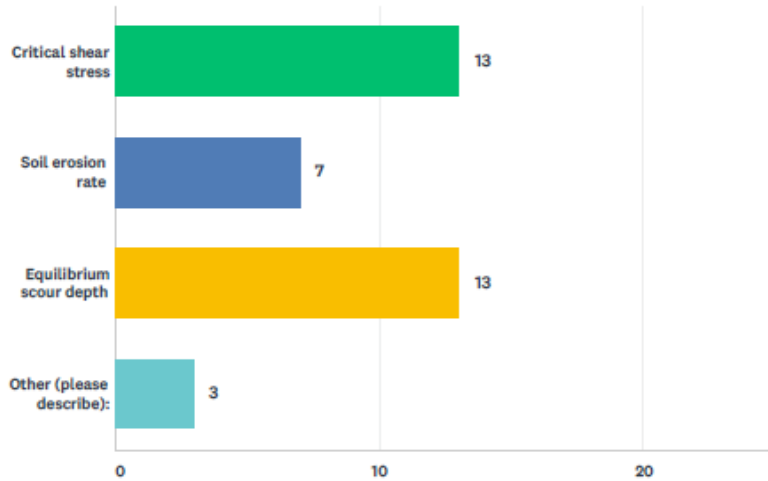
ANSWER CHOICES	RESPONSES	
Critical shear stress	61.90%	13
Soil erosion rate	33.33%	7
Equilibrium scour depth	61.90%	13
Other (please describe):	14.29%	3
Total Respondents: 21		

#	OTHER (PLEASE DESCRIBE):	DATE
1	Critical velocity	8/3/2018 9:59 AM
2	We have not been able to do the geotech analysis to consider cohesive soils	8/2/2018 8:06 AM
3	firm glacial clay	8/2/2018 7:10 AM

6 / 16

Q4 What method does your agency use to measure or determine soil erodibility (check all that apply)?

Answered: 21   Skipped: 0
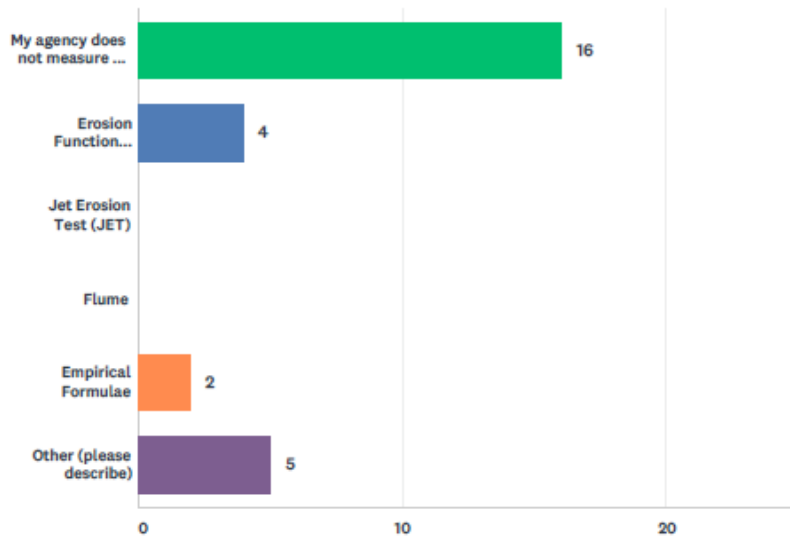
ANSWER CHOICES	RESPONSES	
My agency does not measure or determine soil erodibility	76.19%	16
Erosion Function Apparatus (EFA)	19.05%	4
Jet Erosion Test (JET)	0.00%	0
Flume	0.00%	0
Empirical Formulae	9.52%	2
Other (please describe)	23.81%	5
Total Respondents: 21		

#	OTHER (PLEASE DESCRIBE)	DATE
1	The EFA is seldom used.	8/23/2018 7:38 AM
2	We've only used an EFA on one project.	8/3/2018 9:34 PM
3	We tried the EFA apparatus about 20 years ago but in about 5 years we used it we had multiple problems related to both calibration and reliability. Ultimately, we stopped using it about 10 years ago.	8/3/2018 9:59 AM
4	We have just started to use EFA in conjunction with electrical resistivity at a handful of locations with research project. Typically use (conservative) HEC-18 sand equations.	8/2/2018 9:03 AM
5	soil survey	8/2/2018 8:12 AM

Q5 What methods does your agency use to predict bridge scour in cohesive soils (check all that apply)?

Answered: 21   Skipped: 0
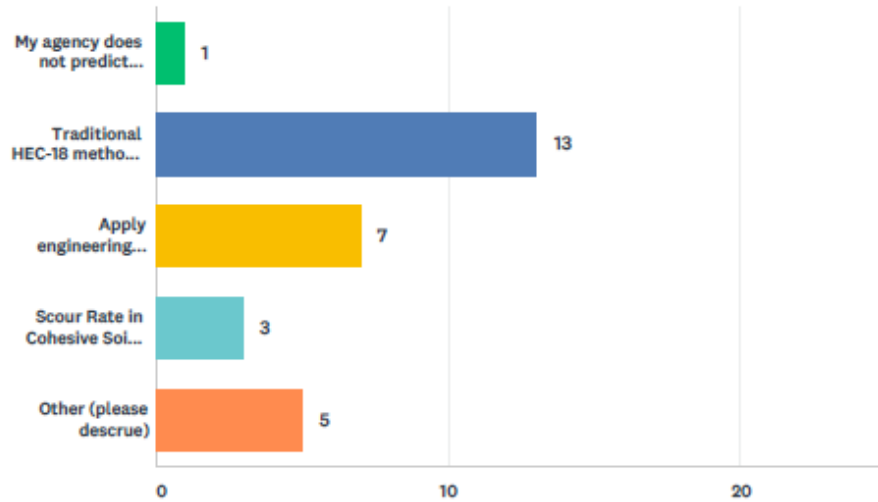
ANSWER CHOICES	RESPONSES	
My agency does not predict scour in cohesive soils	4.76%	1
Traditional HEC-18 method for non-cohesive soils	61.90%	13
Apply engineering judgement to the HEC-18 method	33.33%	7
Scour Rate in Cohesive Soils (SRICOS) method	14.29%	3
Other (please descrue)	23.81%	5
Total Respondents: 21		

#	OTHER (PLEASE DESCRUE)	DATE
1	Annandale's Erodibility Index Method	8/10/2018 6:30 PM
2	Clear-Water Contraction Scour at Selected Bridge Sites in the Black Prairie Belt of Coastal Plain in Alabama, 2006 USGS Scientific Investigation Report 2007-5260	8/10/2018 3:46 PM
3	I am not sure	8/6/2018 8:41 AM
4	Our in-house ABSCOUR software offers a procedure based on the critical velocity concept. The software is described in Appendix A to the Scour Chapter (Chapter 11) in the OOS H&H Design Manual. both can be downloaded using this link: http://www.gishydro.eng.umd.edu/sha_soft.htm	8/3/2018 9:59 AM
5	Although overly conservative, we use HEC-18 sandbed equations for rapid estimation. Just beginning to assess EFA and ER at some sites.	8/2/2018 9:03 AM

Q6 How does your agency decide to use the SRICOS method instead of the traditional HEC-18 method, which does not account for the time rate of scour (check all that apply)?

Answered: 21   Skipped: 0
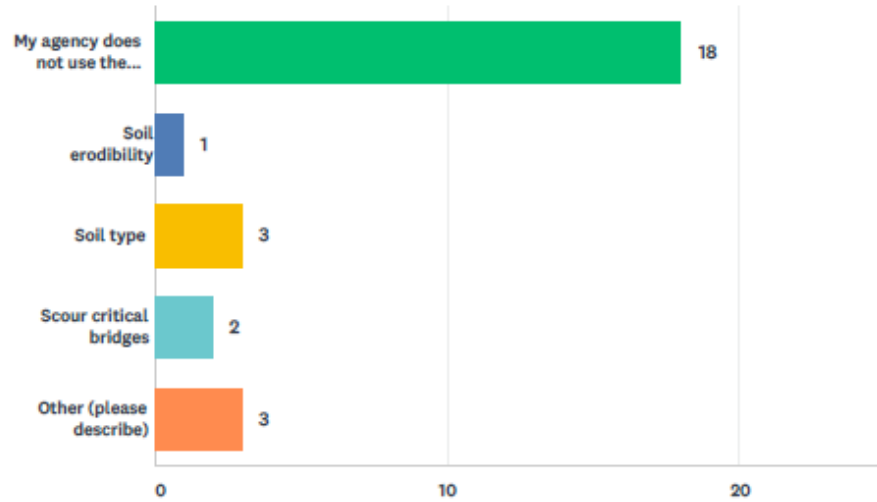
ANSWER CHOICES	RESPONSES	
My agency does not use the SRICOS method for scour analysis	85.71%	18
Soil erodibility	4.76%	1
Soil type	14.29%	3
Scour critical bridges	9.52%	2
Other (please describe)	14.29%	3
Total Respondents: 21		

#	OTHER (PLEASE DESCRIBE)	DATE
1	Back in 2000 SRICOS was one of the methodologies used in analyzing scour depths for the bascule piers of the new WW Bridge on I-95 over the Potomac River. It computed scour depths of about 25 ft. At the other end of the spectrum was the Annandale's method that yielded depths of about 105 ft. We ended up selecting the results of the physical studies in the FHWA flume (scour depths of about 60 ft.).	8/3/2018 9:59 AM
2	SRICOS is an optional method for cohesive or layered soil	8/2/2018 9:09 AM
3	Bridge designers (structural) also do hydraulics. Agency does not have time nor experience to develop hydrographs.	8/2/2018 9:03 AM

9 / 16

Q7 Has your agency ever used time series of streamflow to predict scour?

Answered: 21   Skipped: 0
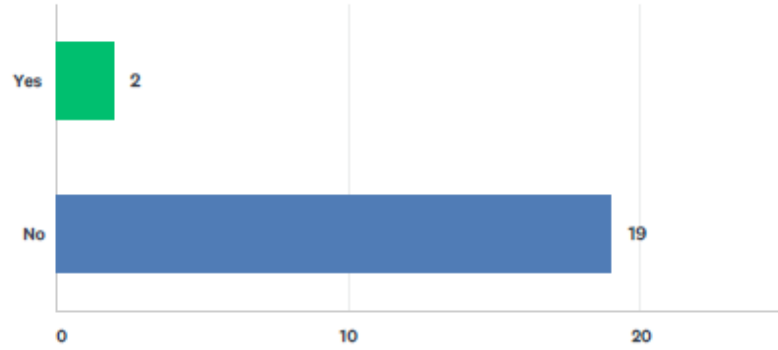
ANSWER CHOICES	RESPONSES	
Yes	9.52%	2
No	90.48%	19
TOTAL		21

10 / 16

Q8 If your agency has estimated streamflow for an un-gauged stream, please identify which methods you have used (check all that apply):

Answered: 21   Skipped: 0
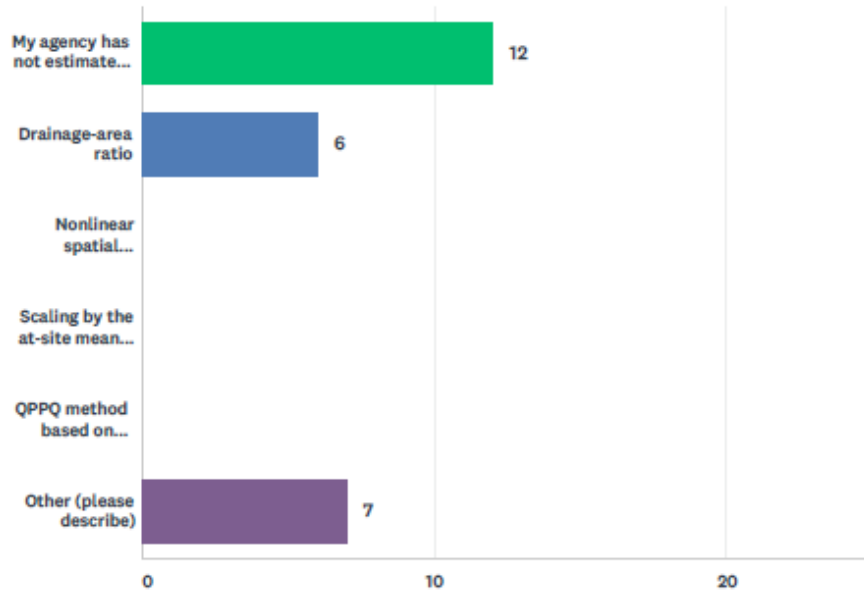
ANSWER CHOICES	RESPONSES	
My agency has not estimated streamflow time series for an ungauged stream	57.14%	12
Drainage-area ratio	28.57%	6
Nonlinear spatial interpolation	0.00%	0
Scaling by the at-site mean variance	0.00%	0
QPPQ method based on flow-duration curves at an index streamgage	0.00%	0
Other (please describe)	33.33%	7
Total Respondents: 21		

#	OTHER (PLEASE DESCRIBE)	DATE
1	Need to contact Saul Nuccitelli in the Hydraulics Branch of the Design Division for other possible methods. Saul.Nuccitelli@txdot.gov	8/10/2018 6:33 PM
2	U.S.G.S. Regression Equation.	8/10/2018 1:10 PM
3	Streamstats	8/6/2018 12:18 PM
4	National Water Model	8/2/2018 3:56 PM
5	Regression equations.	8/2/2018 2:48 PM
6	USGS StreamStats regression equations. Other statewide regression equations for peak discharge.	8/2/2018 9:06 AM
7	Regional regression formulas	8/2/2018 8:22 AM

11 / 16

Q9 If your agency has used synthetic streamflow data in scour analysis, please identify how you constructed the synthetic hydrograph (check all that apply):

Answered: 21   Skipped: 0
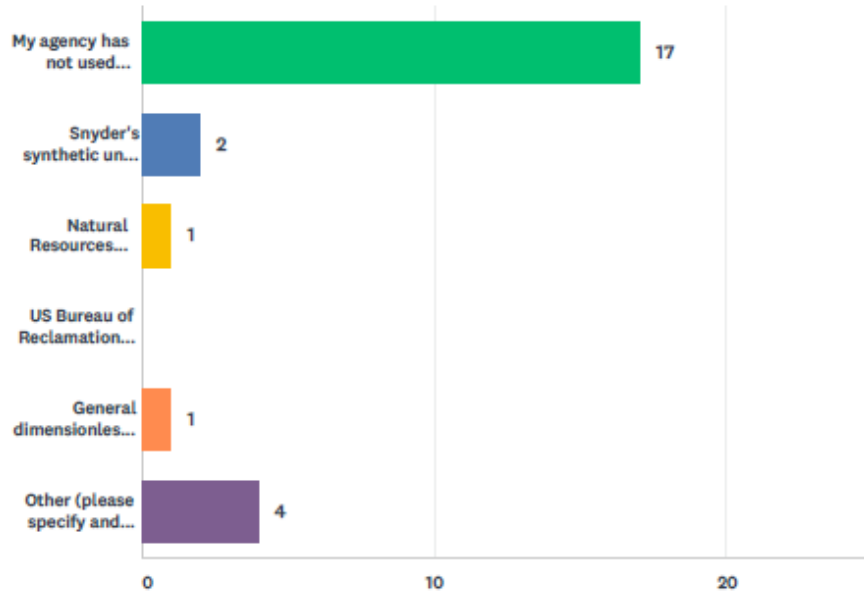
ANSWER CHOICES	RESPONSES	
My agency has not used synthetic streamflow data	80.95%	17
Snyder's synthetic unit hydrograph	9.52%	2
Natural Resources Conservation Service (NRCS) synthetic unit hydrograph	4.76%	1
US Bureau of Reclamation (USBR) synthetic unit hydrograph	0.00%	0
General dimensionless unit hydrograph (GDUH)	4.76%	1
Other (please specify and describe)	19.05%	4
Total Respondents: 21		

#	OTHER (PLEASE SPECIFY AND DESCRIBE)	DATE
1	Need to contact Saul Nuccitelli in the Hydraulics Branch of the Design Division for other possible methods. Saul.Nuccitelli@txdot.gov	8/10/2018 6:33 PM
2	USGS WRI 80-80 flood hydrograph	8/6/2018 9:31 AM
3	Have used Snyder's and NRCS - but very rare, special cases.	8/2/2018 9:06 AM
4	didn't use a hydrograph	8/2/2018 8:22 AM

12 / 16

Q10 Please describe the type of situations where your agency has used flood duration in scour analysis, if any:

Answered: 21   Skipped: 0
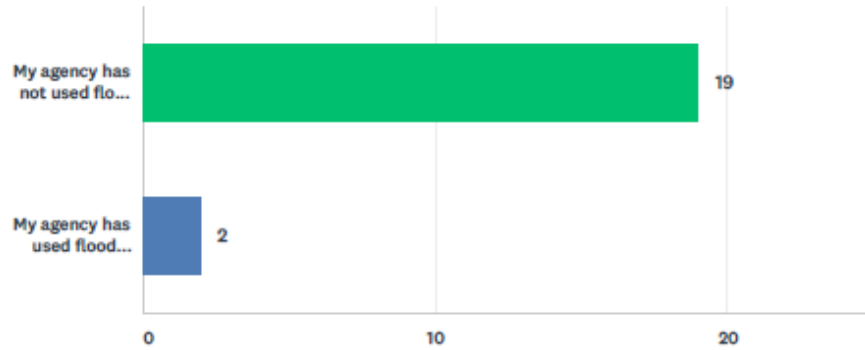
ANSWER CHOICES		RESPONSES	
My agency has not used flood duration in scour analysis		90.48%	19
My agency has used flood duration in scour analysis of these types of situations:		9.52%	2
TOTAL			21

#	MY AGENCY HAS USED FLOOD DURATION IN SCOUR ANALYSIS OF THESE TYPES OF SITUATIONS:	DATE
1	Bridges on rivers that are controlled by the outflow of dams on lakes	8/10/2018 6:35 PM
2	State owned Scour Critical Bridges.	8/10/2018 1:14 PM

Q11 How has your agency estimated flood duration for scour analysis (check all that apply)?

Answered: 21   Skipped: 0
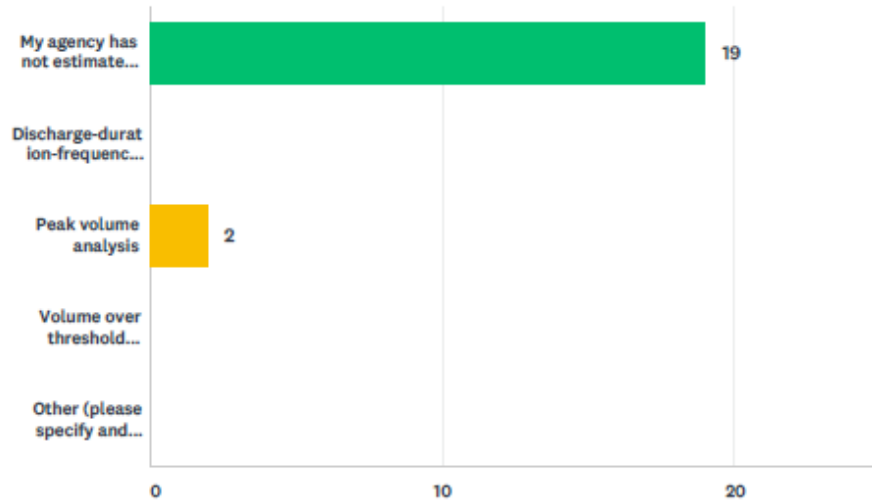
ANSWER CHOICES	RESPONSES	
My agency has not estimated flood duration for scour analysis	90.48%	19
Discharge-duration-frequency (QdF) analysis	0.00%	0
Peak volume analysis	9.52%	2
Volume over threshold analysis	0.00%	0
Other (please specify and describe)	0.00%	0
Total Respondents: 21		

#	OTHER (PLEASE SPECIFY AND DESCRIBE)	DATE
	There are no responses.	

14 / 16

Q12 What forecasting models has your agency used to predict flood time series (check all that apply)?

Answered: 21   Skipped: 0
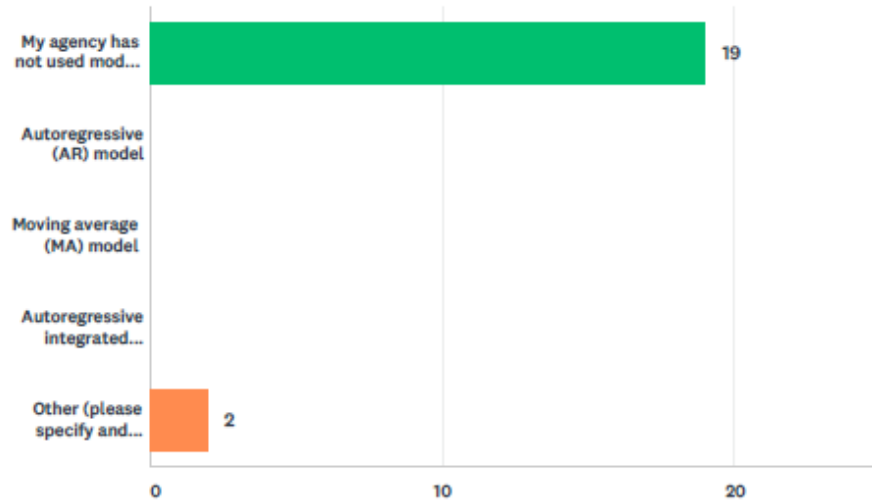
ANSWER CHOICES	RESPONSES	
My agency has not used models to predict flood time series	90.48%	19
Autoregressive (AR) model	0.00%	0
Moving average (MA) model	0.00%	0
Autoregressive integrated moving average (ARIMA) model	0.00%	0
Other (please specify and describe)	9.52%	2
Total Respondents: 21		

#	OTHER (PLEASE SPECIFY AND DESCRIBE)	DATE
1	Need to contact Saul Nuccitelli in the Hydraulics Branch of the Design Division for other possible methods. Saul.Nuccitelli@txdot.gov	8/10/2018 6:35 PM
2	National Water Model	8/2/2018 3:58 PM

15 / 16

Q13 Please provide any other comments that you'd like regarding your agency's practices in predicting scour in cohesive soils:

Answered: 5   Skipped: 16

#	RESPONSES	DATE
1	We assume that equilibrium will eventually be realized and use hec 18 for scour estimation.	8/6/2018 12:20 PM
2	We are looking forward to seeing the test results of the new FHWA in-situ apparatus/methodology.	8/3/2018 10:02 AM
3	Primary contact for TxDOT scour is John Delphia. I forwarded this survey to him to complete as well.	8/2/2018 3:58 PM
4	Would really like to see outcome - worthwhile project. Results must be pared-down, quickly applied, and easily understood by practitioners to be of use. Recommend providing multiple real-world worked examples. DOT's staff and resources are generally so diminished, most use the very conservative non-cohesive equations of HEC-18. Unsteady flow conditions very time-consuming to develop. With 1,000's of cohesive bed stream crossings statewide, don't have time nor confidence to assess (less conservative) results for foundations.	8/2/2018 9:19 AM
5	Cohesive soils at bridges are not common in our state.	8/2/2018 8:10 AM

APPENDIX II OUTPUT FROM PEAKFQ FOR BIG SIOUX RIVER

near Brookings Streamflow Gauging Station (06480000)

```
Program PeakFq            U. S. GEOLOGICAL SURVEY          Seq.002.000
Version 7.1            Annual peak flow frequency analysis  Run Date / Time
3/14/2014                                                   05/03/2017 10:37

                  --- PROCESSING OPTIONS ---

          Plot option          = Graphics device
          Basin char output    = None
          Print option         = Yes
          Debug print          = No
          Input peaks listing  = Long
          Input peaks format   = WATSTORE peak file

          Input files used:
             peaks (ascii)  - P:\nt00f9j\Peaks\EMA Dr Ting\BS\2016 hist\06480000.TXT
             specifications - P:\nt00f9j\Peaks\EMA Dr Ting\BS\2016 hist\PKFQWPSF.TMP
          Output file(s):
             main - P:\nt00f9j\Peaks\EMA Dr Ting\BS\2016 hist\06480000.PRT




Program PeakFq            U. S. GEOLOGICAL SURVEY          Seq.001.001
Version 7.1            Annual peak flow frequency analysis  Run Date / Time
3/14/2014                                                   05/03/2017 10:37

          Station - 06480000  BIG SIOUX RIVER NEAR BROOKINGS,SD


              I N P U T   D A T A   S U M M A R Y

          Number of peaks in record          =        63
          Peaks not used in analysis         =         0
          Systematic peaks in analysis       =        63
          Historic peaks in analysis         =         0
          Beginning Year                     =      1881
          Ending Year                        =      2016
          Historical Period Length           =       136
          Generalized skew                   =    -0.400
                Standard error               =     0.550
                Mean Square error            =     0.303
          Skew option                        =  WEIGHTED
          Gage base discharge                =       0.0
          User supplied high outlier threshold =      --
          User supplied PILF (LO) criterion  =        --
          Plotting position parameter        =      0.00
          Type of analysis                          EMA
          PILF (LO) Test Method                    MGBT
          Perception Thresholds:
             Begin    End     Low     High     Comment
             1881    1881     INF     INF     1881 NOT EXCEEDED UNTIL 1969
             1881    1953  33900.0    INF     1969 LARGEST SINCE 1881
             1954    2016     0.0     INF     SYSTEMATAIC
          Interval Data             =     None Specified




********* NOTICE -- Preliminary machine computations.     *********
********* User responsible for assessment and interpretation. *********

  WCF002J-CALCS COMPLETED.  RETURN CODE =  2
  EMA001W-VARIANCE OF ESTIMATE WARNING, HISTORIC PERIOD > 2* SYS
  EMA002W-CONFIDENCE INTERVALS ARE NOT EXACT IF HISTORIC PERIOD > 0


                  Kendall's Tau Parameters

                                    MEDIAN   No. of
                     TAU    P-VALUE  SLOPE   PEAKS
                   ------------------------------------
   SYSTEMATIC RECORD  0.078   0.370  14.959    63
```

```
Program PeakFq                U. S. GEOLOGICAL SURVEY              Seq.001.002
Version 7.1                 Annual peak flow frequency analysis    Run Date / Time
3/14/2014                                                          05/03/2017 10:37

              Station - 06480000  BIG SIOUX RIVER NEAR BROOKINGS,SD


            ANNUAL FREQUENCY CURVE PARAMETERS -- LOG-PEARSON TYPE III

                                      LOGARITHMIC
                          ---------------------------------
                                     STANDARD
                            MEAN     DEVIATION    SKEW
                          ---------------------------------
EMA W/O REG. INFO          3.3857     0.4885     -0.276
EMA W/REG. INFO            3.3866     0.4894     -0.315

EMA ESTIMATE OF MSE OF SKEW W/O REG. INFO (AT-SITE)     0.0784
EMA ESTIMATE OF MSE OF SKEW W/SYSTEMATIC ONLY (AT-SITE) 0.0996



        ANNUAL FREQUENCY CURVE -- DISCHARGES AT SELECTED EXCEEDANCE PROBABILITIES

    ANNUAL     EMA W/     EMA W/O     <------ FOR EMA ESTIMATES ------->
  XCEEDANCE   REG INFO   REG INFO     VARIANCE   95% CONFIDENCE INTERVALS
  ROBABILITY  ESTIMATE   ESTIMATE     OF EST.        LOWER        UPPER
    0.9950       95.9      100.3       0.0432        20.7         192.0
    0.9900      136.8      141.7       0.0320        38.1         251.9
    0.9500      346.9      351.4       0.0137       165.8         536.2
    0.9000      556.1      558.6       0.0091       321.2         808.9
    0.8000      963.6      960.6       0.0061       641.5        1338.0
    0.6667     1576.      1564.        0.0048      1123.0        2143.0
    0.5000     2584.      2560.        0.0043      1904.0        3487.0
    0.4292     3150.      3121.        0.0042      2339.0        4245.0
    0.2000     6370.      6339.        0.0041      4769.0        8582.0
    0.1000     9886.      9898.        0.0046      7292.0       13560.0
    0.0400    15420.     15590.        0.0062     10920.0       22450.0
    0.0200    20290.     20670.        0.0082     13720.0       31520.0
    0.0100    25760.     26440.        0.0110     16450.0       43140.0
    0.0050    31820.     32920.        0.0146     19080.0       57930.0
    0.0020    40740.     42600.        0.0207     22330.0       83590.0
```

224

```
Program PeakFq              U. S. GEOLOGICAL SURVEY           Seq.001.003
Version 7.1            Annual peak flow frequency analysis    Run Date / Time
3/14/2014                                                     05/03/2017 10:37

             Station - 06480000  BIG SIOUX RIVER NEAR BROOKINGS,SD


                    I N P U T   D A T A   L I S T I N G


    WATER      PEAK   PEAKFQ   <--- Intervals --->
    YEAR      VALUE   CODES      LOW        HIGH    REMARKS
    1954     1970.0
    1955     1180.0
    1956      287.0
    1957     5320.0
    1958      382.0
    1959      240.0
    1960     9620.0
    1961     1340.0
    1962    10600.0
    1963     1880.0
    1964      952.0
    1965     7700.0
    1966     4560.0
    1967     1880.0
    1968      230.0
    1969    33900.0
    1970     3350.0
    1971     2100.0
    1972     5060.0
    1973     3010.0
    1974      950.0
    1975      696.0
    1976     1080.0
    1977     1750.0
    1978     5960.0
    1979     4720.0
    1980     3820.0
    1981      143.0
    1982      718.0
    1983     3300.0
    1984    13700.0
    1985     8440.0
    1986     6690.0
    1987     2400.0
    1988      950.0
    1989     1900.0
    1990     1990.0
    1991     1430.0
    1992     5760.0
    1993    13300.0
    1994     5660.0
    1995     6910.0
    1996     2990.0
    1997    11000.0
    1998     2180.0
    1999     1870.0
    2000      683.0
    2001     6680.0
    2002     2340.0
    2003      965.0
    2004      521.0
    2005     1020.0
    2006     2790.0
    2007     6520.0
    2008     2780.0
    2009     3740.0
    2010    19800.0
    2011    15400.0
    2012     2520.0
    2013     3480.0
    2014     1840.0
    2015     1320.0
    2016     1020.0
```

APPENDIX III OUTPUT FROM PEAKFQ FOR JAMES RIVER

near Forestburg Streamflow Gauging Station (06477000)

```
Program PeakFq              U. S. GEOLOGICAL SURVEY          Seq.001.001
Version 7.1             Annual peak flow frequency analysis   Run Date / Time
3/14/2014                                                     05/03/2017 09:36

             Station - 06477000   JAMES R NEAR FORESTBURG,SD


              I N P U T   D A T A   S U M M A R Y

          Number of peaks in record         =        69
          Peaks not used in analysis        =         2
          Systematic peaks in analysis      =        67
          Historic peaks in analysis        =         0
          Beginning Year                    =      1881
          Ending Year                       =      2016
          Historical Period Length          =       136
          Generalized skew                  =    -0.228
              Standard error                =     0.550
              Mean Square error             =     0.303
          Skew option                       =   WEIGHTED
          Gage base discharge               =       0.0
          User supplied high outlier threshold =    --
          User supplied PILF (LO) criterion =      --
          Plotting position parameter       =      0.00
          Type of analysis                         EMA
          PILF (LO) Test Method                   MGBT
          Perception Thresholds:
              Begin    End     Low     High    Comment
              1881    1881     INF     INF    1881 NOT EXCEEDED UNTIL 1997
              1882    1949  25600.0    INF    1997 LARGEST SINCE 1881
              1950    2016     0.0     INF     SYSTEMATIC
          Interval Data                 =    None Specified




 *********  NOTICE  --  Preliminary machine computations.      *********
 *********  User responsible for assessment and interpretation. *********

 **WCF109W-PEAKS WITH MINUS-FLAGGED DISCHARGES WERE BYPASSED.      2
 **WCF113W-NUMBER OF SYSTEMATIC PEAKS HAS BEEN REDUCED TO NSYS =   67
   WCF002J-CALCS COMPLETED.   RETURN CODE =   2
   EMA001W-VARIANCE OF ESTIMATE WARNING, HISTORIC PERIOD > 2* SYS
   EMA002W-CONFIDENCE INTERVALS ARE NOT EXACT IF HISTORIC PERIOD > 0



                        Kendall's Tau Parameters

                                          MEDIAN   No. of
                         TAU    P-VALUE   SLOPE    PEAKS
                    -------------------------------------
   SYSTEMATIC RECORD    0.164    0.050    21.191     67
```

Station - 06477000   JAMES R NEAR FORESTBURG,SD

ANNUAL FREQUENCY CURVE PARAMETERS -- LOG-PEARSON TYPE III

LOGARITHMIC

                              STANDARD
                    MEAN   DEVIATION   SKEW

EMA W/O REG. INFO   3.2648   0.5607   -0.174
EMA W/REG. INFO   3.2653   0.5612   -0.189

EMA ESTIMATE OF MSE OF SKEW W/O REG. INFO (AT-SITE)   0.0699
EMA ESTIMATE OF MSE OF SKEW W/SYSTEMATIC ONLY (AT-SITE) 0.0881

ANNUAL FREQUENCY CURVE -- DISCHARGES AT SELECTED EXCEEDANCE PROBABILITIES

ANNUAL EXCEEDANCE PROBABILITY	EMA W/ REG INFO ESTIMATE	EMA W/O REG INFO ESTIMATE	<------ FOR EMA ESTIMATES ------->		
			VARIANCE OF EST.	95% CONFIDENCE INTERVALS LOWER	UPPER
0.9950	52.5	53.6	0.0460	11.6	108.5
0.9900	76.3	77.5	0.0342	21.4	144.2
0.9500	205.6	206.9	0.0151	96.5	324.6
0.9000	343.3	344.1	0.0101	193.8	510.6
0.8000	629.3	628.5	0.0070	408.5	896.3
0.6667	1092.	1089.	0.0058	757.1	1526.0
0.5000	1919.	1910.	0.0052	1372.0	2658.0
0.4292	2412.	2401.	0.0051	1737.0	3336.0
0.2000	5521.	5506.	0.0050	4002.0	7620.0
0.1000	9379.	9378.	0.0056	6698.0	13260.0
0.0400	16230.	16290.	0.0076	11160.0	25000.0
0.0200	22920.	23080.	0.0103	15100.0	38810.0
0.0100	31070.	31400.	0.0140	19390.0	58630.0
0.0050	40840.	41430.	0.0188	23930.0	86600.0
0.0020	56540.	57620.	0.0268	30160.0	141000.0

Station - 06477000   JAMES R NEAR FORESTBURG,SD

I N P U T   D A T A   L I S T I N G

WATER YEAR	PEAK VALUE	PEAKFQ CODES	<--- Intervals ---> LOW HIGH	REMARKS
1920	-8888.0			
1922	-8888.0			
1950	5180.0			
1951	1600.0			
1952	6290.0			
1953	2080.0			
1954	332.0			
1955	1210.0			
1956	920.0			
1957	864.0			
1958	924.0			
1959	80.0			
1960	10900.0			
1961	702.0			
1962	12000.0			
1963	599.0			
1964	561.0			
1965	1010.0			
1966	2800.0			
1967	1910.0			
1968	372.0			
1969	12500.0			
1970	1320.0			
1971	980.0			
1972	2990.0			
1973	2770.0			
1974	280.0			
1975	1040.0			
1976	308.0			
1977	4050.0			
1978	4830.0			
1979	1920.0			
1980	336.0			
1981	63.0			
1982	1050.0			
1983	925.0			
1984	6140.0			
1985	3330.0			
1986	7740.0			
1987	4530.0			
1988	415.0			
1989	3080.0			
1990	260.0			
1991	2520.0			
1992	743.0			
1993	3450.0			
1994	8180.0			
1995	13000.0			
1996	3790.0			
1997	25600.0			
1998	4530.0			
1999	5060.0			
2000	911.0			
2001	17400.0			
2002	428.0			
2003	751.0			
2004	931.0			
2005	1920.0			
2006	2010.0			
2007	21300.0			
2008	965.0			
2009	9400.0			
2010	19800.0			
2011	28400.0			
2012	1790.0			
2013	3260.0			
2014	1520.0			
2015	1720.0			
2016	968.0			

APPENDIX IV OUTPUT FROM PEAKFQ FOR SPLIT ROCK CREEK

```
Program PeakFq              U. S. GEOLOGICAL SURVEY           Seq.001.001
Version 7.1              Annual peak flow frequency analysis   Run Date / Time
3/14/2014                                                      03/29/2018 09:38

                Station - 06482610  SPLIT ROCK CR AT CORSON,SD


                     I N P U T   D A T A   S U M M A R Y

            Number of peaks in record        =        48
            Peaks not used in analysis       =         0
            Systematic peaks in analysis     =        48
            Historic peaks in analysis       =         0
            Beginning Year                   =      1966
            Ending Year                      =      2017
            Historical Period Length         =        52
            Generalized skew                 =    -0.358
                 Standard error              =     0.550
                 Mean Square error           =     0.303
            Skew option                      =  WEIGHTED
            Gage base discharge              =       0.0
            User supplied high outlier threshold =    --
            User supplied PILF (LO) criterion    =    --
            Plotting position parameter      =      0.00
            Type of analysis                        EMA
            PILF (LO) Test Method                  MGBT
            Perception Thresholds:
                 Begin     End    Low     High    Comment
                 1966     2017    0.0     INF     DEFAULT
                 1991     1991   500.0    INF     PEAK < STATED VALUE
                 1998     2001 18900.0    INF     1993 EXCEEDS ANY IN INTERVAL
            Interval Data:
                          Year    Low     High    Comment
                          1991    0.0    500.0    PEAK < STATED VALUE



  *********  NOTICE  --  Preliminary machine computations.     *********
  *********  User responsible for assessment and interpretation. *********

   WCF002J-CALCS COMPLETED.   RETURN CODE =  2
   EMA002W-CONFIDENCE INTERVALS ARE NOT EXACT IF HISTORIC PERIOD > 0


                         Kendall's Tau Parameters

                                        MEDIAN   No. of
                        TAU    P-VALUE   SLOPE    PEAKS
                       ---------------------------------------
  SYSTEMATIC RECORD    0.103    0.307   15.876     48
```

at Corson Streamflow Gauging Station (06482610)

```
              Station - 06482610  SPLIT ROCK CR AT CORSON,SD


            ANNUAL FREQUENCY CURVE PARAMETERS -- LOG-PEARSON TYPE III

                              LOGARITHMIC
                     -------------------------------
                                  STANDARD
                        MEAN     DEVIATION    SKEW
                     -------------------------------
  EMA W/O REG. INFO    3.3826     0.4482      0.099
  EMA W/REG. INFO      3.3826     0.4496     -0.038

  EMA ESTIMATE OF MSE OF SKEW W/O REG. INFO (AT-SITE)       0.1112
  EMA ESTIMATE OF MSE OF SKEW W/SYSTEMATIC ONLY (AT-SITE)   0.1157



        ANNUAL FREQUENCY CURVE -- DISCHARGES AT SELECTED EXCEEDANCE PROBABILITIES

     ANNUAL     EMA W/    EMA W/O    <------ FOR EMA ESTIMATES ------->
   EXCEEDANCE  REG INFO  REG INFO   VARIANCE   95% CONFIDENCE INTERVALS
   PROBABILITY ESTIMATE  ESTIMATE   OF EST.        LOWER        UPPER

     0.9950      161.5     186.1     0.0293       44.5         299.0
     0.9900      210.9     235.9     0.0220       70.7         363.1
     0.9500      434.7     455.2     0.0103      223.3         649.6
     0.9000      637.6     650.4     0.0073      382.6         911.6
     0.8000     1012.     1008.      0.0055      682.4        1402.0
     0.6667     1553.     1526.      0.0048     1105.0        2125.0
     0.5000     2429.     2373.      0.0046     1769.0        3324.0
     0.4292     2921.     2854.      0.0047     2136.0        4015.0
     0.2000     5778.     5722.      0.0057     4191.0        8368.0
     0.1000     9055.     9153.      0.0078     6398.0       14440.0
     0.0400    14580.    15220.      0.0125     9760.0       27890.0
     0.0200    19800.    21220.      0.0176    12560.0       44380.0
     0.0100    26050.    28700.      0.0242    15530.0       68990.0
     0.0050    33460.    37910.      0.0322    18620.0      105300.0
     0.0020    45270.    53290.      0.0453    22860.0      180000.0
```

Station - 06482610   SPLIT ROCK CR AT CORSON,SD

I N P U T   D A T A   L I S T I N G

WATER YEAR	PEAK VALUE	PEAKFQ CODES	<--- Intervals ---> LOW	HIGH	REMARKS
1966	550.0				
1967	925.0				
1968	1850.0				
1969	17800.0				
1970	2500.0				
1971	1300.0				
1972	1900.0				
1973	840.0				
1974	5240.0				
1975	446.0				
1976	900.0				
1977	2470.0				
1978	3250.0				
1979	10500.0				
1980	2230.0				
1981	1110.0				
1982	3090.0				
1983	4500.0				
1984	9020.0				
1985	4100.0				
1986	7920.0				
1987	1840.0				
1988	491.0				
1989	1200.0				
1990	1150.0				
1991	500.0	L	0.0	500.0	PEAK < STATED VALUE
1992	4800.0				
1993	18900.0				
1994	4700.0				
1995	5820.0				
1996	956.0				
1997	8290.0				
2002	1320.0				
2003	1130.0				
2004	3400.0				
2005	1180.0				
2006	8020.0				
2007	4050.0				
2008	1710.0				
2009	400.0				
2010	13100.0				
2011	4730.0				
2012	4730.0				
2013	1340.0				
2014	13100.0				
2015	2510.0				
2016	1480.0				
2017	946.0				